Developing safer HIV drugs: Elucidating the mechanistic pathway of Tenofovir-induced cytotoxicity via mitochondrial dysfunction.

Thesis submitted in accordance with the requirements of The University of Liverpool for the degree of Doctor of Philosophy

Claire Louise Mellor

2013

DECLARATION

This thesis is the result of my own work. The material within this thesis has not been presented, nor is currently being presented, either wholly or in part for any other degree or qualification

Claire Louise Mellor

This research was carried out in the Department of Pharmacology and Therapeutics, The University of Liverpool, UK.

ACKNOWLEDGEMENTS

I would like to thank my supervisors Dr. Amy Chadwick, Dr Neill Liptrott, Prof. David Back and Prof. Kevin Park for all of their help and guidance throughout my PhD, for this I am eternally grateful.

I would like to thank everyone in H Block and in the Pharmacology and Therapeutics labs for their friendship and help when it was needed especially to Bhavana Jagota for 7 years of friendship.

I would also like to thank my family for the encouragement they have given me throughout the years of education. Finally a special thank you to Clint Orlik for his continued help and support whilst I carried out my PhD and for making my life easier so I could concentrate on getting my PhD finalised, without him this would not have been possible. I therefore dedicate this thesis and the work presented within it to him and my beautiful girls Leah-Rose Orlik and Alexa Orlik.

CONTENTS

ABSTRACT

Human immune deficiency virus (HIV) currently affects around 34 million people worldwide, but due to recent advancements in antiretroviral treatments the morbidity and mortality of HIV has greatly improved (UNIAIDS, 2009). Tenofovir (TFV) is a nucleoside reverse transcriptase inhibitor (NRTI) that is currently widely used in most HIV regimens due to its favourable pharmacokinetic and pharmacodynamic properties, which allows for once daily dose (Gallent *et al*., 2004). TFV is used to treat HIV in both treatment experienced and treatment naive patients; it is also used as a treatment for hepatitis B and has recently been approved for use as a pre-exposure prophylaxis treatment. The preclinical trials for TFV showed that it had a good safety profile, however there has been an increasing number of patients presenting with TFV induced renal damage specifically proximal tubule dysfunction (Cooper *et al*., 2010). It was hypothesised that TFV was inducing this tubule damage via mitochondrial dysfunction, as this has been widely reported as an adverse reaction associated with NRTI's (Kontorinis *et al*., 2003). Within these studies *in vitro* cell models were modified via culturing them in galactose media in order to probe for mitotoxins (Marroquin *et al*., 2007). The cytotoxicity and mechanisms of cell death induced via TFV were elucidated within these modified cell lines. Work presented has shown that TFV causes delayed mitochondrial cytotoxicity, which causes a cell cycle arrest within the G_2/M phase leading to an accumulation of cell within the S phase. It was shown that the cell cycle arrest is likely due to the inhibition of mitochondrial polymerase γ leading to decreased mitochondrial DNA and ultimately cell death firstly via apoptosis (caused by release of caspase 3/ 7), and then necrosis when cellular ATP levels become too low to sustain apoptosis. Work presented also showed that autophagy induced by TFV, may play a protective role within cells at lower time period. A study within this thesis using patient urine samples was presented to look for a possible biomarker of TFV proximal tubule dysfunction. Kidney injury molecule-1 (KIM-1)

was selected as previous studies have shown that it is specific to proximal tubule cells (Ichimura *et al*., 2008). Results demonstrated that TFV did not significantly alter the KIM-1 / creatinine ratio within patient urine samples. However the data from this pilot study are novel and should be used for future research into the possible use of KIM-1 as a biomarker for TFV induced proximal tubule dysfunction. The biomarker work presented within this thesis should be carried forward to power a future study using a larger and adequate patient cohort. The work presented within this thesis has now opened doors for further study into this subject area especially with regards to the study of KIM-1 as a biomarker, which is a pressing matter as TFV is now widely available for use as a PrEP treatment.

ABBREVIATIONS

- ABC Abacavir
- ADEF Adefovir
- ADRs Adverse Drug Reactions
- AIDs Autoimmune deficiency virus
- Apaf-1 Apoptotic protease activating factor 1
- ATP Adenosine TriPhosphate (ATP)
- ATV Atazanavir
- AZT Zidovudine
- BAF Bio-Analytical Facility
- BUN Blood Urea Nitrogen
- CAR Cellular Accumulation Ratio
- CARD Caspase Activation and Recruitment Domain
- CKD Chronic Kidney Disease
- Cmax maximum Concentration
- CNS Central Nervous System
- C-path Critical path Institute
- CYP450 human Cytochrome P450
- d4T Stavudine
- ddC Zalcitabine
- ddI Dianosine
- DED Death Effector Domain
- DHE DiHydroEthidium
- DISC Death-Inducing Signal Complex
- DMF n-DiMethylFormamide
- DMSO DiMethylSulphOxide
- DNA Deoxyribonucleic acid
- EFV Efavirenz
- eGFR estimated Glomerular Filtration Rate
- ELISA Enzyme-Linked Immuno-Sorbant Assay
- EMA European Medicines Agency
- ETC Electron Transport Chain (ETC)
- EU European Union
- FACs Flow Cytometry
- FADD Fas- Associated Death Domain
- FBS Foetal Bovine Serum
- FDA Food and Drug Administartion
- FS Forward Scatter
- FTC Emtricitabine
- GFR Glomerular Filtration Rate
- GUM GenitoUrinary Medicine
- HAART Highly Active Antiretroviral Therapy
- HAVCR-1 Hepatitis A Virus Cellular Receptor 1
- HBSS Hanks Balanced Salt Solution
- HEK293 a human renal cell line
- hENT-1 human Equilibrative Nucleoside Transporter 1
- Hep B Hepatitis B
- HEPES N-(2-Hydroxyethyl)piperazine-N′-(2-ethanesulfonic acid)
- HepG2 cells a human hepatic cell line
- hOAT human Organic Anion Transporter's
- II Integrase Inhibitors

- KIM-1 Kidney Injury Molecule -1
- KO KnockOut
- LPV Lopinavir
- MI Maturation Inhibitors
- MRP Multi Drug resistant transporters
- MSD Meso Scale Discovery
- mtDNA mitochondrial DNA
- mtDNA pol γ mitochondrial DNA polymerase γ
- MTT 3-(4,5-Dimethylthiazol-2-yl)-2,5-diphenyltrazolium bromide
- NAG N-Acetyl-β-D-Glucosaminidase
- NIAID National Institute of Allergy and Infectious Diseases
- NKC Natural Killer Cells
- NNRTIs Non-Nucleoside Reverse Transcriptase Inhibitors
- NR Neutral Red
- NRTI Nucleoside Reverse Transcription Inhibitors
- OXPHOS mitochondrial Oxidative Phosphorylation
- PBMCs Peripheral Blood Mononuclear Cells
- PI Propidium Iodide
- PI's Protease Inhibitors
- PI3K Phosphyatidylinositol-3-Kinase
- PMOM Permeabilisation of the Mitochondrial Outer Membrane
- PNS Peripheral Nervous System
- PrEP Pre-Exposure Prophylaxis
- PS PhosphatidylSerine
- RIs Reverse transcriptase Inhibitors
- RNA Ribonucleic acid
- ROS Reactive Oxygen Species
- RTV Ritonavir
- SCr Serum Creatinine
- SD Standard Deviation of the mean
- SDS Sodium Dodecyl Sulfate
- SIVcpz Simian immunodeficiency virus
- SNPs Single Nucleotide Polymorphisms
- SS Side Scatter
- TDF Tenofovir Disoproxil Fumarate
- TFV Tenofovir
- TIM-1 T cell Immunoglobulin Mucin domains-1
- TMRE TetraMethylRhodamine Ethyl ester
- TNF Tumour Necrosis Factor
- UNAIDS United Nations programme on HIV/AIDS
- US United States
- WHO World health organisation
- [^{3}H] tritiated
- 3MA 3-MethylAdenine
- 3TC Lamivudine

Chapter One

GENERAL INTRODUCTION

Contents

1.1 Introduction

The World Health Organisation (WHO) recommends the use of Tenofovir (TFV) in all regimens for the treatment of human immunodeficiency virus (HIV), both for HIV treatment-naive and treatment-experienced patients due to its good efficacy and tolerability properties [1]. TFV acts through the inhibition of the viral reverse transcriptase enzyme and thus prevents further viral replication [2]. Although TFV has a relatively good safety profile, there have recently been clinical reports of patients developing chronic kidney disease (CKD). This renal specificity has been linked to its accumulation in the proximal tubules of the kidney [3].

1.2 Tenofovir as a pharmacological agent

1.2.1 The problem of HIV

The HIV infection was first defined in 1981 when autoimmune deficiency virus (AIDs) was first recognised as a disease [4]. The virus is thought to have originated from Simian immunodeficiency virus (SIVcpz) which infects chimpanzees [5]. The SIVcpz virus is known to infect chimpanzees in central Africa but the origins of this virus itself is still unknown [6]. More than 20 species of African primates have been identified to have species-specific strains of the SIVcpz virus [7]. Recent evidence suggests that the SIVcpz virus in chimpanzees arose from a recombination of two different simian immunodeficiency viruses, SIV rem (from red -capped mangabeys) and SIVgsn (from greater spot -nose monkeys) [8-9]. These primate species are both preyed upon by chimpanzees which are where cross contamination and the production of SIVcpz occurred [6].

Evidence suggests that cross contamination of humans occurred during butchering of infected primates for food in sub-Saharan Africa [7]. Whilst butchering the animals the humans came into contact with the contaminated blood which passed into humans via open wounds [10].

This cross contamination between primates and humans went unnoticed for a long period of time [11]. The African continent at that time provided optimal conditions for the viral spread of HIV, such as mass migration from urban to rural areas leading to the breakup of family units and conditions that meant commercial sex was favoured. Once the virus was deeply spread in Africa the development of increased sexual freedoms and the increase in global travel, led to the spread of the HIV virus to more developed countries and eventually global contamination occurred [11].

If left untreated then HIV becomes the more serious form of AIDs which ultimately leads to death of the patient. HIV currently affects more than 34 million people worldwide [12]. It can be spread through contact with other infected patients via sexual transmission, sharing of infected needles or through contact with infected bodily fluids [13]. According to the United Nations programme on HIV/AIDS (UNAIDS) the spread of HIV in richer countries has decrease dramatically by a third over the last few years. This is largely due to better education and increased access to contraception that prevents the spread of the virus. However, there are still an estimated 6000 new cases of HIV reported in the United Kingdom (UK), alone each year. In the poorer areas of the world there has been an increase in the access to treatment, however more education about how the virus spreads is needed in order to prevent further cases of HIV infection. Since the early 1990's the impact of AIDs has decreased life expectancy of African people by at least 25 years. Recent development in HIV drug regimens has led to an increase in the number of people who have HIV and survive leading to the figures for the total global amount of people with HIV has increased. This can be seen when comparing the number of AIDS related deaths in 1998 (2.8 million) to the amount of AIDS related deaths in 2008 (2 million), and when comparing the number of people living with HIV in 1998 (33 million) to the number of people living with HIV in 2008

(34 million). HIV treatment has led to a better quality and quantity of life for HIV patients and has dramatically decreased the number of HIV patients that develop AIDs [14-15].

1.2.2 The different phases of HIV-1 infection.

Once HIV enters the body and infects the CD4 cells, it can become dormant by hiding within the cytoplasm of the cell or by incorporation into the cellular genetic material. Once hidden, the HIV virus can evade immune response and lay dormant for months or even years [16]. These cells are known as latent reservoirs of the virus [17]. Even though HIV can be treated with antiretrovirals, which suppresses the viral load to undetectable within blood, the virus cannot be eliminated completely due to these reservoirs [17].

There are three main phases of HIV infection. The first phase, known as acute infection, covers the period from first patient contact with the infection [12]. After 2-4 weeks from contracting the virus the patients usually experience an acute illness called acute retroviral syndrome [12]. During the acute period the virus undergoes rapid replication within the CD4 cells; this leads to a rapid decline in patient CD4 count [12]. The risk of viral transmission is higher during this acute phase, as viraemia is at its peak. After the rapid replication period, viral replication becomes stable (known as a viral set point). This stability results in an increase in patient CD4 count, however the patients CD4 count will still remain lower than before they contracted the virus [18].

The second phase of HIV infection is the asymptomatic phase. It is during this stage that the virus undergoes low levels of replication and patients will have no symptoms and feel generally well. Their CD4 counts will be at healthy levels and viral load will be undetectable. This phase can last up to 8 years, creating the problem of further viral spread throughout the general population [19].

Later on during this second phase the CD4 count of patients will begin to decline as viral load steadily increases; it is at this point that patients are usually diagnosed with HIV. The final phase is the development of AIDS [14]. AIDS can be prevented by the regular use of an antiretroviral regimen. AIDS is defined as a CD4 cell count that is below 200 cells/mm^3 (a healthy person has a CD4 cell count of between 500- 1600 cells/mm^3) [12]. When a patient develops AIDS they have an extremely weakened immune system and are vulnerable to opportunistic infections. Without treatment life expectancy of a patient with AIDS is three years, which shortens to one year if they develop an opportunistic infection [19].

1.2.3 How HIV replicates in the human body and the role of the immune cells

When outside the host system viruses are termed virions. They are very small (20-30nm) infective agents that cannot function without a host as they contain no metabolic systems of their own. Virions consist of a nucleic acid core that is encapsulated in a protein coat (capsid). The nucleic acid core and the capsid coat together are termed the nucleocapsid and are contained inside a lipoprotein envelope. The difference between other virions and that of HIV-1 is the presence of viral enzymes unique to HIV-1, such as reverse transcriptase (**Figure 1.1**). The HIV-1 virion contains the docking glycoprotein gp120 and the transmenbrane glycoprotein gp41 [20].

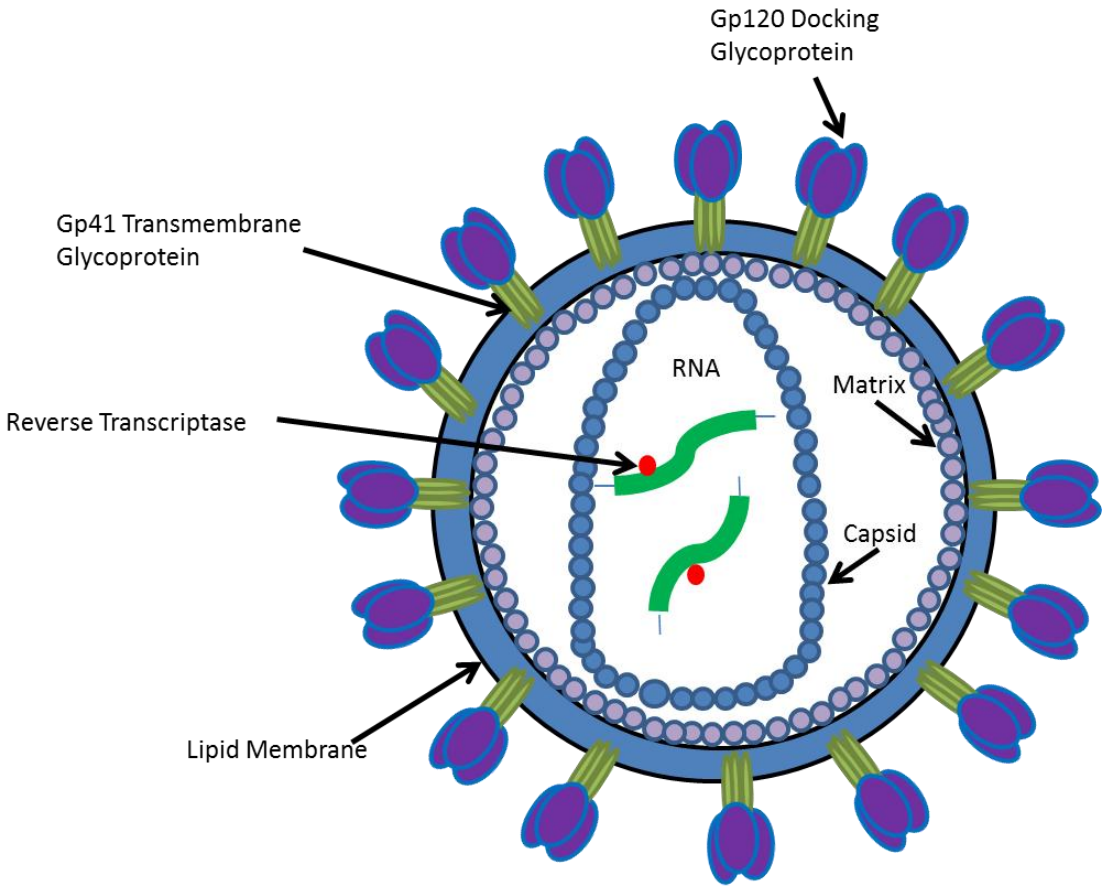

Figure 1.1: A schematic image of the contents of a HIV-1 virion

Once the HIV-1 virus enters the blood stream, its docking glycoprotein gp120 recognises $CD4^+$ cells and their co-receptors CCR5 or CXCR4 [21]. Once recognised, the HIV-1 virus will bind to the surface of the host $CD4^+$ T-cells via its gp120 glycoprotein [22-23]. The binding to the surface receptor activates other surface proteins and allows the virus to fuse to the outside of the cell (**Figure 1.2)** [24].

The first site of viral replication is within the lymph nodes closest to the site of viral entry (e.g. viral contraction through sharing of needles, the viral entry site will be the arm and the regional lymph node will be the draining lymph nodes) [25]. This primary replication site has only a few viral variants and is the point that modest viral amplification takes place [12]. Within this primary replication site the HIV-1 virus targets specific white blood cells (the

white blood cells that the HIV-1 virus infects are the $CD8^+$ T cells, macrophages and the $CD4^+$ cells (main target)) and ultimately leads to their destruction [26].

The main function of $CD8^+$ T cells is to directly kill virally-infected cells and to release cytokines that are antiviral (e.g. interferon-γ). Macrophages are involved in cellular phagocytosis either to engulf and destroy bacteria or to clean up cellular debris and dead cells. The main function of $CD4^+$ cells is to release cytokines (e.g. interleukin-2 / interleukin 4) and stimulate the B cells and natural killer cells (NKC) [25]. B cells are involved in the production of antibodies to fight off foreign bodies and NKC eliminate infected cells [25]. When HIV-1 infects these white blood cells it leads to the depletion of these cells and causes the immune system to become immunocompromised leading to a decreased defence against the disease or against other invading pathogens [12]. Thus HIV-1-infected patients are at risk of contracting opportunistic infections. Secondary replication takes place within the spleen, bone marrow and gastrointestinal tract due to migration of infected T lymphocytes [26].

Following binding the viral capsid is released into the host cell; the viral enzyme reverse transcriptase is released from the capsid and converts the two viral Ribonucleic acid (RNA) strands into double stranded Deoxyribonucleic acid (DNA) which can then be incorporated into the host genome allowing further viral replication (**Figure 1.2**) [24].

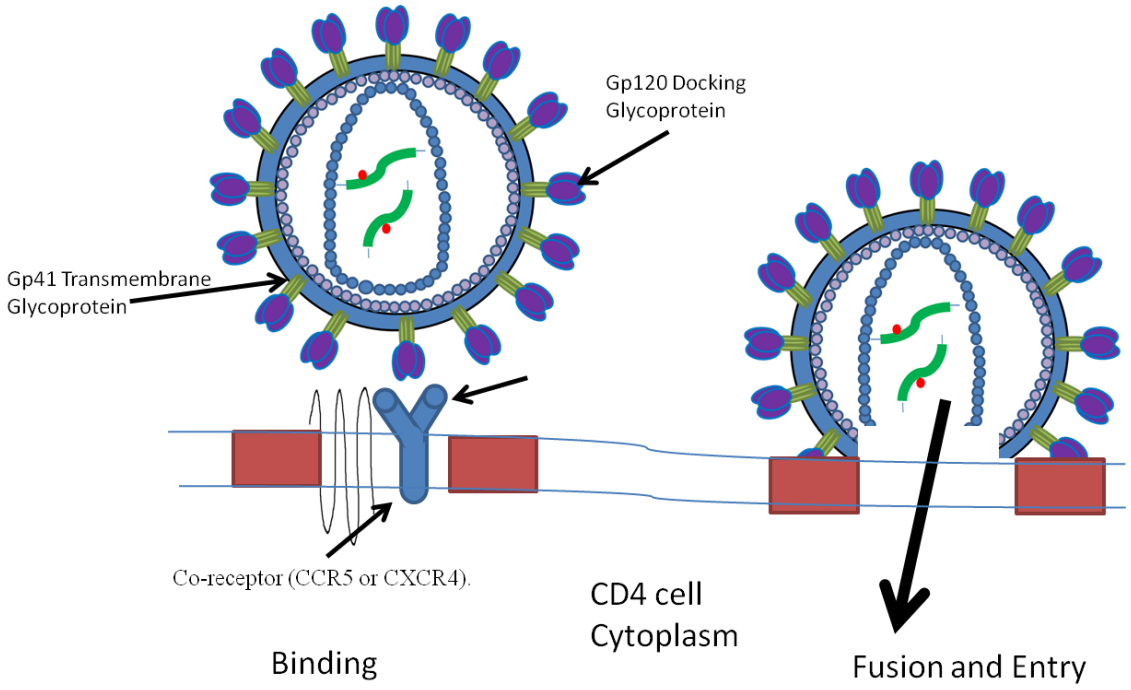

Figure 1.2: A schematic image showing HIV-1 binding to $CD4^+$ surface receptors

Once transcribed, the HIV-1 DNA locates to the host cell's nucleus. Another viral enzyme, integrase, is responsible for inserting the proviral DNA into the host's DNA [27-28]. This integration step also masks the viral DNA's location, making removal impossible. When the host cell replicates to produce new proteins, it will simultaneously produce new HIV-1 virions [27-28]. Upon integration, HIV-1 directs the cell to produce new proteins. The strands of viral DNA produced in the nucleus separate and undergo translation where a complementary strand of genetic material is produced [24]. The result of the translation step is many long protein strands which are then processed into smaller strands by the viral enzyme protease [29-30]. Some of these smaller proteins become structural parts of new HIV-1 virions and others become the vital viral enzymes [29-30]. Once the viral particles are assembled they bud off from the host cell to create a new virus. This new virus then undergoes maturation which involves viral protein processing [12, 31]. This processing is the cleavage of the gag-pol polyprotein via the viral enzyme protease [12, 31]. Maturation of the

virus enables the new virus to become infectious [29-30]. After all the stages of viral production are complete the newly matured virus can proceed to infect more cells [29-30].

1.2.4 Current HIV treatments

There are many different classes of drugs which act upon separate targets within the HIV cycle (**Figure 1.3**) currently approved for the treatment of HIV-1.

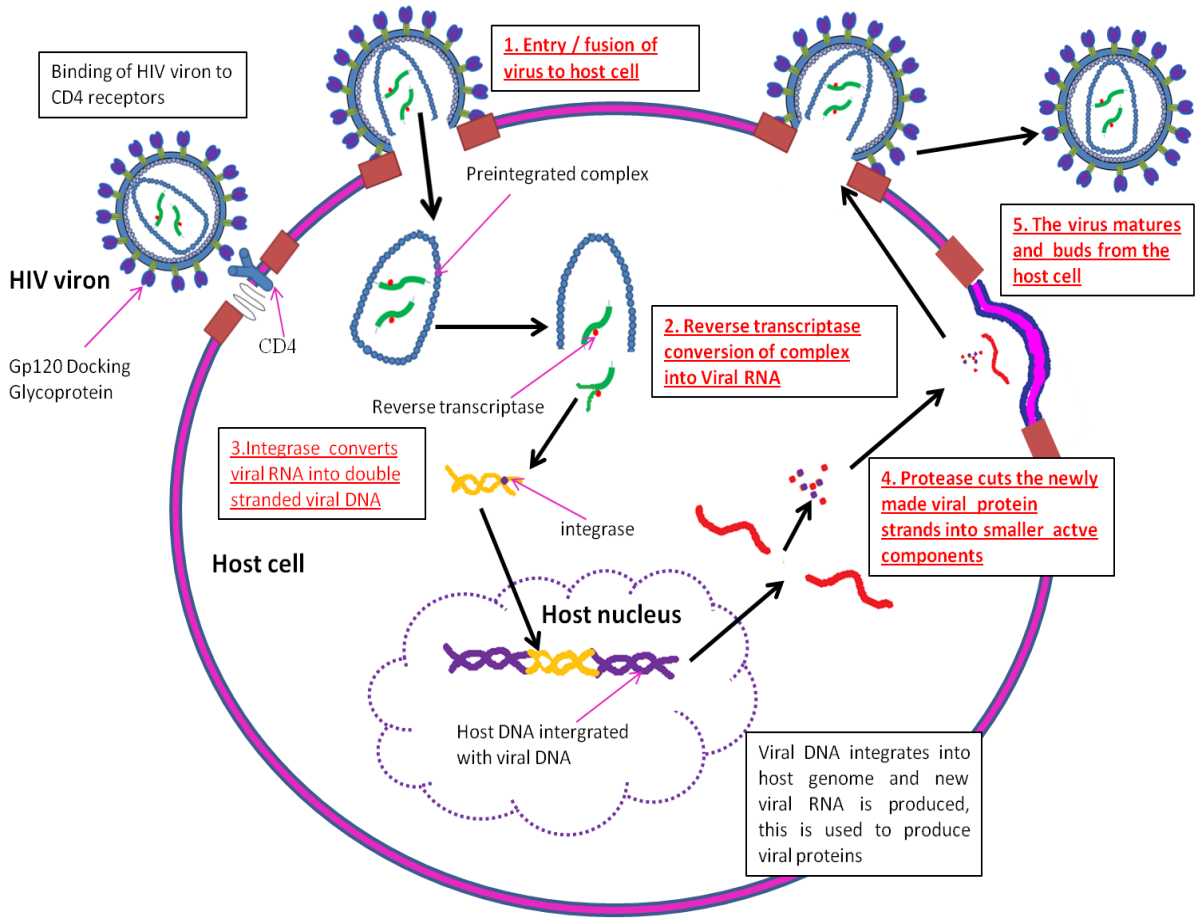

Figure 1.3: A schematic diagram showing the replication stages of HIV-1 and where current treatments target this process.

Entry/ fusion of HIV-1 can be prevented by the use of entry/ fusion inhibitors (act at labelled number 1 in **Figure 1.3**). This class of drugs interfere with the binding of the HIV-1

gp120 glycoprotein with the CD4 cell surface and therefore prevent fusion and entry into the host cell [32]. Examples include Pfizer's drug selzentry (generic name Maraviroc) which was first approved in august 2007 [33]. Selzentry works by binding to CCR5 and prevents interaction with HIV-1 gp120 glycoprotein therefore inhibiting HIV-1 from binding to CD4 surface [34]. Also Roche's drug fuzeon (generic name Enfuvirtide first approved in March 2007) which acts by inhibiting gp140 glycoprotein on the HIV virion's surface preventing binding and entry of HIV into the host's cell [33]. There are currently a few novel drugs in this class that are still in experimental stage of drug discovery [35]. They include Progenics drug PRO 140 which is a monoclonal antibody that blocks the action of CD4 cells co-receptor CCR5. In 2008 PRO 140 entered into phase 2 clinical trials and is still currently within this phase [36]. Also Tanox's drug TNX-355 which acts by targeting and binding to the CD4 protein on CD4 cells preventing HIV binding [35].

Reverse transcriptase inhibitors (RIs) (act at labelled number 2 in **Figure 1.3**). These drugs inhibit the action of the viral enzyme reverse transcriptase [37]. Reverse transcriptase is responsible for converting the two viral single RNA strands into double stranded viral DNA, so that it can then be incorporated into the host's genome [37]. Inhibiting this step means new HIV virions cannot be produced. There are two types of RIs and they are:

1) Nucleoside / nucleotide reverse transcriptase inhibitors (NRTIs) which act as analogues and mimic the naturally occurring deoxynucleotides which make up the viral DNA chain. NRTIs compete with the naturally occurring deoxynucleotides for incorporation into the viral DNA chain. Once incorporated, DNA synthesis is blocked as the NRTIs lack a 3' hydroxyl group that is essential for the formation of a 5' to 3' phosphodiester bond between the growing DNA chain and a new nucleotide base. This results in termination of DNA synthesis. As NRTIs compete with naturally occurring nucleotides they are known as competitive

substrate inhibitors [37]. All Food and Drug Administration (FDA) approved NRTI's are pro-drugs lacking the 3'hydroxyl group which forces chain termination in the viral RT enzyme [38]. Examples of NRTI's include Abacavir (ABC) which is a guanosine analogue produced by ViiV healthcare and Lamivudine (3TC) produced by GalxoSmithKline [33]. TFV is an example of a nucleotide reverse transcriptase inhibitor it is produced by Gilead and its trade name is Trvuda [33]. An example of a discontinued NRTI is Adefovir (ADEF) [33]. ADEF was manufactured by Gilead Sciences under the trade name of Preveon for the treatment of HIV. However, in 1999 its use for HIV treatment was not granted by the FDA and the development of this drug was discontinued due to its severe renal impairment [39]. ADEF was later granted FDA approval under the drug name Herpsera, when used at lower doses for the treatment of hepatitis B (Hep B) [39].

2) Non-nucleoside reverse transcriptase inhibitors (NNRTIs) have a different mechanism of action and are not incorporated into the HIV virus due to their structure. They bind at a different active site on the viral reverse transcriptase enzyme compared to the NRTIs [40]. NNRTIs do not compete with naturally occurring nucleotides for incorporation into DNA during DNA synthesis, instead they bind at their active site [40]. Binding of NNRTIs to the active site causes a conformational change to the structure of reverse transcriptase that limits the movement of protein domains needed to carry out DNA synthesis [40]. NNRTIs are classified as non-competitive inhibitors [38]. Examples of NNRTIs include Efavirenz (EFV) which is produced by the company Bristol-Myers Squibb under the trade name sustiva [33].

Despite NRTI's and NNRTI's being highly effective at inhibiting the actions of the viral reverse transcriptase and decreasing viral load, the problem patients encounter is resistance [41]. The viral reverse transcriptase enzyme can undergo mutations as it does not have any proof reading activity [42]. This is especially prominent whilst a patient is on NRTI/ NNRTI

treatments due to the selective pressure placed upon reverse transcriptase [42]. Patients who experience resistance whilst taking the antiretroviral drugs within the classes NRTI's, NNRTI's or PI, can benefit from using entry/ fusion inhibitors as they have a different mode of action and therefore a decreased chance of experiencing the same resistance problems [42].

Integrase inhibitors (II) (act at labelled number 3, **Figure 1.3**), act to inhibit the action of the viral enzyme integrase, therefore they prevent the incorporation of the viral genetic material into the host cells genome [43]. Examples include Raltegravir [3].

Protease inhibitors (PI's) are an alternative class of antiretroviral drugs (act at labelled number 4 in **Figure 1.3**) that target the viral protease enzyme. Protease is responsible for cutting up the newly made viral proteins. Without this step no new functional HIV virions can be produced, preventing the further spread of HIV [44]. It is currently recommended that this drug class is taken alongside at least two other HIV approved drugs in order to treat the HIV treatment effectively (e.g. 1 PI + 2 NRTI's is a usual combination) [44]. Examples of PIs include Genetech's invirase (generic name is Saquinavir) and Bristol-Myers Squibb's reyataz (generic name is Atazanavir) [33].

There is another class of drugs termed maturation inhibitors (MI) (act at point labelled 5 in **Figure 1.3**), which are currently in development. MIs act by inhibiting the final step in the gag processing. The inhibition of this step results in the production of non-infectious virions, which prevents further spread of the virus in the host's body [45]. At present there are no approved MIs, but there is a few that are in development such as Bevirimat [33]. This drug class would be useful for those patients who have experienced resistance to the other antiretroviral drugs [45].

The WHO recommends that patients be treated using the highly active antiretroviral therapy (HAART) approach [33]. This method was developed by the National Institute of Allergy and Infectious Diseases (NIAID) and involves using two or more classes of antiretrovirals at the same time in order to increase the CD4 count and to decrease the risk of the patient developing resistance [46]. HAART can be achieved by either giving the patient a single drug that contains more than one agent (a multidrug combination product) such as Truvada, which is a combination of Tenofovir and Emtricitabine. Alternatively, the patient can be given more than one drug to be taken alongside each other for example 2 NRTI's alongside a PI [46].

1.3 Tenofovir as a toxicological agent

1.3.1 Tenofovir current indications

Tenofovir (TFV) belongs to the NRTI class of drugs. It was approved for use against HIV by the FDA on October 28th 2001 and for use against hepatitis B on August 11th 2008. It is given to patients as tenofovir disoproxil fumarate (TDF) which is the pro-drug form of TFV, to increase its oral bio-availability (**Figure 1.4**) [47]. TDF is phosphorylated to form TFV inside cells via cellular enzymes [13].

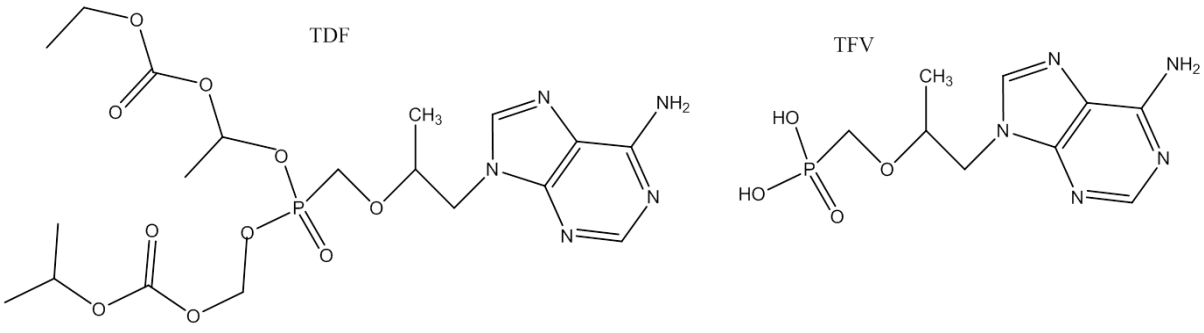

Figure 1.4: The structure of the pro-drug TDF and its active form TFV

TFV is currently indicated to treat both HIV and hepatitis B infections in patients (both treated with 300mg daily of Viread in adults). TFV is indicated to treat HIV in adults and

paediatric patients as young as two and to treat hepatitis B (Hep B) in adults and paediatric patients as young as 12 [48].

Hep B is an infectious inflammatory virus that affects the liver; it is epidemic in Asia and Africa and is endemic in China [49]. Hep B is spread in a similar way as HIV. Recent studies showed to be 180,000 people within the UK currently infected with Hep B [50]. Hep B can be treated with TFV, Viread and a low dose of Adefovir, Hepsera [49].

TFV is also currently used to prevent mother to baby transfer of HIV through the placenta [13]. Usually a typical regimen to prevent mother to baby transmission of HIV consists of TDF + 3TC + EFV [13].

TDF was the first of the NRTI class approved for the treatment of HIV [51]. It is widely used in many, if not all, HIV regimens due to its excellent properties, which include good potency, good tolerability and its convenience (one pill daily) [51]. TDF possesses good pharmacokinetic and pharmacodynamic properties, such as long serum (17 hours) and intracellular ($\geq$ 60 hours) half-lives, allowing a one daily dose regimen [1]. The convenience of TDF regimens being one pill daily via oral administration allows for better patient compliance [1]. This is essential for HIV patients as they must keep their plasma HIV RNA levels consistently low to prevent further viral growth [51]. TFV regimens can be administered as TDF alone (Viread) or TDF co formulated with either emtricitabin (Truvada) or emtricitabin and efavirenz (Atripla) [33].

TFV is not a substrate, inducer or inhibitor of human cytochrome P450 (CYP450) enzymes *in vitro* or *in vivo* and its oral bioavailability can be enhanced through its administration with a high-fat meal [51]. TFV can be used in both treatment-naive and treatment-experienced patients, as the pharmacokinetics is dose-proportional and similar in healthy volunteers and

HIV-infected individuals [1]. In patients with renal and/ or hepatic impairment TFV can still be used as long as TFV levels are monitored via plasma liquid chromatography [51].

Drug-drug interactions may result in increased or inadequate drug concentrations. If drug concentrations are increased, the risk of the patient developing adverse drug reactions (e.g. renal dysfunction) (ADRs) also increases [52]. If the drug levels become inadequate, in the case for HIV-1 patients, this leads to poor management of viral load. For this reason doctors and clinicians devote great attention to the potential drug-drug interactions of each antiretroviral [52]. This is essential as many HIV-1 patients take a HARRT regimen that usually involves the use of 2 NRTI's and one PI alongside each other.

The known drug-drug interactions associated with TFV treatment are similar to those with the NRTI diadanosine (ddI), the PI atazanavir (ATZ) and lopinavir (LPV) / ritonavir (RTV) [33]. When the coadministration of TFV with DDI takes place patients must be monitored for ddI associated ADRs (pancreatitis and neuropathy), as clinical monitoring has shown TFV to significantly increase the maximum concentration (Cmax) and the area under the curve (AUC) of ddI [53]. The mechanism of this interaction is unknown, however; research has demonstrated that the monophosphate and diphosphate forms of TFV are inhibitors of the purine nucleoside phophorylase enzyme, which is essential for ddI clearance and breakdown, thus increasing the circulating levels of ddI within patients [53]. Coadministration of TFV with ATV has shown to increase circulating TFV concentrations within patients [54]. The mechanism of this interaction is still unknown. Patients taking both drugs should be monitored for TFV associated ADRs, such as renal dysfunction and Fanconi syndrome [54]. LPV and RTV are taken in combination in a fixed dose regimen [55]. RTV is a known inhibitor of the CYP450 enzymes for this reason it is used as a PI booster as it increases circulating PI concentrations [55]. Studies have shown that coadministration of TFV with

LPV/ RTV increases circulating TFV concentrations [54-55], but the mechanisms of this interaction are unknown [55]. Patients who are taking TFV and LPV/ RTV should be monitored for TFV associated ADRs [55].

Coadministration of drugs that affect renal function alongside TFV, will affect circulating TFV concentrations as TFV is metabolised primarily via the kidneys [56]. Certain drugs (e.g. cyclovir, ganciclovir cidofovir, and valganciclovir), may reduce renal function or compete for active tubular secretion thus increasing serum concentrations of TFV and/or increase the concentrations of other drugs eliminated renally [56].

Although TFV has a relatively good safety profile, it has been linked to a number of renal dysfunctional problems especially when patients have been on TFV regimens long term which is usually the case for HIV patients [57].

1.3.2 Tenofovir pharmacodynamics

TFV can be taken as a once daily tablet for oral administration (300mg Viread). As TFV is polar and ionised, it has low oral bioavailability and so it must be administered as a pro-drug (TDF). TDF (**Figure 1.4**) was designed to mask the two main ionic regions of TFV to enhance its penetration thorough the gut wall and increase bioavailability [13]. Upon absorption into the intestinal wall, TDF is converted to a monoester by the carboxylesterase enzyme. This monoester is then converted into TFV upon first pass metabolism through the liver making TFV the main circulating species [13].

After first pass metabolism within the liver circulating TFV reaches the kidneys. TFV is excreted unchanged into the urine via a combination of glomerular filtration and proximal tubule secretion [58]. TFV enters the proximal tubule cells via active transport through the

basolateral membrane. This active transport is mediated by the human organic anion transporter's (hOAT) 1 and to a lesser extent 3 (hOAT-1, hOAT-3). OAT transporters are part of a superfamily that facilitates the transmenbrane transport of endogenous and exogenous compounds (**Figure 1.5)** [58].

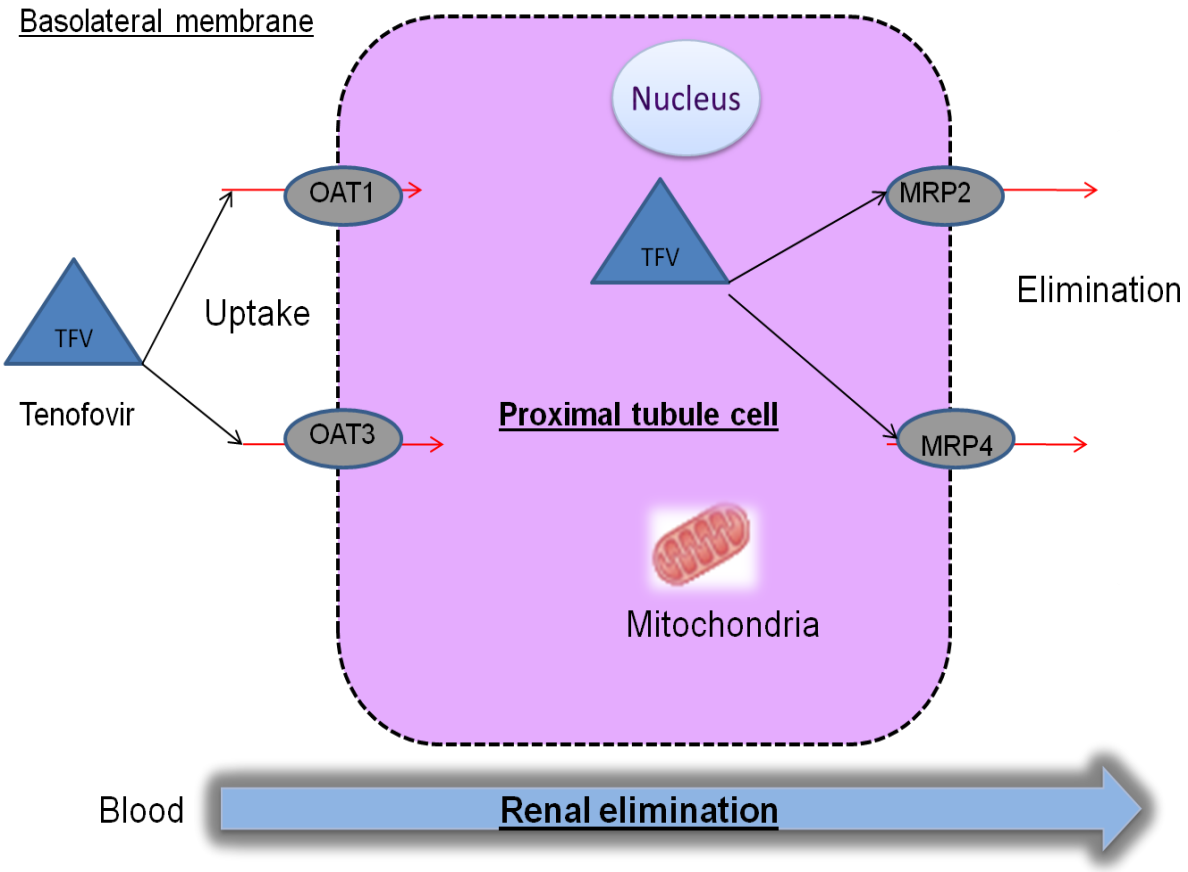

Figure 1.5 A schematic image of the uptake and elimination of TFV.

TFV is excreted from proximal tubule cells into the urine via the apical membrane multi drug resistant transporters 2 and 4 (MRP2, MRP4), which are highly expressed within the apical membranes of renal proximal tubule cells [58].

1.3.3 The anatomy of the kidneys

The kidneys are key organs that help to regulate volume, electrolyte content and pH of extracellular fluid. Several hundred litres of plasma enter the kidneys daily, 120 litres of this

plasma is filtered [59]. Water is filtered through the kidneys and 99% is reabsorbed along with reabsorbtion of most of the sodium ions. The average adult human kidneys produce 1.5 litres of urine in an average 24 hour period.

The kidney is made up of an outer cortex, an inner medulla and a hollow pelvis which empties into the urethra [59]. The main functional component of the kidneys is the nephrons. Each average adult kidney contains approximately $1.4x10^6$ nephrons (this number declines with age). Each of these nephrons are made up of 5 main sections including the glomerulus, proximal tubule, loop of Henle, distal convoluted tubule and the collecting ducts (**Figure 1.6**) [59].

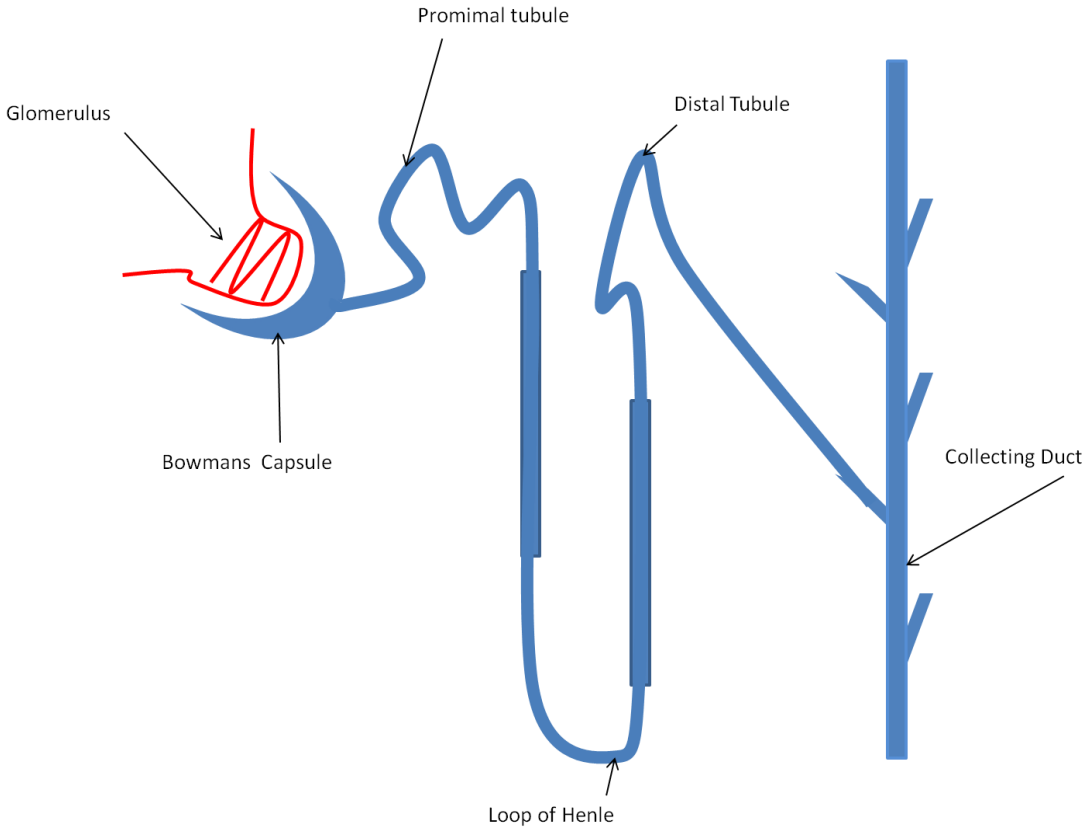

Figure 1.6 A schematic diagram of the anatomy of the kidneys

The glomerulus is made up of a bundle of blood capillaries that enter the renal tubule at the dilated end. Fluid enters the Bowmans capsule (**Figure 1.6**) through the capillaries under hydrodynamic pressure [59]. The first set of cells that the filtrate encounters are the proximal tubule cells. At this meeting point the filtrate is at its most concentrated, therefore these cells are at greater risk of toxicity caused by the components of the filtrate [59]. The proximal tubule cells are permeable to ions and water and permit passive flow in either direction. Around 60-70% of sodium reabsorption occurs in the proximal tubule cells [59]. Sodium ions enter the proximal tubule cells via sodium/ hydrogen exchange. The enzyme carbonic anhydrase is an intracellular enzyme and is essential for the production of hydrogen ions that are exchanged for sodium ions [59]. The main active transport of the proximal tubule cells happens via the sodium potassium ATPase pump (sodium pump). This pump is located in the basolateral membrane of the proximal tubules and is responsible for expelling the excess sodium ions that have built up inside the proximal tubule cells into the blood [59]. The excess bicarbonate that is produced intracellularly and exchanged for the sodium ions is broken down in the extracellular fluid by the carbonic anhydrase enzyme into water and carbon dioxide. This reaction occurs at the brush border of the proximal tubules [59]. As the proximal tubule cells are responsible for the active transport of many ions, they are highly abundant in mitochondria needed for the production of cellular ATP. This makes the proximal tubule cells more susceptible to mitochondrial toxicity induced by mitotoxins [60].

Upon leaving the proximal tubule the filtrate is only 30-40% of its original volume and passes to the loop of Henle (**Figure 1.6**), where further reabsorption of ions and water takes place [59]. After filtrate from the loop of Henle enters the distal tubule, further reabsorbtion of ions occurs, regulated via the hormones paratharmore and calcitrol [59]. The filtrate leaves the distal tubule and enters the collecting ducts via the collecting tubules [59]. Within this section movement of ions and water are controlled only by the hormones aldosterone

(reabsorption of sodium chloride) and the anti-diuretic hormone (reabsorption of water) [59]. The kidneys control the pH of the urine and favour an acidic pH to facilitate the removal of phosphoric/ sulphuric acids and sulphur containing amino acids from the diet [59]. After leaving the collecting ducts the filtrate leaves the kidneys as urine via the urethra [59].

1.3.4 Tenofovir induces toxicity via kidney injury

1.3.4.1 Tenofovir induces renal dysfunction

Current antiretroviral therapies that contain NRTI's are plagued with toxicity and RT resistance [61]. Although TFV is known to be less toxic than other nucleoside analogues such as adefovir and cidofovir it is still well reported as a nephrotoxin [58-61]. Specifically clinical cases of TFV induced renal toxicity include Fanconi's Syndrome, acute renal failure, nephrogenic diabetes insipides and chronic kidney disease (CKD) [58-61]

Initial pre-clinical trials and the post clinical studies reported that TFV is safe due to low incidence of renal impairment (1-3%), which was characterised by elevated serum creatinine clearance [58]. However recent case reports and data from cohort studies show a clear association between prolonged TFV use and the development of nephrotoxicity; this was recently reported as a 20% incidence rate within HIV-1 infected patients [58].

The first report of kidney disease induced via TFV use was published in 2002. The patient presented with normal baseline renal function, however further investigations confirmed that the patient had developed TFV induced Fanconi syndrome (Verhelst *et al*., 2002). Fanconi syndrome is a disease that affects the renal proximal tubules and leads to excessive loss of glucose, uric acid, phosphates, bicarbonate and amino acids within the urine. The onset of Fanconi syndrome can lead to further complications such as renal tubular acidosis due to loss

of bicarbonate ions and bone diseases e.g. rickets due to loss of phosphates. Since 2002, the onset of renal disease induced via TFV use has been reported both in numerous singular cases or cases within a small subset of patients. The symptoms that the patients presented with varied, some develop acute renal failure [63-73], whilst most patients had developed tubulopathy, occasionally with overt Fanconi syndrome [61,74-80]. The signs and symptoms associated with kidney tubulopathy (including glucosuria in cases when patients had normal serum glucose levels), include hypokalemia (with or without acute renal failure), phosphate wasting (with hypophosphateamia), acidosis and proteinuria (usually mild); these were among the most frequent renal dysfunctions in patients experiencing TFV induced nephrotoxicity. There was also a small subset of patients with nephrogenic diabetes insipidus [63, 81-82].

The risk factors for the development of TFV-induced nephrotoxicity include baseline renal dysfunction (this has also been linked to the age of a patient, as renal function declines as a person ages), low CD4 counts and low body weight [83, 84]. Patients are at higher risk if they have pre-existing systemic conditions or are taking a regimen that involves the use of potential nephrotoxins [70-71, 81, 85]. The antiretroviral medications that were associated with a higher onset of TFV-induced renal dysfunction were; LPV [63, 67-68, 70-71, 74-75, 78, 82, 86-87] or ddI [66, 76, 81]. A review of the cases reported to the FDA on the onset of TFV induced renal dysfunction within patients from 2001 through to 2006, showed that of those cases, 164 met the definition for Fanconi syndrome [88]. Of those 164 cases, 83% of the patients were coadministered TFV and a PI as part of their HIV-1 HAART regimen, 34% of these patients were also taking ddI [58].

Patient data that was obtained from patients not involved in clinical trials reported significant increase in the serum creatinine levels as well as a reduction in the estimated glomerular

filtration rate (eGFR) in patients on TFV compared to those taking other nucleoside regimens [89].

Kidney damage is usually seen in patients on TFV containing antiretroviral treatment after 6 months post treatment; however a recent study reported cases where renal dysfunction did not develop until 18 months after initiation of treatment and suggest that patients should be monitored for this period post initiation [77]. Renal dysfunction usually presents as acute renal failure with decreased glomerular function [61]. The renal damage is usually seen as tubular dysfunction which is specific to the proximal tubules and has an incidence rate of 20% within HIV-1 infected patients who may already be renally compromised due to the HIV-1 infection [58].

Although data from clinical trials suggest that TFV toxicity affects 2% of the population this may be an under estimation due to the use of only healthy volunteers vs. the target population [90], who are immunocompromised. Therefore the patient cohort data that shows a 20% incidence rate of TFV associated renal dysfunction may provide a more reliable figure [58].

1.3.4.2 Tenofovir induced chronic kidney disease

Upon discontinuation of TFV treatment the acute kidney damage is shown to reverse in cohort studies. However, once the kidney damage has developed into chronic kidney disease (CKD) the effects of TFV induced renal toxicity cannot be reversed. Therefore, it is important to detect damage earlier in TFV treatment in order to prevent long lasting renal dysfunction [58]. As a gold standard, the clinical marker of kidney function is serum creatinine that is determined via the estimated Glomerular Filtration Rate (eGFR). When a person has an eGFR of 90 ml /min/ 1.73^2 or above is considered normal. A patient is

diagnosed with CKD if their eGFR falls below 60 ml /min/ 1.73^2 for a period longer than 3 months [91].

Patients with CKD are at increased risk of suffering a stroke or of having a heart attack. A decline in eGFR to 30-59 ml /min/ 1.73^2 is considered as moderate CKD [91]. At this stage hormones and mineral levels within patients become unbalanced; this can lead to anaemia and weakened bones [91]. Sever reduction in eGFR is classified as an eGFR in the range 15-29 ml /min/ 1.73^2 [91]. At this stage the kidneys are damaged and patients must undergo invasive treatment including haemodialysis, peritoneal dialysis and in some cases patients undergo kidney transplant (a healthy kidney donated from a family member or a matched donor) [91]. Kidney failure will occur when patient's eGFR is below 15 ml /min/ 1.73^2; it is at this point that a patient will need to undergo either dialysis or a transplant to sustain life. CKD is irreversible and cannot be cured, but if identified early stages patients will be able to maintain kidney function if the perpetrator of the kidney damage is inhibited [91]. Upon discontinuation of TFV in patients on TFV, kidney function will remain at a steady stage; CKD effects will not be reversed, but further damage will be prevented [58-61]. This is why early identification if TFV induced renal damage is essential; development of a new biomarker is needed [58].

1.3.5 Mechanisms of Tenofovir induced renal toxicity

As TFV has only been approved as a HIV drug since late October 2001 the current *in vitro* and *in vivo* experiments to determine TFV's mechanistic pathways and associated toxicities are not well established. A summary of the main *in vitro* and *in vivo* experiments used to study TFV-induced toxicity can be seen in **Table 1.1**. This table highlights that there needs to be further investigations into the molecular pathways of TFV *in vitro* and *in vivo* to elucidate its toxicological pathways.

Table 1.1: Summary of the *in vitro* and *in vivo* research into TFV

Authors	Drugs being tested	*ex vitro /in vivo* model/s used	Experimental Aims	Results
Birkus *et al*., 2001	TFV toxicity vs. other NRTI's	HepG2 cells, skeletal muscle cells and proximal tubule epithelial cells	3 weeks treatment with concentrations from 3 - 300 µM of NRTI drugs. The mtDNA levels and COX II / COX IV mRNA levels were assessed and lactate levels were determined.	TFV did not induce any significant effects on mtDNA levels in all cell types. TFV did not affect COX II or COX IV . Lactate production was decreased by < 20% at 300 µM TFV. No toxicities were associated with TFV dosing.
Cihlar *et al* .,2001	TFV in comparison to other NRTI's (ZDV, ddC, ddI, d4T, abacavir (ABC) and 3TC)	HepG2 cells, skeletal muscle cells, erythroid progenitor cells, renal proximal tubule epithelial cells and myeloid cell lineage	to examine the cytotoxic effects of TFV in comparison to other NRTI's	TFV inhibited proliferation of HepG2 cells and normal skeletal muscle cells with CC50 values of 398 and 870 µM. This > CC50 values for the other NRTI's. TFV was less cytotoxic within erythroid progenitor cells than ZDV, d4T, and ddC. the inhibitory activity of NRTIs in myeloid cell lineage, was (highest severity to lowest) ddC>ZZDV>D4t>TFV>3TC. TFV showed weaker effects on proliferation and viability of renal proximal tubule epithelial cells than cidofovir
Rompay et al., 2004	TFV	rhesus macaque in vivo and using isolated rhesus macaque PBMC cells	determining affect of TFV on interleukin-12 (IL-12) expression	TFV caused a small increase in vivo and in vitro of IL-12. IL-12 has been shown to mediate anti-apoptotic responses
Ray *et al*., 2006	TFV	CaCO transfected with human MRP2 and MDCKII	to determine which transporters are responsible for TFV uptake and efflux	OAT1 / 3 are responsible for TFV uptake and MRP4 is responsible for TFV efflux. It was found that TFV was not a substrate for MRP2
Vidal *et al*., 2006	TFV alone and in combination with AZT (zidovudine), ddI, RTV and LPV	renal proximal tubule epithelial cells	cytotoxicity was determined after a 22 day period, mtDNA levels and cytochrome oxidase II (COX II) mRNA levels were assessed	TFV alone and in combination showed no associations with toxicity therefore taking TFV in combinations will not increase toxicity
Tong *et al*., 2007	TFV + PIs (DRV/RTV, LPV/RTV, ATV/RTV)	human ovarian carcinoma cell line (CaCo-2) and Mandin-Derby canine kidney cell line (MDCKII)	To determine the effect of PIs on TFV intestinal absorption	It was demonstrated that TFV permeabilisation was decreased due to ester cleavage, this is possible reason for increased circulating TFV when coadministered with PI'S
Venhoff *et al*., 2007	TFV alone and in combination with FTC, ABC	HepG2 cells	evaluation of the mitochondrial toxicity of the drugs via assessment of cell growth, lactate production, intracellular lipids, mtDNA and COX II / COX IV	TFV showed no or minimal toxicity . FTC + TFV slightly reduced proliferation without affecting mitochondrial parameters. TFV attenuated ddI related cytotoxicity but worsened the cytotoxic effects of CBV and AZT
Cihlar *et al* .,2007	TFV and ADEF	Isolated human proximal tubule cells	to determine if transporter expression of hOAT -1 is responsible for TFV / ADEF induced nephrotoxicity	There was no associated TFV cytotoxicity within the proximal tubule cells. TFV was transported via hOAT1

Cihlar *et al* .,2007	TFV + PIs (DRV/RTV, LPV/RTV, ATV/RTV)	Isolated human proximal tubule cells	to determine how PI affects TFV transport (human OAT 1 / 3 and MRP4 assessed)	The PI's did not affect cytotoxicity of TFV. It was shown that PI's caused < 20 % inhibition of TFV transport via the hOAT1. hOAT3 saw a 62% decline in TFV transport with RTV and a 37 % decline with LPV. Outcome: low potential of PI's to interfere with active secretion of TFV
Bousquet *et al*., 2008	TFV + EFV + FTC (emtricitabine)	peripheral blood mononuclear cells (PBMC)- obtained from healthy volunteers	transporter expression in response to drugs (p-glycoprotein and MRP 1-6)	TFV significantly reduced MRP1, MRP5 and MRP6 MRNA expression

The conclusion from previous work [92-100], is that TFV causes nephrotoxicity due to its accumulation within the proximal tubules. The exact molecular mechanisms of TFV toxicity are not fully understood however there are two main hypotheses.

1.3.5.1 Tenofovir toxicity is linked to cellular transporters

The first hypothesis is an increase in the activity of OAT 1/3 transporters, or a decrease in the activity of the MRP2/4 transporters will lead to increased accumulation of TFV in the proximal tubules [101]. (**Figure 1.7)**

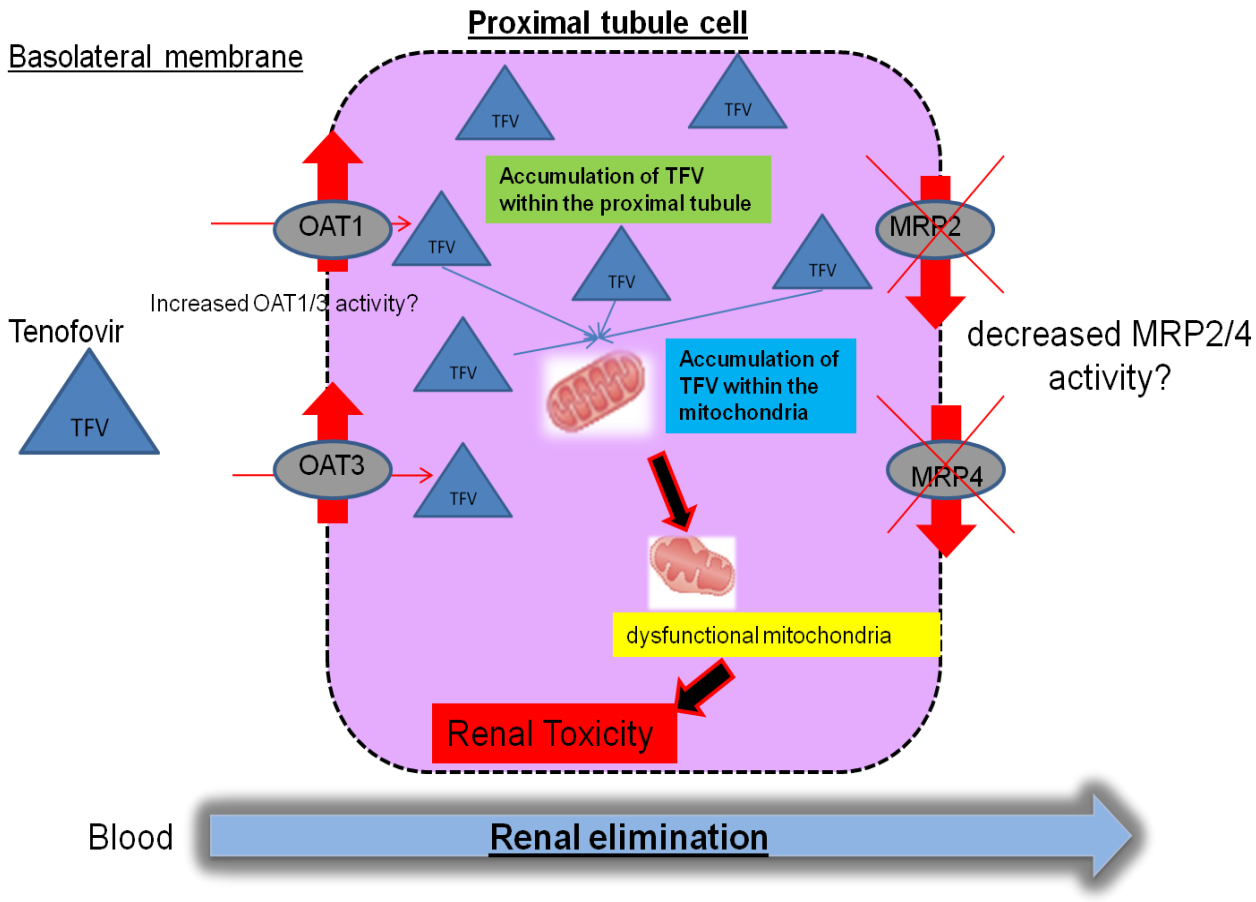

Figure 1.7 A schematic diagram of renal dysfunction induced by TFV when the transport of TFV is changed

This increased accumulation of TFV leads to greater exposure of the mitochondria to TFV and increases any mitochondrial toxicity that TFV may induce (**Figure 1.7**). This hypothesis states that a person's pharmacogenetics could predispose them to TFV induced renal dysfunction. For example an increased expression of OAT1 within an individual will lead to increased TFV accumulation within the proximal tubules, therefore increasing their risk of developing TFV induced proximal tubule toxicity [53].

Transporter levels may also alter due to taking multi-drug therapies such as the HIV regimens [53]. These therapies can lead to a change in the activity of the transporters key to TFV uptake and/ or elimination. An example is a patient taking TFV alongside a protease inhibitor

(e.g. ritonavir), ritonavir is eliminated from proximal tubule cells via the MRP2 transporters. This will lead to increased circulating TFV concentrations as both drugs compete for the same MRP2 transporter [53].

In vivo studies have utilised MRP4 -/- knockout (KO) mice to study TFV. It was reported that the KO mice became more susceptible to TFV induced nephrotoxicity. This was reportedly due to a decreased elimination of TFV into the urine. This supports the hypothesis that patients may have polymorphisms in specific transporter genes which may lead to up/ down regulation of transporters responsible for TFV influx and efflux, making some patients more susceptible to TFV induced toxicity [60]. It has also been suggested in the literature that TFV itself can cause the up/down regulation of these key transporter's leading to increased accumulation of TFV within the proximal tubule cells and a higher incidence of renal dysfunction [60].

Other studies showed that there are differences in the activity or expression in genes coding for the key transporters involved in TFV efflux according to race [13]. Studies showed single nucleotide polymorphisms (SNPs) in the MRP2 genes (c-24T and G1249A) and MRP4 genes (A3463G and T4131G) have been shown to be linked to differences in expression due to race [13].

Smaller cohort studies have shown associations between gender (males have a higher metabolic rate than females, this may lead to an increased rate of TFV accumulation), or race (different races have variations in the expression of transporters needed for TFV influx and efflux), of patients and the increased risk factors for TFV induced renal toxicity [102]. Studies have shown females to have a higher incidence rate of developing renal dysfunction when taking TFV regimens [102]. These findings may be essential for developing relevant PrEP treatments for different patient populations [103].

1.3.5.1 Tenofovir toxicity is linked to mitochondrial damage

The second hypothesis is based on the interaction of TFV with mitochondria. Once TFV is transported into the proximal tubule cells they gain access to the mitochondria which are present in abundance in these cells to help facilitate active transport. It is hypothesised that TFV can non-specifically inhibit mitochondrial DNA (mtDNA) polymerase γ, causing mitochondrial dysfunction [38, 93]. This hypothesis is based on the known mechanistic pathway of ADEF-induced proximal tubule dysfunction [38, 93]. Mitochondrial dysfunction can lead to anaerobic respiration, oxidative damage, lactic acid production and renal damage leading eventually to CKD. MtDNA damage may lead to the disruption of the electron transport chain which is essential for cellular energy production. This damage and disruption of mitochondrial function may also cause the activation of apoptosis via the many intrinsic cell death pathways that mitochondria are essential for [93]. NRTI's can inhibit mtDNA in a similar fashion as how they inhibit the viral reverse transcriptase.

Pre-clinical trials, *in vitro* studies and enzymatic assays of TFV toxicity have demonstrated that TFV is not as effective in inhibiting mtDNA pol γ as other NRTI's [13]. However, recent clinical data has linked TFV to mitochondrial toxicity which was observed as a decrease in the reabsorbtion of glucose, uric acid, phosphates or amino acids. These data also reported TFV effects on bone density [53, 58, 62]. Patients on long term TFV treatment have presented with significantly reduced bone density, which could be due to the alteration in phosphate metabolism within the proximal tubule cells caused via mitochondrial dysfunction. This impacts on bone mineral density [94].

Many *in vitro* and *in vivo* studies support the hypothesis that NRTI exposure leads to mitochondrial impairment [46, 53, 58, 62, 104]. Studies have demonstrated that NRTI's, such as ADEF, induce renal toxicity primarily by mitochondrial toxicity via the inhibitation of

mitochondrial pol γ [53, 58, 93]. As ADEF and TFV have similar structures with only the addition of a methyl group on TFV compared to ADEF (**Figure 1.8**), the adverse affects of ADEF and the other NRTI's may be mechanistically shared by TFV. Therefore the effect of TFV on cellular mitochondria needs to be investigated within an adequate cell model.

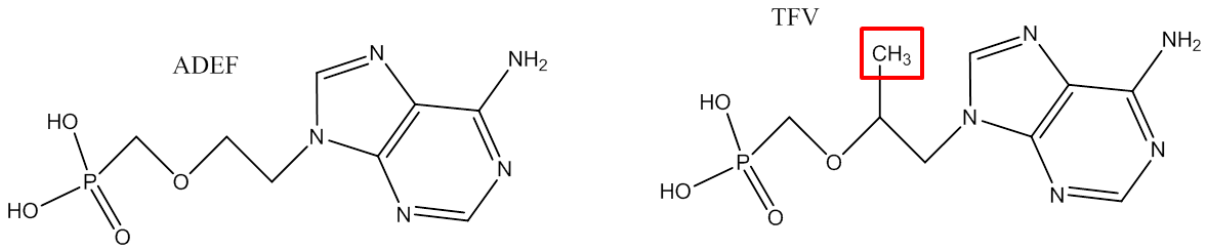

Figure 1.8: The structure of ADEF and TFV (only an additional methyl group compared to ADEF)

1.4 Thesis Aims

TFV is the backbone of most HIV regimens due to its good pharmacodynamic and pharmacokinetic properties [1]. Many pre-clinical studies showed that TFV was a safe drug in comparison to previous HIV-1 treatments; however recent data from cohort studies have reported a significant number of patients that develop TFV induced renal dysfunction [46, 53, 58, 62, 104]. For this reason it was the aim of this Ph.D. to elucidate the mechanistic pathway of TFV induced toxicity in order to develop safer HIV treatments in future, either via the identification of potential biomarkers to monitor TFV induced renal dysfunction, or by identifying those patients who are more susceptible to TFV induced renal dysfunction.

The cytotoxicity induced by TFV will be investigated by developing *in vitro* models with which to probe the mechanistic pathway and to understand TFV induced cytotoxicity. Within these *in vitro* models the mechanisms of cell death induced by TFV will be elucidated via the assessment of apoptosis, and necrosis determined by different markers including caspase activity, mitochondrial membrane depolarisation, reactive oxygen species (ROS) production and DNA content. Finally the possible use of kidney injury molecule-1 as a biomarker for TFV induced proximal tubule dysfunction will be assessed using the urine from a cohort of HIV-1 patient.

Chapter Two

GENERATION AND VALIDATION OF METABOLICALLY MODIFIED CELL LINES TO PROBE MITOCHONDRIAL TOXICITY

Contents

1.1 Introduction

In this chapter the methodology and results from the work to generate and validate metabolically modified cell lines will be presented. These studies were essential in order to generate an *in vitro* model that could be used as a mechanistic tool for the elucidation of TFV induced cytotoxicity. Previous work has shown that TFV does not cause any cellular injury during *in vitro* studies [1-4].

Clinical toxicity caused by therapeutic drugs is referred to as an adverse drug reaction (ADR) [5]. ADRs are a major health problem worldwide; there are two main types of ADRs which are called on target and off target responses. On target ADRs are always predictable from the known pharmacology of the drug and are dose-dependent. Off target ADRs are also referred to as idiosyncratic or immune-mediated responses. These idiosyncratic responses are not predictable from the known pharmacology of the drug and the mechanisms behind them are not understood [5]. In order to predict these ADRs both during drug development in order to prevent toxicity before the drug is licensed, and to monitor ADRs after drug licensing via the use of biomarkers, the mechanistic pathways of toxicity must be elucidated and understood [5].

TFV toxicity is usually a time-delayed event clinically, that accumulates when a patient is on TFV long term [6]. This delayed accumulative toxicity means previous attempts at studying TFV toxicity *in vitro* have not been successful as discussed in **Chapter 1** [1-4]. Therefore, careful consideration had to be taken in order to define the most relevant cell model for the study of TFV-induced cytotoxicity. As previously discussed in **Chapter 1**, the use of NRTIs including TFV, have been associated with the induction of mitochondrial dysfunction. Human cells rely heavily on mitochondria for their energy production, however the *in vitro* models previously used to study TFV cytotoxicity were immortalised cell lines, which

produce their energy mainly via glycolysis. To elucidate the effect of TFV on mitochondrial function and viability, cell lines would need to be modified to produce a cellular system that closely represents the aerobic conditions of human cells.

The most ideal cell model would have been to use primary human proximal tubule cells as these are the target cell of TFV-induced toxicity clinically [7]. Primary cells have the advantage that they are not glycolytic and are abundant in mitochondria, therefore are a better representation phenotypically to *in vivo* cells. However, practically the use of primary cells has distinct disadvantages. The main disadvantage is the problem of isolation of the primary cells which can be technically challenging and can lead to contamination of the cells with other cell types thus altering the results gained. Another problem with using primary cell lines is their survival rate which is short (2- 4 passages), making long term study difficult; the use of these cells is limited as their phenotype begins to change the longer they are left in culture, which may make results unreliable. When using primary cells they have to be replaced after a maximum of 4 passages making their usage expensive. The kidney biopsy used to obtain these cells is a high risk procedure as the kidney is highly vascular; also there will be patient variation in the health of their mitochondria. All these disadvantages mean that for *in vitro* studies, primary cell lines whilst representing more closely the patient cellular conditions, are rarely used [8]. As the study of TFV induced cytotoxicity was to be studied, primary cells would not have a viable option due to the time delayed toxicity that has been associated with TFV use clinically [9]. Therefore we considered other in vitro options that will have a high survival rate, allowing longer culturing, whilst still retaining enough resemblance phenotypically to human proximal tubule cells in order to gain reliable results.

1.1.1 The importance of the mitochondria for cellular energy production

The mitochondria are considered the powerhouse of the cell. The mitochondria are essential for many functions within the cell; the main functions being the production of energy in the form of adenosine triphosphate (ATP) via mitochondrial oxidative phosphorylation (OXPHOS) [10]

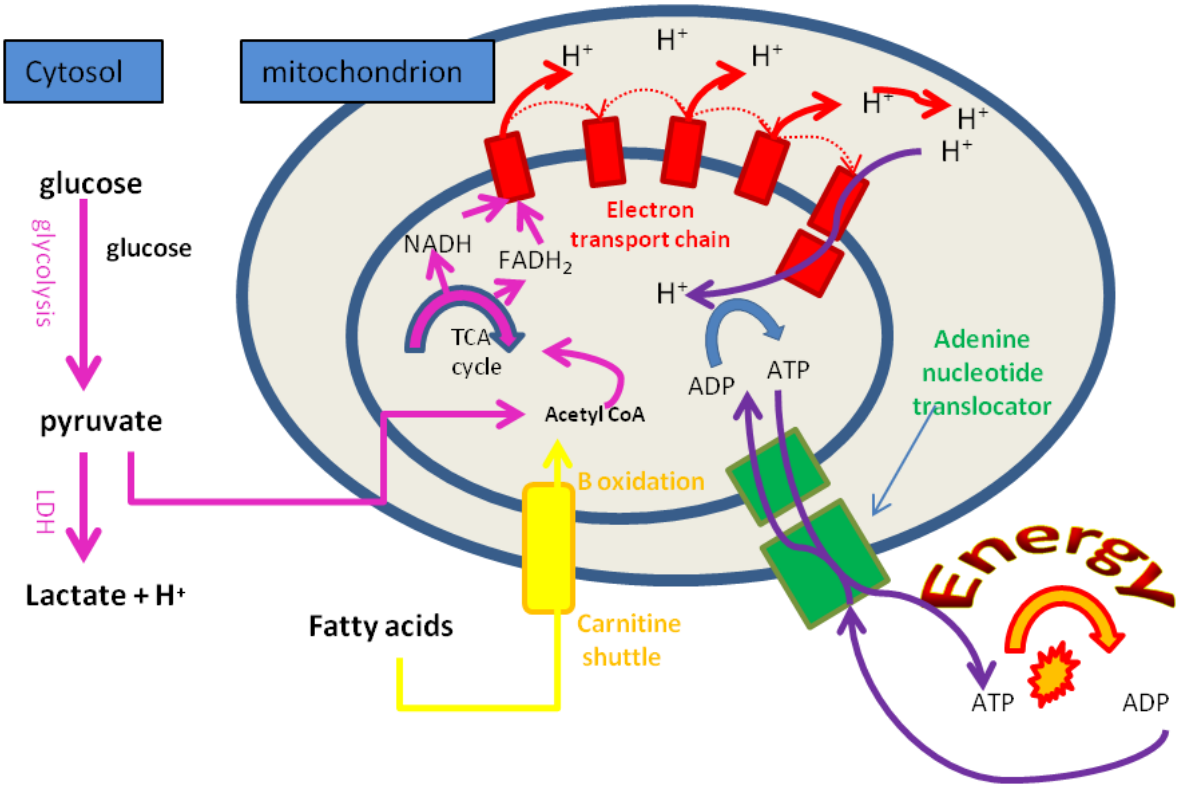

Figure 2.1: A schematic diagram of the production of ATP via the mitochondrial OXPHOS pathway (modified from a picture in White *et al*., 2010)

The mitochondrial respiratory chain (**Figure 2.1)** is responsible for catalysing the transfer of electrons from reduction donors (NADH and $FADH_2$) to molecular oxygen (O_2), producing water (H_2O). Acetyl CoA which is generated either by glycolysis (in the cytosol) or by the oxidation of fatty acids (inside the mitochondria), is passed through the tricarboxylic acid cycle. This cycle leads to the generation of the reduction donors NADH and $FADH_2$ which are essential for the electron transport chain (ETC). There is a large redox potential difference

between the electron donors and the final electron acceptor within the ETC. The electron flow along the respiratory chain is accompanied by a decrease in the Gibbs potential (which results in the release of free energy). This energy is used to pump protons across the inner mitochondrial membrane. This leads to production of an electrochemical gradient, allowing protons to return to the mitochondria via specific channels. As the protons pass through these channels the synthesis of ATP is catalysed. ATP is then exchanged for cytosolic ADP via the ADP/ATP translocator. Another key function of the mitochondria is their involvement in the intrinsic apoptotic pathway (discussed in detail in **Chapter 4**), showing mitochondria are essential regulators of cellular survival [10]

Tumour-derived immortalised cell lines have become the most widely used type of cellular systems used for *in vitro* work. These cell lines have the advantage of rapid growth and long survival periods under culture conditions. However, they produce their energy mainly via glycolysis instead of mitochondrial oxidative phosphorylation (OXPHOS); this is known as the Crabtree effect [8]. Immortalised cell lines derive their energy in this way despite the fact that they contain fully functional mitochondria. It has been shown that this Crabtree effect is due to the allosteric modulation of glycolytic enzymes [8], and the binding of the enzyme hexosekinosine to the mitochondrial porin [11]. As these immortalised cell lines generate their energy mainly via glycolysis, they are not reliant on mitochondria for ATP production. Therefore, in these cell lines mitochondrial toxicity is virtually non-existent, due to the fact that mitochondrial toxins have little or no effect on cell viability or cell growth [8].

Studies have shown that when HepG2 cells are grown in glucose-free media supplemented with galactose, the glycolysis pathway becomes inhibited. Therefore, cells become more reliant on mitochondrial OXPHOS, thus making them more susceptible to mitochondrial toxins [8]. This study showed that when HepG2 wild type (HepG2 WT) cells are incubated

with the classical mitochondrial toxin rotenone, no cytotoxicity is seen, however when the HepG2 cells were grown in galactose media cytotoxicity induced by rotenone was clear showing that rotenone is causing mitochondrial specific toxicity [8]. These galactose grown cells more closely represent human cells, as human cells use 95 % OXPHOS to generate cellular ATP [12]. Other studies showed that when grown in galactose media HepG2 cells increase their respiration rate to maintain the cellular ATP levels, this is known as the Warburg effect as can be seen in **Figure 2.2** below [13].

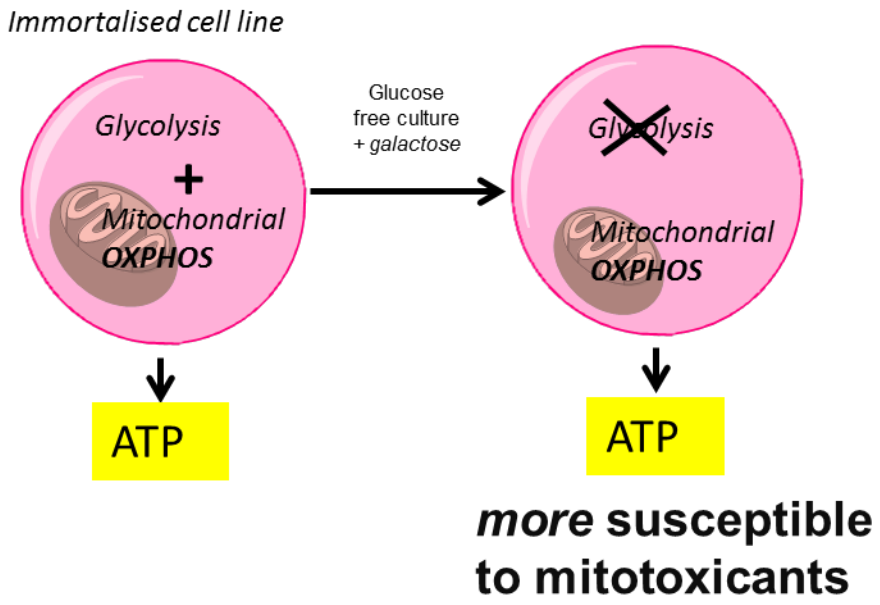

Figure 2.1 A schematic diagram showing how growing cells in galactose media makes them more susceptible to mitochondrial toxins

2.1.2 Aims of Chapter

The aim of this chapter was to aerobically modify cell lines in order to elucidate the effect of TFV on cellular mitochondria. The cell lines that were chosen for generation and validation were HepG2 cells (a human hepatic cell line) and HEK293 (a human renal cell line). The HepG2 cells were chosen as they had previously been grown in galactose media; results showed they became susceptible to mitochondrial toxicity induced by rotenone these cells were used alongside HEK293 cells that have not been aerobically modified before. The HEK293 cells used were transfected with human kidney injury molecule-1 (KIM-1) so that further studies into using KIM-1 as a possible biomarker for TFV induced proximal tubule dysfunction could be carried out (**Chapter 5**). All work carried out in the HEK293 KIM-1 cells was also carried out within HEK293 PcDNA cells which are HEK293 cells transfected with an empty vector so that any effects of the transfection could be identified. The progression of this metabolic switch was monitored using rotenone, a classical mitotoxin. Rotenone is used in solution as a pesticide and is known to cause mitochondrial toxicity via a specific inhibition of Complex I (NADH –dehydrogenase, inhibiting this enzyme inhibits mitochondrial respiration) [14]. Rotenone toxicity is observed when glycolysis pathways are inhibited, thus cells must rely on mitochondrial OXPHOS [8]. The following states the aims of this chapter:

1) In order to validate when the glucose grown cells were dependent solely on the mitochondrial OXPHOS pathway, 24 hr rotenone MTT assays were carried out at each passage point until the point when rotenone cytotoxicity was prominent after only 24hrs [8].

2) In order to verify the use of the cells in a TFV study, the presence of transporters needed for TFV accumulation were examined. The levels of the transporters MRP2, MRP4, MRP7, OAT1 and OAT3 were determined within both cells lines when grown in glucose and galactose, via PCR methods.
3) Finally the accumulation of TFV within the HepG2 cells grown in glucose (HepG2 WT) and galactose (HepG2 galactose) was determined using radiolabelled TFV to determine the profile of TFV accumulation in these cells.

2.2 Materials and Methods

2.2.1 Materials

Basal culture media (DMEM high glucose and DMEM no glucose) were ordered from life technologies, Invitrogen (Paisley, UK) Hanks balanced salt solution (HBSS), 3-(4,5-Dimethylthiazol-2-yl)-2,5-diphenyltrazolium bromide (MTT), Sodium dodecyl sulfate (SDS), N-(2-Hydroxyethyl)piperazine-N′-(2-ethanesulfonic acid) (HEPES), sodium pyruvate, trypan blue (0.4%) solution, dimethylsulphoxide (DMSO), ethanol, acetic acid, Neutral Red, Adefovir, Lamivudine**,** n-dimethylformamide (DMF), chloroform, isopropanol, nuclease free water, Foetal bovine serum (FBS) and D-(+)-Galactose were all purchased from Sigma (Poole, UK). Primers and probes, master mix, and kit containing all components of the PCR reaction mix were purchased from Applied Biosystems, (Warrington, UK). Tenofovir was ordered from Toronto Research Chemicals **(**Toronto, Canada)

2.2.2 Cell Culture and Experimental Preparation

HepG2 and HEK293 cell lines were maintained in either DMEM high glucose or DMEM no glucose. Under both conditions, the media was supplemented with 10% v/v FBS, 1% v/v sodium pyruvate and 5 % v/v HEPES. To the cells grown in DMEM no glucose, galactose was added to a final concentration of 10 mM. Once cells were confluent, 1 x 10^6 cells were then seeded in 30 ml of freshly supplemented media in a new 75 cm^2 flask. The cells were incubated in a humidified incubator with 5% CO_2 and were maintained at of 37^oC.

The viability of the cells was based upon a trypan blue exclusion from the cells that was carried out using haemocytometer and a light microscope (x 10; Axioskop, Welwyn Garden City, UK). 20µl of trypan blue 4% solution was added to a 100µl aliquot of cells, this was then counted. Cell viability was above 95% for all experiments carried out. During

experiments cells were exposed to drug stock solutions which were made up in DMSO the final concentration of the DMSO was below 1 % v/v in each incubation. Experimental conditions were carried out in quadruplicate on at least 3 separate occasions.

2.2.3 The assessment of cytotoxicity using MTT assays

The MTT assay is a colorimetric assay that is based upon the reduction of the soluble tetrazolium MTT dye to its insoluble formazan salt via the dehydrogenase enzymes found within viable cells [15]. This assay produces a colour change from the original yellow MTT to purple when incubated with viable cells. The quantity of formazan present is directly proportional to cell viability [15],

All cell lines were plated at a density 0.4 x 10^6 cells/ml. Cells were plated, in triplicate, in flat-bottom 96-well plates and were exposed to a range from 0 µM to 100 µM of each compound for 24 hours. Following incubation of the cells with the compound 20 µl of MTT solution (5 mg / ml in HBSS) was added to each well. After 2 hour incubation at 37 ^{0}C, 100 µl of lysis buffer (20 % w / v SDS; 50 % v / v DMF) was added to each well. The lysis step was to dissolve the formazan crystals, after this step the plate was again incubated for 4 hours. The absorbance of the wells was read using a test wavelength of 570 nm and a reference wavelength of 590 nm using a plate reader (MRX, Dynatech Laboratories). The results were expressed as a percentage of the non-treated vehicle only cells. The EC_{50} values were estimated from the inhabitation curves that were plotted using the GraFit software.

2.2.4 The assessment of cytotoxicity using Neutral Red Assays

The Neutral Red (NR) assay is based upon the cell's ability to bind the NR dye within its lysosomes. The quantity of retained dye is directly proportional to the number of viable cells [16].

All cell lines were plated at a density 0.4 x 10^6 cells / ml. Cells were plated, in triplicate, in flat-bottom 96-well plates and were exposed to a range from 0 µM to 100 µM of each compound for 24 hours. On the day before carrying out the NR assay, the NR solution (40 mg/ml in appropriate media) was prepared and left in the incubator overnight. Following incubation of the cells with the compound, the NR solution was centrifuged for 10 min at 600 g to remove any precipitated dye crystals. The cell media was decanted from all wells and 100 µl of NR solution was added to each well. After 2 hour incubation at 37^0C, the NR solution was decanted from all wells and the plate was washed with HBSS. After the wash step 150 µl of NR destain solution (50 % v / v of 96 % ethanol, 49 % v / v distilled water and 1 % v / v acetic acid). The plate was then shaken on a microtilter (300 g) for at least 10 minutes. The plate was then read using spectrophotometer at a wavelength of 540 nm this measures the optical density of the NR in each well. The EC_{50} values were estimated from the inhibitation curves that were plotted using the GraFit from Erithacus software.

2.2.5 The determination of cellular Tenofovir accumulation

1 x 10^6 cells/ml were incubated in their usual media that contained tritiated ([^{3}H])-TVF. The cells were incubated at 37 ^{o}C, with 5 % CO_2 with the antiretroviral drug TFV (1 µM). The cells were incubated with the radiolabelled drugs for 1 hour (37 ^{o}C) then they were removed from the incubator and spun at 9000g for 1 min. 100µl of supernatant was put into a scintillation vial and the rest of the supernatant was discarded. The pellet from each sample was kept and underwent 3 wash steps with ice-cold HBSS (after each step the samples were spun at 9000 g for 1 min). The pellet samples were then resuspended in 100 µl of water and were added to scintillation vials. Scintillation fluid (4 mls) was added to all scintillation vials. All samples were then counted on a scintillation counter (assuming a cell volume of 1 pl for each cell) and the cellular accumulation ratio (CAR, which is a ratio of pellet [^{3}H]-TVF association compared to extracellular media [^{3}H]-TFV) was estimated.

2.2.6 PCR Analysis of transporter mRNA levels in cell lines

The levels of mRNA expression of MRP2, MRP4, MRP7, OAT1 and OAT3 were assessed in each cell line. Total RNA extraction was extracted using phenol-chloroform extraction and Tri reagent. Cells (1 x 10^6 cells / ml) were incubated at room temperature for 5 minutes, then centrifuged for 10 minutes at 12,000 g (4 ^{0}C). After centrifuging 200µl of chloroform was added to all cells, they were mixed vigorously and incubated at room temperature for 15 minutes this incubation step was repeated 2 times. The aqueous phase was removed, 500µl of isopropanol was added and the cells were vortexed for 10 seconds. The cells were incubated at room temperature for 10 minutes and then centrifuged for 8 minutes at 12,000 g (4 ^{0}C). The supernatant was discarded and to the resultant pellet, 1ml of 75 % ethanol was added. The cells were spun (7,500 g, 5 minutes), the ethanol was removed and the RNA pellet was dissolved in 15 µl Nuclease-free water.

After RNA extraction spectrophotometric analysis was carried out on all samples to determine the amount of RNA in each sample (ng / µl). All samples were made up to a volume of 20 µl, in nuclease free water to a final concentration of 2 ng / µl of RNA. All samples (20 µl) were added to a white PCR plate and 31.5 µl of reverse transcription reaction mix was added to each well (reaction mix for each well consist of 5µl reverse transcriptase buffer, 11 µl magnesium chloride, 10 µl DNTP's, 2.5 µl random Heks, 1 µl RNAse inhibitor, 1.75 µl reverse transcriptase). The plate was loaded into a PCR machine (Bio-Rad / MJ Research Opticon 2 Real-Time PCR) and reverse transcription was carried out.

The final step was to carry out PCR using the separate probes for each transporter. To each well of a white PCR plate, 12.5 µl master mix, 1.25 µl probe (specific to the transporter of interest or to the housekeeper gene), 1.5 µl DNA sample (from the reverse transcription PCR plate or from human kidney cDNA samples- used to test if probes are working correctly),

9.75 µl nuclease-free water was added. Samples were run in triplicate. The plate was then read on a PCR machine (Bio-Rad / MJ Research Opticon 2 Real-Time PCR) and the levels of transporter of interest were estimated using Opticon 2 software.

2.2.7 Statistical Analysis

Data are expressed as a mean ± standard deviation. A Shapiro-Wilk test was first carried out to assess the distribution of the data. A Student's t-test was used for all normally distributed data and a Mann-Whitney U test was carried out on non-normally distributed data. All calculations were carried out using the StatsDirect software. Significance is indicated as follows * $P < 0.05$, ** $P < 0.01$, *** $P < 0.001$.

2.3 Results

2.3.1 Metabolic modification of glucose dependent cells into galactose dependent cells

Cells were grown in galactose media over a period of 8 passages, as previously reported [8]. In order to assess the progression of metabolic modification, cytotoxicity assays were carried out using the classic mitochondrial toxin rotenone. The cytotoxicity assays carried out were MTT and NR assays after 24 hr incubations with rotenone.

2.3.1.1 The assessment of cytotoxicity using MTT assays in the presence of rotenone for 24 hours.

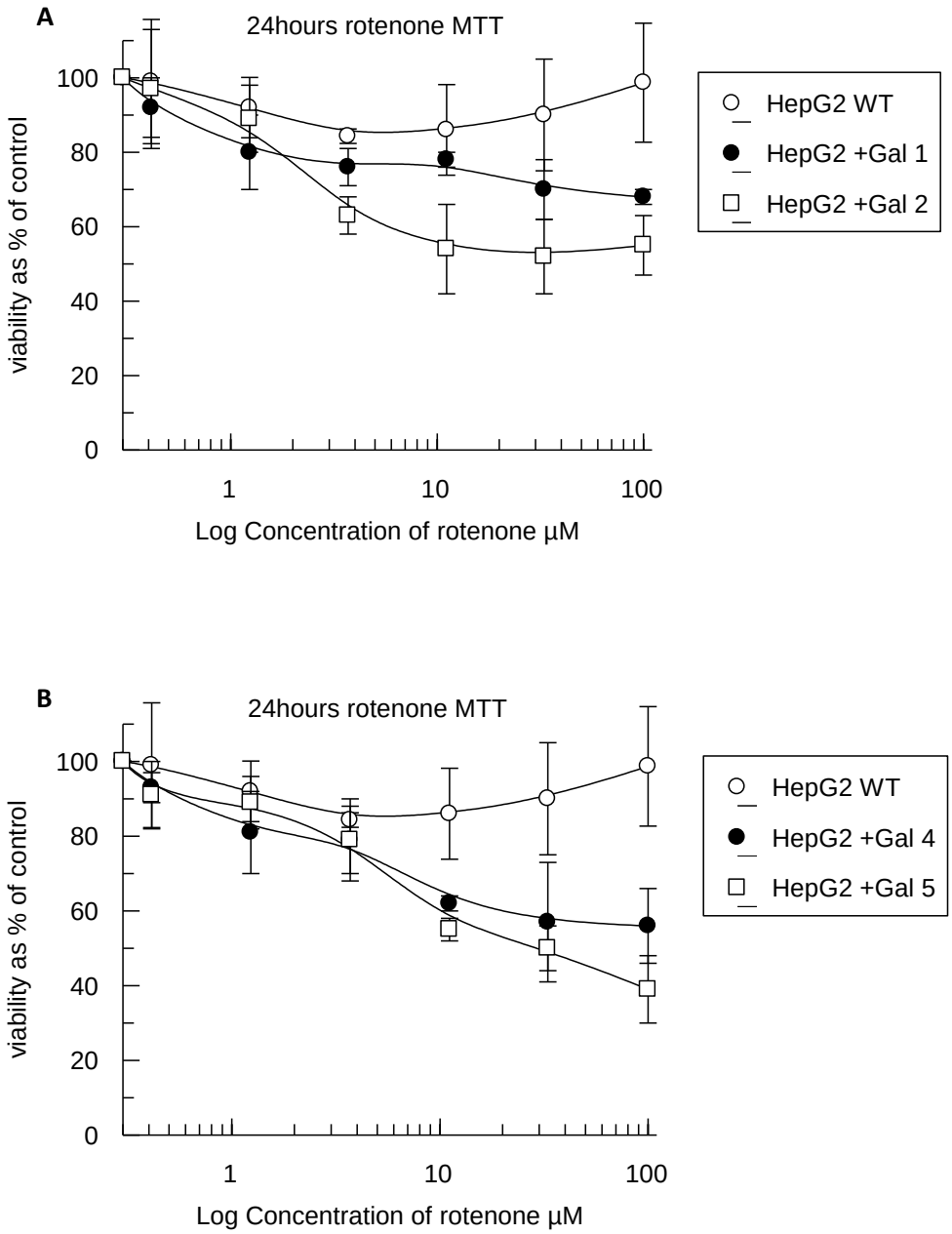

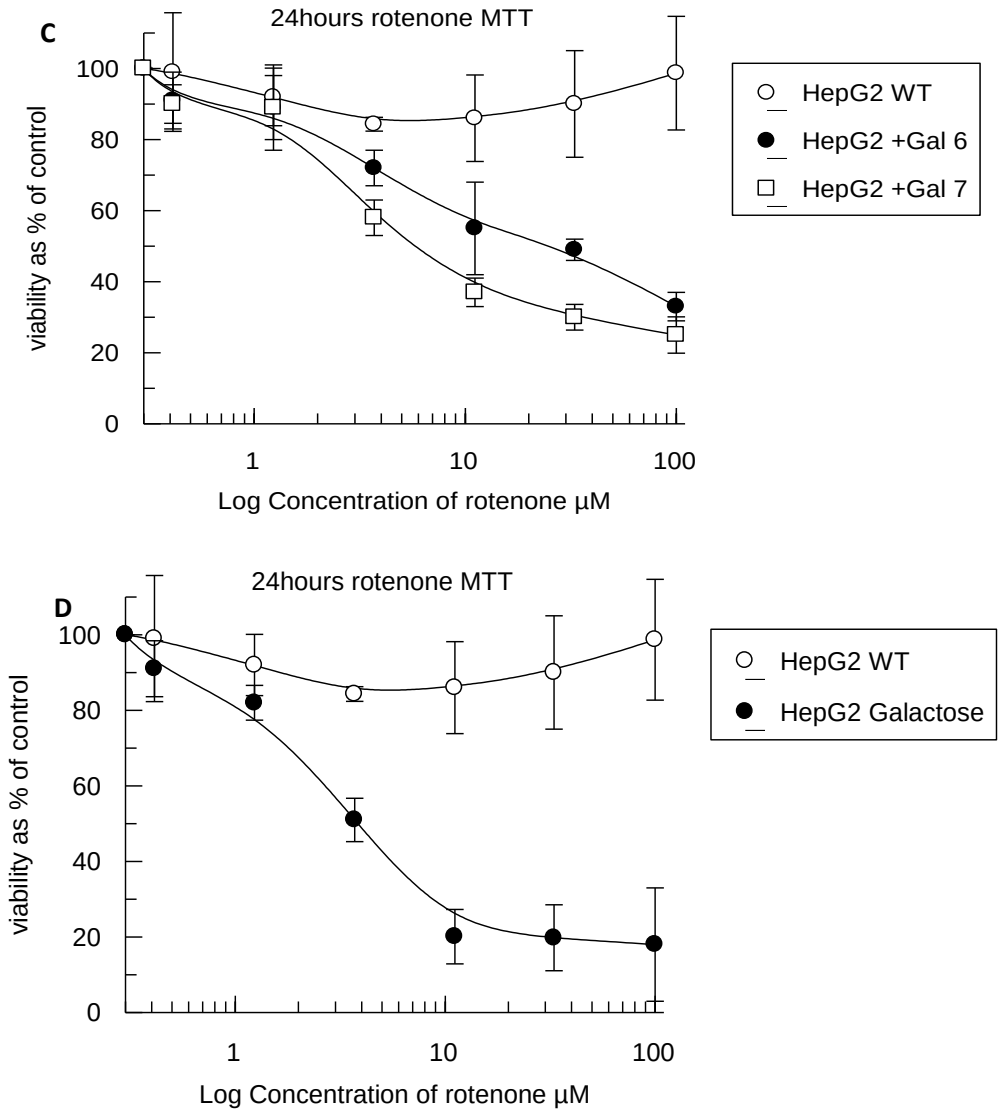

Figure 2.3-Dose-response curves of HepG2 cells grown in galactose media treated with rotenone 24hr. A =MTT of HepG2 WT and HepG2 at passages 1 and 2 with galactose media. **B** = HepG2 WT and HepG2 at passages 4 and 5 with galactose media. **C** = HepG2 WT and HepG2 at passages 6 and 7 with galactose media. **D** = HepG2 WT and HepG2 cultured in galactose for > 8 passages. Results are the mean $\pm$S.D of three or more independent experiments.

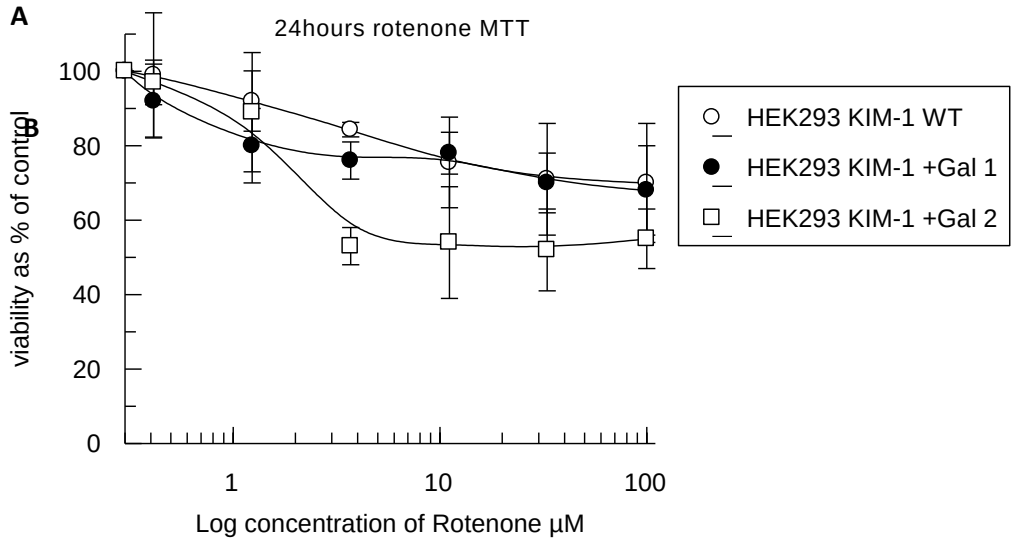
A
24hours rotenone MTT
viability as % of control
100
80
60
40
20
0
1
10
100
Log concentration of Rotenone µM
HEK293 KIM-1 WT
HEK293 KIM-1 +Gal 1
HEK293 KIM-1 +Gal 2

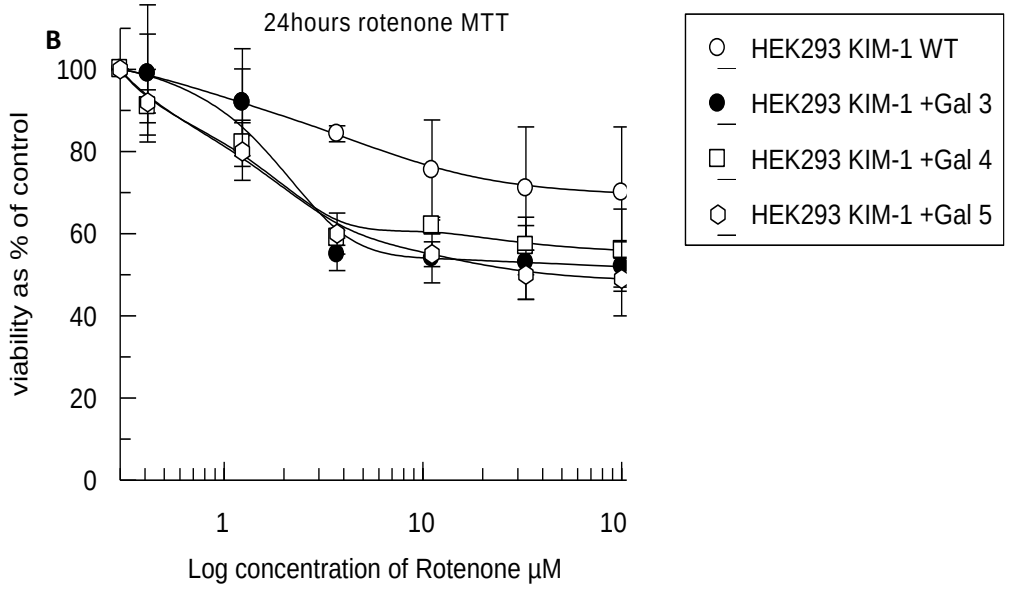
B
24hours rotenone MTT
viability as % of control
100
80
60
40
20
0
1
10
10
Log concentration of Rotenone µM
HEK293 KIM-1 WT
HEK293 KIM-1 +Gal 3
HEK293 KIM-1 +Gal 4
HEK293 KIM-1 +Gal 5

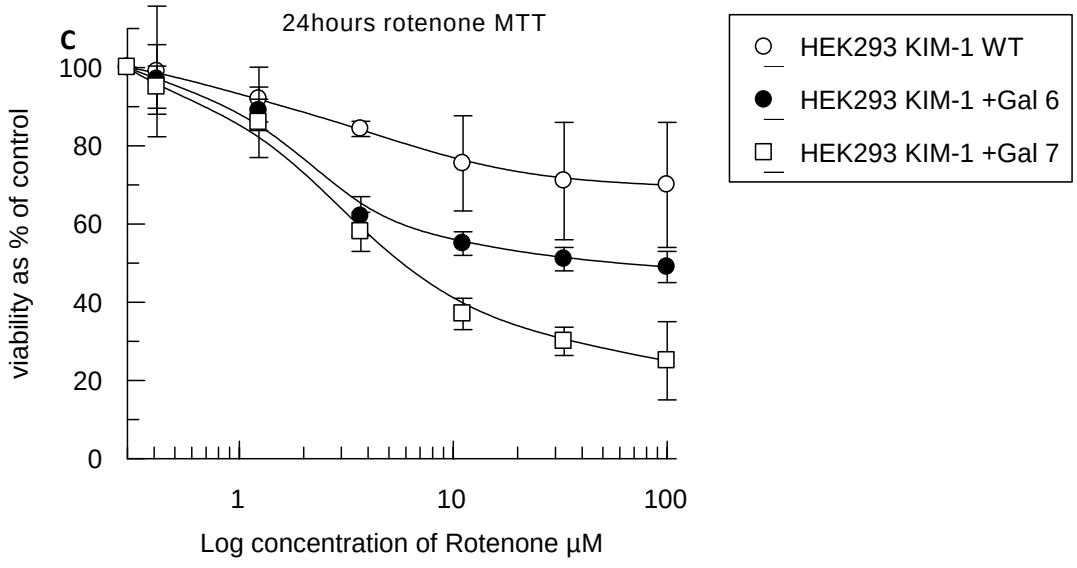
C
24hours rotenone MTT
viability as % of control
100
80
60
40
20
0
1
10
100
Log concentration of Rotenone µM
HEK293 KIM-1 WT
HEK293 KIM-1 +Gal 6
HEK293 KIM-1 +Gal 7

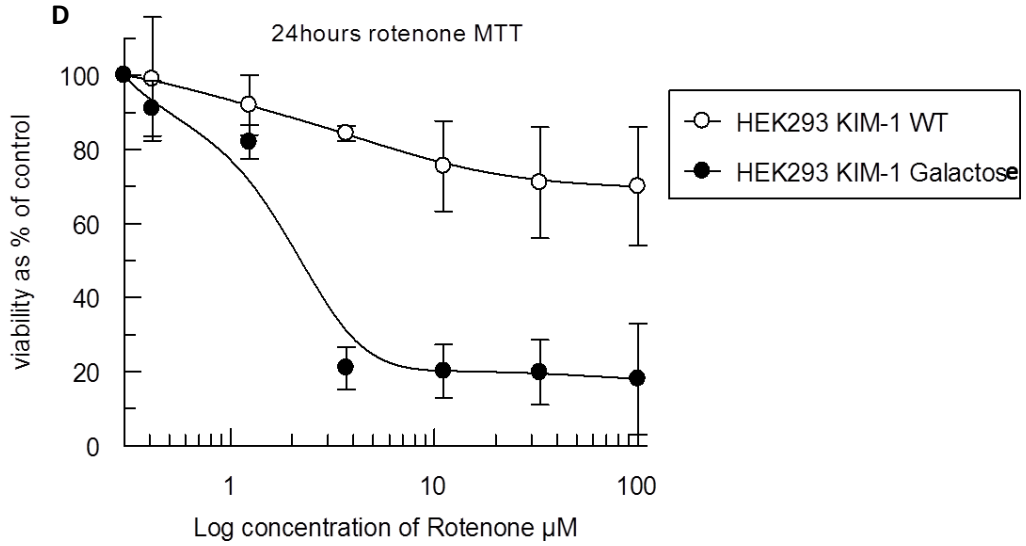

Figure 2.4 -Dose-response curves of HEK293 KIM-1 cells grown in galactose media treated with rotenone 24hr. A =MTT of HEK293 KIM-1 WT and HEK293 KIM-1 at passages 1 and 2 with galactose media. **B** = HEK293 KIM-1WT and HEK293 KIM-1 at passages 3, 4 and 5 with galactose media. **C** = HEK293 KIM-1WT and HEK293 KIM-1 at passages 6 and 7 with galactose media. **D** = HEK293 KIM-1 WT and HEK293 KIM-1 cultured in galactose for > 8 passages. Results are the mean ±S.D of three or more independent experiments.

Table 2.1 A and **2.1 B.** Table 2.1 **A-** EC_{50} values for 24hr MTT for the HEK 293 KIM-1 cells.**B-** EC_{50} values for 24hr MTT for the HepG2 cells. The IC_{50} values are shown ± standard error, n was ≥ 3.

A

Passage number HEK293 KIM-1	EC_{50} values ± standard deviation (µM)
WT 0	> 100
Galactose 1	> 100
Galactose 2	> 100
Galactose 3	> 100
Galactose 4	> 100
Galactose 5	29.0 ± 3.5
Galactose 6	24.9 ± 2.1
Galactose 7	7.16 ± 2.8
>8 passages in galactose	2.6 ± 1.3

B

Passage number HepG2	EC_{50} values ± standard deviation (µM)
WT 0	> 100
Galactose 1	> 100
Galactose 2	> 100
Galactose 3	> 100
Galactose 4	> 100
Galactose 5	12.4 ± 3.1
Galactose 6	9.3 ± 1.6
Galactose 7	2.8 ± 1.7
>8 passages in galactose	2.2 ± 2.2

Table 2.2A and **B. 2.2A** – Shows the results for the statistical analysis performed on the HepG2 MTT data**. 2.2B** - Shows the results for the statistical analysis performed on the HEK293 KIM-1 MTT data. Significance is indicated as follows * P < 0.05, ** P < 0.01, *** P < 0.001.

A

	Concentration of rotenone (µM)						
Passage number (HepG2)	**0.1**	**1**	**5**	**10**	**50**	**100**	**WT vs Galactose**
WT	-	-	-	-	-	-	-
Galactose 1	-	-	-	-	*	*	*
Galactose 2	-	-	-	-	**	**	**
Galactose 3	-	-	-	-	*	**	**
Galactose 4	-	-	-	*	**	**	**
Galactose 5	-	-	-	*	**	***	**
Galactose 6	-	-	-	*	**	***	***
Galactose 7	-	-	*	**	***	***	***
> 8	-	-	*	***	***	***	***

B

	Concentration of rotenone (µM)						
Passage number (HEK293 KIM-1)	**0.1**	**1**	**5**	**10**	**50**	**100**	**WT vs Galactose**
WT	-	-	-	-	-	-	-
Galactose 1	-	-	-	-	-	-	-
Galactose 2	-	-	-	*	*	-	-
Galactose 3	-	-	-	*	*	*	*
Galactose 4	-	-	*	*	*	*	*
Galactose 5	-	-	*	*	*	**	*
Galactose 6			*	**	**	**	**
Galactose 7	-	-	*	**	***	***	***
> 8	-	-	***	***	***	***	***

As time in galactose media increased the susceptibility to rotenone induced cytotoxicity also increases (**Figures 2.3** and **2.4**). This is demonstrated when comparing the EC_{50} value for HepG2 WT cells (EC_{50} was > 100), to the EC_{50} for HepG2 cells passaged in galactose 7 times (EC_{50} was 2.8 µM). This increase in susceptibility to rotenone induced cytotoxicity as passaging in galactose increases is also seen in the HEK293 KIM-1 cells, for example

rotenone is 14 times more toxic in HEK293 KIM-1 cells at passage 7 (EC_{50} was 7.1 µM) compared to HEK293 KIM-1 WT (EC_{50} was > 100 µM). Interestingly the EC_{50} values remains at > 100 µM up until passage 5 in both cell lines where it falls to 12.4 µM in the HepG2 cells and 29µM in the HEK293 KIM-1 cells (**Tables 2.1A** and **2.1B**). **Figures 2.3D** and **2.4D** illustrate that when the cell are considered fully modified they are susceptible to rotenone induced cytotoxicity when compared to glucose grown cells (WT). The EC_{50} values decrease from >100 µM for both WT cell lines to 2.2 µM for the HEK293 KIM-1 galactose cells and to 2.6 µM for the HepG2 galactose cells (**Tables 2.1A** and **2.1B)**

2.3.1.2 The assessment of cytotoxicity using NR assays in the presence of rotenone for 24 hrs.

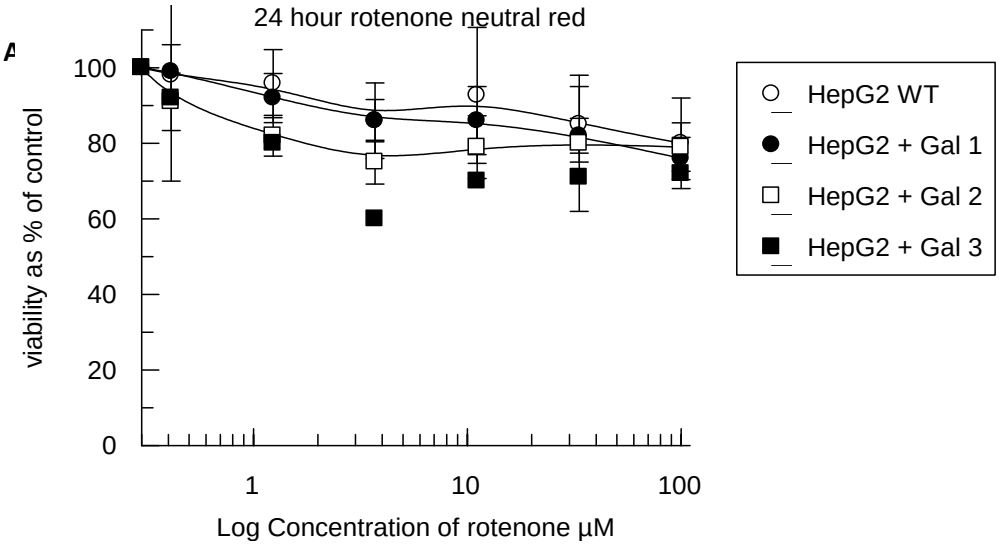

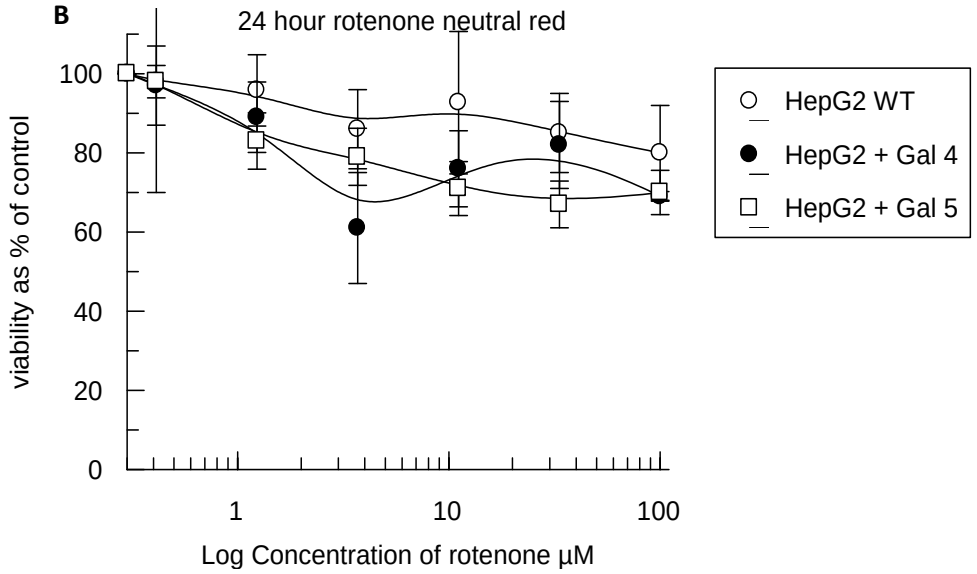

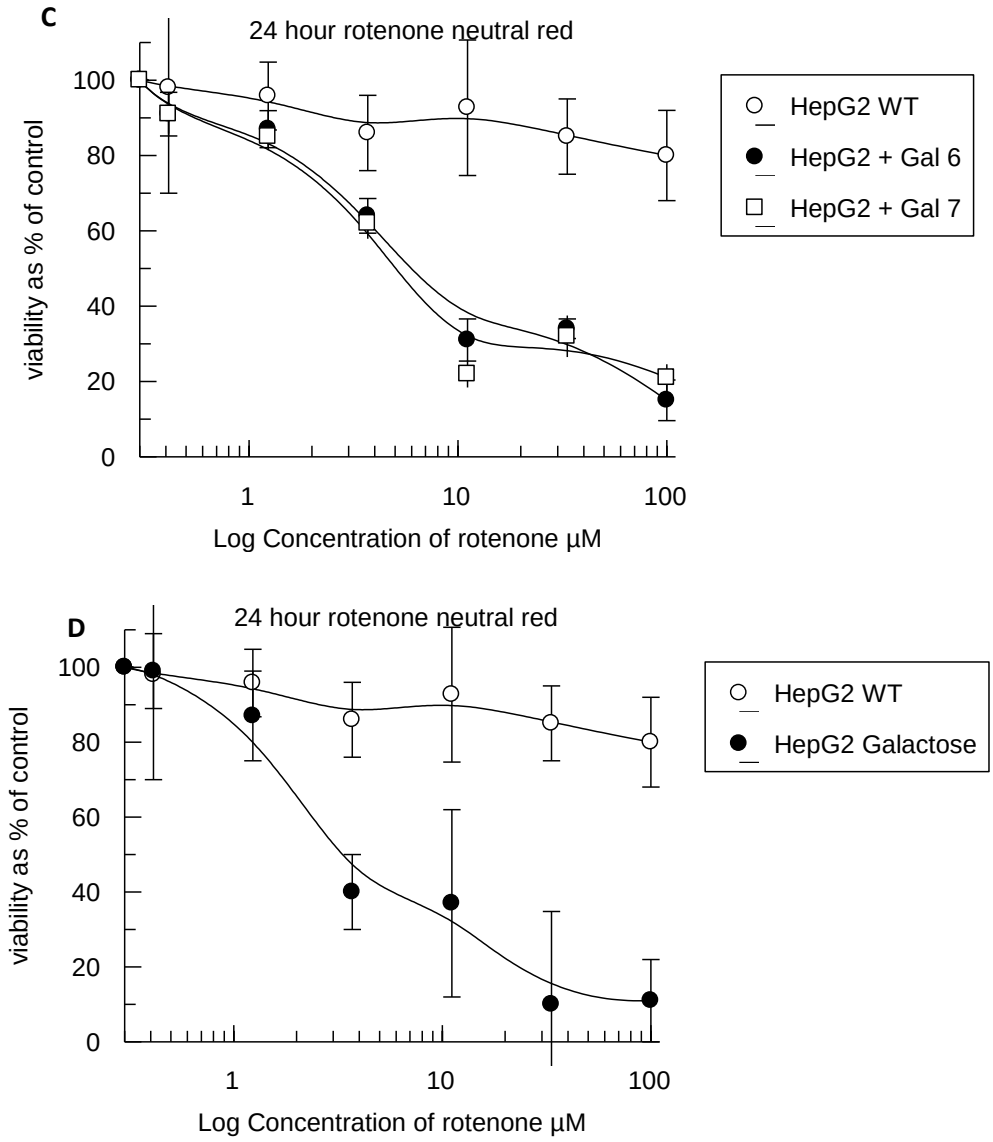

Figure 2.5-Dose-response curves of HepG2 cells grown in galactose media treated with rotenone 24hr. A =MTT of HepG2 WT and HepG2 at passages 1 and 2 with galactose media. **B** = HepG2 WT and HepG2 at passages 3, 4 and 5 with galactose media. **C** = HepG2 WT and HepG2 at passages 6 and 7 with galactose media. **D** = HepG2 WT and HepG2 cultured in galactose for > 8 passages. Results are the mean ±S.D of three or more independent experiments.

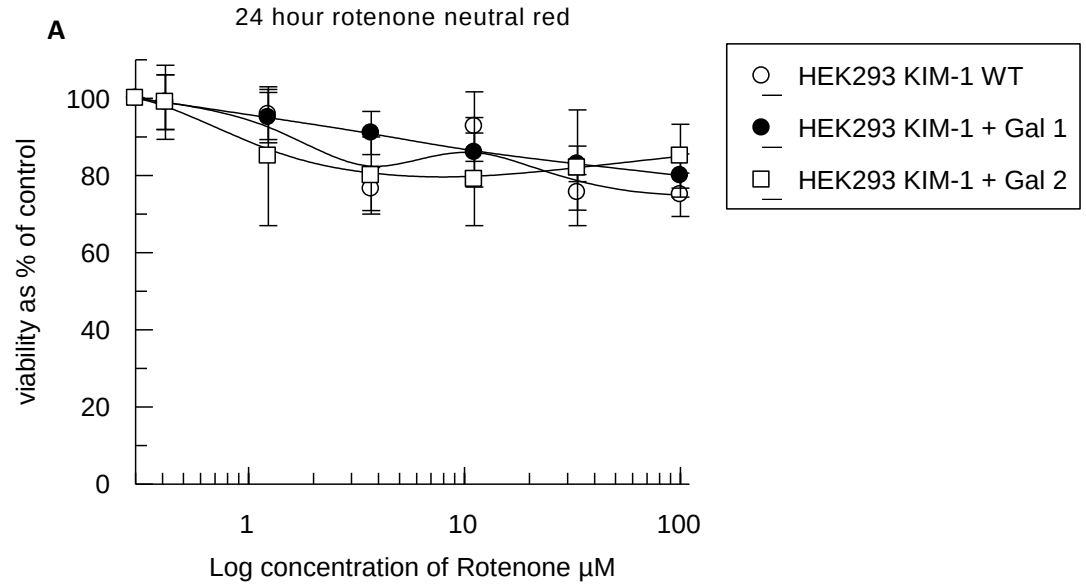
A
24 hour rotenone neutral red
viability as % of control
100
80
60
40
20
0
1
10
100
Log concentration of Rotenone µM
HEK293 KIM-1 WT
HEK293 KIM-1 + Gal 1
HEK293 KIM-1 + Gal 2

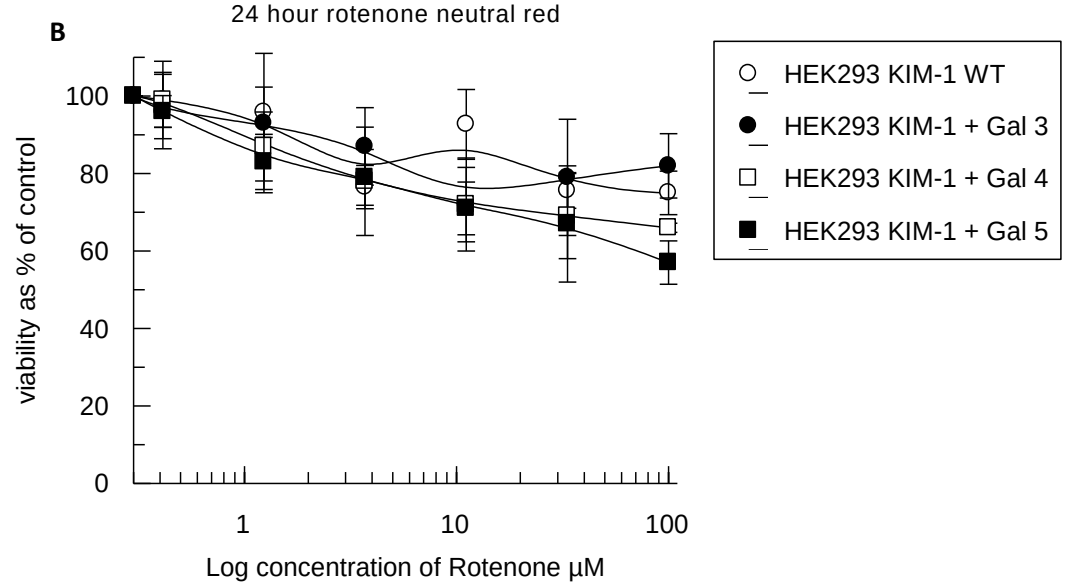
B
24 hour rotenone neutral red
viability as % of control
100
80
60
40
20
0
1
10
100
Log concentration of Rotenone µM
HEK293 KIM-1 WT
HEK293 KIM-1 + Gal 3
HEK293 KIM-1 + Gal 4
HEK293 KIM-1 + Gal 5

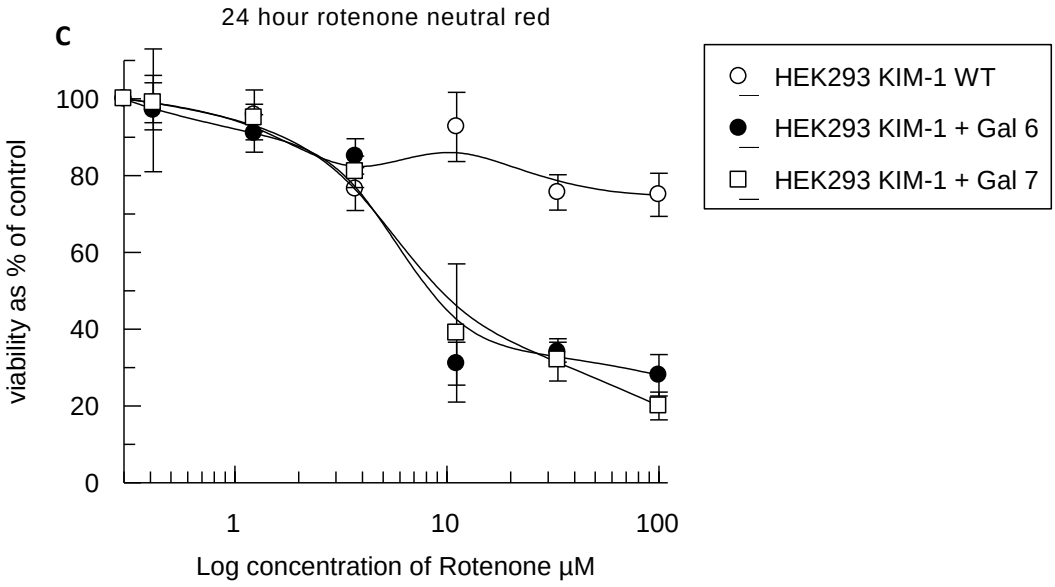
C
24 hour rotenone neutral red
viability as % of control
100
80
60
40
20
0
1
10
100
Log concentration of Rotenone µM
HEK293 KIM-1 WT
HEK293 KIM-1 + Gal 6
HEK293 KIM-1 + Gal 7

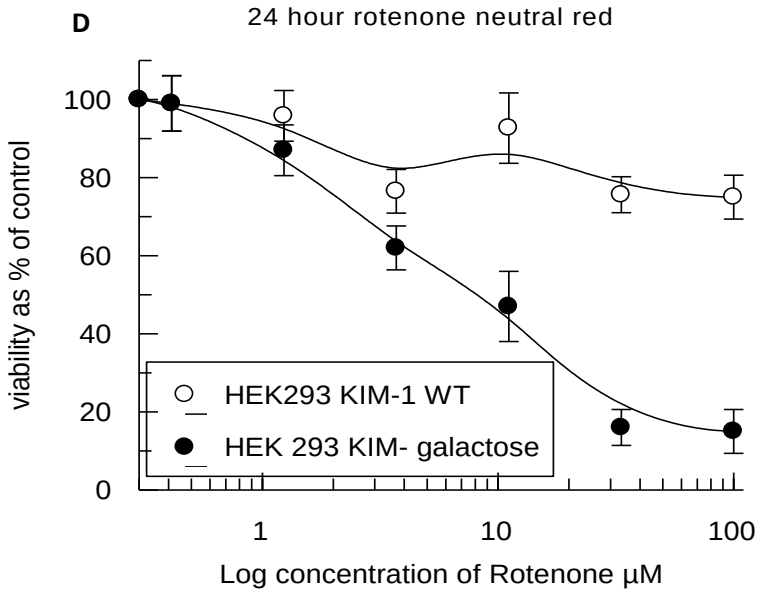

Figure 2.6 -Dose-response curves of HEK293 KIM-1 cells grown in galactose media treated with rotenone 24hr. A =MTT of HEK293 KIM-1 WT and HEK293 KIM-1 at passages 1 and 2 with galactose media. **B** = HEK293 KIM-1WT and HEK293 KIM-1 at passages 3, 4 and 5 with galactose media. **C** = HEK293 KIM-1WT and HEK293 KIM-1 at passages 6 and 7 with galactose media. Results are the mean ±S.D of three or more independent experiments. **D** = HEK293 KIM-1 WT and HEK293 KIM-1 cultured in galactose for > 8 passages. Results are the mean ±S.D of three or more independent experiments.

Table 2.3A and 2.3 B. Table 2.2 **A**- IC_{50} values for 24hr NR for the HepG2 cells. Table 2.2 **B**- EC_{50} values for 24hr NR for the HEK 293 KIM-1 cells. The EC_{50} values are shown +/- standard error, n was ≥ 3.

A

Passage number HepG2	EC_{50} values ± standard deviation (µM)
WT 0	> 100
Galactose 1	> 100
Galactose 2	> 100
Galactose 3	> 100
Galactose 4	> 100
Galactose 5	> 100
Galactose 6	4.4 ± 3.9
Galactose 7	2.2 ± 4.4
>8 passages in galactose	2.9 ± 1.7

B

Passage number HEK293 KIM-1	EC_{50} values ± standard deviation (µM)
WT 0	> 100
Galactose 1	> 100
Galactose 2	> 100
Galactose 3	> 100
Galactose 4	> 100
Galactose 5	> 100
Galactose 6	9.4 ± 4.0
Galactose 7	7.0 ± 3.6
>8 passages in galactose	5.8 ± 1.8

Table 2.4A and **B. 2.4A** – Shows the results for the statistical analysis performed on the HepG2 NR data**. 2.4B** - Shows the results for the statistical analysis performed on the HEK293 KIM-1 NR data. Significance is indicated as follows * $P < 0.05$, ** $P < 0.01$, *** $P < 0.001$.

A	Concentration of rotenone (µM)						
Passage number (HepG2)	0.1	1	5	10	50	100	WT vs Galactose
WT	-	-	-	-	-	-	-
Galactose 1	-	-	-	-	-	-	-
Galactose 2	-	-	-	-	-	-	-
Galactose 3	-	-	-	-	-	-	-
Galactose 4	-	-	-	-	-	-	-
Galactose 5	-	-	-	-	-	-	-
Galactose 6	-	-	*	**	**	***	***
Galactose 7	-	-	*	**	**	***	***
> 8	-	-	**	**	***	***	***

B	Concentration of rotenone (µM)						
Passage number (HEK293 KIM-1)	0.1	1	5	10	50	100	WT vs Galactose
WT	-	-	-	-	-	-	-
Galactose 1	-	-	-	-	-	-	-
Galactose 2	-	-	-	-	-	-	-
Galactose 3	-	-	-	-	-	-	-
Galactose 4	-	-	-	-	-	*	
Galactose 5	-	-	-	-	-	*	*
Galactose 6	-	-	-	**	**	***	***
Galactose 7	-	-	-	**	**	***	***
> 8	-	-	-	**	**	***	***

With increased galactose passage the susceptibility to rotenone induced cytotoxicity also increases (**Figures 2.5** and **2.6**). This is shown when comparing the EC_{50} value for HepG2 WT cells (EC_{50} was > 100 µM), to the EC_{50} for HepG2 cells at passage 7 (EC_{50} was 2.2 µM). This increase in susceptibility to rotenone induced cytotoxicity as time spent in galactose increases is also observed in the HEK293 KIM-1 cells. In the HEK293 KIM-1 cells at passage 7, the EC_{50} was 7 µM compared to HEK293 KIM-1 WT EC_{50} was > 100 µM. Interestingly the EC_{50} values remains at > 100 µM up until passage 6 in both cell lines where it falls to 4.4 µM in the HepG2 cells and 9.4 µM in the HEK293 KIM-1 cells (**Table 2.3A** and **2.2B**). **Figures 2.5D** and **2.6 D** show that at the point that the cells are considered fully

modified (> 8 passages) they are susceptible to rotenone induced cytotoxicity when compared to glucose grown cells (WT). The EC_{50} values decrease from > 100µM for both WT cell lines to 5.8 µM for the HEK293 KIM-1 galactose cells and to 2.9 µM for the HepG2 galactose cells (**Table 2.3A** and **B**).

2.3.2 Accumulation of Tenofovir in HepG2 cells

Accumulation studies using the cell lines HepG2 and HEK293 KIM-1 (both grown in glucose and galactose-containing media) of the antiretroviral drug TFV were carried out. The aim of this study was to show, with the use of radioactively labelled TFV [^{3}H], that it accumulates in the cell lines used in this study. An additional aim of this study was to demonstrate if the metabolic switch affects the rate of TFV [^{3}H], accumulation.

A

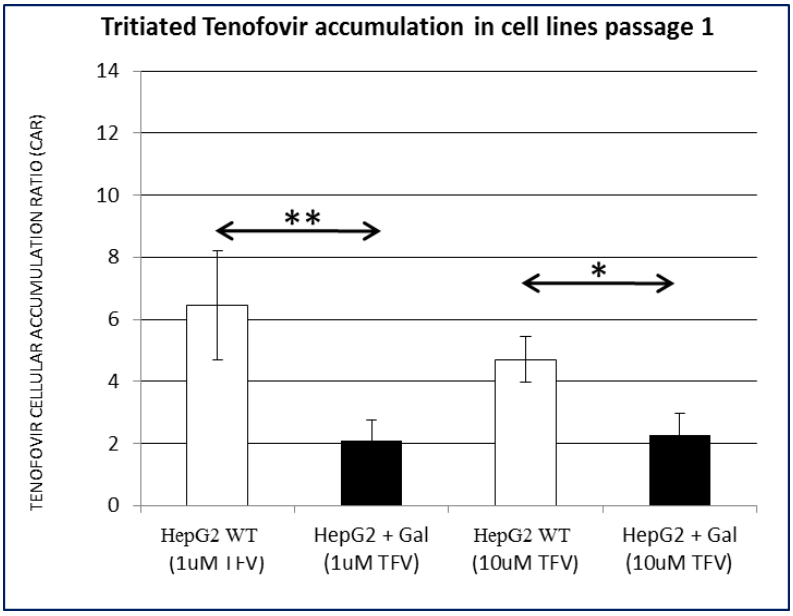

B

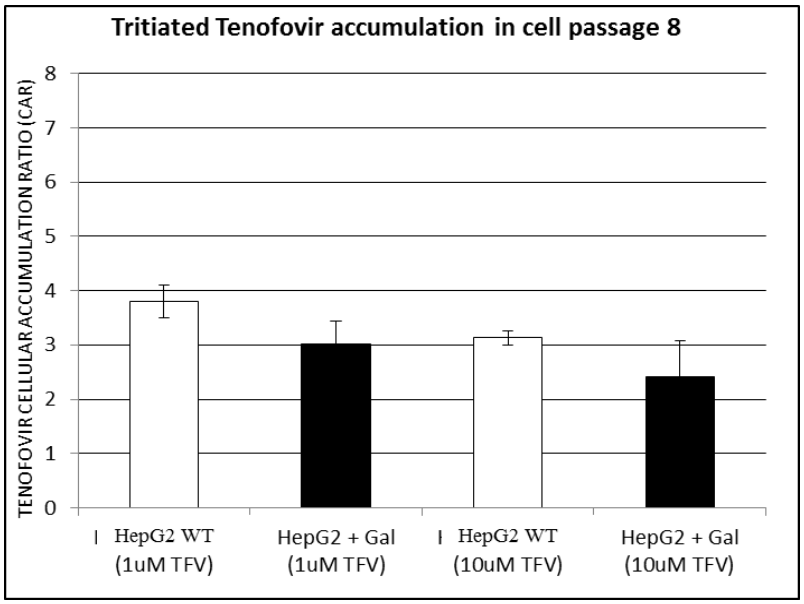

Figure 2.7 A and 2.7 B. A = accumulation of TFV [^{3}H], in HepG2 WT and HepG2 galactose passage 1. **B =** accumulation of TFV [^{3}H], in HepG2 WT and HepG2 galactose passage 8. Results are the mean $\pm$ S.D of three or more independent experiments. **KEY** ** $P \leq 0.01$ * $P \leq 0.05$. S.D. is shown as significance between HepG2 WT compared to the HepG2 galactose cells.

At passage point 1 there is a significant difference between the HepG2 WT (at 1 μM TFV the CAR was 6.4 ±) and the HepG2 galactose passage 1 cells (at 1 μM TFV the CAR was 2.1±) **(Figure 2.7A)**. At galactose passage point 8 there is no significant difference in the TFV accumulation between the HepG2 WT (at 1 μM TFV the CAR was 3.8 ±) and the HepG2 Galactose cells (at 1 μM TFV the CAR was 3.0 ±) (**Figure 2.7B**).

2.3.3 The determination of cellular transporter levels via PCR methods

PCR analysis of drug transporters was carried out and determined by calculating the relative ΔΔCT values which were normalised to a housekeeping gene. The aim of this study was firstly to show that these cell lines contained the key transporters for TFV transport (MRP2, MRP4, MRP7, OAT1 and OAT3) [17]. Secondly this study would show how / if galactose culturing affects the cellular physiology or transporter expression within each cell line.

2.3.3.1The determination of cellular transporter levels within HEK293 KIM-1 cells and HepG2 cells via PCR methods.

A

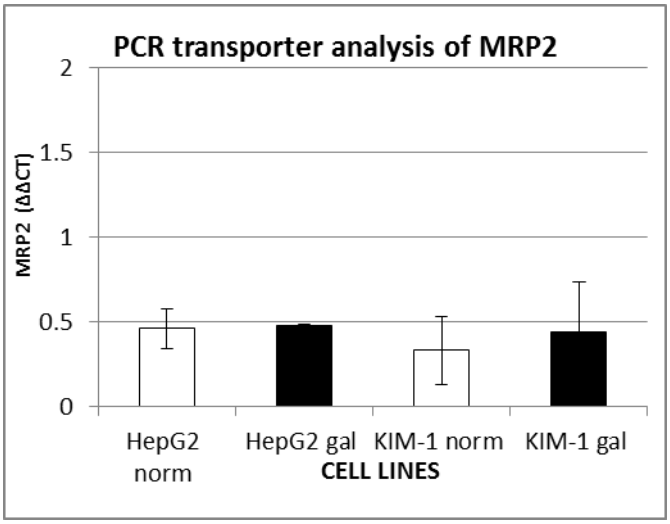

B

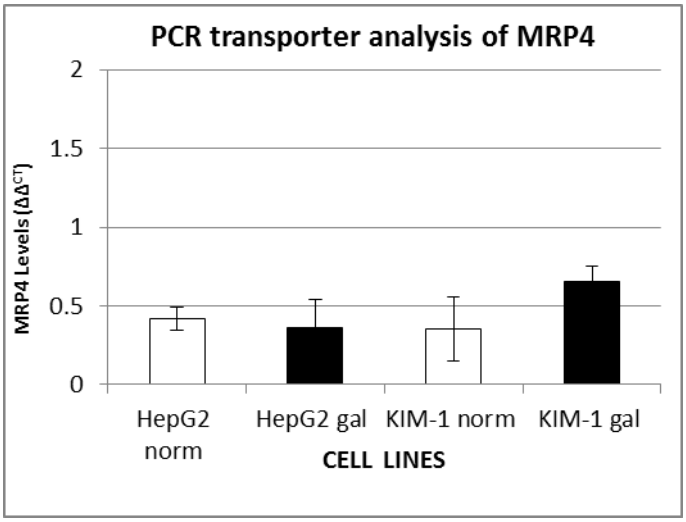

C

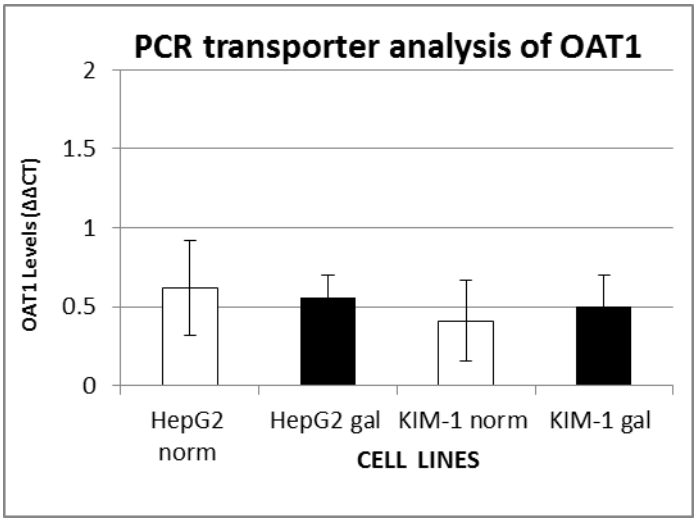

D

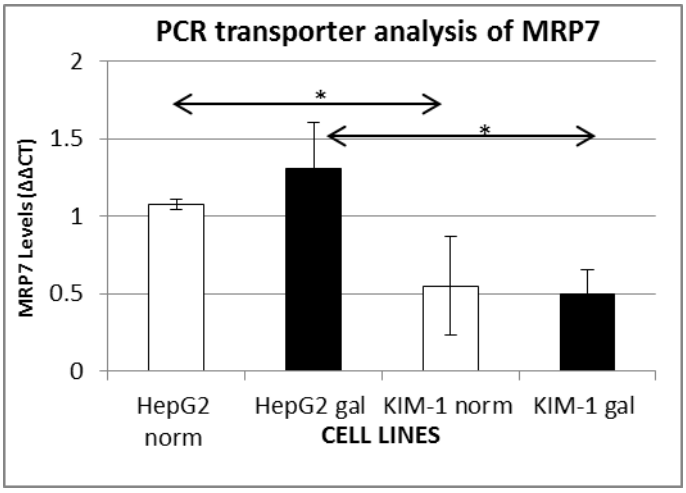

E

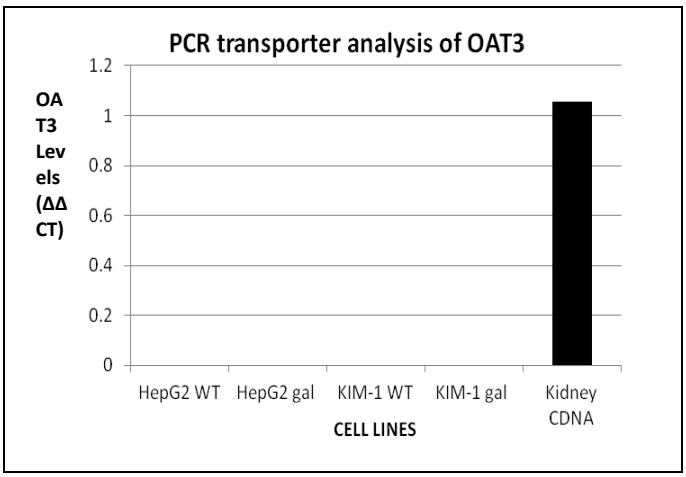

Figure 2.8 A, B, C, D and E Transporter analysis in HepG2, HEK293 KIM-1(KIM-1) and HEK293 PcDNA cells grown in glucose and galactose media. A= MRP2 analysis. **B=** MRP4 analysis. **C=** OAT1 analysis. **D** =MRP7. **E=** OAT 3 analysis. Results are the mean ±

S.D of three or more independent experiments. **KEY:** * P≤ 0.05. S.D. is shown as significance between those data sets as indicated by the arrow bars.

These studies have determined transporter levels (ΔΔ CT) within HepG2 WT/ galactose cells and HEK293 KIM-1 cells WT/ galactose cells (**Figure 2.8 A, B, C** and **D**) demonstrated that all cell lines expressed MRP2, MRP4, MRP7 and OAT1 however OAT3 was not detected in these cell lines. The MRP2 levels in the HepG2 WT were 0.46 and for the HepG2 galactose cells it was 0.47(**Figure 2.8 A**). There was no significant difference in the levels of transporters between the cell lines when cultured in glucose (WT) compared to when cultured in galactose for example; MRP4 levels detected for HepG2 galactose cells was 0.36 and for HepG2 WT it was 0.41(**Figure 2.8 B**). The OAT 1 levels detected for the HEK293 KIM-1 WT was 0.41 and for the HEK293 KIM-1 galactose OAT1 levels were 0.50 (**Figure 2.8 C**). The MRP2 levels in the HepG2 WT were 0.46 and for the HepG2 galactose cells it was 0.47(**Figure 2.8 A**). The MRP7 transporter values for the HEK293 KIM-1 WT was 0.54 and for the HEK293 KIM-1 galactose cells it was 0.50 (**Figure 2.8 D**). As a positive control human kidney DNA was tested using the OAT 3 probe to verify that the OAT3 probe was working correctly. This confirmed that the cells did not have OAT 3 (**Figure 2.8 E**). There was no significant difference between transporter levels detected in the HepG2 cells compared to the HEK 293 KIM-1 cells except for MRP7 (**Figure 2.8 D**).

2.3.3.2 The determination of transporter levels within HepG2 cells throughout the modification into galactose cultured cells using PCR methods.

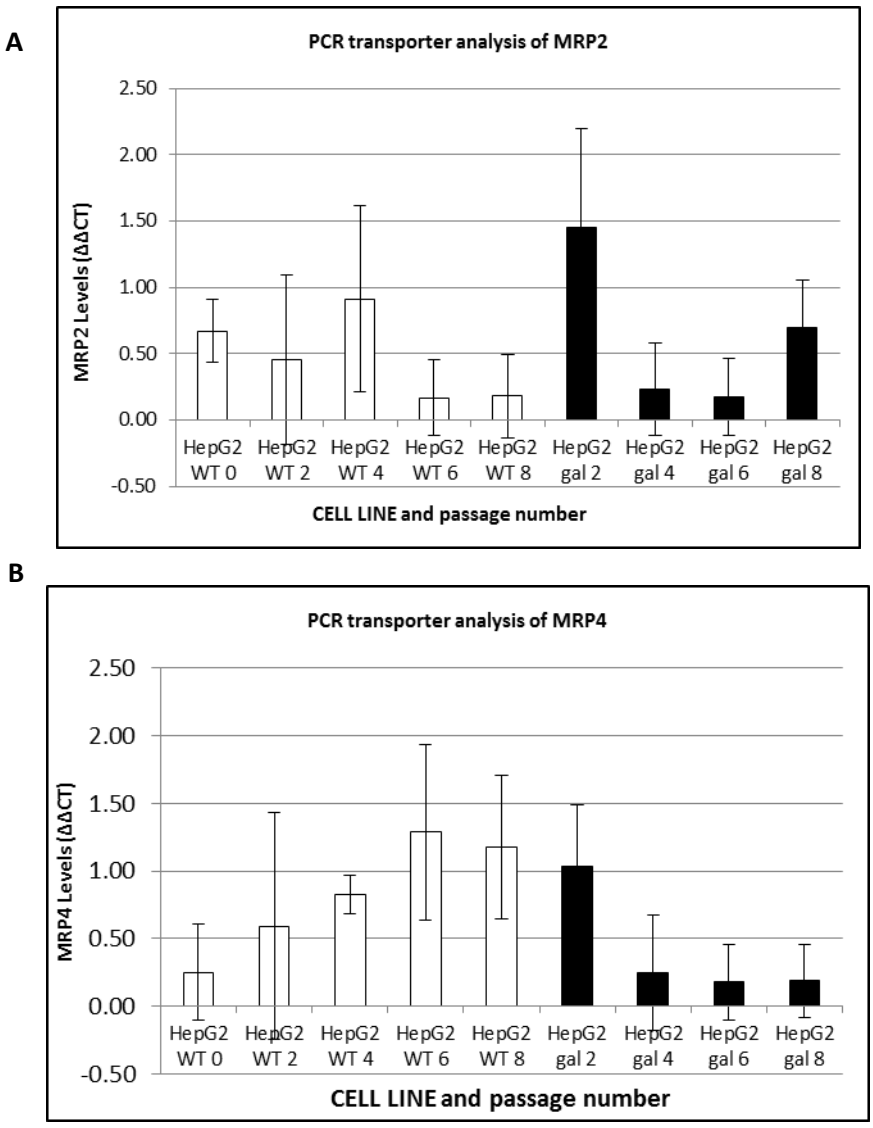

Figure 2.9 A, B, C and D Transporter analysis in HepG2 WT and HepG2 Galactose cells. 2.9 **A=** MRP2 analysis. 2.9 **B=** MRP4 analysis. 2.9 **C=** MRP7 analysis. 2.9 **D =** OAT 1 analysis. Results are the mean ± S.D of three or more independent experiments.

The graphs showing the determined transporter levels (ΔΔCT) throughout the modification of WT cells to galactose grown cells (**Figure 2.9 A, B, C** and **D**) showed that there was no significant difference in the levels of transporters between the HepG2 WT and HepG2 cells

grown in galactose for 8 passages. However, there seemed to be a general trend of an increase in transporters levels when HepG2 cells were cultured with galactose over 2 passages the transporter levels for MRP2 in HepG2 WT was 0.67 and when cultured in galactose 2 times this increased to 1.45 (**Figure 2.9 A**). After this increase the transporter levels within the HepG2 galactose cells lowered to be the same as HepG2 for MRP2 after culturing in galactose for 8 passages the transporter levels were 0.69 (**Figure 2.9 A**). For MRP4 the transporter levels where higher until passage 8 (The HepG2 WT MRP4 levels were 0.25 and after 8 passages the HepG2 WT MRP4 level was 1.17) (**Figure 2.9 B**). There was variable transporter expression for MRP7, levels initially increased after 2 passages within galactose media to 1.4, this level then decreased at each passage point to 0.2 at passage 8within galactose media (**Figure 2.9C**). and then Finally for OAT1 the HepG2 WT transporter levels increased from 0.25 to 0.73 at passage 4, there was a decrease to 0.30 at passage 6 and finally the transporter levels increase at passage 8 to 1.09 (**Figure 2.9 D**).

2.4 Discussion

Work presented within this chapter has focussed on the generation and validation of a cell model that could be used to study the mechanistic pathway of TFV-induced cytotoxicity. These studies were essential as the mechanistic pathway of TFV-induced cytotoxicity has previously not been reported due to lack of a suitable cell model [1-5]. Cells (HepG2 / HEK293 KIM-1) were cultured in galactose containing media in order to modify them to rely on mitochondrial OXPHOS for cellular ATP production which has been shown in other studies [8]. These modified cells better represent the physiological aerobic conditions; this study has shown that human cells rely on 95 % OXPHOS for the generation of cellular ATP [12]. When the cells become reliant on the mitochondrial OXPHOS they become more susceptible to mitotoxins because they are reliant solely on mitochondria for the production of cellular ATP [8].

To determine when the cells had become fully modified galactose passaging cells were incubated with the known classical mitotoxin rotenone for a period of 24 hours and cytotoxicity was determined either by MTT or NR assays [8]. NR assays were used to ensure that galactose culturing was not interfering with the cytotoxicity determined via MTT assays, as the NR assay is not influenced by mitochondrial enzymes [16]. MTT assays were chosen as they measure mitochondrial cytotoxicity and it has been hypothesised that TFV induces its cytotoxic effects via inhibitation of mitochondrial polymerase γ which leads to mitochondrial specific toxicity [6]. The MTT/NR results (**Figures 2.3** to **2.6**), showed that cells became fully reliant on the mitochondrial OXPHOS by passage 7 seen by the increase to in susceptibility to rotenone induced cytotoxicity. It was decided that cells would be used after 8 passages within galactose media which supports previous studies [8] (MTT and NR results showing fully modified galactose cells can be seen in **Figures 2.7** and **2.8**). The kinetics of the transition towards relying solely on mitochondrial OXPHOS for cellular energy

production can be clearly seen within the dose response curves. For the MTT assays the transition can be seen after 5 passages in galactose containing media for both the HepG2 and HEK293 KIM-1 cells which is shown by the sharp decrease in EC_{50} values at this passage point (**Figure 2.3 C** and **2.4 C**). For the NR assays the transition is seen later after 6 passages cultured in galactose media (for both HepG2 and HEK293 KIM-1 cells), shown again by a sharp decrease in EC_{50} values at this passage point (**Figure 2.5 C** and **2.6 C**). The difference between the two assays shows that the cytotoxicity being induced is mitochondrial specific as the MTT assay shows cytotoxicity at an earlier passage point. The delay seen in the determined cytotoxicity via the NR assay, could be due to previously established observation that the cell has an abundance of mitochondria, a certain threshold point in the percentage of dysfunctional mitochondria must be reached before any cellular cytotoxicity is seen [10]. A recent study has shown that this transition toward relying on mitochondrial OXPHOS for cellular energy production can be induced after only 2 hours when culturing cells in serum free media containing galactose [18]. The switch over can be achieved within 2 hours due to the use of serum-free media. Serum contains a small amount of glucose therefore these cells have no option but to convert to mitochondrial OXPHOS for cellular ATP production. Whilst this method would benefit the study of mitochondrial cytotoxicity within immortalised cells induced by most drugs, TFV toxicity is reported clinically to be delayed toxicity only induced after long term-exposure, and cells could not be cultured for long in serum-free media as they would not survive. Also these cells may become stressed due to these extreme conditions and may produce less reliable results [18].

Accumulation studies were carried out to determine if TFV accumulated within the HepG2 cells and to show if culturing the cells in galactose-containing media alters the accumulation rate of TFV. The accumulation results (**Figure 2.9**) showed that TFV was able to accumulate within the HepG2 cells and that there was no significant difference in accumulation n the

HepG2 WT compared to the fully modified HepG2 cells grown in galactose-containing media. However, there was a significant difference in accumulation between HepG2 WT and HepG2 cultured with galactose for one passage; this could be due to a decrease in cellular ATP levels which has been shown to happen initially after culturing cells in galactose-containing media, as transport is active and reliant upon cellular ATP levels [18]. However, as cells were only used in further experiments following 8 passages this finding is unlikely to affect the experiments.

The mRNA levels of MRP2, MRP4, MRP7, OAT1 and OAT3 were determined via PCR analysis as these transporters are essential for the uptake and efflux of TFV within human proximal tubule cells [19]. The transporter results (**Figures 2.10** and **2.11**) showed that all transporters except for OAT3 were expressed in both HepG2 and Hek293 cells grown in glucose and galactose media. As OAT3 was absent from both cell lines and because it has been shown that TFV uptake is dependent mainly on OAT1 which is present within all cell lines [19], it was decided that the absence of this transporter whilst not ideal would not greatly affect the cytotoxicity studies. This is supported by the fact that the level of accumulation of TFV was the same in both cell lines. These results showed there was no significant difference between the transporter expression in the WT cells compared to the expression in the fully modified galactose-grown cells. This shows that at the point that the galactose cells will be used for subsequent experiments their transporter expression is not affected by galactose culturing. Interestingly, it was observed that the accumulation of TFV initially decreased following galactose culturing; this was unexpected and would require further investigation to find a reason for this reduction in accumulation (**Figure 2.7 A** and **B**). During the modification of the WT cells into galactose-grown cells, transporter expression increased after the initial culturing with galactose. This could be due to an increase in the expression of cellular transporters in response to cell stress. This has previously been reported

in vitro and *in vivo* using kidney cells treated with gentamicin in which the expression of MRP2 increased due to cellular stress [20]. There was variation in the HepG2 WT transporter expression over time; this could be due to cellular aging which could result in difference in transporter expression. However, none of the variations were significant.

Recent studies have highlighted how the human equilibrative nucleoside transporter 1 (hENT-1), which is located on mitochondrial membranes, is essential for mitochondrial accumulation of antivirals [21]. Studies have shown that an increased expression of this transporter can lead to enhanced mitochondrial toxicity of NRTI's [21]. Therefore future studies could determine the expression of hENT-1 within the different cell lines and see if its expression is influenced by cells adapted in galactose-containing media.

Future work could involve using seahorse technology to measure the glycolytic vs. mitochondrial OXPHOS rates within the cells when culturing the cells within galactose media vs. glucose media.

Using immortalised cells is not the ideal method for studying mechanistic pathways; however they are currently the best option available as TFV toxicity is delayed clinically, making it difficult to use primary cells. Overall the data presented within this chapter show that culturing cells in galactose media made them more susceptible to mitochondrial toxins, without compromising or changing the physiological characteristics of the cells. Thus these modified cells are good tools for studying the mechanistic pathway of TFV induced cytotoxicity. It was decided that HepG2 cells would be used for the majority of the subsequent studies as they were more reliable during culturing than the HEK293 KIM-1 cells.

Chapter Three

INVESTIGATION OF THE MECHANISM OF CYTOTOXICITY INDUCED BY TENOFOVIR IN HUMAN RENAL AND HEPATIC CELL LINES

Contents

3.1 Introduction

Current evidence links HARRT and its adverse effects to impaired mitochondrial replication [1]. Many *in vitro* and *in vivo* studies support the hypothesis that NRTI exposure leads to mitochondrial impairment [2-5]. The clinical evidence of mitochondrial impairment due to NRTI treatment is demonstrated by the development of lactic acidosis within patients [6-8]. The hallmark of mitochondrial dysfunction is the onset of hyperlactatemia, which can be symptomatic or asymptomatic and is caused by an increase in the cellular lactate / pyruvate ratio. Lactic acidosis arises due to the reduced ability of the mitochondria to oxidise lactate and by an increased glycolytic flux which compensates for a reduction in mitochondrial OXPHOS [6-8].

The pathogenesis of NRTI-induced mitochondrial dysfunction can be split into three distinct steps. The first step is the competition of the NRTI triphosphates with the naturally occurring nucleotide triphosphates within the cell [9]. Upon successful competition the second step takes place. NRTI's are incorporated into the mitochondrial DNA (mtDNA) strands, leading to chain termination as the NRTI's lack a second hydroxyl group required for the addition of new DNA bases. Finally the result of chain termination is impaired mitochondrial polymerase γ (mtDNA pol γ), leading to mtDNA depletion and a reduction in mtDNA copy number [9].

The mitochondrial effect of NRTI's arises from the DNA polymerase γ hypothesis of Lewis [10]. This hypothesis states that as NRTI's act to inhibit HIV-1 reverse transcriptase, they can also inhibit mtDNA pol γ in a non-selective manner [2-3, 11]. MtDNA pol γ is essential for the replication of the mitochondria and depletion will lead to impaired cellular ATP production [10]. This decrease in the cellular physiological scope dramatically impacts on cellular function and structure, and is considered the perpetrator responsible for the long term side effects associated with NRTI use [10].

The extent of NRTI mtDNA pol γ inhibition is dependent upon the type of NRTI and the tissue being affected [2, 10-12]. The type of NRTI can influence the extent of pol *γ* inhibition as they all have different affinities for pol *γ*. Previous studies have shown the order of NRTI pol γ affinity to be the following (highest to lowest): zalcitabine (ddC) > dianosine (ddI) > stavudine (d4T) ≥ lamivudine (3TC) ≥ abacavir (ABC) ≥ tenofovir disproxil fumarate (TDF) ≥ emtricitabine (FTC) [2-5].

In vitro studies have been carried out to look at mtDNA depletion caused by NRTIs in peripheral blood mononuclear cells (PBMCs) and in HepG2 cells (these cells have a high mtDNA copy number making the study of mtDNA easier) [2-5]. The depletion of mtDNA was detected using PCR methods in the above mentioned cells treated with different NRTI's [2-5]. The depletion of mtDNA was detected with the following rank; ddC >, ddI >, d4T >, zidovudine (AZT) >, ABC= 3TC = TDF [2-5]

The tissue type can influence susceptibility to mitochondrial toxicity induced by NRTI's via a number of factors such as the size of the nucleotide pools, the kinase activity of the cells and the bio-energetic demand of specific tissues [2, 10-12]. Previous research showed there to be precursor nucleotide pools within cells that are specific for mtDNA [13]. Studies have also showed that these pools selectively resist depletion until a threshold point; if a cell has a smaller nucleotide pool, it will be more susceptible to mitochondrial toxicity induced by NRTI's [14-16]. The kinase enzymes within a cell are responsible for the activation of NRTI's via phosphorylation [14-16]. Research has shown a direct correlation between NRTI phosphorylation and mitochondrial toxicity induced by NRTI use [14-16]. The bio-energetic energy demands of the tissue may be high, for example proximal tubule cells require higher cellular ATP levels due to the large amount of active transport carried out within the cell. For

this reason, proximal tubules are highly abundant in mitochondria, making them more susceptible to mitochondrial toxicity induced by NRTI's [16].

Studies have shown that specific genotypes make an individual more susceptible to the NRTI-induced toxicity [17-18]. For example one study showed that individuals with variations in the tumour necrosis factor (TNF) α promoter have increased associations with the onset of lipoatrophy [17-18]. Other genetic studies have shown that variations in mtDNA pol *y* itself can increase an individual's susceptibility to NRTI induced mitochondrial toxicity [19].

3.1.1 Mitochondrial DNA and its importance to cell survival

The mitochondria has its own DNA, making it unique compared to other organelles; this feature was first described in the 1960's [20]. MtDNA is a double-stranded circular DNA molecule that is around 16,000 bases. It codes for 13 polypeptides (such as membranes), 2 ribosomal RNAs and 22 transfer RNAs [21].

Mitochondrial diseases result from both mtDNA and nuclear DNA mutations or rearrangements, which mostly affect post-mitotic tissues [22]. Mitochondrial diseases can affect the following organs: bone marrow, skeletal / cardiac muscles, the kidneys, the central nervous system (CNS), the peripheral nervous system (PNS), the pancreas, the gastrointestinal tract and the liver [22].

Those diseases resulting from mtDNA mutations are inherited maternally and lead to diseases such as Pearson syndrome, which is a disease affecting the pancreas and bone marrow [23]. The diseases that arise due to mutations within the nuclear DNA are acquired and include diseases such as Alzheimer's which leads to impaired memory function [24].

There are currently 9 known polymerases that play a key role in the maintenance and replication of the cellular DNA; however, polymerase γ (pol γ) is the only polymerase responsible for mtDNA replication [25]. The genome for human pol γ was first studied, characterised and eventually cloned by Ropp and Copeland in the year 1996 [25]. *In vitro* studies have shown that when cells have depleted mtDNA, pol γ becomes expressed and translated as a protective mechanism within the cell [26]. Pol γ mediates both replication and repair of mtDNA, although until recently, it was believed that mtDNA had no capacity to repair itself [27].

In vitro studies have shown that toxicity affecting mtDNA pol γ will only present itself in patients after a threshold of mutated mitochondria is reached (**Figure 3.1**) [23]. In a normal healthy cell, the mitochondria are said to be in a homoplastic state. When the cellular mtDNA pol γ becomes inhibited due to toxicity (e.g. from exposure to NRTIs), some of the mitochondria become mutated and dysfunctional [23]. *In vitro* studies have shown that these dysfunctional mitochondrial populations can co-exist with normal mitochondria within cells in a state called heteroplasmy [23]. During cellular replication the segregation of the mitochondria is completely random; this leads to the production of daughter cells that contain different ratios of dysfunctional mitochondria. When the ratio of dysfunctional mitochondria is above the threshold for the specific tissue (which could be from 70 - 95 %) mitochondrial dysfunction will result [28].

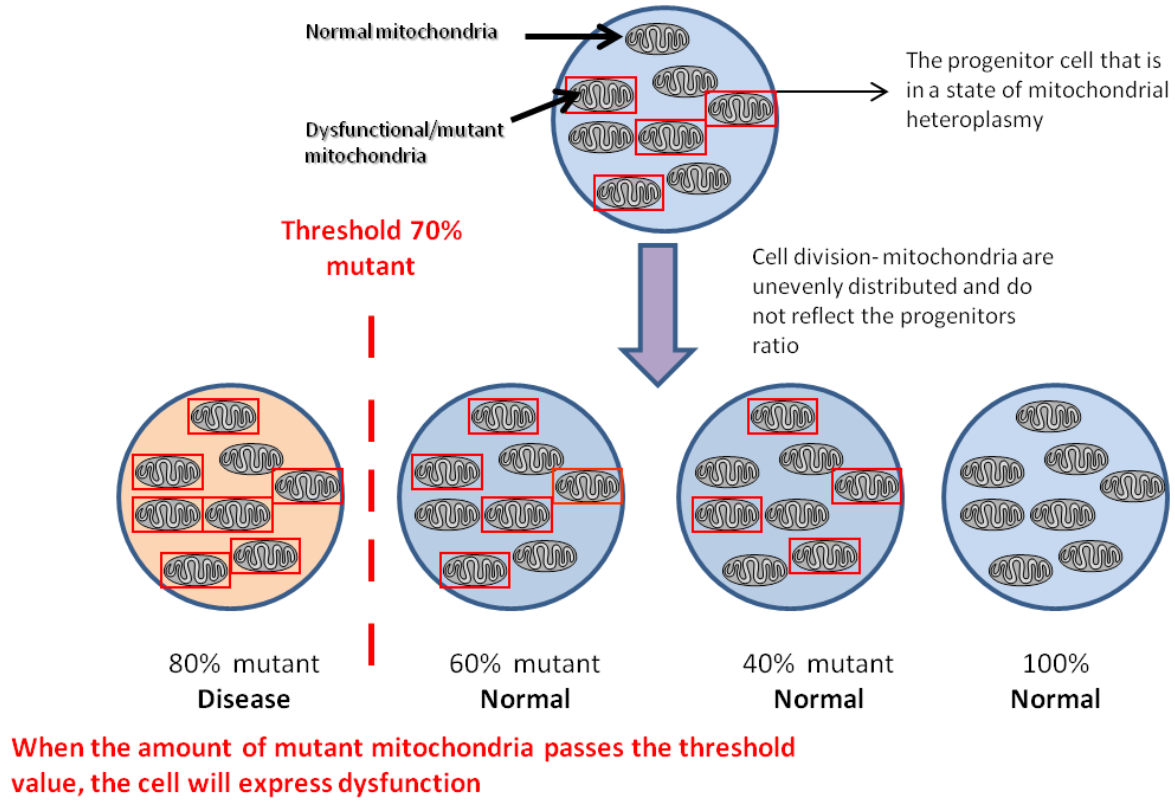

Figure 3.1: A schematic diagram showing the threshold effect within the mitochondria (modified from White *et al*., 2010)

3.1.2 Aims of Chapter

In this chapter the investigation of cytotoxicity induced by the antiretroviral drugs, tenofovir (TFV), Adefovir (ADEF) and Lamivudine (3TC) were assessed.

ADEF was manufactured by Gilead Sciences under the trade name of Preveon for the treatment of HIV. However, in 1999 its use as for HIV treatment was not granted by the Food and Drug Administration (FDA) and the development of this drug was discontinued [29]. The FDA did not approve its use at the doses needed for HIV treatment (60 - 120 mg) as at these doses of ADEF caused severe renal toxicity [29]. Gilead Sciences developed this drug for use as hepatitis B (HBV) treatment using a much lower dose of 10 mg under the trade name Hepsera [29]. The FDA approved this drug for HBV treatment on the 20th September 2002 and it was later approved for HBV treatment in the European Union (EU) in March 2003

[29]. Further studies into ADEF renal toxicity found that its primary cause was due to mitochondrial toxicity via the inhibition of mitochondrial pol γ [30]. As ADEF and TFV have similar structures (as seen in **Figure 3.2** below) with only the addition of a methyl group on TFV compared to ADEF, the adverse effects of ADEF may be mechanistically shared by TFV. Therefore, ADEF will be used as a positive control for mtDNA depletion and mitochondrial dysfunction. 3TC will be used as a negative control as previous studies have shown it to have no effect on the mitochondria [2]. The negative and positive controls were selected to keep the study focused around NRTI's as this is the drug class that TFV belongs to.

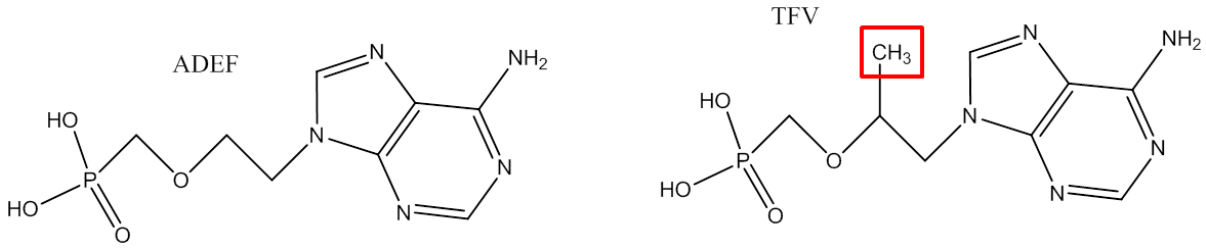

Figure 3.2: Structure of TFV and ADEF showing the extra methyl group on TFV

The first aim of this chapter was to establish a novel *in vitro* cell model in order to study NRTI cytotoxicity using aerobically modification *in vitro* cell models.

The cytotoxicity of ADEF, TFV and 3TC was assessed and compared using MTT, NR and ATP assays. The effects of ADEF and TFV on cellular ATP levels were determined as any change in ATP can give an indication of the effects of drugs on energy production specifically in the galactose-grown cells that are reliant on mitochondrial OXPHOS. The accumulation of TFV and ADEF was assessed using titrated ([^{3}H]) forms of the drugs.

The second aim of this study was to utilise this *in vitro* model to examine the effects of the antiretroviral TFV and ADEF upon mtDNA, using similar PCR methods as used in [31].

3.2 Materials and Methods

3.2.1 *Materials*

The cell culture media (DMEM high glucose and DMEM no glucose) were ordered from life technologies, Invitrogen (Paisley, UK) Hanks balanced salt solution (HBSS), 3-(4,5-Dimethylthiazol-2-yl)-2,5-diphenyltrazolium bromide (MTT), Sodium dodecyl sulphate (SDS), N-(2-Hydroxyethyl)piperazine-N′-(2-ethanesulfonic acid) (HEPES), sodium pyruvate, trypan blue (0.4%)solution, dimethylsulphoxide (DMSO), ethanol, acetic acid, Neutral Red, Adefovir, Lamivudine **,** n-dimethylformamide (DMF),Foetal bovine serum (FBS) andD-(+)-Galactose were all purchased from Sigma (Poole, UK). Tenofovir was ordered from Toronto Research Chemicals **(**Toronto, Canada). The probes were ordered from Applied Biosystems, (Warrington, UK) and the ATP bioluminescence kit was purchased from Roche (Hertfordshire, UK)

3.2.2 *Cell culture and experimental preparation*

As in section 2.2.2, Chapter 2. For > 5 day incubations the media + treatment (e.g. drug / vehicle) was removed and fresh media + treatment was added every 72 hours.

3.2.3 The assessment of cytotoxicity using MTT assays

As in section 2.2.3, Chapter 2. For > 5 day incubations the media + treatment (e.g. drug / vehicle) was removed and fresh media + treatment was added every 72 hours.

3.2.4 The assessment of cytotoxicity using Neutral Red assays

As in section 2.2.4, Chapter 2. For > 5 day incubations the media + treatment (e.g. drug / vehicle) was removed and fresh media + treatment was added every 72 hours.

3.2.5 The determination of cellular Tenofovir and Adefovir accumulation

As in section 2.2.5, Chapter 2, with a few modifications. The accumulation of both TFV ([^{3}H]-TFV) and ADEF ([^{3}H]-ADEF) will be determined. Accumulation studies will be carried out at both 37^{0}C and 4^{0}C. At 4^{0}C studies have shown that cellular transporters are not active therefore any passive transport of the antiretroviral drugs TFV and ADEF will be determined.

3.2.6 The luminescent analysis of cellular ATP.

A kit that is commercially available (Roche, Hertfordshire, UK) was used for the detection of cellular ATP. This ATP kit quantifies the phosphorylation of glycerol to generate a product that is detected by luminescent methods. The Kit was used according to manufactures instructions. The plate was read using a plate reader (MRX, Dynatech Laboratories).

3.2.7 The determination of cellular mtDNA and nuclear DNA levels using PCR methods

3.2.7.1 Identification of unique regions of the mitochondrial genome for use as primers / probes

The method found within [31] was followed, which utilised unique regions of the mitochondrial genome (**Table 3.1**) that are not replicated within the nuclear genome for quantification. This study used BLAST in order to find the regions of the mitochondrial genome that were duplicated within the nuclear genome and ENSEMBL was used to find those unique mitochondrial regions that were not duplicated within the nuclear genome [31]. The mitochondrial specific primer was synthesised at Sigma-Genosys UK, the predesigned

RNaseP taqman probe was used (Applied Biosystems) to determine nuclear DNA and the RLPO probe was used as a housekeeping gene (AppliedBiosystems)

Table 3.1: Primers and probes sequences used.

Gene accession number	primner / probe	Oligonucleotide sequence	Product size (bp)
Human mitochondrial genome NC_012920	hmito F3	CACTTTCCACACAGACATCA	129
	hmito R3	TGGTTAGGCTGGTGTTAGGG	
Human RNaseP AF479321	hRNaseP F1	CCCCGTTCTCTGGGAACTC	175
	hRNaseP R1	TGTATGAGACCACTCTTTCCCATA	

3.2.7.2 Genomic DNA preparation

Cellular genomic DNA was obtained using the QIAMP MINI DNA kit (Qiagen), following the manufacturer's instructions. The concentration of the DNA was adjusted to 10 ng / µl. Shearing was carried out, at least 100 ng / µl of DNA was passed repeatedly through a 1 mm needle for 25 seconds. DNA in a total volume of 100 ng / µl was subjected to sonication for 2–10 minutes using a Bath Sonicator (Kerry, Pulsa-tron 55). To avoid errors arising due to repeated freeze thaw cycles, the cellular DNA samples were kept at $4^{O}C$ for the duration of this study [31]

3.2.7.3 Real time qPCR

MtDNA and nuclear DNA were determined using probes specific to both regions. The RLPO probe was used as a house keeping gene in order to normalise both the mtDNA and nuclear DNA content. A 62-bp fragment of mtDNA was amplified using the following primers: hmito-319F5 and hmito-383R5, and hmitoP5 used as the hybridisation probe, containing the FAM (6-carboxy fluorescein) as a fluorescent reporter dye and NFQ as a quencher dye at the 30 end [31]. Nuclear content was quantified by targeting a unique region of the RNaseP gene, using the FAM™ dye–labelled probe (Applied Biosystems). The RLPO gene was determined using the VIC /TAMRA™ probe (Applied Biosystems). The PCR machine used was the Bio-

Rad / MJ Research Opticon 2 Real-Time PCR. Relative gene expression was calculated using the comparative C_T method also referred to as the $2^{-\Delta\Delta CT}$ method [32]. After C_T values were calculated, the mtDNA vs. nuclear DNA ratio was determined.

3.2.8 Statistical analysis

Statistical analysis was carried out on all data. Values are expressed as a mean $\pm$ standard deviation of the mean (SD), this is represented as error bars on all graphs. A Shapiro-Wilk test was first carried out on the data to see if it was considered normal. A Student's t-test was used for all normally distributed data and a Mann-Whitney U test was carried out on non-normally distributed data. All calculations were carried out using the StatsDirect software. Significance is indicated as follows * $P < 0.05$, ** $P < 0.01$, *** $P < 0.001$.

3.3 Results

3.3.1 The assessment of Tenofovir, Adefovir and Lamivudine-induced cytotoxicity using MTT assays.

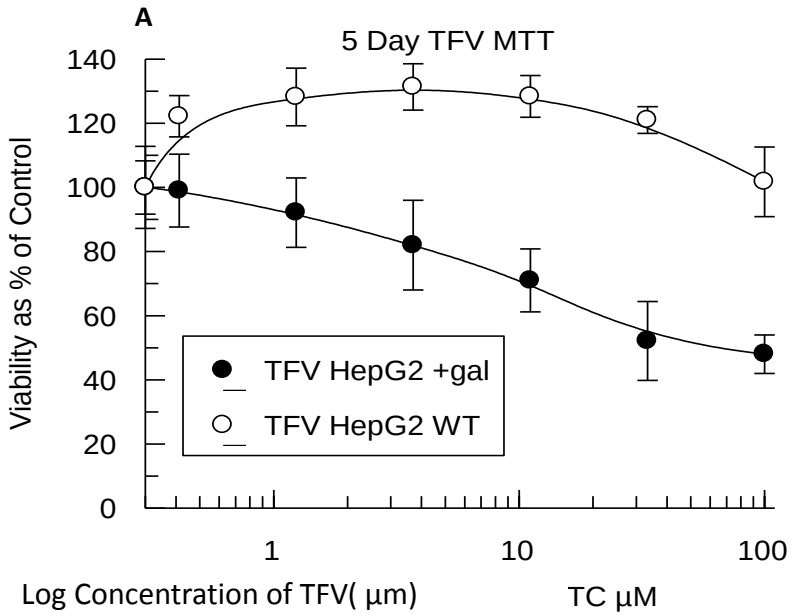

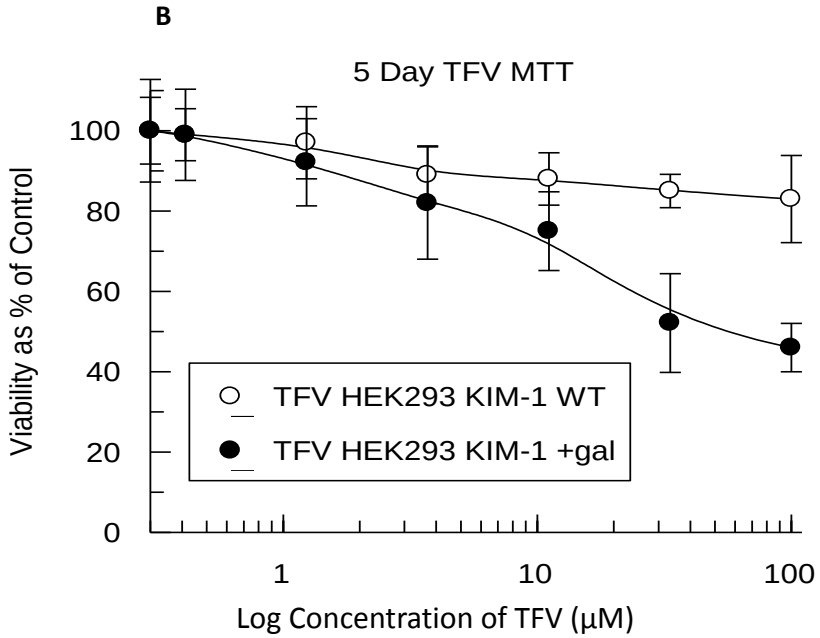

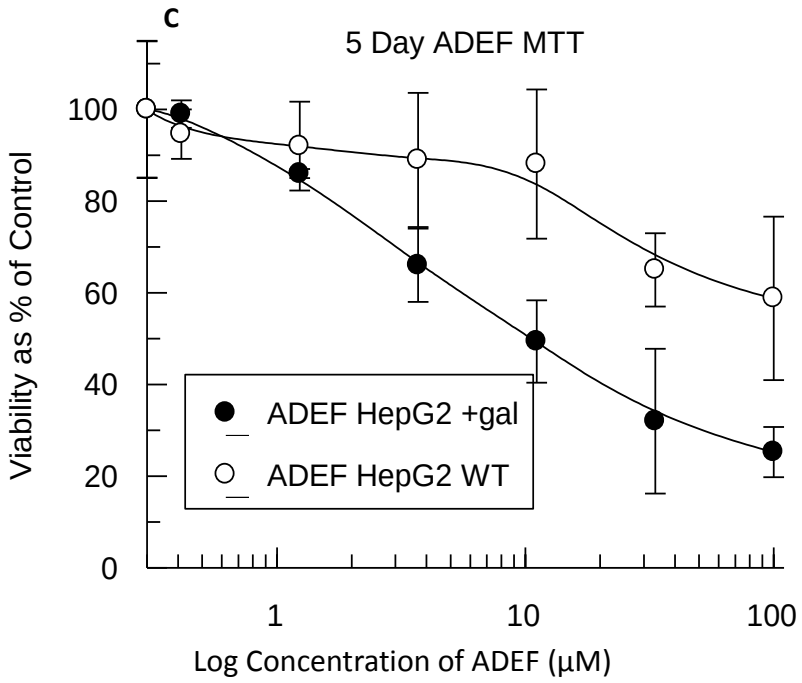
C
5 Day ADEF MTT
Viability as % of Control
100
80
60
40
20
0
1
10
100
Log Concentration of ADEF (µM)
ADEF HepG2 +gal
ADEF HepG2 WT

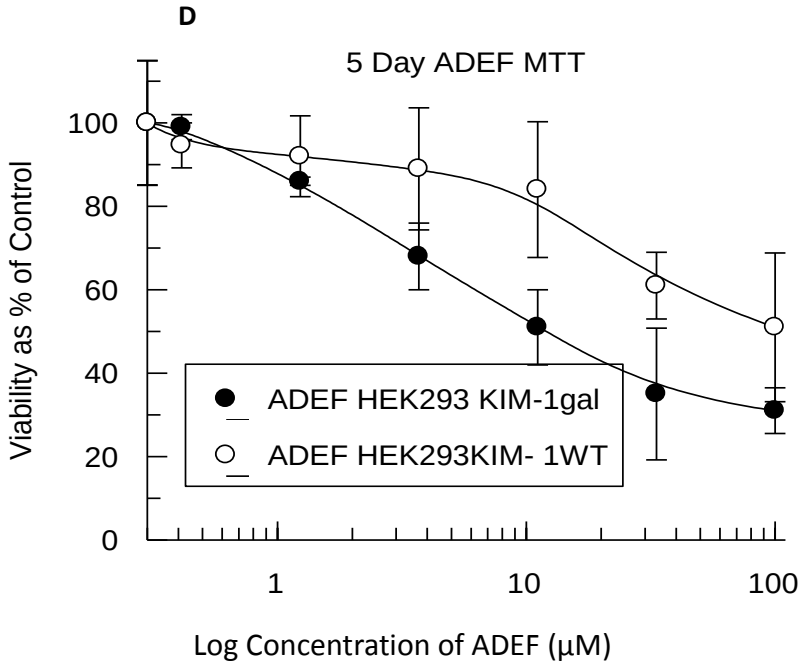
D
5 Day ADEF MTT
Viability as % of Control
100
80
60
40
20
0
1
10
100
Log Concentration of ADEF (µM)
ADEF HEK293 KIM-1gal
ADEF HEK293KIM- 1WT

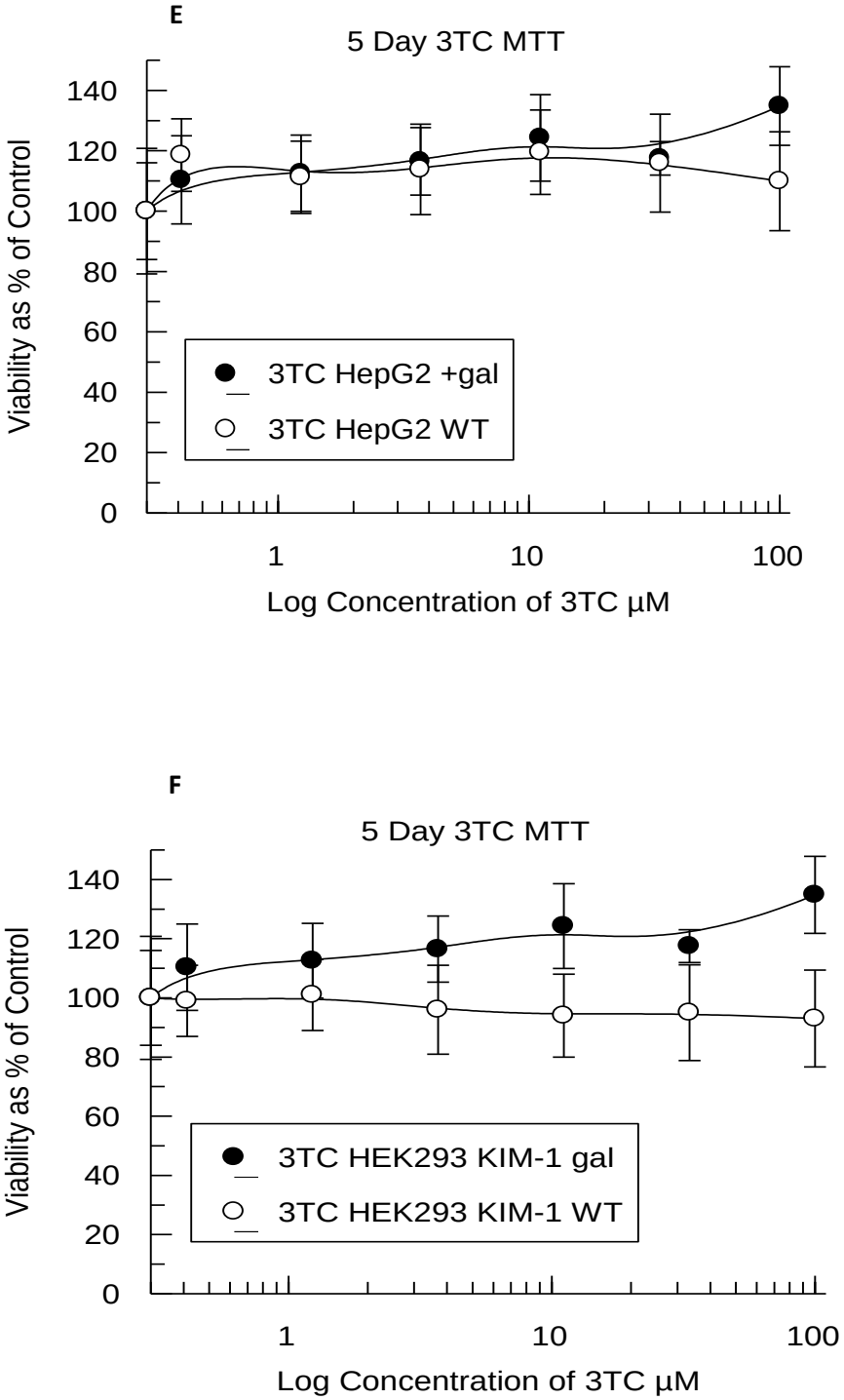

Figure 3.3 Dose-response curves of HepG2 and HEK 293 KIM-1 cells with TFV/ ADEF/3TC for 5 days A = HepG2 galactose /WT treated with TFV. **B** = HEK293 KIM-1 galactose / WT treated with TFV. **C** = HepG2 galactose /WT treated with ADEF. **D** = HEK293 KIM-1 galactose /WT treated with ADEF. **E** = HepG2 galactose/ WT treated with 3TC. **F** = HEK293 KIM-1 galactose / WT treated with 3TC. Results are the mean ± S.D of three or more independent experiments**.**

Table 3.2 Table showing EC50 values for MTT incubations of HepG2 / HEK293 KIM-1 galactose and HepG2 / HEK293 KIM-1 WT in the presence

MTT EC_{50} ± SE (µM)	TFV				ADEF				3TC			
	5 Day	10 Day	15 Day	20 Day	5 Day	10 Day	15 Day	20 Day	5 Day	10 Day	15 Day	20 Day
HepG2 Galactose	25.0 ± 8.5	12.8 ± 5.2	10.5 ± 6.6	9.5 ± 3.9	9.3 ± 1.8	9.4 ± 7.0	8.7 ± 7.7	8.0 ± 1.8	> 100	> 100	> 100	> 100
HepG2 WT	> 100	> 100	> 100	> 100	> 100	27.9 ±11.0	17.6 ± 2.4	13.1 ± 3.4	> 100	> 100	> 100	> 100
HEK 293 KIM-1 Galactose	38.4 ± 4.9	11.2 ± 7.8	10.9 ± 3.6	9.8 ± 2.7	9.1 ± 2.8	8.1 ± 6.1	7.1 ± 4.5	7.8 ± 2.7	> 100	> 100	> 100	> 100
HEK 293 KIM-1 WT	> 100	> 100	> 100	> 100	> 100	29.3 ± 6.3	15.3 ± 16.6	13.7 ± 10.0	> 100	> 100	> 100	> 100

Table 3.3 Table showing average control values for MTT incubations (5 -20 day) for HepG2/ HEK293 galactose and

Cell type	Average control value ± standard deviation			
	5 days	10 days	15 days	20 days
HepG2 Galactose	0.852 ± 0.54	0.824± 0.55	0.744 ± 0.51	0.754 ± 0.41
HepG2 WT	0.895 ± 0.85	0.867± 0.24	0.787 ± 0.24	0.798 ± 0.19
HEK293 KIM-1 Galactose	0.821 ± 0.95	0.793± 0.47	0.713± 0.73	0.785 ± 0.61
HEK293 KIM-1 WT	0.879 ± 0.21	0.851± 0.34	0.771± 0.11	0.759 ± 0.22

Table 3.4 A, B, C, D, E and **F. Show the statistical analysis** performed on the MTT data (5, 10, 15 and 20 days) for the HepG2 WT /HepG2 galactose-cultured cells[in the presence of TFV (**3.4A**), ADEF (**3.4 B**) and 3TC (**3.4C**)] and for the HEK 293 KIM-1 WT / HEK293 KIM-1 galactose-cultured cells[in the presence of TFV (**3.4D**), ADEF (**3.4 E**) and 3TC (**3.4F**)] Significance is indicated as follows * P < 0.05, ** P < 0.01, *** P < 0.001.

A

Incubation period (HepG2)	culture media	Concentration of TFV (µM) 0.1	1	5	10	50	100	WT vs Galactose
5 day	WT	-	-	-	-	-	-	**
	GAL	-	-	-	*	**	**	
10 day	WT	-	-	-	-	-	-	*
	GAL	-	-	-	*	*	*	
15 day	WT	-	-	-	-	-	-	**
	GAL	-	-	-	**	***	***	
20 day	WT	-	-	-	-	-	-	**
	GAL	-	-	**	**	***	***	

B

Incubation period (HepG2)	culture media	Concentration of ADEF (µM) 0.1	1	5	10	50	100	WT vs Galactose
5 day	WT	-	-	*	**	***	***	*
	GAL	-	-	-	-	**	**	
10 day	WT	-	-	-	*	**	**	-
	GAL	-	-	-	**	***	**	
15 day	WT	-	-	**	**	**	**	*
	GAL	-	-	**	***	***	***	
20 day	WT	-	-	**	**	**	**	*
	GAL	-	-	**	***	***	***	

C

Incubation period (HepG2)	culture media	Concentration of 3TC (µM) 0.1	1	5	10	50	100	WT vs Galactose
5 day	WT	-	-	-	-	-	-	*
	GAL	-	-	-	-	*	*	
10 day	WT	-	-	-	-	-	-	-
	GAL	-	-	-	-	-	-	
15 day	WT	-	-	-	-	-	-	-
	GAL	-	-	-	-	-	-	
20 day	WT	-	-	-	-	-	-	-
	GAL	-	-	-	-	-	-	

D

Incubation period (HepG2)	culture media	Concentration of TFV (µM) 0.1	1	5	10	50	100	WT vs Galactose
5 day	WT	-	-	-	-	-	-	**
	GAL	-	-	-	-	**	**	
10 day	WT	-	-	-	-	-	-	*
	GAL	-	-	-	*	*	**	
15 day	WT	-	-	-	-	*	-	**
	GAL	-	-	*	**	**	**	
20 day	WT	-	-	-	-	-	-	**
	GAL	-	-	**	**	**	***	

E

Incubation period (HepG2)	culture media	Concentration of ADEF (µM) 0.1	1	5	10	50	100	WT vs Galactose
5 day	WT	-	-	-	-	*	*	*
	GAL	-	-	-	*	**	***	
10 day	WT	-	-	-	*	**	***	-
	GAL	-	-	-	**	***	***	
15 day	WT	-	-	-	*	*	**	*
	GAL	-	-	-	**	***	***	
20 day	WT	-	-	*	**	**	***	*
	GAL	-	-	**	**	***	***	

F

Incubation period (HepG2)	culture media	Concentration of 3TC (µM) 0.1	1	5	10	50	100	WT vs Galactose
5 day	WT	-	-	-	-	-	-	*
	GAL	-	-	-	-	*	*	
10 day	WT	-	-	-	-	-	-	-
	GAL	-	-	-	-	-	-	
15 day	WT	-	-	-	-	-	-	-
	GAL	-	-	-	-	-	-	
20 day	WT	-	-	-	-	-	-	-
	GAL	-	-	-	-	-	-	

The dose response data showing the determination of TFV induced cytotoxicity via MTT analysis (**Figures 3.3 A- 3.3F / Tables 3.2, 3.4A-3.4F**) show that TFV induces cytotoxicity in a time and dose dependent manner within the galactose grown HepG2 and HEK293 KIM-1 cells. TFV cytotoxicity is only seen after 5 days as shown in **Figures 3.3 A** and **B** where the EC_{50} for the HepG2 galactose cells is 25.1µM and for the HEK293 KIM-1 galactose cells the EC_{50} was 38.4 µM (for the WT cells of both cell lines the EC_{50} was >100 µM). The EC_{50} value reduces for both cells lines grown in galactose media as the incubation time increases, for the HepG2 galactose cells the EC_{50} at 20 days is 9.5 µM and for the HEK293 KIM-1 galactose cells the EC_{50} at 20 days the EC50 is 9.8 µM. The EC_{50} for the WT of both cell lines remains at > 100 µM for all incubation periods. This demonstrated that the galactose cultured cells have become more susceptible to toxicity.

The dose response data showing the determination of ADEF induced cytotoxicity measured by MTT analysis (**Figures 3.3 C** and **D**) demonstrate that ADEF induces time and dose dependent cytotoxicity in both HepG2 / HEK293 KIM-1 cells grown in glucose and galactose media. This is demonstrated after 5 days when the maximal EC_{50} is reached for the galactose cultured for the HepG2 galactose cells the EC_{50} is 9.3, and for the HEK293 KIM-1 galactose cells the EC_{50} 9.1 µM. However for the HepG2 / HEK293 KIM-1 WT the maximal EC_{50} value is not observed until 10 days when the EC_{50} for the HepG2 WT cells is 27.9 µM, and for the HEK293 KIM-1 WT the EC_{50} is 29.3 µM (**Table 3.2**).

The dose response data showing the determination of 3TC induced cytotoxicity measured by MTT analysis (**Figures 3.2 E** and **F**) shows that 3TC did not cause any cytotoxicity at all incubation periods in these cell lines, this can be seen by the EC_{50} values (**Table 3.2**) which remain at > 100 µM for all cell lines at all incubation periods.

3.3.2 The assessment of cytotoxicity using Neutral red assays in the presence of Tenofovir, Adefovir and Lamivudine

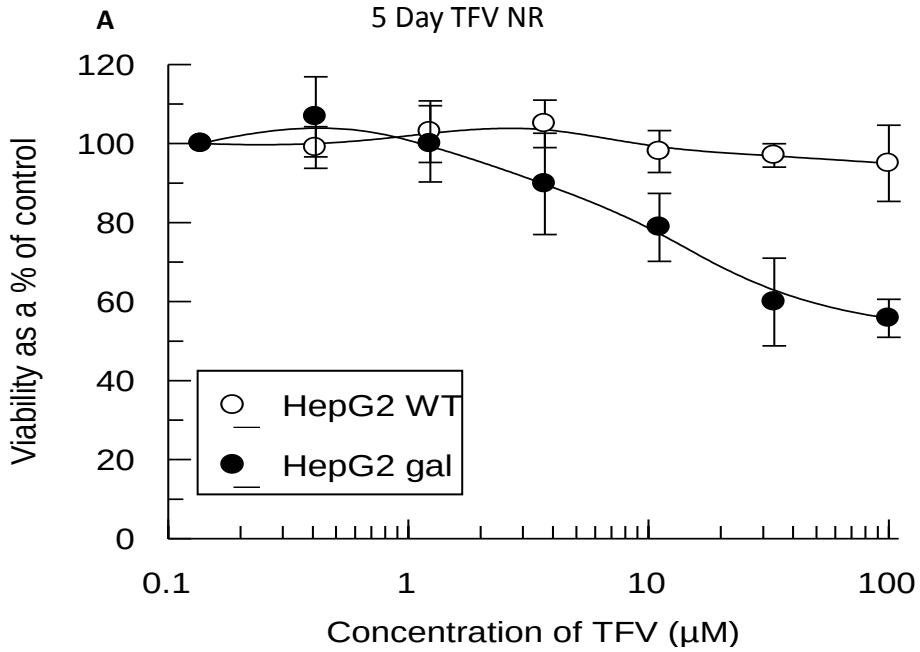

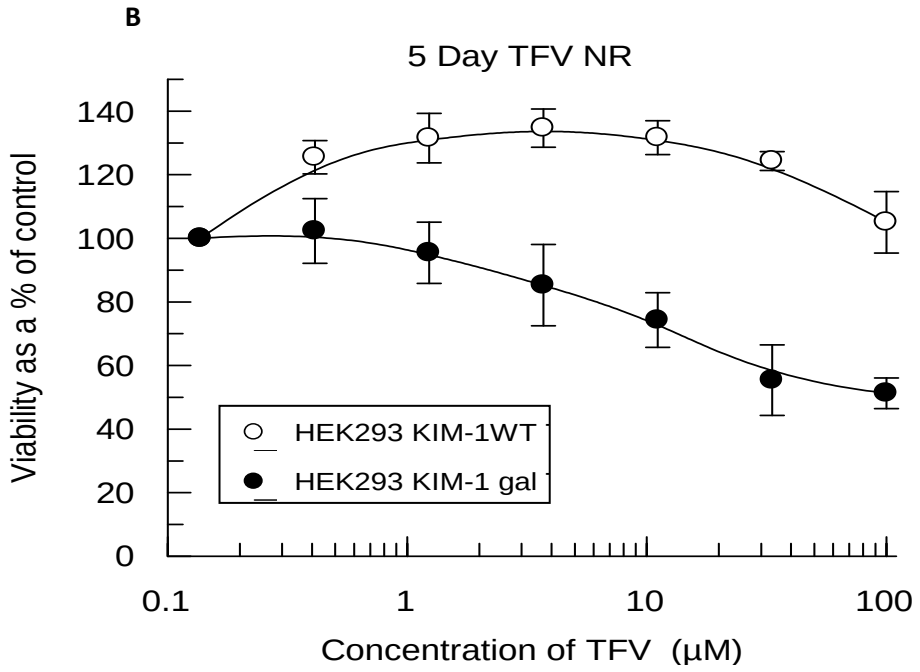

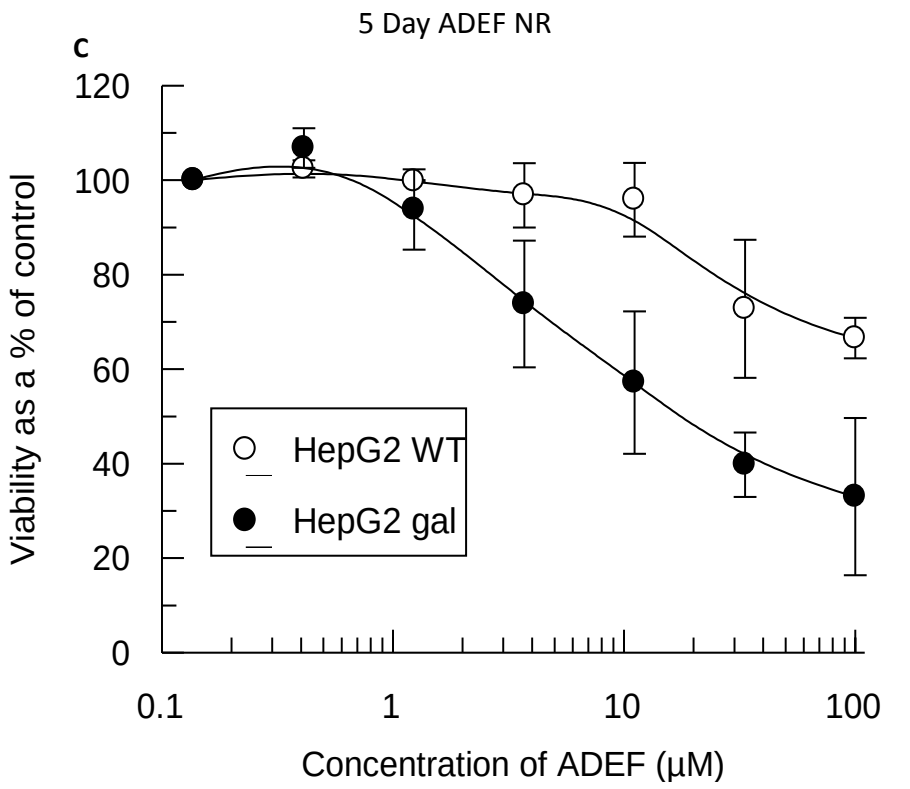
C
5 Day ADEF NR
120
100
80
60
40
20
0
Viability as a % of control
HepG2 WT
HepG2 gal
0.1
1
10
100
Concentration of ADEF (µM)

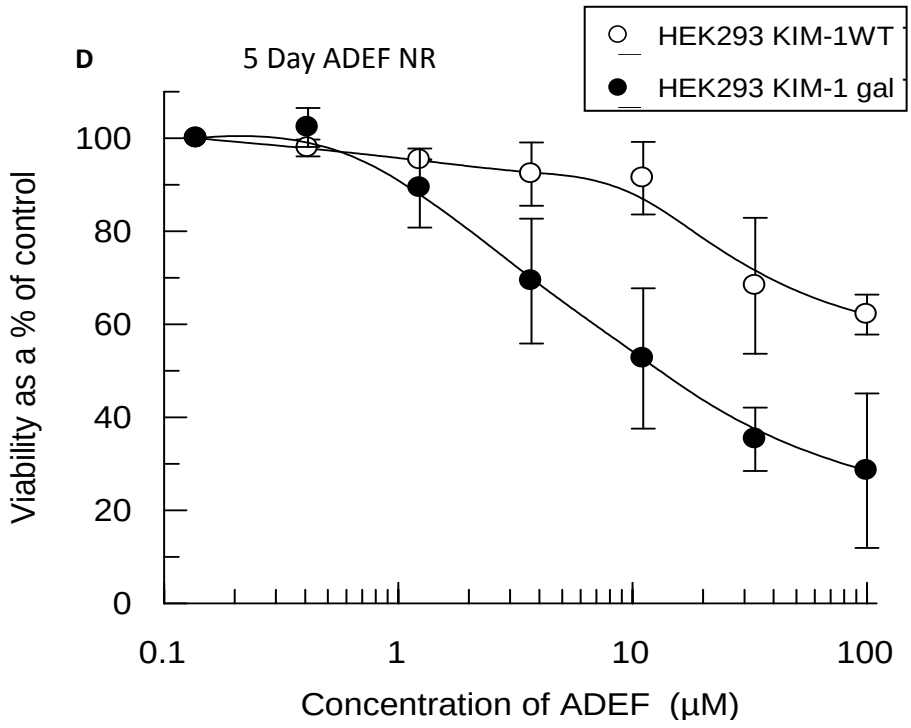
D
5 Day ADEF NR
HEK293 KIM-1WT
HEK293 KIM-1 gal
100
80
60
40
20
0
Viability as a % of control
0.1
1
10
100
Concentration of ADEF (µM)

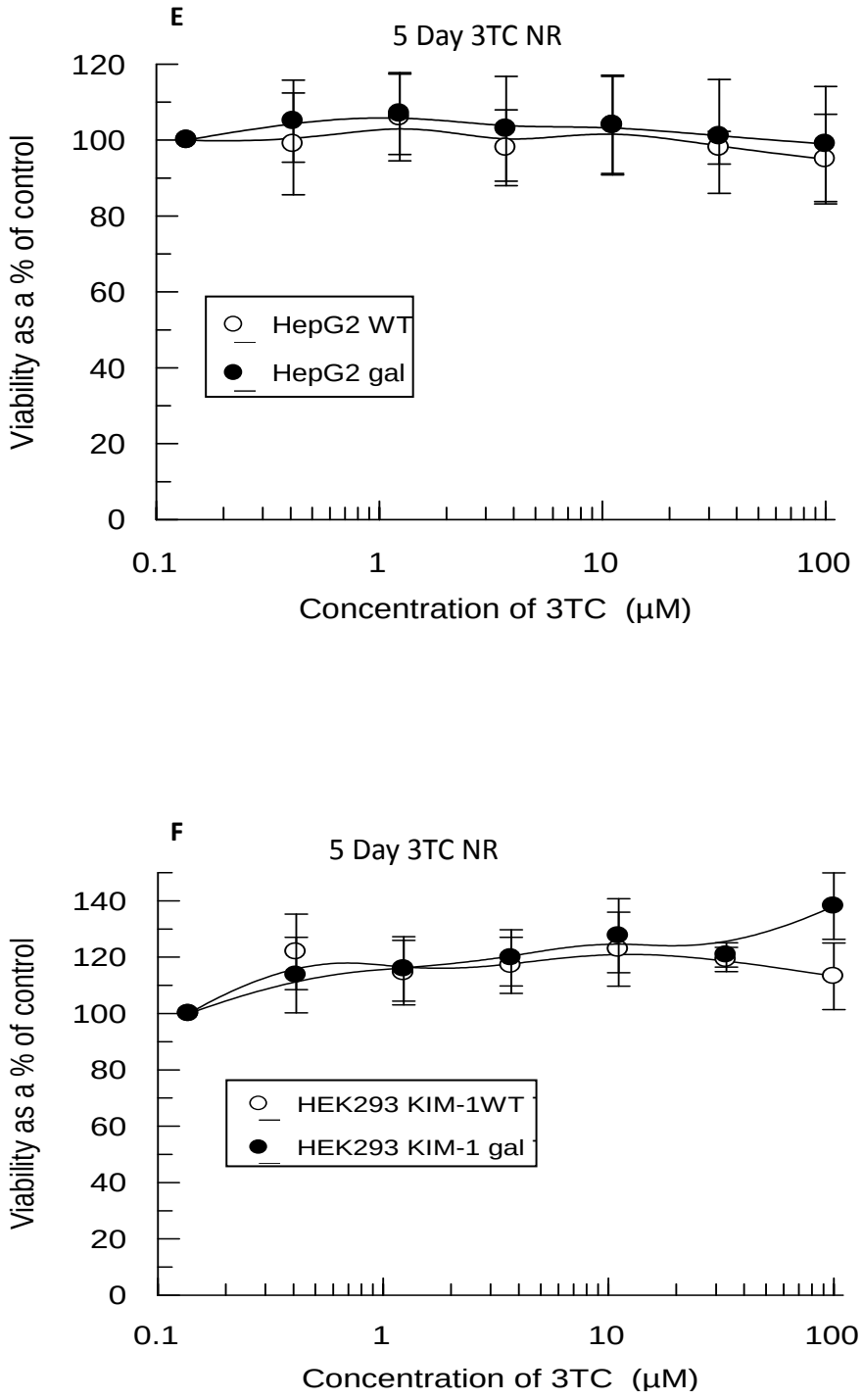

Figure 3.4 Dose-response curves of HepG2 and HEK 293 KIM-1 cells with TFV/ ADEF/3TC for 5 days A = HepG2 galactose / WT treated with TFV. **B** = HEK293 KIM-1 galactose / WT treated with TFV. **C** = HepG2 galactose / WT treated with ADEF. **D** = HEK293 KIM-1 galactose WT treated with ADEF. **E** = HepG2 galactose / WT treated with 3TC. **F** = HEK293 KIM-1 galactose / WT treated with 3TC. Results are the mean ± S.D of three or more independent experiments.

Table 3.5 Table showing EC50 values for NR incubations of HepG2 / HEK293 KIM-1 galactose and HepG2 / HEK293 KIM-1 WT in the presence

Neutral Red EC_{50} ± SE (µM)	TFV				ADEF				3TC			
	5 Day	10 Day	15 Day	20 Day	5 Day	10 Day	15 Day	20 Day	5 Day	10 Day	15 Day	20 Day
HepG2 Galactose	54.9 ± 8.1	37.7 ± 3.3	28.5 ± 6.0	28.6 ± 6.0	12.7 ± 6.2	10.9 ± 16.4	13.8 ± 8.1	7.6 ± 6.6	> 100	> 100	> 100	> 100
HepG2 WT	> 100	> 100	> 100	> 100	> 100	36.8 ± 9.8	34.4 ± 12.6	26.6 ± 5.7	> 100	> 100	> 100	> 100
HEK 293 KIM-1 Galactose	53.0 ± 1.3	21.9 ± 3.2	18.9 ± 5.7	12.2 ± 2.6	11.3 ± 3.8	14.0 ± 1.3	14.9 ± 6.9	10.9 ± 1.4	> 100	> 100	> 100	> 100
HEK 293 KIM-1 WT	> 100	> 100	> 100	> 100	> 100	> 100	25.9 ± 8.5	18.8 ± 6.2	> 100	> 100	> 100	> 100

Table 3.6 Table showing average control values for NR incubations (5 -20 day) for HepG2/ HEK293 KIM-1 ga and

Cell type	Average control value ± standard deviation			
	5 days	10 days	15 days	20 days
HepG2 Galactose	1.002 ± 0.28	0.927± 0.9	0.857 ± 0.15	0.837 ± 0.46
HepG2 WT	1.045± 0.39	0.97± 0.84	0.9 ± 0.11	0.881 ± 0.57
HEK293 KIM-1 Galactose	0.971 ± 0 .43	0.896± 0.13	0.826 ± 0.54	0.806 ± 0.06
HEK293 KIM-1 WT	1.029± 0.10	0.954± 0.41	0.884± 0.17	0.864 ± 0.64

Table 3.7 A, B, C, D, E and **F. Show the statistical analysis** performed on the NR data for the HepG2 WT /HepG2 galactose-cultured cells[in the presence of TFV (**3.4A**), ADEF (**3.4 B**) and 3TC (**3.4C**)] and for the HEK 293 KIM-1 WT / HEK293 KIM-1 galactose-cultured cells[in the presence of TFV (**3.4D**), ADEF (**3.4 E**) and 3TC (**3.4F**)] Significance is indicated as follows * P < 0.05, ** P < 0.01, *** P < 0.001.

A

Incubation period (HepG2)	culture media	Concentration of TFV (µM) 0.1	1	5	10	50	100	WT vs Galactose
5 day	WT	-	-	-	-	-	-	**
	GAL	-	-	-	*	*	**	
10 day	WT	-	-	-	-	-	-	*
	GAL	-	-	-	**	**	**	
15 day	WT	-	-	-	-	-	-	**
	GAL	-	-	-	**	**	**	
20 day	WT	-	-	-	-	-	-	**
	GAL	-	-	*	**	**	***	

B

Incubation period (HepG2)	culture media	Concentration of ADEF (µM) 0.1	1	5	10	50	100	WT vs Galactose
5 day	WT	-	-	-	-	**	**	**
	GAL	-	-	*	*	*	**	
10 day	WT	-	-	-	-	-	-	*
	GAL	-	-	-	**	**	**	
15 day	WT	-	-	-	*	**	**	**
	GAL	-	-	-	**	**	**	
20 day	WT	-	-	-	*	**	**	*
	GAL	-	-	-	**	**	***	

C

Incubation period (HepG2)	culture media	Concentration of 3TC (µM) 0.1	1	5	10	50	100	WT vs Galactose
5 day	WT	-	-	-	-	-	-	-
	GAL	-	-	-	-	-	-	
10 day	WT	-	-	-	-	-	-	-
	GAL	-	-	-	-	-	-	
15 day	WT	-	-	-	-	-	-	-
	GAL	-	-	-	-	-	-	
20 day	WT	-	-	-	-	-	-	-
	GAL	-	-	-	-	-	-	

D

Incubation period (HepG2)	culture media	Concentration of TFV (µM) 0.1	1	5	10	50	100	WT vs Galactose
5 day	WT	-	-	-	-	-	-	**
	GAL	-	-	*	*	**	**	
10 day	WT	-	-	-	-	-	-	**
	GAL	-	-	-	**	**	**	
15 day	WT	-	-	-	-	-	-	**
	GAL	-	-	*	**	**	***	
20 day	WT	-	-	-	-	-	-	
	GAL	-	-	*	**	***	***	

E

Incubation period (HepG2)	culture media	Concentration of ADEF (µM) 0.1	1	5	10	50	100	WT vs Galactose
5 day	WT	-	-	-	-	*	*	*
	GAL	-	-	*	**	**	***	
10 day	WT	-	-	-	*	**	**	-
	GAL	-	-	*	**	**	***	
15 day	WT	-	-	*	**	**	***	-
	GAL	-	-	*	**	**	***	
20 day	WT	-	-	*	**	**	**	-
	GAL	-	-	*	**	**	***	

F

Incubation period (HepG2)	culture media	Concentration of 3TC (µM) 0.1	1	5	10	50	100	WT vs Galactose
5 day	WT	-	-	-	-	-	-	-
	GAL	-	-	-	-	-	-	
10 day	WT	-	-	-	-	-	-	-
	GAL	-	-	-	-	-	-	
15 day	WT	-	-	-	-	-	-	-
	GAL	-	-	-	-	-	-	
20 day	WT	-	-	-	-	-	-	-
	GAL	-	-	-	-	-	-	

The dose response data showing the determination of TFV induced cytotoxicity via NR analysis (**Figures 3.4 A** and **B and Table 3.5**) show that TFV causes cytotoxicity in a time and dose dependent manner within the galactose grown HepG2 and HEK293 KIM-1 cells. TFV cytotoxicity is seen after 5 days as shown in **Figures 3.4 A** and **B** where the EC_{50} for the HepG2 galactose cells is 54.9 µM and for the HEK293 KIM-1 galactose cells the EC_{50} was 53.0 µM (for the WT cells of both cell lines the EC_{50} was > 100 µM). The EC_{50} value reduces for both cells lines grown in galactose media as the incubation time increases, thus demonstrating their increased susceptibility. For the HepG2 galactose cells the EC_{50} at 20 days is 13.9 µM and in the HEK293 KIM-1 galactose cells the EC_{50} at 20 days is 12.2 µM. The EC_{50} for the WT of both cell lines remains at > 100 µM for all incubation periods.

The dose response data showing the determination of ADEF induced cytotoxicity measured by NR analysis (**Figures 3.4 C** and **D / Table 3.5**) demonstrated that ADEF causes time and dose dependent cytotoxicity in both HepG2 / HEK293 KIM-1 cells grown in glucose and galactose media. For the galactose grown cells the maximal EC_{50} (**Table 3.5**) was reached after 5 days. For the HepG2 galactose cells the EC_{50} at 5 days is 12.6 µM and for the HEK293 KIM-1 galactose cells the EC_{50} at 5 days is 11.3 µM. However for the HepG2 WT cells the maximal EC_{50} is not reached until 10 days when the EC_{50} is 36.8 µM. For the HEK293 KIM-1 WT the maximal EC_{50} was reached at 15 days when EC_{50} was 25.9 µM.

The dose response data showing the determination of 3TC induced cytotoxicity measured by MTT analysis (**Figures 3.4 E** and **F** / **Table 3.5**) shows that 3TC did not cause any cytotoxicity at all incubation periods in these cell lines, this can be seen by the EC_{50} values (**Table 3.3**), which remain at > 100 µM for all cell lines at all incubation periods.

3.3.3 The determination of cellular TFV and ADEF accumulation

3.3.3.1 Tenofovir and Adefovir accumulation at 37 ^{o}C

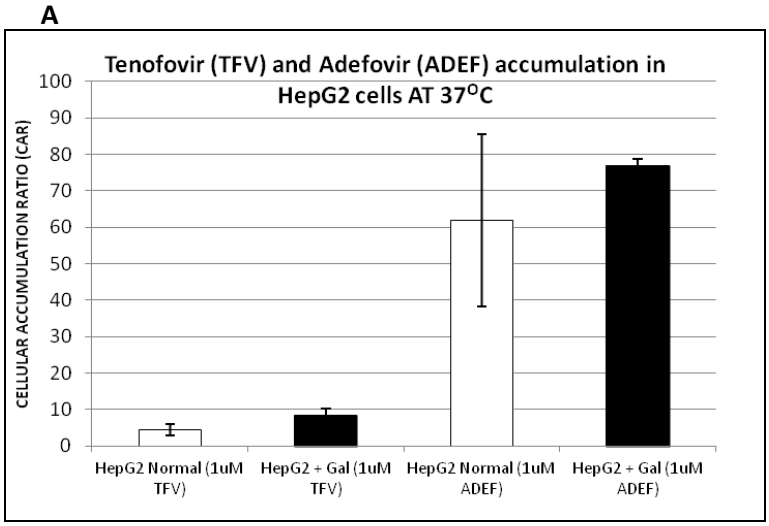

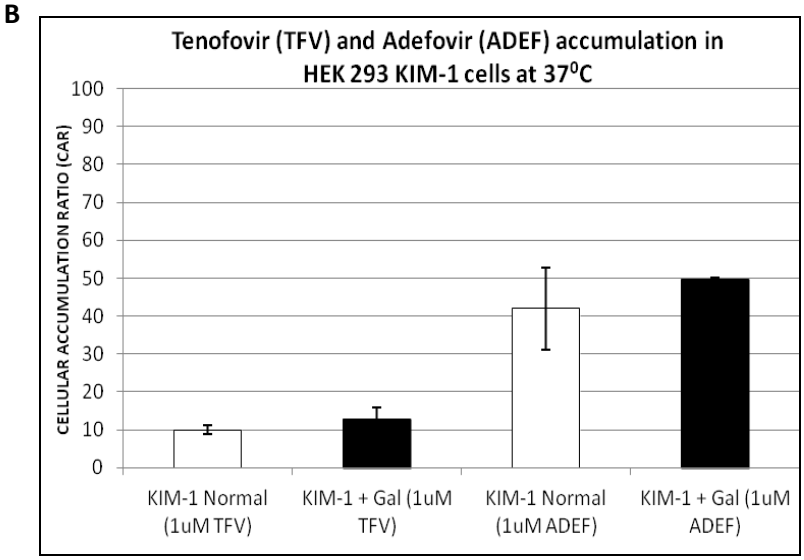

Figure 3.5 A and B. The assessment of TFV and ADEF accumulation within HepG2 WT and HepG2 galactose-cultures cells at 37^{o}C. A = accumulation of TFV and ADEF in HepG2 WT and HepG2 galactose cells for 1 hour. **B =** accumulation of TFV and ADEF in HEK293 KIM-1 WT and HEK293 KIM-1 galactose cells for 1 hour. Results are the mean $\pm$ S.D of three or more independent experiments.

The accumulation at 37^{o}C graphs show that there is almost 6 times more ADEF getting into the HepG2 WT cells compared to the HepG2 WT TFV accumulation. Also there is no significant difference between the accumulation of TFV or ADEF in the WT cells compared to the cells grown in galactose (**Figure 3.5A** and **B**).

3.3.3.2 Tenofovir and Adefovir accumulation at 4 ^{o}C

A

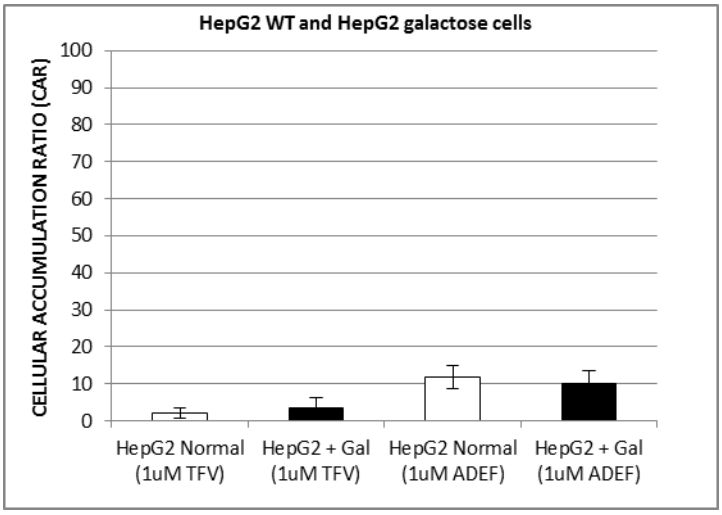

B

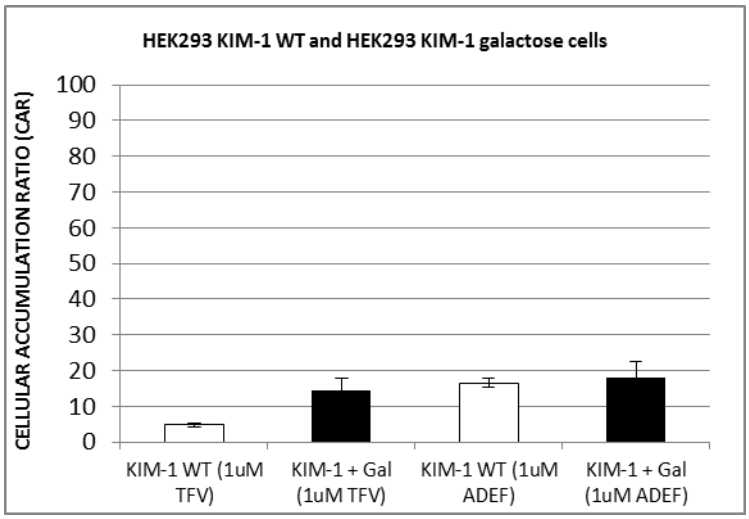

Figure 3.6 A and 3.6 B. The assessment of TFV and ADEF accumulation within HepG2 WT and HepG2 galactose-cultures cells at 4^{o}C. A= accumulation of TFV and ADEF in HepG2 WT and HepG2 galactose cells. **B=** accumulation of TFV and ADEF in HEK293 KIM-1 WT and HEK293 KIM-1 galactose cells. Results are the mean $\pm$ S.D of three or more independent experiments.

The accumulation at 4^{o}C graphs show that there no significant difference between ADEF and TFV accumulation in both cell lines. Also there is no significant difference between the accumulation of TFV or ADEF in the WT cells compared to the cells grown in galactose (**Figure 3.6 A** and **B**).

3.3.4 The luminescent analysis of cellular ATP in the presence of tenofovir and adefovir.

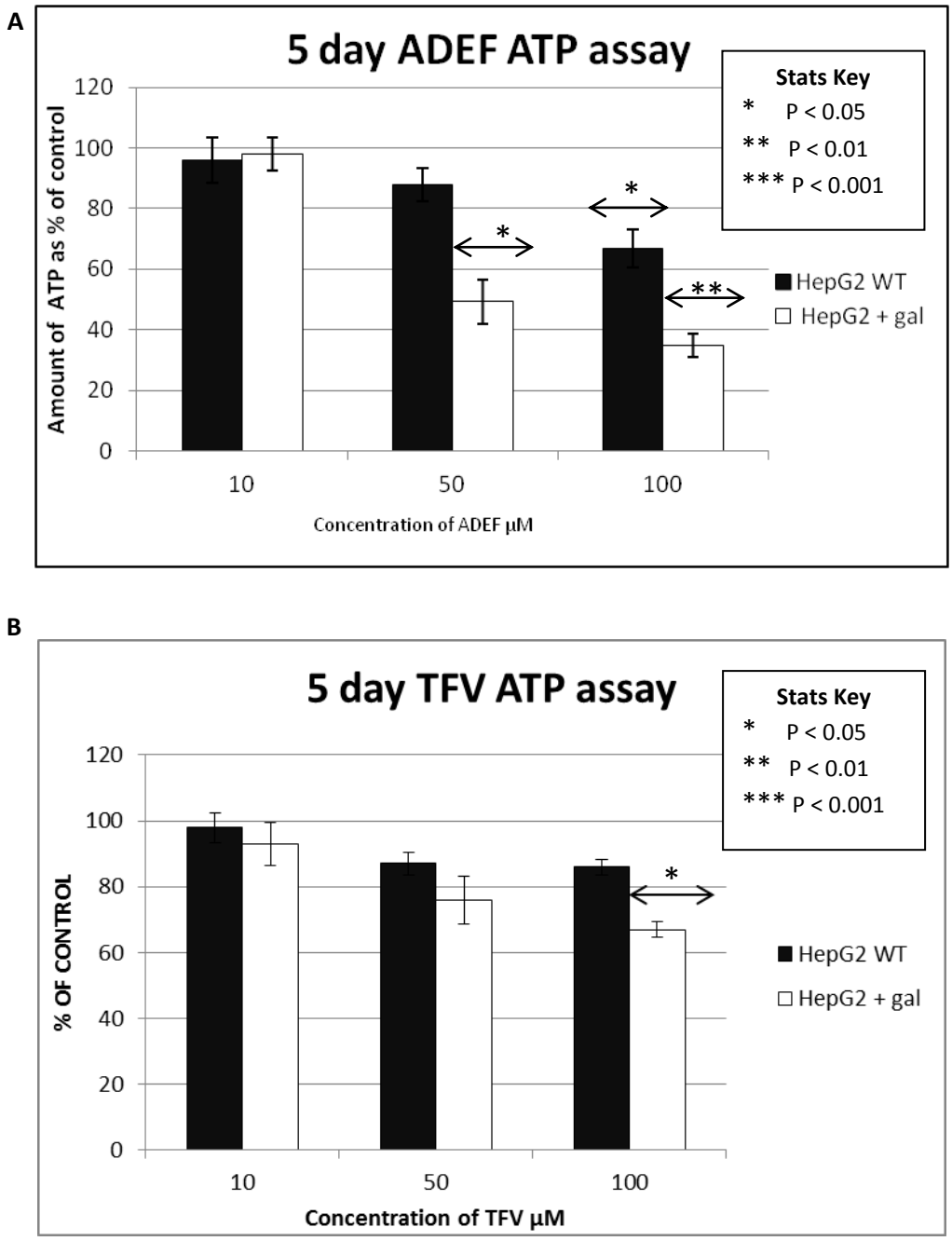

Figure 3.7 - ATP analysis of HepG2 cells treated with TFV. A = HepG2 galactose and Hepg2 WT treated with ADEF for 5 days. **B** = HepG2 galactose and HepG2 WT treated with TFV for 5 days. Results are the mean ± S.D of three or more independent experiments

ATP analysis demonstrated that ADEF causes significant reduction in the ATP levels in both the HepG2 WT (reduces to 65.4 %, a 1.5 fold reduction) and the HepG2 galactose (reduces to 37.9 %, a 2.64 fold decreased) cells at 50 μM (**Figure 3.7 A**). HepG2 cells treated with TFV caused a significant decrease in the cellular ATP levels in the HepG2 galactose cells (decreases to 65.4 %, a 1.5 fold decrease). At 100 μM TFV, however the HepG2 WT ATP levels were only decreased to 82.7 % which is not significant (**Figure 3.7 B**).

3.3.5 Effects of Tenofovir and Adefovir on cellular mtDNA and nuclear DNA levels using real-time PCR.

A

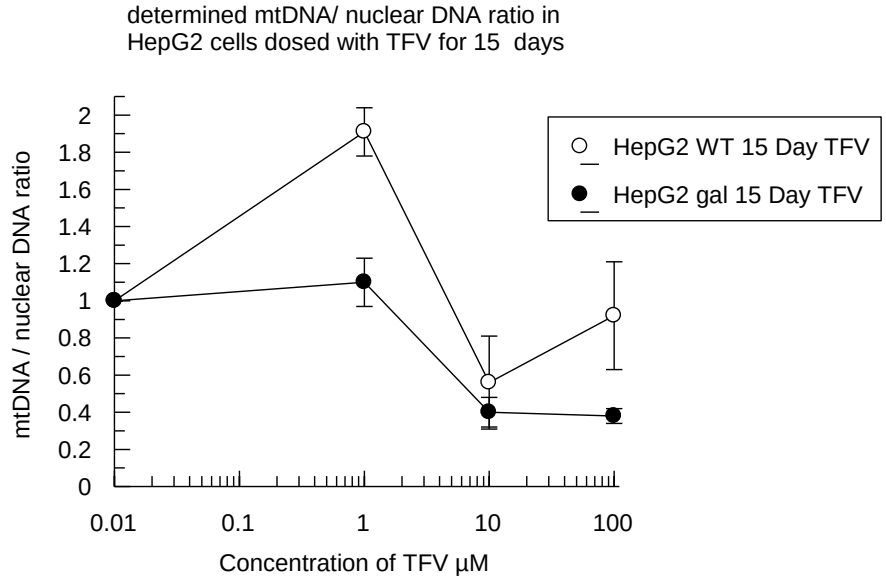

B

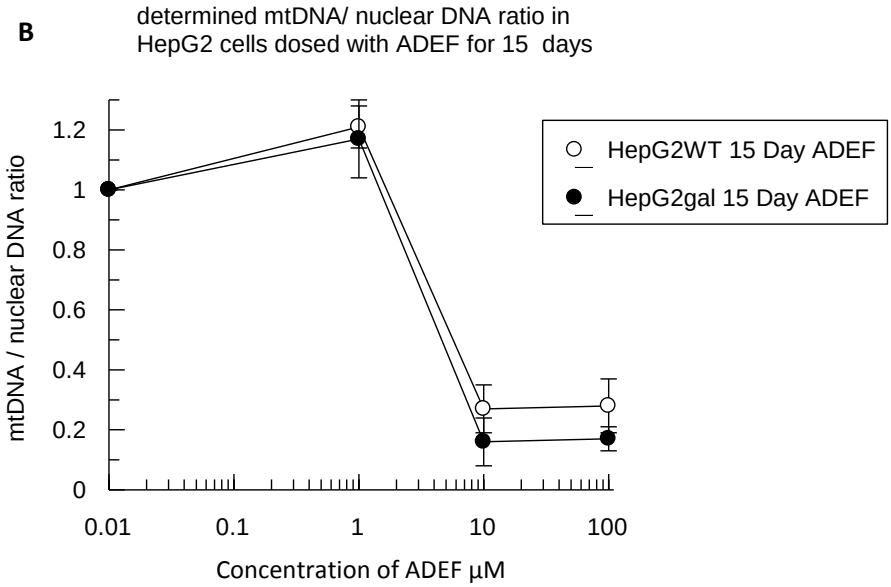

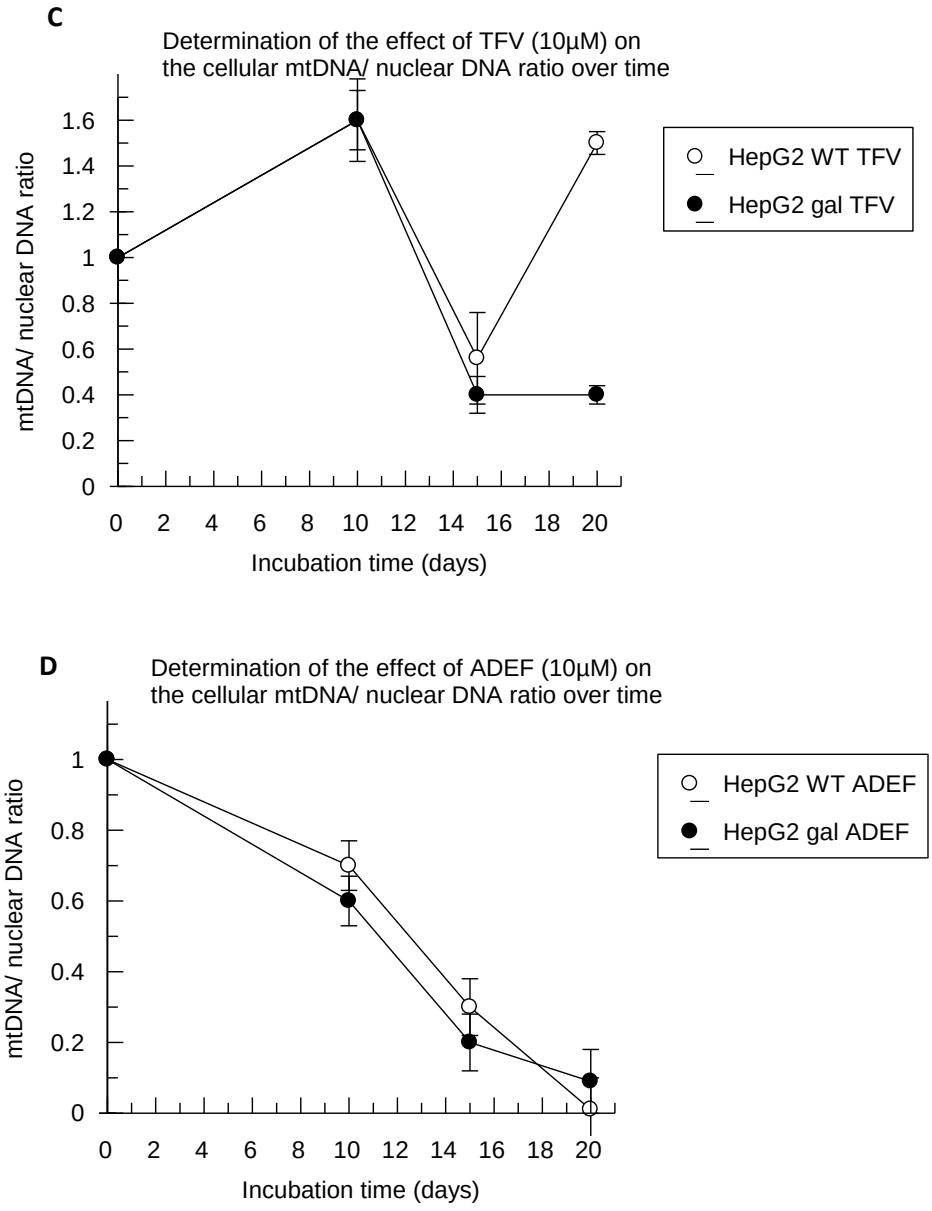

Figure 3.8: The effect of varying concentrations of TFV and ADEF on the mtDNA / nuclear DNA ratio and the effect of incubation length on mtDNA/ nuclear DNA ration upon treatment. **A** = HepG2 WT / galactose dosed with TFV for 15 days. **B** = HepG2 WT / galactose dosed with ADEF for 15 days **C** = HepG2 WT/ galactose dosed with TFV (10 μM) for 10, 15 and 20 days. **D** = HepG2 WT/ galactose dosed with ADEF (10 μM) for 10, 15 and 20 days.

MtDNA / nuclear DNA ratio in HepG2 cells in the presence of TFV were estimated (**Figure 3.8 A** and **C).** Results demonstrated that after an initial increase (> 1) TFV decreased this ratio in HepG2 galactose cells in a time dependant manner. This can be observed in **Figure 3.8 C** which shows a time course with a TFV (10 μM), at 10 days TFV dosing induced an increase in the mtDNA / nuclear DNA to 1.7, however at 15 and 20 days the mtDNA /

nuclear DNA ratio in the HepG2 galactose cells is lower in those cells dose with higher concentrations of TFV concentration increases (for the 20 day the ratio is 0.3). Interestingly the mtDNA / nuclear DNA ratio in HepG2 WT cells is higher after 10 days TFV (10 μM) dosing (**Figure 3.8C,** ratio > 1) , the ratio then reduces at the 15 day incubation (0.9) but for the 20 day incubation the mtDNA/ nuclear DNA ratio again increased to 1.6.

The determined mtDNA / nuclear DNA ratio in HepG2 cells dosed with ADEF (**Figure 3.8 B**and **D**), shows that after an initial increase in the ratio (> 1) ADEF reduces this ratio in a time dependant way for both the galactose and WT cells this is shown by the decrease in the ratio at each time point (**Figure 3.8D**). For example in the HepG2 galactose cells at 10 days the ratio was 0.6 (100 μM ADEF), at 15 days it decreases to 0.2 (100 μM ADEF) and finally at 20 days the mtDNA / nuclear DNA ratio decreases to 0.1 (100 μM ADEF). This effect was also seen within the HepG2 WT cells at 10 days the ratio was 0.7 (100 μM ADEF), the ratio then decreased to 0.3 at 15 days (100 μM ADEF), and finally at 20 days the mtDNA / nuclear DNA ratio decreases to 0.01(100 μM ADEF).

3.4 Discussion

In this chapter the cytotoxic effects and mechanisms of action of the antiretroviral drug TFV was investigated in human hepatic and renal cell lines. ADEF and 3TC were included as positive and negative controls, respectively [2-3].This is important as previous *in vitro* studies have not adequately demonstrated TFV cytotoxicity [33].

The cytotoxicity of these drugs was assessed using MTT and NR assays. The cytotoxicity data contained in this chapter demonstrated that ADEF causes cytotoxicity after 5 days incubation in both HepG2 / HEK293 KIM-1 galactose and WT cells. This cytotoxicity was dose and time dependent and increased as the incubation period increased. TFV caused slight cytotoxicity after 5 days in HepG2 /HEK293 KIM-1 galactose cells. This cytotoxicity increased at 10, 15 and 20 days.

3TC did not cause any cytotoxicity in HepG2 / HEK293 KIM-1 galactose or WT cells at the highest concentration tested (100 μM), which can be seen by the EC_{50} values for both MTT (**Table 3.2**) and NR (**Table 3.5**) as the EC_{50} remains at > 100 for all incubation periods and all concentrations of 3TC.

Previously, *in vitro* studies have not been able to reproduce that TFV does not cause any cytotoxicity [33]. Work within this chapter has shown that upon metabolic modification of the cell lines in order to make them more susceptible to mitotoxins TFV cytotoxicity can be seen from 5 days. This supports the original hypothesis that culturing the cells in galactose media would make them more susceptible to mitotoxins and therefore TFV induced mitochondrial dysfunction would become apparent. The cytotoxicity of TFV seems to have a delayed occurrence when compared to the cytotoxicity of ADEF, however at 15 and 20 days the EC_{50} values of TFV are similar to those of ADEF (**Tables 3.2** and **3.5**) showing that TFV caused time delayed mitochondrial dysfunction. Previous *in vitro* studies of TFV cytotoxicity

used immortalised cell lines that derive their energy from the glycolytic pathway. This makes the study of mitotoxins non-existent, as they have no impact on cellular growth or viability [34]. The models used within this chapter are novel and have not previously been used to study NRTI cytotoxicity. Therefore, these novel cell models, used within this chapter will be useful for future both within academia and in industry, to study NRTI-induced toxicity.

The accumulation of the antiretroviral drugs TFV and ADEF was studied in order to demonstrate that both drugs were entering the cells and to determine if any differential uptake may account for the differences in cytotoxicity. No previous studies regarding TFV / ADEF uptake into HepG2 or HEK293 KIM-1 cells have been reported. It was found that both drugs did accumulate appreciably within both cell lines (**Figures 3.5 A/B** and **3.6A/ B**). The accumulation study carried out at 4^{o}C showed that ADEF and TFV may enter the cell lines through the transporters not via passive diffusion, at this temperature when the transporters are not active the accumulation of both drugs decreased. The most interesting thing found in this study was that the accumulation of ADEF was 7 times higher than TFV accumulation (**Figure 3.5 B**) which may explain why TFV cytotoxicity is reduced and delayed when compared to ADEF cytotoxicity, as shown in the cytotoxicity assays within this chapter. As previously discussed, ADEF and TFV are analogues of each other with only an extra methyl group added to TFV when compared to ADEF (**Figure 3.2**). It could be that this extra methyl group reduces transport of TFV when compared to ADEF (**Figures 3.3 A** and **C**). The addition of the methyl group to TFV's structure does not affect physiochemical properties such as its viral inhibition, when compared to ADEF. It is a possibility that this extra methyl group decreases the affinity of TFV to the transporter in comparison to ADEF leading to a lower accumulation rate; however this will need to be investigated.

The effects of the antiretroviral drugs TFV and ADEF on cellular ATP levels were assessed as any change in cellular ATP could create a clearer picture of the type of cytotoxicity being

induced by these drugs. In the galactose cells ATP is only being synthesised via mitochondrial OXPHOS, therefore any determined effect on the ATP levels is reflective of the electron transport chain activity. A decrease in cellular ATP due to cytotoxicity is a hallmark of cell death via necrosis as apoptosis requires energy in order to proceed [35]. The decrease in ATP levels for the HepG2 galactose cells dosed with TFV for 5 days were not as prominent as expected when comparing the EC_{50} values determined via cytotoxicity assays at these time points, but is significant (**Figure 3.7B** and **Table 3.2**). This was unexpected and could be due to a protective effect taking place within the cells, and therefore preventing the reduction in cellular ATP. This protective effect could possibly be due to the up-regulation of pol γ [36].

The final step in this chapter was to determine whether the antiretroviral drugs TFV and ADEF induced a detrimental effect on mtDNA levels. This was done by estimating the mtDNA / nuclear DNA ratio. A decreased ratio indicates loss of mtDNA relative to nuclear DNA. Loss of mtDNA could be due to decreased mtDNA synthesis or due to a decrease in the quality of DNA; both are direct results of the inhibitation of pol γ [2-4]. ADEF is known as being an inhibitor of mitochondrial pol γ and therefore decreases cellular mtDNA levels [2-4]. As it has been hypothesised that TFV is also acting in a similar way to ADEF by inhibiting mitochondrial pol *y* the mtDNA / nuclear DNA ratios were determined using the comparative C_T method [32]. The results showed that ADEF caused a decrease in the mtDNA/ nuclear DNA ratios in HepG2 galactose and HepG2 WT from 10 days. The quotient point from this study was that TFV caused a significant decrease in the mtDNA / nuclear DNA ratio from 15 days in the HepG2 galactose cells. This data show that TFV is causing a decrease in this ratio which is similar but not as significant as ADEF's effects and this difference could be due to more ADEF being transported into the cell as shown in (**Figure 3.5A)**. The result showed that upon initial ADEF / TFV dosing, the mtDNA/ nuclear DNA

ratio increased. This increase could be due to the up-regulation of pol γ, which previous studies have shown to take place as a protective response when cellular mtDNA levels begin to decline [36]. The difference in response to TFV dosing between the HepG2 WT and HepG2 galactose could be due to a potential increase in mtDNA synthesis to support the continued dependence on the electron transport chain (ETC), as components from the ETC are encoded for by mtDNA. This could lead to an increased rate of accumulation of dysfunctional mitochondrial induced via TFV or ADEF. Previous studies have reported that TFV did not cause a decrease in cellular mtDNA levels *in vitro* [3]. The results determined within in this study are different to the results previously reported possibly because the cell model used here has been modified to better represent the aerobic conditions within human cells, thus making the cells more susceptible to TFV-induced mitochondrial dysfunction. Whilst the comparative C_T method used within this study to calculate the mtDNA / nuclear ratio is a widely used and valid method, another method that establishes the mtDNA/ nuclear DNA ratio via calculating the mitochondrial copy number vs. nuclear copy number has been recently cited as a more reliable method [31]. This method takes into account the structural variation that has been described recently as copy number variation. The variable copy numbers within a sample are determined and compared to a standard reference genome which has been reported as being more accurate method [31]. Recently the study of the mtDNA/ nuclear DNA ratio has been used clinically, within patient PBMC's as a biomarker for the early detection of mitochondrial dysfunction [31]. Future studies should look into this as a possible bio-marker for TFV induced mitochondrial dysfunction.

Overall the work presented within this chapter shows that TFV is inducing cytotoxicity that is causing cellular mitochondrial DNA depletion, this leads to a decrease in the cellular ATP levels, as mitochondria become dysfunctional and this could ultimately lead to cell death via necrosis. The cytotoxicity caused by TFV is similar to that induced by ADEF but is time

delayed and reduced in comparison; this difference could be due to differences in cellular accumulation as it was shown that ADEF has a higher accumulation rate.

Chapter Four

INVESTIGATION OF THE MECHANISM OF TENOFOVIR - INDUCED CELL DEATH IN HUMAN RENAL AND HEPATIC CELL LINES

Contents

4.1 Introduction

Cell death can proceed via three pathways, apoptosis (programmed cell death), necrosis and autophagy and all then contribute to the balance of cell cycle progression. Cell death can be caused by external or internal toxins that disrupt cellular physiology, leading to the death of the cell. Previous studies into the mechanism of TFV-induced cell death have had mixed results, therefore in this chapter, the study of TFV-induced cell death and its effects on cell cycle progression will be elucidated *in vitro* using the validated aerobically modified cell models used in previous chapters.

4.1.1 Apoptosis

Apoptosis or programmed cell death is essential for maintaining cellular homeostasis in multicellular organisms [1]. Apoptosis is key to maintaining cell numbers and to ensure that cells are positioned for optimal function within their specific tissues [1]. The process of apoptosis was first noted in 1972, when it was observed and described after scientists repeatedly found the same morphological features of cell death across many different cell types [2].

Apoptosis is highly conserved as it is such an important process [1]. Apoptosis is essential during development, as many more cells are produced than are needed. These excess cells are broken down via programmed cell death, which contributes to the sculpting of tissues and organs [1]. It is a tightly regulated and balanced physiological process, with disruption to the balance resulting in pathological conditions such as neurodegeneration, developmental defects, cancer or autoimmune diseases [3].

The characteristic features of apoptosis include blebbing of the cell membrane, condensation of chromatin, fragmentation of the DNA, cell shrinkage and the final step is cellular

engulfment via macrophages or neighbouring cells. The final step of apoptosis ensures that inflammatory responses in nearby tissues are avoided, hence the reason why apoptosis is defined as the 'clean' form of cell death [1].

There are two types of apoptosis in mammalian cells: the intrinsic pathway and the extrinsic pathway (**Figure 4.1**).

4.1.1.2 The extrinsic pathway.

The extrinsic pathway is mediated via the death receptor pathway. Death receptors are located on the cell surface and involve Fas, tumour necrosis factor (TNF) and TRAIL receptors [4]. Death receptors become activated by the extrinsic binding of death-inducing ligands (**Figure 4.1**). Once the death ligand binds to the death receptor, oligomerisation is induced and subsequent Fas-associated death domain (FADD) and caspase 8 are recruited to form a death-inducing signal complex (DISC) (**Figure 4.1**). The activation of caspase 8 leads to subsequent activation of effector caspases (caspase -3, -6 and -7). These effector caspases act down stream in the cell death programme, ultimately leading to the activation of cell death via apoptosis [4] (**Figure 4.1**).

4.1.1.4 The intrinsic apoptotic pathway.

The mitochondria act as the key regulators of the intrinsic apoptotic pathway. These pathways are activated inside the cell and evidence shows that the mitochondria act as the central regulators [5]. The essential mitochondrial change involved in the apoptotic pathway is the permeabilisation of the mitochondrial outer membrane (PMOM). PMOM is activated by family members of the Bcl-2 protein and leads to loss of essential functions [5]. Activation of PMOM leads to cell death via one of two mechanisms. The first mechanism is based upon

the release of pro-apoptotic molecules, most of which lead to the induction of caspases [5] (**Figure 4.1**).

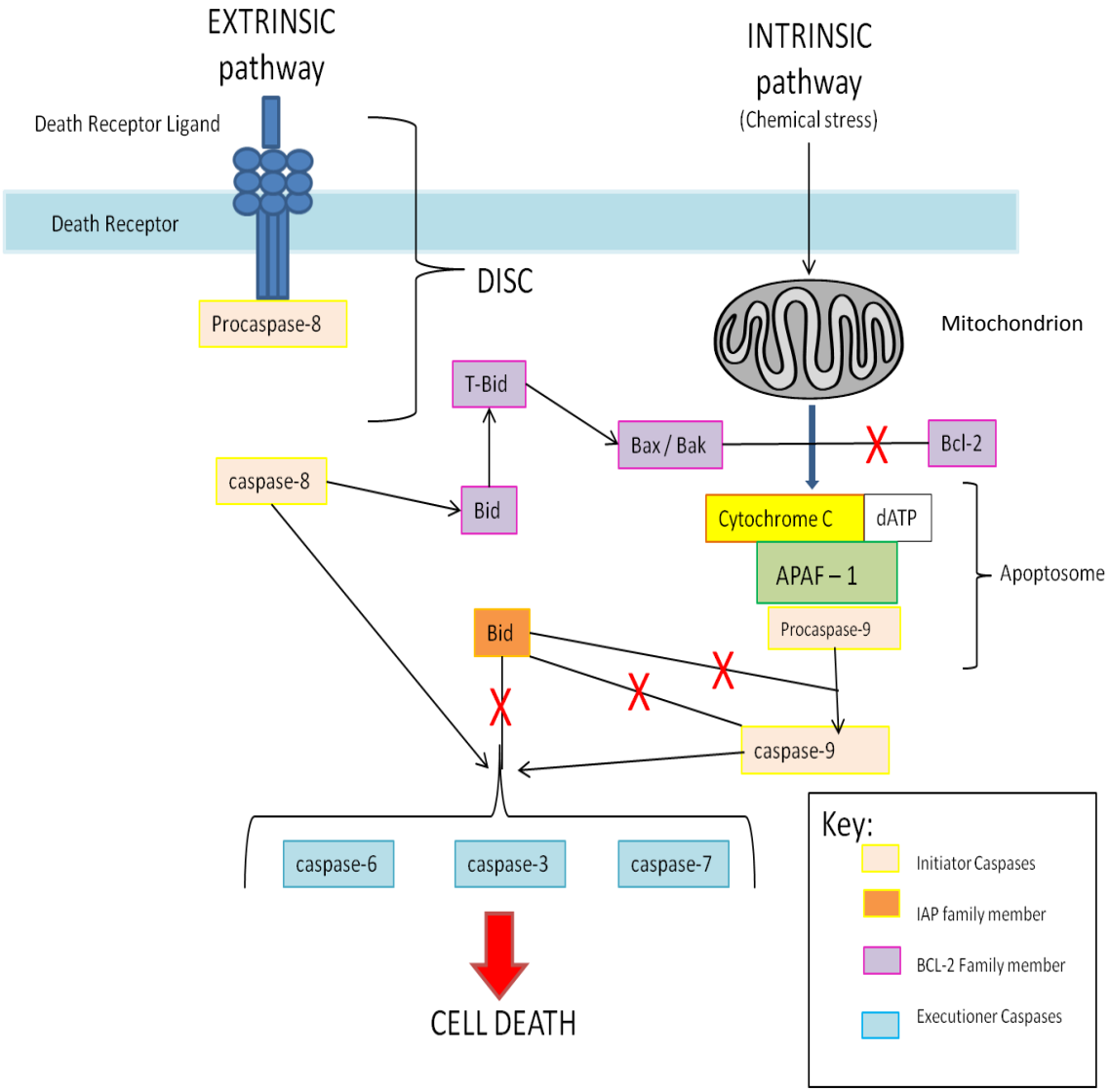

Figure 4.1 A schematic diagram of the apoptotic pathways (modified from a picture in the thesis of Amy Mercer). The red crosses show the point that the pathway can become inhibited

The main molecule released in this way is cytochrome c (**Figure 4.1**), which normally functions as an electron shuttle within the electron transport chain (ETC) [6]. Upon release it has been shown that cytochrome c binds to Apoptotic protease activating factor 1 (Apaf-1), forming an apoptosome once recruited along with caspase-9 (**Figure 4.1**). Caspase-9

becomes activated and subsequently leads to the activation of the executioner caspases-3, -6 and -7(**Figure 4.1**) [6].

The second mechanism is the disruption of the essential mitochondrial functions leading to cell death [1]. A Study has shown that drug induced tubular cell death (shown to be induced via TFV clinically), can proceed via the apoptotic and necrotic cell death pathways, determined via histological sections from the kidneys of patients who experienced drug induced proximal tubule dysfunction [7].

4.1.1.3 The caspase family

Caspases are essential initiators and executioners of the apoptosis pathway. Caspases make up a family of proteins; their activation is the main predecessor of apoptosis [8]. There are currently 14 mammalian caspases that have been identified, all share common features. These caspases can be separated into three main categories [8]. The first is made up of inflammatory caspases (caspase -1, -4, -5, -11, -12, -13 and -14) which are not associated with apoptosis. The second caspase group consists of apoptotic initiator caspases [8]. The initiator caspases have extended pro-domains that consist of either a death effector domain (DED) (caspase -8 and -10), or a caspase activation and recruitment domain (CARD) (caspase -2 and -9) (**Figure 4.1**). The CARD caspases interact with the adaptor molecules that are upstream in the extrinsic pathway. The final caspase group are known as the effector caspases (caspase -3, -6, and -7) (**Figure 4.1**). These characteristically contain a short pro-domain. The effector caspases become activated by upstream caspases in a cascade. Their activation leads to the start of the apoptotic execution process, which is found downstream and causes cleavage of the many cell substrates ultimately leading to cell death [8].

It has previously been shown that the pro-caspase-3 and pro-caspase-7 can become activated via the upstream initiator caspases (caspase -6, - 8, -9 and -10) (**Figure 4.1**) [9]. It was also

shown that effector caspases are found in greater abundance than the initiator caspases [9]. The importance of the executioner caspases has been demonstrated by genetic studies. Results demonstrated that the loss of caspase-3 leads to malfunction of the brain and premature death [10]. *In vivo,* animal studies showed that caspase-3 knock out (KO) mice could not activate apoptosis, when stimulated by the intrinsic and extrinsic apoptotic pathways; this leads to the survival of defective cells which could lead to pathological conditions such as cancer [10].

4.1.2 Necrosis

Necrosis differs form apoptosis as it is unregulated and is energy-independent [11]. Necrosis takes place when the physiological pathway needed for normal cellular homeostasis is disrupted. For example, energy production (ATP generation), ion transport and PH balance, disturbance to these processes leads to necrosis [11]. The key morphological characteristics of necrosis are the vacuolation of cellular cytoplasm, the plasma membrane breakdown and induced inflammatory response in the area around the dying cell, due to leakage of cellular contents and the pro-inflammatory molecules (e.g.TNF-α) [11]. The classical example of necrosis is ischemia, when oxygen levels are drastically depleted along with depletion of glucose and other key tropic factors. This dramatic depletion of essential cellular molecules leads to dramatically large levels of necrosis in the endothelial and non-proliferating cells that surround the ischemic tissue [12].

Studies have shown that necrosis not only occurs due to pathological events as mentioned above, but can also occur as a component of some physiological pathways [13]. It was shown that both apoptosis and necrosis play a key role in the renewal of enterocytes in the small intestine. Necrosis may take place instead of apoptosis when ATP levels become depleted as necrosis is shown to be ATP-independent [14].

Clinical studies on renal biopsies from patients receiving ADEF who developed acute renal failure showed ADEF-induced cell death via the necrotic pathway [15]. As ADEF and TFV have similar structures it is reasonable to assume that TFV may trigger the same cell death response.

4.1.3 Autophagy

A recent study reported that the antiretroviral drug Efavirenz (EFV), induced autophagy at clinically relevant concentrations [16]. EFV is a non-nucleoside reverse transcriptase inhibitor (NNRTI), which has previously been linked to the onset of mitochondrial dysfunction within hepatic cells [16-17]. The induction of autophagy via EFZ was shown within both Hep3B (primary hepatocytes) and HeLa cells [16].

It has been shown that autophagy is an intracellular catabolic mechanism that is mediated via the lysosomes [18]. Autophagy becomes stimulated due to cellular stresses, including oxidative stress, cell volume changes, starvation of the cell, disrupted hormonal signalling, increased concentrations of misfolded proteins, irradiation and xenobiotic treatments [19]. Autophagy is also induced in situations when apoptosis becomes inhibited which has been shown during in vitro studies using etoposide in Bax/ Bak double knockout mice [30]. Autophagy switches cells to a catabolic state that leads to degeneration of cellular components to produce energy for cellular survival during periods of depleted nutrients [14]. Upon activation of autophagy, the endoplasmic reticulum's membrane-bound double layered structures begins to undergo assembly and expansion. This leads to the formation of autophagosomes [20]. The function of autophagosome is to engulf materials in the cytosol; the autophagosome then binds and fuses to lysosomes [20]. The fusion with the lysosomes leads to the autophagosomal contents being degraded [20]. Evidence has shown that the

signalling pathway linked to the induction of autophagy includes phosphyatidylinositol-3-kinase (PI3K) and the kinase target of rampicin [20].

EFV-induced autophagy was determined via the detection of autophagic vacuoles and the presence of the specific autophagic marker proteins, microtubule-associated protein 1A/1B light chain 3 (LC-3) and Beclin-1 [16]. Using an autophagy inhibitor, showed that autophagy was acting as an adaptive mechanism of cell survival [16]. This study highlighted the importance of autophagy for cellular survival, the study of TFV and its possible induction of autophagy will be determined within this chapter.

A previous study has linked diseases such as neurodegenerative diseases, cancer and myopathies to alterations in the autophagic pathway [21]. Autophagy was first noticed in Saccharomyces Cerevisae yeast, which allowed better understanding of the autophagic pathway [22-23]. Studies have shown that upon caspase- 8 inhibition, autophagy is activated. This evidence shows that caspases are involved in the regulation of apoptotic and non-apoptotic cell death [23].

4.1.4 Aims of Chapter

Current evidence is conflicting with regards to TFV-induced cell death. Some *in vitro* studies using human primary renal proximal tubule cells, have shown that TFV does not cause apoptosis [24], however, an *in vitro* study that used the breast cancer cell line MCF-7 reported that TFV did not induce cytotoxicity, but induced morphological features that shows cell death was being induced via apoptosis [25]. Therefore the aim of this chapter is to elucidate the mechanism of cell death induced by TFV in the novel susceptible cell models. The effects of TFV on cell cycle progression were studied using propidium iodide (PI) staining. The effects of TFV on the status of the cell (viable, apoptotic or necrotic) was studied using a double staining method (annexin V / PI). The activation of cellular caspase-3 / -7 and reactive oxygen species (ROS) was determined in the presence of TFV. Mitochondrial depolarisation was studied in the presence of TFV using tetramethylrhodamine, ethyl ester (TMRE) staining. The potential role of autophagy due to TFV was studied using the autophagy inhibitor 3-methyladenine (3MA) and assessed by MTT assays.

4.2 Materials and Methods

4.2.1 Materials

The cell culture media (DMEM high glucose and DMEM no glucose) were ordered from life technologies, Invitrogen (Paisley, UK). All other reagents were purchased from Sigma-Aldrich (Poole, UK). Tenofovir was ordered from Toronto Research Chemicals **(**Toronto, Canada). The caspase -3/7 glo assay was purchased from Promega life sciences (Southampton, UK)

4.2.2 Cell culture and experimental preparation

As in section 2.2.2, Chapter 3. HepG2 cells were used for all cell death assays as they are well characterised for use as mechanistic tools to study cell death.

4.2.3 Analysis by flow cytometry.

Flow cytometry (FACs) was carried out using an Epics XL and XL MCL - Beckman Coulter, flow cytometry machine. The parameters were set using control cells, these were used to adjust the forward scatter (FS) and side scatter (SS), to obtain a population of viable cells, with a voltage threshold set to exclude cell debris (**Figure 4.2**). The FS is used to determine cell size and the SS is used to determine granularity. For all FACs experiments at least 5000 cells were analysed from each sample. The fluorescence channel FL-1 or FL-3 was used to measure fluorescence.

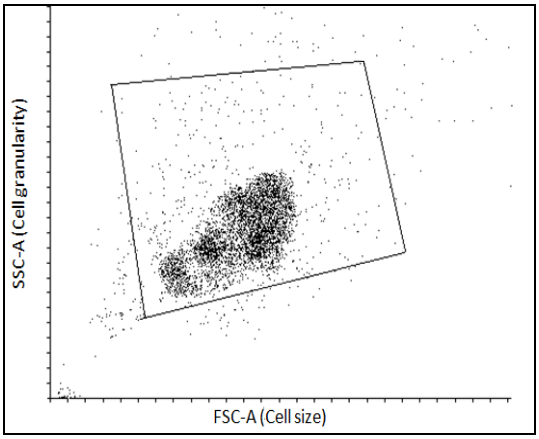

Figure 4.2: representation of cell gating to exclude cell debris

4.2.3.1 The determination of cellular DNA content using Propidium Iodide upon Tenofovir treatment.

Propidium iodide (PI) can be used to measure cellular DNA content, as it is a major groove binder of DNA. When it intercalates with DNA it produces a red fluorescence shift which can be detected [26].

The cells (4×10^5) that had been incubated (24 hours to 15 days) with the drugs (0 to 100 µM) were centrifuged (1400 rpm, 5 minutes). After centrifuging the supernatant was removed and the cells were washed twice in HBSS (1ml), by centrifugation (1400 rpm, 5 minutes). The supernatant was discarded and the cell pellet was resuspended in 70 % ice-cold ethanol (1 ml) and then frozen at $-4\ ^0$C (2 hours) to fix the cells. After 2 hrs the ethanol was removed and the cell pellet was resuspended in 1 ml of PI stock solution (1 % RNAse (50 µM), 1 % citric acid (380 µM)). The cells were then incubated for 30 minutes before being analysed using flow cytometry (Epics XL and XL MCL - Beckman Coulter, flow cytometry machine). The intensity of PI fluorescence was measured using the fluorescence channel, FL-3. The quantification of cells in each stage of the cell cycle was calculated from the DNA content of the cell using WinMDI, version 2.8. Etoposide (10 µM) was used as a positive control as it is a known inducer of apoptosis [27].

4.2.3.2 The determination of cell death using Annexin v / Propiduim Iodide upon Tenofovir treatment.

The annexin V and PI (annexinV/ PI kit from Sigma-Aldrich, Poole, UK) stains are used in conjunction in order to determine the cytotoxic status of the cells, apoptotic, necrotic, viable or in the state of secondary necrosis. The stains are able to do this through the differences in plasma membrane permeability and integrity upon exposure to damaging affects [26]. PI does not stain viable cells; its accumulation within the cell is dependent upon membrane permeability, and for this reason PI stains necrotic or secondary necrotic cells due to their loss of plasma / nuclear membranes. The loss of membranes allows PI to intercalate with cellular nucleic acids which releases a red shift in fluorescence [26]. During apoptosis, major changes take place to the cell surface. One of these changes involves the externalisation of phosphatidylserine (PS) [28]. Annexin V binds to phospholipids in a calcium-dependent manner, therefore annexin V stains for apoptotic and secondary necrotic cells [28].

The cells (4×10^5) that had been incubated (24 hours to 15 days) with the drugs (0 to 100µM) were centrifuged (1400 rpm, 5 minutes). After centrifuging the supernatant was removed and the cells were washed twice in HBSS (1ml) by centrifugation (1400 rpm, 5 minutes). The supernatant was discarded and the cell pellet was resuspended in 195 µl binding buffer and 5 µl annexin. The cells were then incubated in the dark (room temperature, 10 minutes). The samples were centrifuged (4000 rpm, 5 minutes); after centrifuging the supernatant was removed and the cells were washed twice in HBSS (1ml) by centrifugation (1400 rpm, 5 minutes). The supernatant was removed and the cells were re-suspended in 190 µl binding buffer and 10 µl PI. Then 600µl HBSS was added to the cells before being analysed on the flow cytometer (Epics XL and XL MCL - Beckman Coulter, flow cytometry machine). The FL1 channel was used and at least 5000 cells where counted. The proportion of cells in the

different cellular states (viable, apoptotic, necrotic and secondary necrotic) were quantified and data were analysed using WinMDI, version 2.8. Etoposide (10 µM) was used as a positive control as it is a known inducer of apoptosis [27]

4.2.3.3 The determination of cellular mitochondrial depolarisation using tetramethylrhodamine ethyl ester upon Tenofovir treatment.

Tetramethylrhodamine ethyl ester (TMRE) was used to determine mitochondrial depolarisation of cells. TMRE is a positively charged, red dye that is cell membrane-permeable; it labels active mitochondria due to their negative charge. Accumulation of TMRE causes a red shift in TMRE's absorption and fluorescence spectra. Mitochondria that have become depolarised due to cytotoxicity, experience a decrease in membrane potential, therefore the accumulation of TMRE decreases and a decrease in fluorescence can be detected [29].

The cells (4×10^5) that had been incubated (24 hours to 15 days) with the drugs (0 to 100µM were centrifuged (1400 rpm, 5 minutes). The supernatant was removed and the cells were washed twice in 1ml HBSS by centrifugation (1400 rpm, 5 minutes). The supernatant was discarded and the cell pellet was resuspended in TMRE solution (50 µM, 500µl). The samples were then incubated (37 ^{0}C for 10 mins) before being analysed on the FACs machine. The intensity of TMRE fluorescence was measured using the fluorescence channel, FL-3. The quantification of cellular mitochondrial depolarisation was calculated from the TMRE content of the cell using WinMDI, version 2.8. Etoposide (10 µM) was used as a positive control as it is a known inducer of apoptosis [27]

4.2.3.4 The determination of cellular superoxide reactive oxygen species content using dihydroethidium upon Tenofovir treatment.

Dihydroethidium (DHE) was used to determine cellular superoxide ROS content. DHE is cell permeable; when it comes into contact with superoxide anions within the cell it forms the red fluorescent product 2-hydroxyethidium. The production of 2-hydroxyethidium can be detected via a red shift in the fluorescence spectra [31].

The cells (4×10^5) that had been incubated (24 hours to 15 days) with the drugs (0 to 100µM were centrifuged (1400 rpm, 5 minutes). The supernatant was removed and the cells were washed twice in 1ml HBSS by centrifugation (1400 rpm, 5 minutes) and the supernatant discarded after eash wash. The cell pellet was resuspended in DHE (10 µM, 500µl) and incubated (37 ^{0}C, 10 minutes) before being analysed on the FACs machine. The intensity of DHE fluorescence was measured using the fluorescence channel, FL-3. The quantification of cellular ROS production was calculated from the DHE content of the cell using WinMDI, version 2.8. [32]. Menadione (10µM) was used as a positive control as it is a known inducer of apoptosis [32].

4.2.4 The luminescent analysis of cellular Caspase-3 and Caspase-7 upon Tenofovir treatment.

A kit (caspase-glo 3/7, from Promega life sciences (Southampton, UK)) that is commercially available for the detection of caspases -3 and 7 was used to measure the DEVD-ase activity of these caspases. Within the assay is a caspase-3/7 proluminescent substrate; this contains the tetrapeptide sequence DEVD. DEVD is cleaved by caspases which produces a luminescent signal that can be detected.

The manufactures instructions were followed. Cells were plated out on a white plate and incubated (24 hours to 5 days) as in section 3.2.2 (**Chapter 3**). After the required incubation time with the drugs, caspase 3/7 glo reagent (100 µl) was added to all wells and the plate was shaken on a plate shaker (30 seconds, 400 rpm). The cells were incubated at room temperature (30 minutes) and then the luminescence was read using a plate reader (BioTek FL600). Etoposide (10 µM) was used as a positive control as it is a known inducer of apoptosis [27]

4.2.5 The study of the potential role of autophagy induced by Tenofovir, via the use of the autophagy inhibitor 3-methyladenine

MTT cytotoxicity assays were carried out as in sections 2.2.3 in Chapter 2. These were carried out in the presence of the autophagy inhibitor 3MA (3-methyladenine). 3MA is an inhibitor of the phosphatidylinositol 3-kinase (PI3K) pathway, which has been shown to play a key role in the induction of autophagy [16]. All cells were pre-dosed with 3MA (25µM, 2hours, 37^0C).

2.2.6 Statistical Analysis

Statistical analysis was carried out on all data. Values are expressed as a mean $\pm$ standard deviation (SD) of the mean. This is represented as error bars on all graphs. A Shapiro-Wilk test was first carried out on the data to see if they were was considered normal. A Student's t-test was used for all normally distributed data and a Mann-Whitney U test was carried out on non-normally distributed data. All calculations were carried out using the StatsDirect software. Significance is indicated as follows * $P < 0.05$, ** $P < 0.01$, *** $P < 0.001$

4.3 Results

4.3.1 Effects of Tenofovir on cellular DNA content by Propidium Iodide staining.

PI intercalates with nuclear DNA within the cells, this leads to the formation of an adduct that is highly fluorescent. This fluorescence is measured by flow cytometry and is proportional to cellular DNA content. Each stage of the cell cycle (**Figure 4.3 A)**, relates to a distinct region of the histogram (**Figure 4.3 B).** An increase in the G_1/ G_0 (also called G_1 phase) phases is indicative of apoptosis [33].

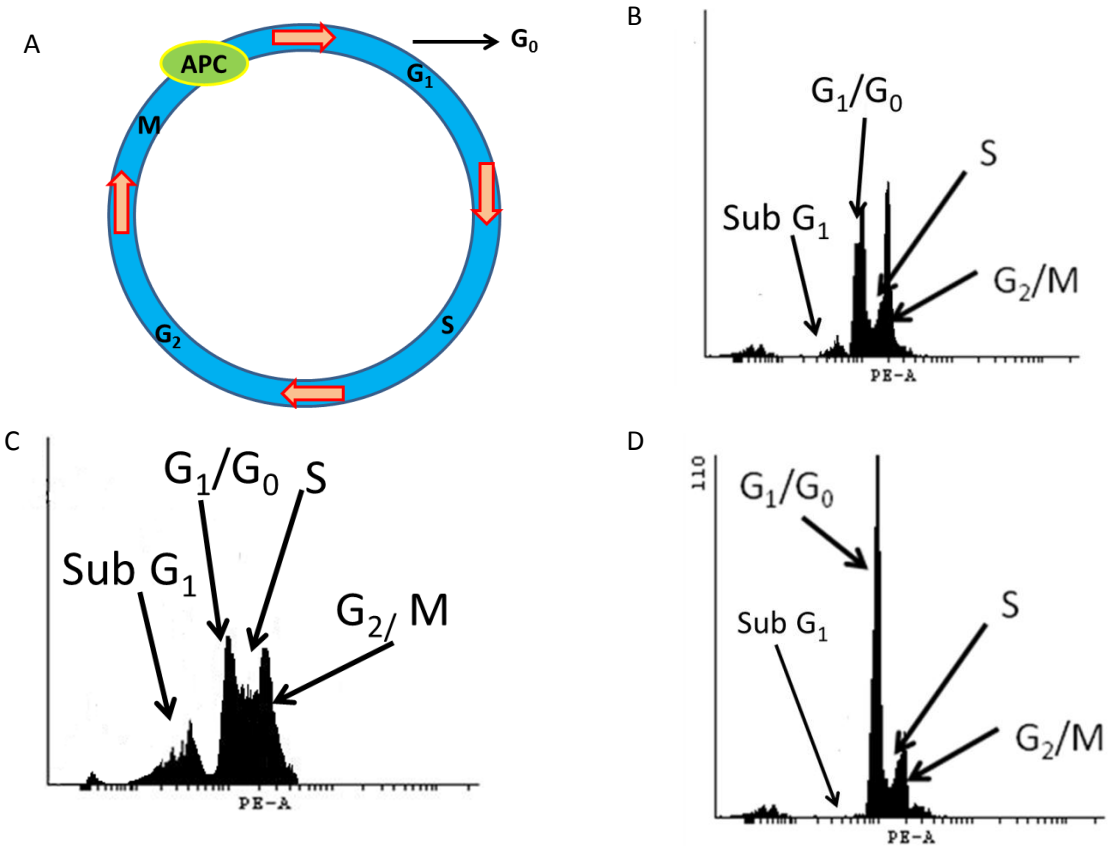

Figure4.3: A– The Cell Cycle **B**– Representative histogram of PI stained HepG2 galactose cells, vehicle only control cells (15 day incubation), where viability > 95 %. **C**- Representative histogram of PI stained HepG2 galactose cells, TFV treated (10 µM for 15 days) **D**- Representative histogram of PI stained HepG2 cells treated with etoposide (10µM for 15 days)

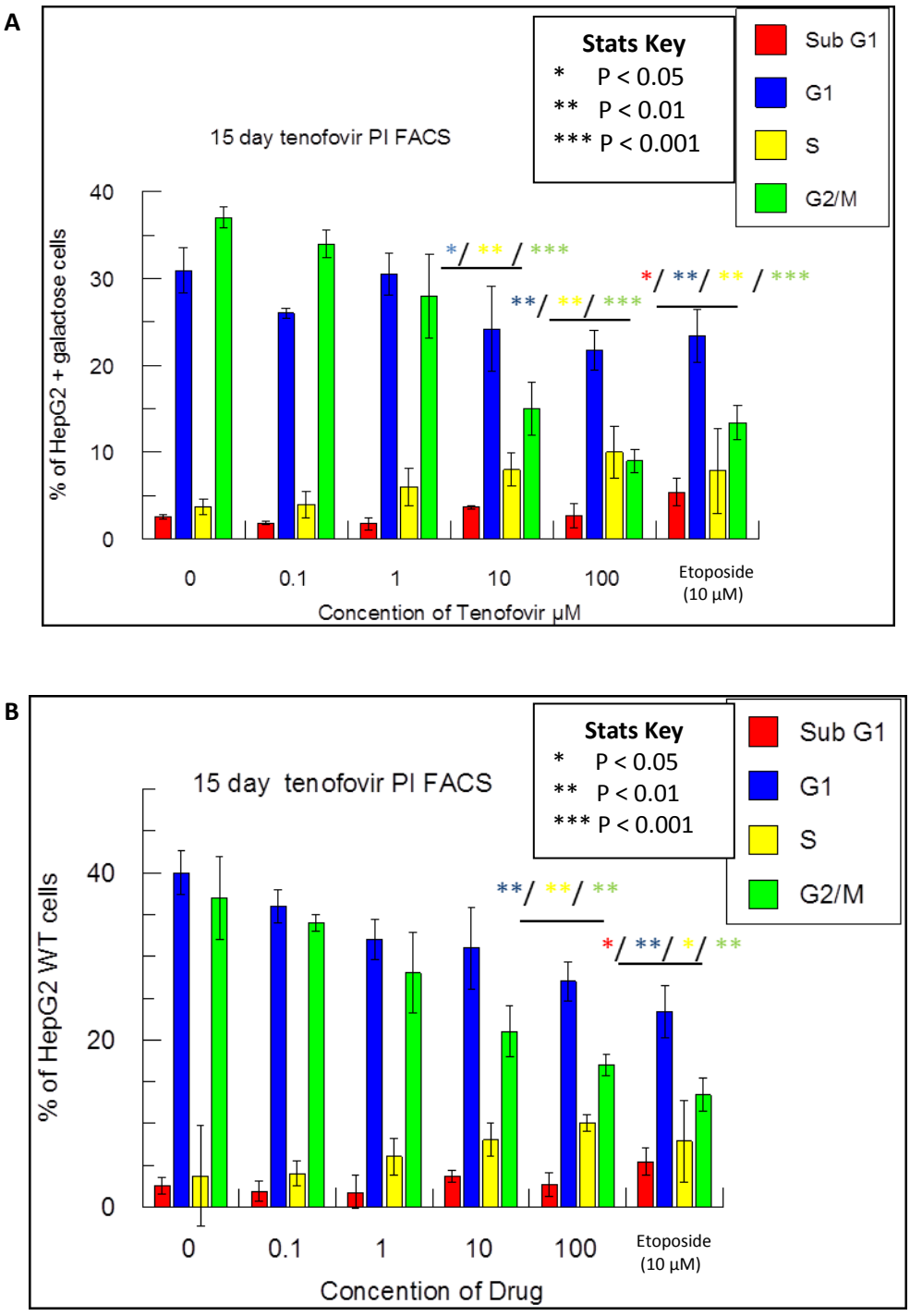

Figure 4.4 – Graphs of PI analysis of HepG2 cells treated with TFV for 15 days. A = HepG2 galactose. **B** = HepG2 WT days Results are the mean ±S.D of three or more independent experiments.

A

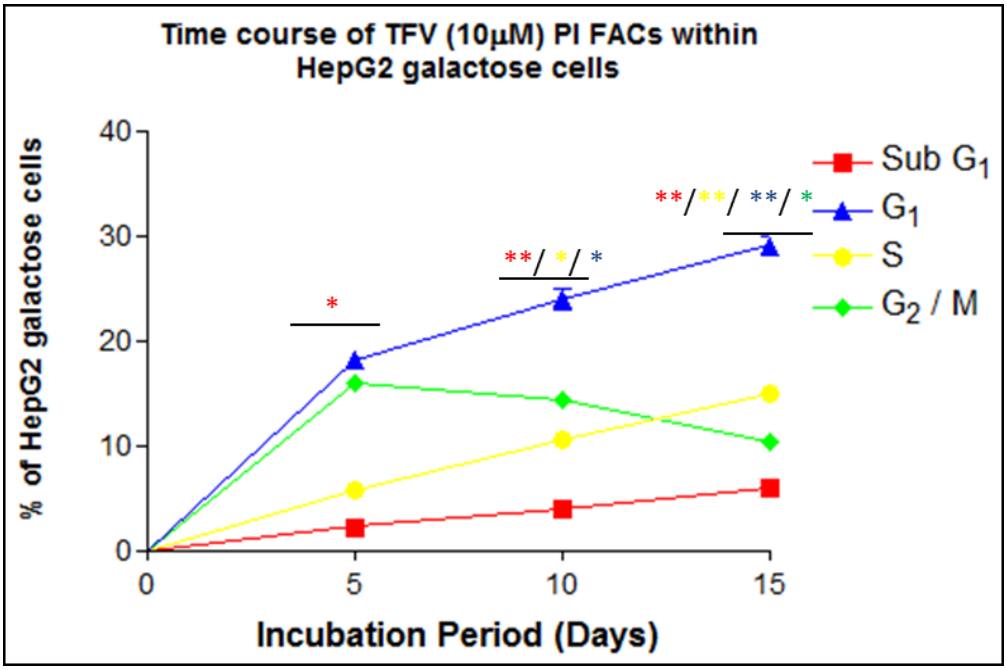

B

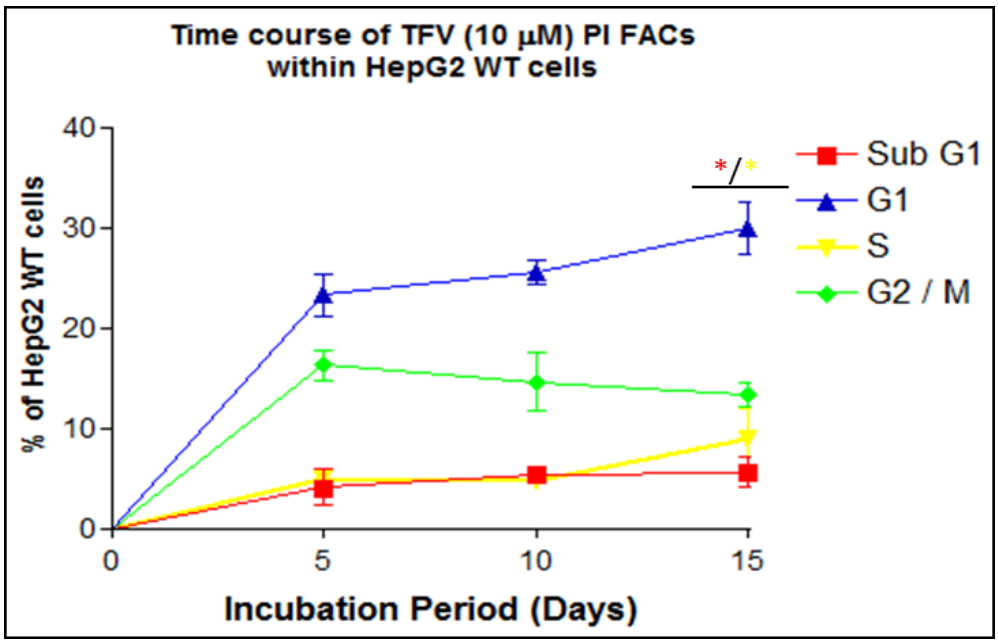

Figure 4.5 – Graphs of time course of PI analysis of HepG2 cells treated with TFV (10µM). A = HepG2 galactose **B** = HepG2 WT. Results are the mean ±S.D of three or more independent experiments. **KEY:** Red = Sub G_1, Blue = G_1, Yellow = S and Green = G_2. * $p < 0.05$, ** $p < 0.01$ and *** $p < 0.001$.

Figure 4.4 A and **Figure 4.5 A** demonstrate that TFV acts in a time dependant and dose dependent manner against the HepG2 galactose cells, causing a G_2 / M cell cycle arrest which leads to an accumulation of cells in the S phase. This can be seen clearly by the significant increase in cells within the S phase at 10 and 15 days (10 µM TFV, S phase is 4.9 % at 5 days and increases to 18.8% at 15 days) (**Figure 4.5 A**). The amount of cells in the G_1 (G_1 / G_0) phase also significantly increased (10 µM TFV, G_1 phase is 20.1 % at 5 days and increases to 31.2 % at 15 days) (**Figure 4.5 A**). There is significant reduction of cells in the G_2 / M phase at 5 , 10 and 15 days (10 µM TFV,G_2/M is 19.9% at 5 days and reduces to 5.7 % at 15 days) (**Figure 4.5 A**). Cells within Sub G_1 also significantly increase at 15 days within the HepG2 galactose cells (10 µM TFV) (**Figure 4.5 A**).Within **Figure 4.5 B,** the time course data (at 10 µM TFV), demonstrates that at 15 days the same effects seen within the HepG2 galactose cells are beginning to take place within the HepG2 WT cells. This can be seen by the significant increase in the S phase and the significant reduction in the G_2 / M phase (**Figure 4.5 B** at 10 µM TFV).

4.3.2 Determination of Tenofovir-induced cell death using Annexin v / Propiduim Iodide dual staining.

Annexin V and PI can be used in conjunction as a dual stain to determine cell status, viable (annexin V - / PI -), apoptotic (annexin V + / PI -), necrotic (annexin V - / PI +) and secondary necrotic (annexin V + / PI +) (**Figure 4.6**).

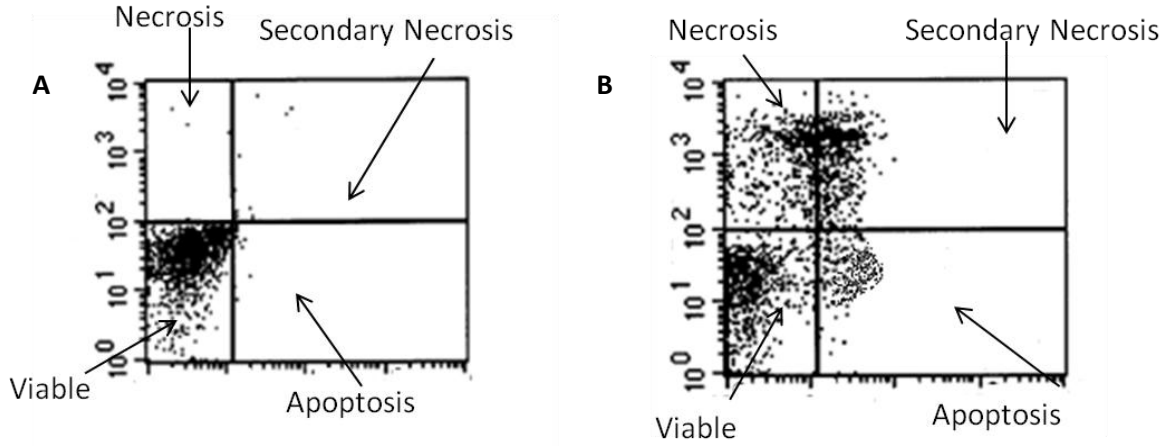

Figure 4.6 representative dot plot of HepG2 galactose cells incubation for 15 days with **A** –vehicle control **B** – TFV (100 µM)

A

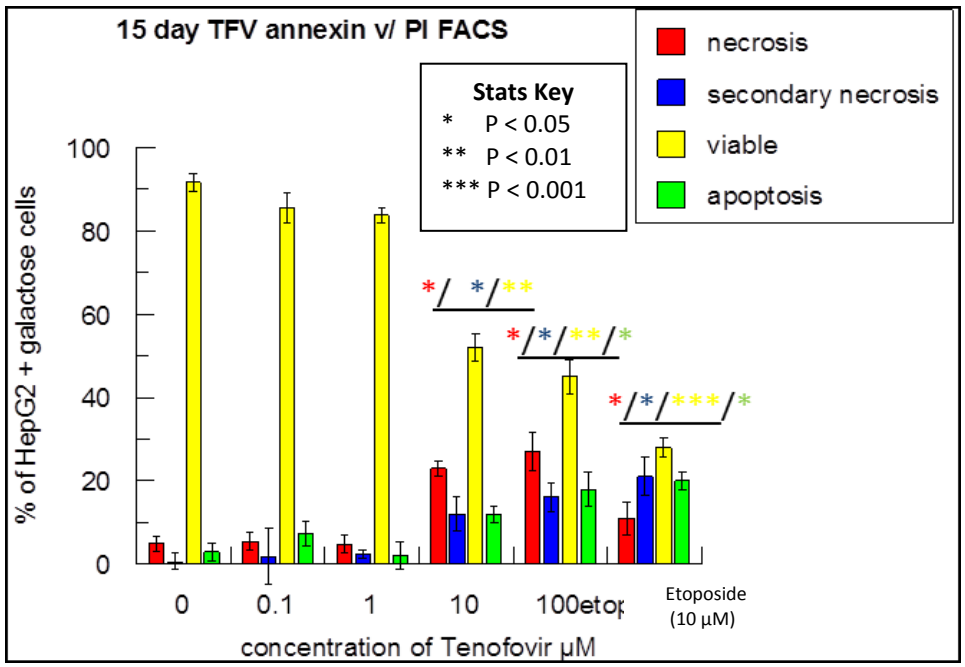

B

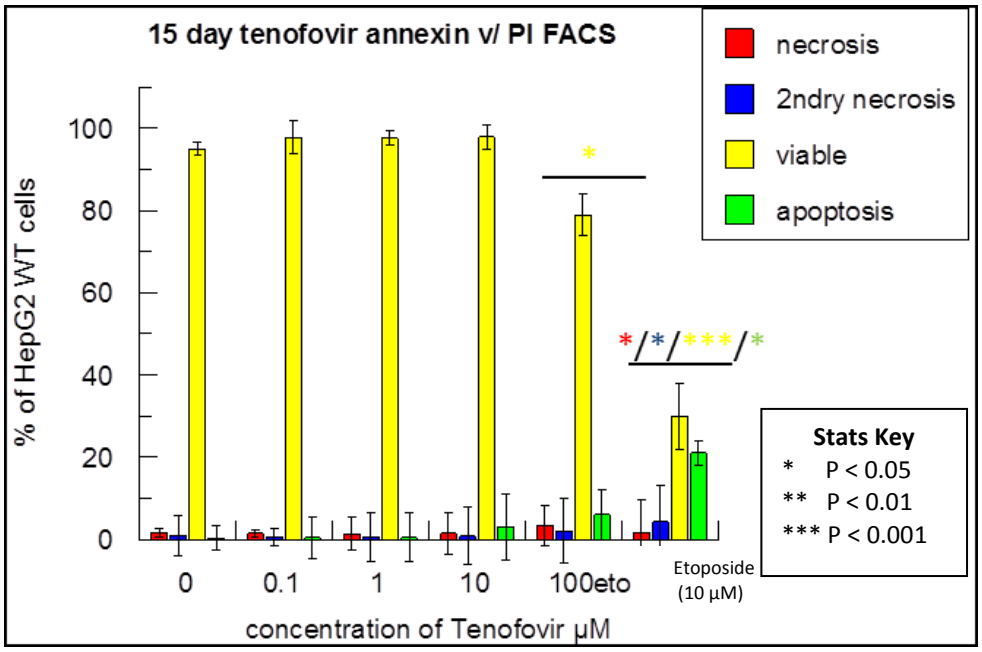

Figure 4.7 – Graphs of annexin V/ PI analysis of HepG2 cells treated with TFV for 15 days. A = HepG2 galactose. **B** = HepG2 WT days Results are the mean ±S.D of three or more independent experiments.

A

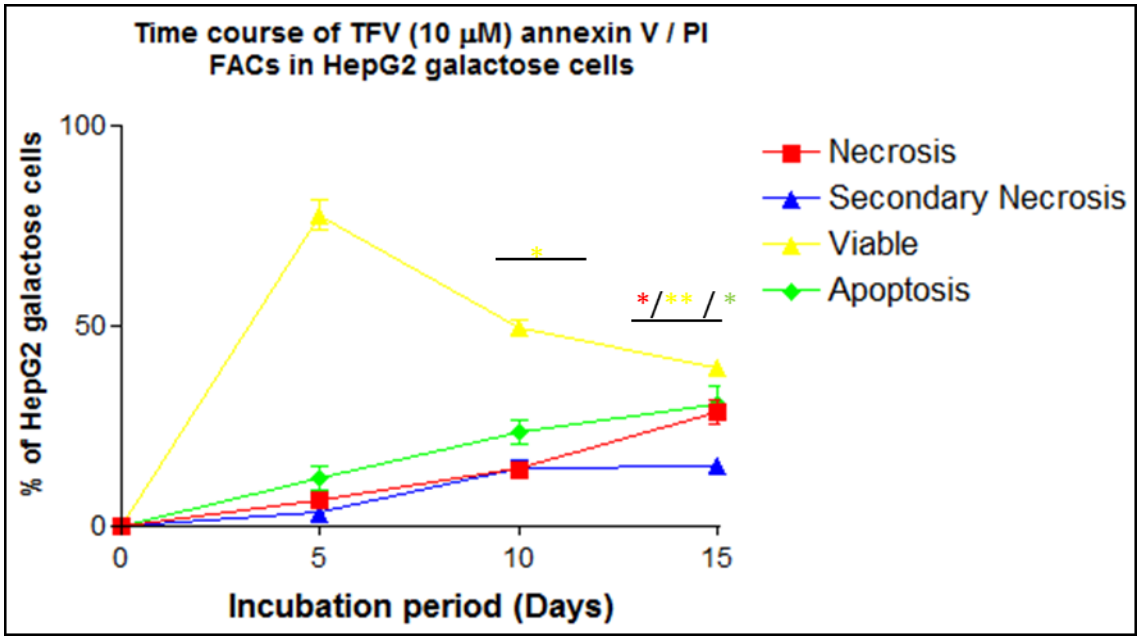

B

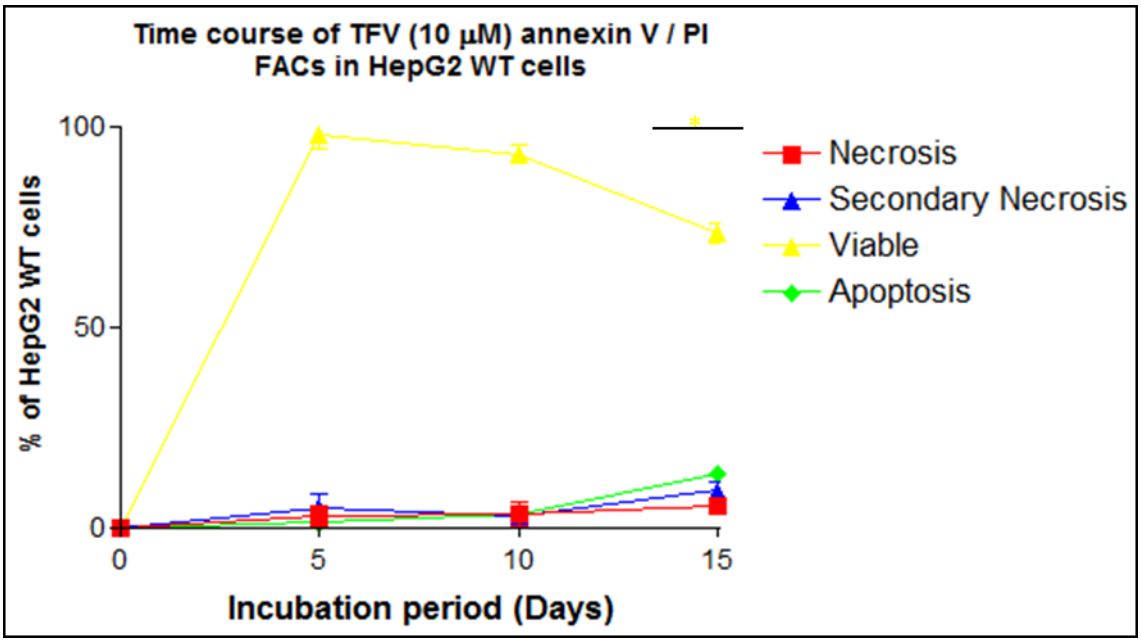

Figure 4.8 – Graphs of time course of annexin V/ PI analysis of HepG2 cells treated with TFV (10µM). A = HepG2 galactose **B** = HepG2 WT. Results are the mean ±S.D of three or more independent data sets of experiments. **KEY:** Red = necrosis, Blue = secondary necrosis, Yellow = viable and Green = apoptosis. * $p < 0.05$, ** $p < 0.01$ and *** $p < 0.001$.

The graphs for the annexin v / PI FACs demonstrate that the HepG2 galactose cells are more susceptible to TFV induced cytotoxicity than the HepG2 WT cells. This can be seen clearly when comparing **Figure 4.7 A** to **Figure 4.7 B**. In **Figure 4.7A** (the HepG2 galactose cells) the amount of viable cells at 15 days was significantly ($p < 0.01$) reduced from 95.0 %

(control) to 48.3 % (at 10 μM TFV), however in **Figure 4.7 B** (the HepG2 WT cells) it can be seen that the percentage of viable cells doesn't significantly change (95.0 % to 96.1 %), when dosed with TFV (10 μM).The data presented in **Figures 4.7 A** and **4.8 A,** demonstrate that TFV acts in a dose-dependent and time-dependent manner to cause cytotoxicity, ultimately leading to cell death via apoptosis or necrosis. This can be seen by the significant ($p < 0.05$) increase in apoptosis and necrosis at 15 days in **Figure 4.8 A** (apoptosis increased from 4.2% to 19.8%; necrosis increased from 5.3% to 14.3 %**.** The amount of secondary necrosis also increases, however it was not significant (**Figure 4.8 A**).

4.3.3 Effects of Tenofovir on mitochondrial membrane potential by tetramethylrhodamine ethyl ester staining.

As discussed in section 4.2.3.3 TMRE staining is used to determine mitochondrial depolarisation. Mitochondrial depolarisation is demonstrated when there is a decrease in quantity of TMRE florescence detected (**Figure 4.9**)

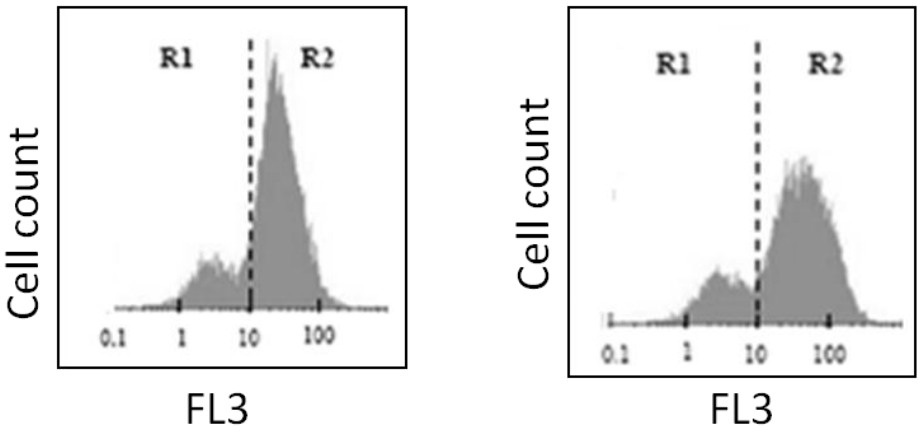

Figure 4.9: A representative histogram of TMRE staining within HepG2 galactose cells (after a 10 day incubation). **A** – Vehicle control **B** – TFV treated (100 μM). R1: cells with low TMRE fluorescence R2: cells with high TMRE fluorescence

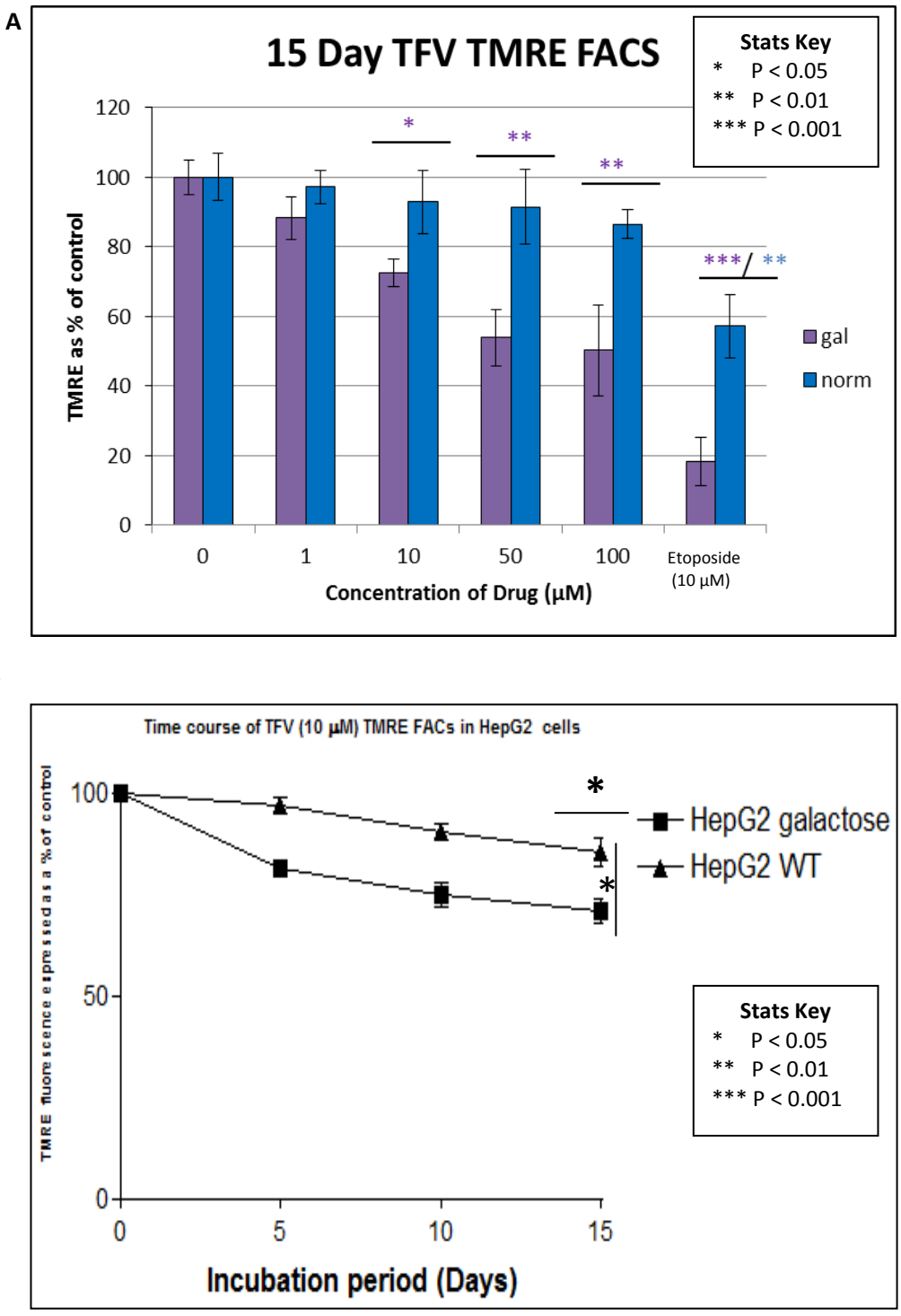

Figure 4.10 – Graphs of TMRE analysis within HepG2 cells treated with varing concentrations of TFV. Etoposide (10µM) was used as a positive control . A = HepG2 galactose/ WT cells treated with TFV for 15 days. **B** = Time course of HepG2 galactose/ WT cells treated with TFV (10µM). Results are the mean ± S.D of three or more independent experiments.

TFV causes dose-dependent (**Figure 4.10 A**) and time-dependent (**Figure 4.10 B**) depolarisation of the mitochondria specifically in the HepG2 cells grown in galactose media. This can be seen in **Figure 4.10 B** (at 10 µM TFV) when comparing the percentage of TMRE in each cell type over the different time points, For the HepG2 WT the percentage of TMRE fluorescence does not significantly reduce any time point, whereas in the HepG2 galactose there is a significant ($p < 0.05$) reduction in TMRE fluorescence at 15 days (reduction from 81.2 % at 5 day to 69.8 % at 15 day).

4.3.4 Effects of Tenofovir on cellular Caspase-3 and Caspase-7 levels by luminescent staining.

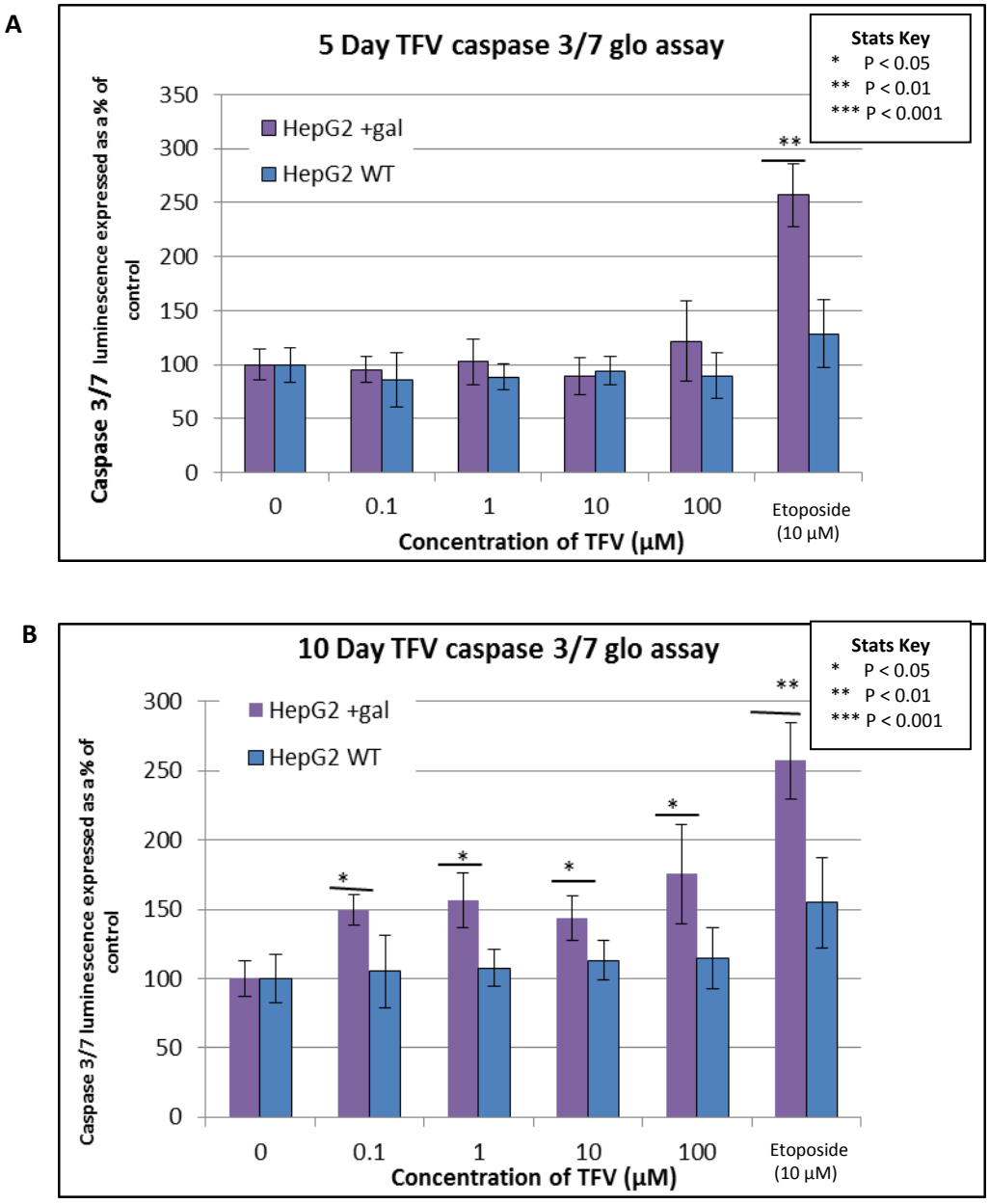

Figure 4.11 –– Graphs of caspase 3/7 glo analysis of HepG2 cells treated with TFV. A = HepG2 galactose/ WT cells treated for 5 days. **B** = HepG2 galactose/ WT cells treated for 10 days. Results are the mean ± S.D of three or more independent experiments.

TFV induces caspase 3/ 7 glo activity of HepG2 cells cultured in galactose media after 5 days (**Figure 4.11B**). The results demonstrate that TFV acts in a time dependent and dose dependent manner and causes a significantly ($p < 0.05$) higher percentage of caspase luminescence within the HepG2 galactose cells at 10 day incubations when compared to vehicle control cells (170.4 % at 100 μM TFV) (**Figure 4.11 B**). However, TFV did not cause and increase in caspase activity within the HepG2 WT cells (the percentage of caspase activity was 109% at 10 days upon treatment with TFV 100μM) (**Figure 4.11 A**), thus showing that the HepG2 + gal cells were more susceptible to TFV cytotoxicity as caspases are released as part of the apoptotic pathway.

4.3.5 Effects of Tenofovir on cellular superoxide reactive oxygen species levels using dihydroethidium staining.

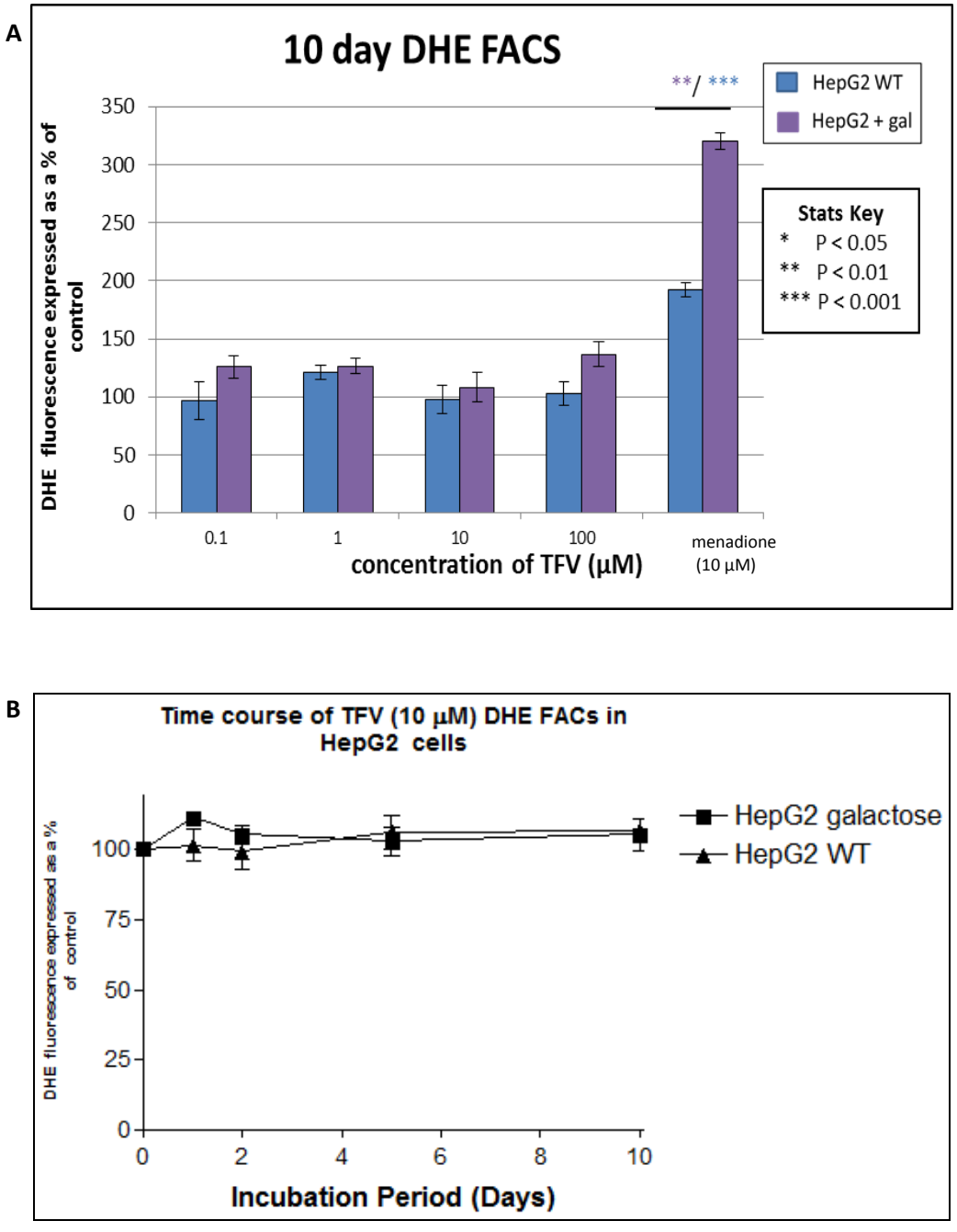

Figure 4.12 – Graphs of DHE analysis of HepG2 cells treated with TFV. A = HepG2 galactose/ WT cells treated with TFV for 15 days. **B** = Time course of HepG2 galactose/ WT cells treated with TFV (10µM). Results are the mean ± S.D of three or more independent experiments.

There was DHE in all samples tested, but the levels in the HepG2 + galactose cells were not significantly different to those in the HepG2 WT cells (**Figure 2.12**). The detection of DHE (Figures **4.12 A and B**) unexpectedly demonstrates that TFV is not inducing any superoxide ROS generation. This can be clearly seen in **Figure 4.12 B** as there is no significant change in the amount of superoxide ROS detected. The positive control (Menadione, 10) induced a significant increase in production of superoxide ROS within both the HepG2 WT and HepG2 galactose cells, with levels being higher in the HepG2 + galactose cells (**Figure 4.12 A**), thus confirming that the assay was working correctly.

4.3.6 Determination of Tenofovir-induced autophagy, via the use of the autophagy inhibitor 3-methyladenine

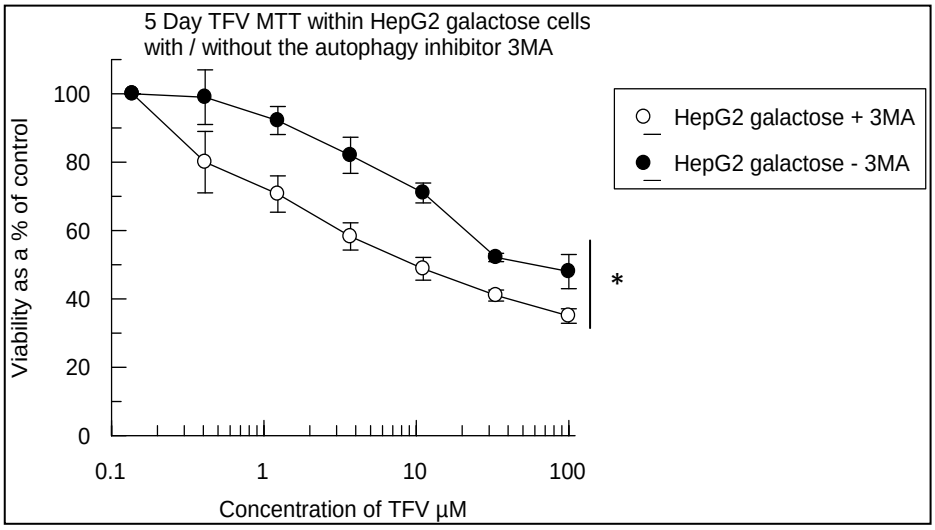

Figure 4.13 – Dose-response curve of HepG2 galactose cells treated with TFV for 5 days, with and without 3MA (25 µM) Results are the mean ± S.D of three or more independent experiments.

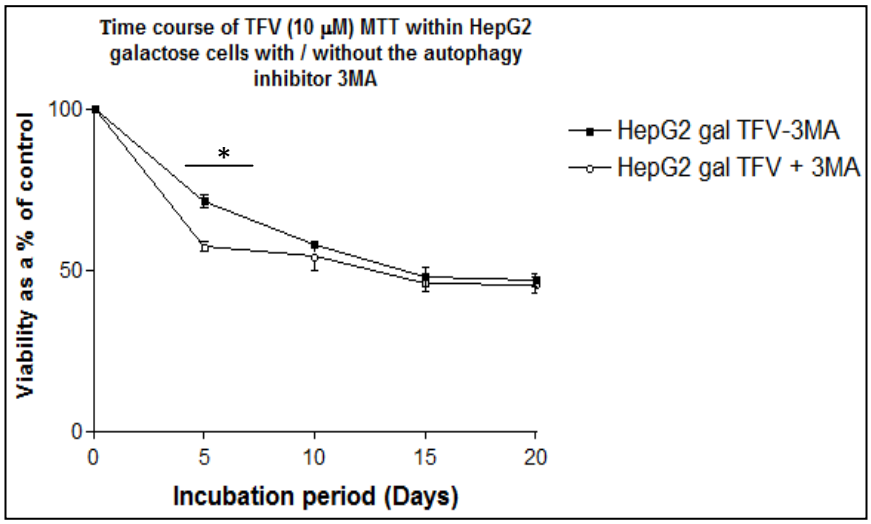

Figure 4.14 – Graph of time course MTT analysis within HepG2 galactose cells treated with TFV (10µM) without or with 3MA (25 µM). Results are the mean ±S.D of three or more independent experiments.

There was a significant ($p < 0.05$) difference in TFV-induced cytotoxicity at 5 days between HepG2 cells + galactose treated with 3MA to without 3MA (**Figure 4.13**). The cytotoxicity

induced by TFV within HepG2 galactose cells at 5 days (**Figures 4.13**), when cultured in the presence of the autophagy inhibitor 3MA, indicate that the autophagy inhibitor acted to exacerbate the cytotoxic effects of TFV, this is indicative that autophagy is acting as an adaptive mechanism of cellular survival induced by TFV dosing. However, this protective effect is only apparent and significant ($p < 0.05$) at the earlier time point of 5 days (**Figure 4.14),** shown by the reduction in the EC_{50} (the EC $_{50}$ for HepG2 galactose cells dosed with TFV (0.1µM – 100 µM) at 5 days is 25.0 µM, when dosed with TFV (0.1µM – 100 µM) in the presence of a fixed dose concentration of 3MA (25µM) the EC_{50} decreases significantly($p < 0.05$) to 11.7 µM (**Figure 4.14 A)**. At all other time points (10, 15 and 20 days), results demonstrate there was no significant difference in the cytotoxicity induced by TFV in both HepG2 galactose / WT, with and without the presence of the autophagy inhibitor 3MA.

4.4 Discussion

The studies presented within this chapter have investigated the mechanistic pathways of TFV induced cell death via the study of biochemical and structural events involved at different points of the various cell death pathways. Previous studies have showed that other NRTI's induce cell death via both apoptotic and necrotic pathways [15], however the mechanistic pathway of TFV induced cell death still remains unknown, due to lack of appropriate *in vitro* models.

These finding can be combined in order to establish a molecular pathway of TFV-induced cell death, **Figure 4.15.**

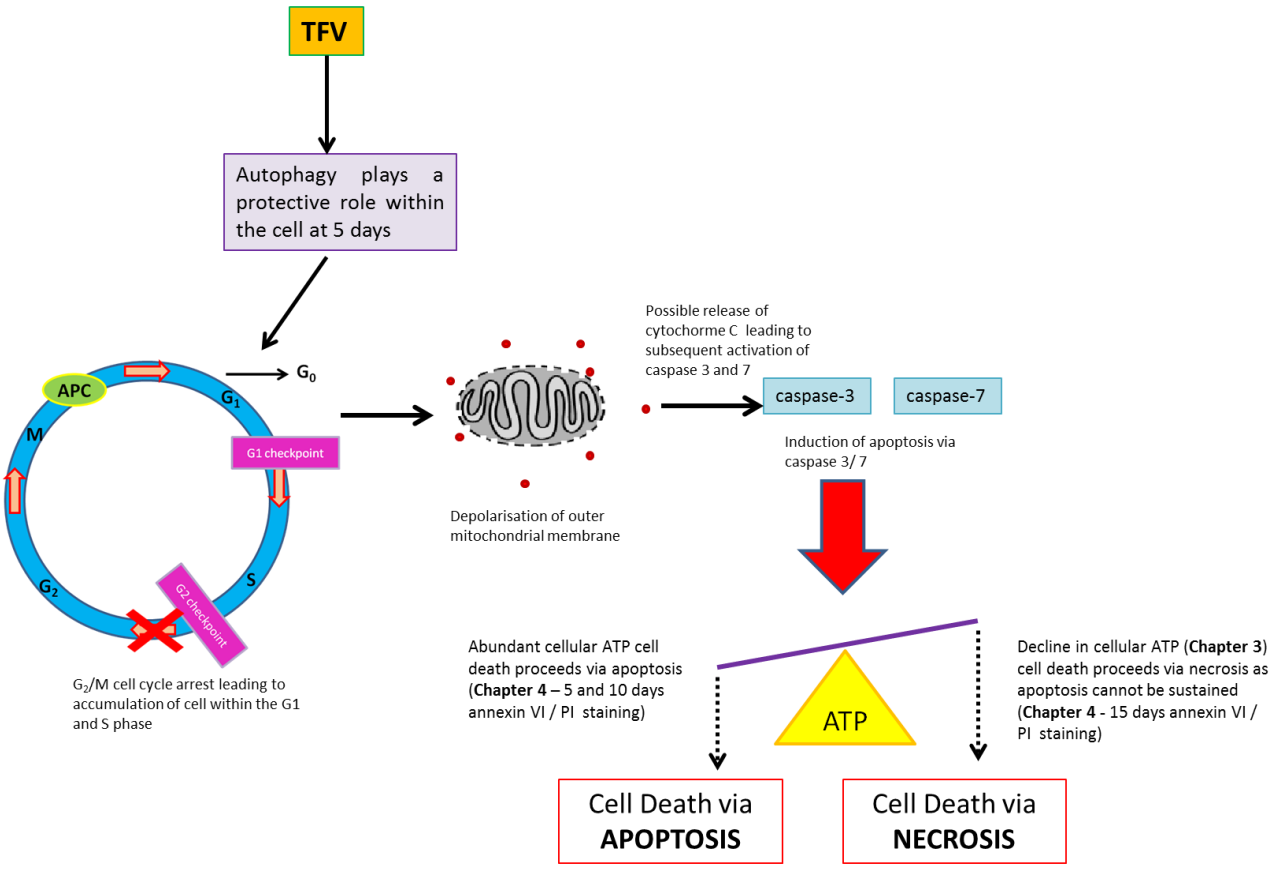

Figure 4.15 A schematic diagram of the determined mechanistic pathway of TFV induced cell death

Due to a recent paper showing that EFZ-induced autophagy acted as an adaptive mechanism of cell survival, the study of the possible role of autophagy induced by TFV was carried out using the autophagy inhibitor 3MA [16]. The results demonstrated that at only the 5 day incubation period, in the presence of 3MA the cytotoxicity of TFV was significantly increased, within both the HepG2 galactose and the HepG2 WT cells (**Figure 4.14**). This is indicative that autophagy is induced by TFV and plays a protective role within the cells at the early time points. This may underline the long time periods required to see TFV-induced cytotoxicity. In future more work needs to be carried out, in order to establish the relationship between TFV dosing, autophagy and cell death. Further studies within *in vitro* and *in vivo* models should be carried out, using western blott analysis to look for the presence of the specific autophagy protein LC-3 induced by TFV [16]. Future intervention studies should be carried out to see if the induction of autophagy may be a possible protective mechanism that could be used in the future. This treatment could benefit those patients that have been identified as predisposed to TFV-induced toxicity.

The determination of cellular DNA content and its position within the cell cycle can be indicative of any DNA damage leading to cell cycle arrest [34]. The cell cycle has two main checkpoints that determine if progression through the cycle continues. The cell cycle has check points within the G_1 (before the S phase), and in G_2 (after the S phase) [34]. Any cellular DNA damage detected by these checkpoints results in cell cycle arrest at the point of detection, ultimately leading to apoptosis (Willis *et at*., 2011). Therefore, the cellular DNA content in the presence of TFV was determined. The results demonstrated that TFV caused a time dependent and dose dependent G_2 /M cell cycle arrest within HepG2 galactose cells at 5 days, which lead to an accumulation of cells in the S phase of the cell cycle. The data presented within this chapter indicate that the G_2 checkpoint was triggered. This may be a result of the DNA damage observed in Chapter 3, resulting in accumulation of cells in the S

phase. Previous *in vitro* work has shown that an accumulation of cells within the S phase is linked to mtDNA damage [35]. These results support evidence that TFV may be inducing mitochondrial DNA damage. It was demonstrated that the G_1 (G_1/ G_0) population also significantly increased within HepG2 galactose cells dosed with TFV after 10 days, this is indicative that TFV is inducing cell death via apoptosis [33].

Disruption in cellular superoxide ROS levels has been cited as an early indicator of apoptosis as a result of ETC disruption, therefore cellular superoxide ROS levels were determined via DHE staining in the presence of TFV [36]. Earlier time points were investigated for the detection of early apoptosis (24 hour / 48 hour), when there was no detection of superoxide ROS at these time points (data not shown), later time points were carried out (5 days and 10 days). Results demonstrated that TFV did not induce ROS production at the early or later time points, which was unexpected, as data within this chapter shows that TFV induces mitochondrial cytotoxicity leading to apoptosis within the HepG2 galactose cells after 5 days (**Figure 4.13**). This could be indicative that whilst TFV is causing mitochondrial damage, it may only reduce the quantity of mitochondria rather than the quality, therefore superoxide ROS production may proceed as usual. But data presented here agrees with previous observations that TFV does not induce cellular ROS production *in vitro* [25].

The depolarisation of the mitochondrial membrane has been cited as an early apoptotic event as it may lead to cytochrome c release, this could mediate the induction of a caspase cascade that leads to cell death via apoptosis [8]. The mitochondrial membrane potential (MMP) was therefore assessed following TFV treatment using TMRE staining [37]. Results demonstrated that after 10 days TFV induced a significant reduction in MMP within the HepG2 galactose cells in a time dependent and dose dependent manner (**Figures 4.10 A and B**). These results do not determine if the reduction in MMP occurs after the initial chemical stress induced by TFV, as part of the apoptotic pathway or whether TFV is targeting the mitochondria

specifically. However, as the PI staining **Figure 4.5A** shows a G_2/M arrest at 5 days, this is indicative that a reduction in MMP has been induced via a cell cycle arrest and the induction of apoptosis.

The caspases 3 and 7 are essential for the execution of apoptosis therefore the activities of these caspases were determined following treatment of the cells with TFV [5]. The results demonstrated that TFV induced caspase 3 /7 activation slightly at 5 days and significantly at 10 days (**Figure 4.11 A** and **B**). At 10 days cytotoxicity of TFV has been shown within these modified cell lines (**Chapter 3, Table 3.2** and **3.5**), this cytotoxicity may be induced via the apoptotic caspase pathway. This could be the intrinsic pathway, although many cell death pathways can lead to the upstream caspase activation and subsequent cascade of caspase activation [5]. Future work could be to look for the release of cytochrome C induced by TFV dosing as this is specific to the intrinsic pathway. Work could also be carried out using caspase inhibitors such as the Caspase 2/3 Inhibitor (Ac-LDESD-CHO can be purchased from sigma-Aldrich, Poole, UK) to see if this is protective to the cell when dosed with TFV.

The induction of apoptosis or necrosis via TFV was determined using annexin V /PI dual staining. Results demonstrated that TFV caused time-dependent and dose-dependent induction of necrosis and apoptosis. Although an increase in both apoptosis and necrosis was detected, the data suggest that cell death is predominantly apoptosis for the 5, and 10 day incubations shown by an increase in apoptosis and secondary necrosis (secondary necrosis is the resultant end point of apoptosis, so cells detected in this state were also apoptotic cells [38]). Results for the 15 day incubation period demonstrated that necrosis was the predominant form of cell death in the HepG2 galactose cells dosed with TFV at this time point; this could be due to a decrease in cellular ATP as seen in **Chapter 3 (Figure 3.7B)**. Apoptosis is an active process that is ATP dependent; when cellular ATP levels fall below a certain threshold, cell death proceeds via the necrotic pathway [11]. Previous *in vitro* work

reported that TFV does not cause cell death [24-27, 30-40]. This could be due to the length of incubation times used for these studies which were 24 – 48 hours, as the data presented within this thesis (**Chapter 3, Table 3.2** and **3.5**) has demonstrated that TFV cytotoxicity is time-delayed requiring at least a 5 day incubation period. Previous studies into ADEF induced cell death showed that it caused cell death via the necrotic pathway [13], which is similar to data shown within this chapter (**Figure 4.7 A**).

When taking into account all the cell death data generated, it has been demonstrated that TFV induces a G_2 /M cell cycle arrest. This causes an accumulation of cells in the S phase which eventually leads to the activation of apoptosis, which may be via the intrinsic pathway, leading to depolarisation of the mitochondrial membrane. This could lead to cytochrome c release that causes subsequent activation of caspases 3 / 7, ultimately leading to cell death via apoptosis. When cellular ATP levels decrease cell death proceeds via the necrotic pathway. Results also demonstrated that autophagy may act as an adaptive mechanism of cellular survival induced by TFV; however this protective effect is only significant at the earlier 5 day time point. Further studies are needed *in vitro* before studying these theories further in a clinical setting.

Chapter Five

ASSESSMENT OF KIM-1 IN HIV PATIENT URINE SAMPLES: POTENTIAL UTILITY AS A BIOMARKER OF TENOFOVIR MEDIATED KIDNEY DAMAGE

Contents

5.1 Introduction

Many drugs induce renal toxicities and TFV has been linked in particular to proximal tubule dysfunction [1-3]. If TFV is not withdrawn in patients experiencing renal injury the onset of CKD could result, leading to irreversible kidney damage [4]. Drug monitoring of kidney function in patients receiving a HAART regimen containing TFV is therefore vital [5].

A number of markers of renal insufficiency are currently used clinically, including blood urea nitrogen (BUN) and serum creatinine (SCr), used for the determination of glomerular filtration rate (GFR). These markers involve the use of histopathology and function tests (such as blood tests). However, *in vitro* and *in vivo* studies of renal dysfunction have shown that these markers have many limitations [6]. The main limitation is they are not region-specific so the area of the kidney undergoing toxicity remains unclear [7]. Another disadvantage of these traditional markers is they will not detect renal insult until 30- 50% renal damage has occurred. This highlights the importance of developing biomarkers that can detect damage at earlier time points in specific regions of the kidney.

Currently the importance of TFV as a front line treatment against HIV-1 outweighs the risks of developing renal dysfunction. Therefore, novel biomarkers must be developed in order to monitor patients and minimise the risk of developing irreversible renal damage as previous studies showed the onset of proximal tubule damage to be 20% in patients receiving TFV [8-10].

Due to the limitations of current markers a working group of scientists in the pharmaceutical industry was set up; named the Predictive Safety Testing group. This group is led by the Critical path Institute (C-path) which is a non-profit organisation. Recently, data for possible urinary proteins that could be used as biomarkers (**Figure 5.1**) for renal dysfunction was

presented by the PSTC to the regulatory bodies, the Food and Drug Administration (FDA) and the European Medicines Agency (EMA) [7]. Amongst these urinary proteins was kidney injury molecule -1 (KIM-1), which emerged as a good possible biomarker for proximal tubule damage due to its specificity to this region of the kidney [11].

Previous prospective studies have evaluated GFR as a predictor of TFV-induced toxicity, as a decline in GFR is an indicator of the onset of kidney dysfunction. All studies reported that TFV did not cause any decline in GFR when comparing patients on TFV treatments against other antiretroviral drugs [12-14]. However, these studies have all focused on the glomerular function when many animal studies have shown TFV to cause proximal tubule dysfunction specifically, therefore they may miss the onset of kidney damage [15-17]. The early clinical indicator of induced proximal tubule damage is hypophosphateamia, which is closely followed by a decline in reabsorbtion of phosphates, causing excessive phosphate loss within the urine [5]. A previous study showed that evaluation of hypophosphateamia revealed that the incidence rate of hypophosphatemia was higher in patients taking TFV compared to patients on other antiretroviral drugs [18]. This demonstrates that hypophosphateamia could be a better biomarker than GFR for predicting TFV-induced proximal tubule damage. In another study, a cohort of 284 HIV-1 patients were evaluated for SCr levels and β_2-microglobulin, proximal tubule damage was defined as the presence of two or more well defined urine abnormalities. It was shown that SCr levels remained normal in all patients including those on TFV, whilst those patients taking TFV had the highest levels of β_2-microglobulin levels within their urine. β_2-microglobulin is thought of as one of the most specific markers of tubular damage [9]. These studies highlight the importance of finding a biomarker that is specific to proximal tubules damage. However, this study shows that although β_2-microglobulin maybe a good biomarker for monitoring TFV induced kidney

damage, other studies have shown that β_2-microglobulin is not specific to just the proximal tubule and is also shed from the glomerulus (**Figure 5.1**) [11].

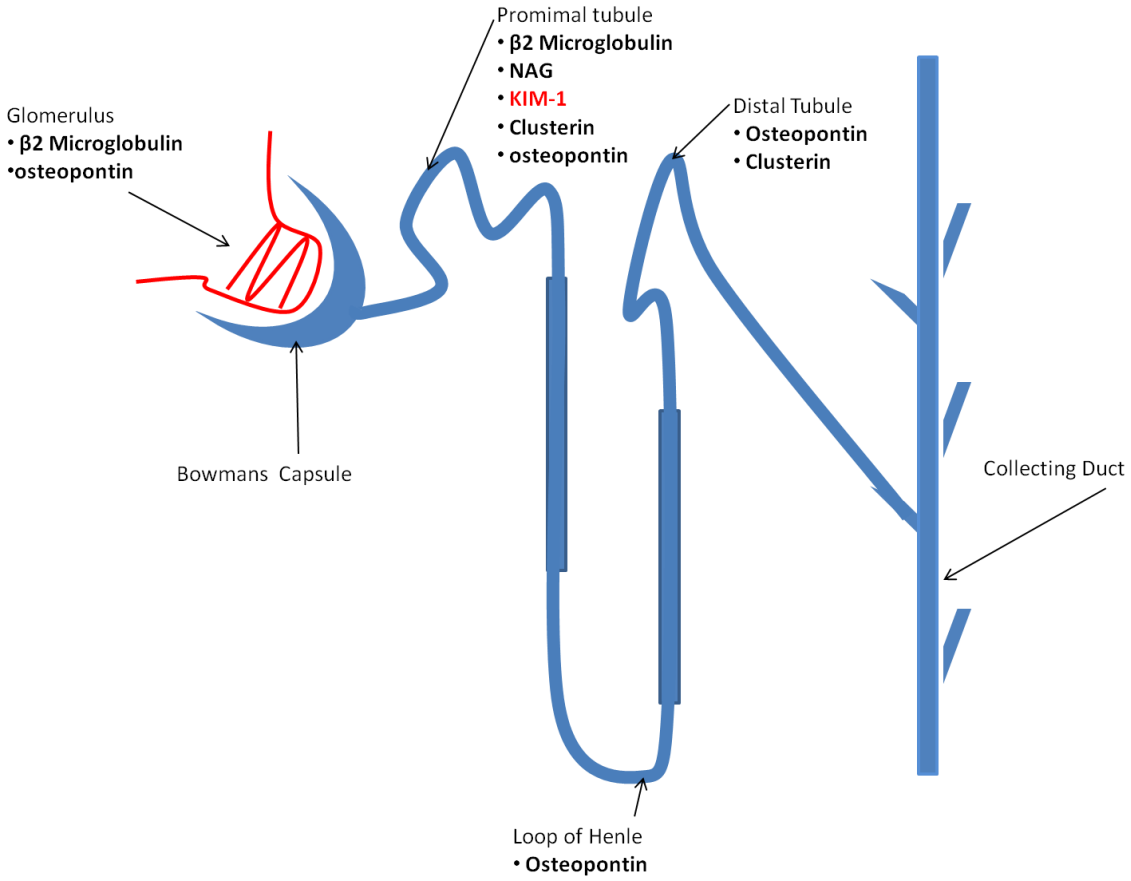

Figure 5.1: A schematic diagram of the kidney showing the localization of the novel biomarkers (modified from a picture in [19])

As TFV is such an important drug for the use in most HAART regimens due to its good pharmacodynamic and pharmacokinetic properties, and has recently been approved for pre-exposure prophylaxis, determination of urinary KIM-1 may become an advantageous tool for monitoring proximal tubule dysfunction TFV patients.

5.1.1 Kidney Injury Molecule -1

When damage occurs to the proximal tubule epithelial cells the morphological changes that occur include loss of polarity, dedifferentiation, apoptosis and loss of the brush border [20]. When advanced damage occurs to these cells it leads to the detachment from the basement membrane of both necrotic and viable tubular epithelial cells, which leads to obstruction of the renal lumen [20], the surviving cells that are dedifferentiated proceed to spread over the broken down basement membrane. They undergo mitogenesis to ultimately re-differentiate and restore normal epithelial polarity / function [21]. These processes are well defined due to extensive studies in *in vitro* and *in vivo* platforms; however the molecular factors that regulate these events are not understood [21].

One key molecule identified through *in vivo* studies involving post-ischaemic rats was KIM-1. KIM-1 is also called T cell immunoglobulin mucin domains-1 (TIM-1) because it is expressed by sub populations of activated T-cells at low levels. KIM-1 is also called hepatitis A virus cellular receptor 1 (HAVCR-1) because it is expressed by hepatocytes.

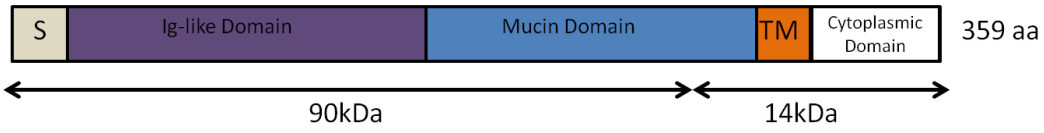

Figure 5.2: A schematic image of KIM-1 modified from a picture in [22]

The KIM-1 gene encodes for a type 1 cellular membrane glycoprotein. This glycoprotein has a unique immunoglobulin domain that contains 6 cysteine residues and an extracellular region that is mucin-rich (As seen in **Figure 5.2**). Studies have shown KIM-1 to be highly conserved in the following species: dogs, rodents, zebra fish, primates and humans which

could be useful in order to bridge information from *in vitro* / *in vivo* investigations and relate them back into man [20].

Studies have found that KIM-1 is undetectable in a normal human kidney and rodent kidney, but that expression increases post kidney injury [20, 23]. The localisation of the KIM-1 expression post renal injury is specific to surviving epithelial cells of the proximal tubules [20]. The localisation of KIM-1 and other novel biomarkers can be seen in **Figure 5.1.** Other studies also showed that the expression of KIM-1 mRNA is increased more than any other gene post kidney injury [23]

In vitro investigations using renal proximal tubular epithelial cells showed that upon kidney insult, the ectodomain of KIM-1 is shed into the urine [24]. This evidence was supported by further *in vitro* studies involving rodent urine [25] and human urine samples [26] which showed shedding of the KIM-1 ectodomain into urine after the initiation of renal insult. The selectivity and sensitivity of KIM-1 compared to the traditional markers BUN and SCr and the novel biomarker N-acetyl-β-D-glucosaminidase (NAG) was assessed *in vivo* using multiple rat models of kidney injury. The results showed that KIM-1 significantly outperformed the 'gold standard' biomarkers BUN and SCr [11]. This was demonstrated in this study by the differences in sensitivity between the gold standard biomarkers: BUN had a sensitivity of 0.48 and 0.29 for SCr whilst the sensitivity of urinary KIM-1 was 0.71 following kidney injuries [11]. KIM-1 is currently the only injury biomarker specific to the kidney to be approved by the FDA and EMA; thus making it an acceptable biomarker for the prediction of TFV-induced proximal tubule dysfunction.

5.1.3 Aims of Chapter

In this chapter KIM-1 analysis will be carried out in urine samples from a small cohort of 30 HIV-1 patients. Of these patients 16 are on a TFV-containing regimen and 14 were not on TFV containing regimens. Urine samples were collected with the full consent of the patients who were asked in advance if they were taking any antiretroviral drugs. The urine samples were anonymised and collected from genitourinary medicine (GUM) clinics and tested for the presence of HIV-1, those found to be HIV-1 positive were then tested to determine presence of antiretroviral drugs. The hypothesis being tested is that those patients on TFV containing regimens will have higher KIM-1 levels in urine in comparison to those patients not receiving TFV.

5.2 Materials and Methods

5.2.1 Materials

The cell culture media (DMEM high glucose and DMEM no glucose) were from life technologies, Invitrogen (Paisley, UK). All other reagents were purchased from Sigma-Aldrich (Poole, UK). Tenofovir was from Toronto Research Chemicals **(**Toronto, Canada). The MSD Toxicology KIM-1 assay kit was ordered from MESO Scale Discovery (Gaithersburg, USA).

5.2.2 Cell culture and experimental preparation

As in section 3.2.2, Chapter 3. Only HEK293 KIM-1 cells were use in this chapter as they are transfected with human KIM-.1

5.2.3 Clinical sample collection and preparation

The clinical HIV-1 urinary patient samples were supplied from the University of Liverpool Bio-Analytical Facility (BAF) and full ethical approval had been previously granted for work from a previous cohort study that was carried out.

The urine from healthy volunteers was obtained with the volunteer's full consent. With these samples the heat / formalin inactivation methods were validated to find the best method to inactivate the HIV-1 within the clinical samples. For formalin treatment, urine samples were incubated with 10 % formalin (500 µl at room temperature) overnight. For the heat treatment urine samples were left in a water bath for 1 hour at 56 ^{o}C.

5.2.4 The determination of sample creatinine concentrations.

Serum creatinine is currently used as a marker for kidney injury [27]. For these studies the urinary creatinine was measured in order to normalise the concentration of urinary KIM-1. This normalisation step minimises the influence of the volume of patient urine output and is the current method used when determining urinary KIM-1 values [27].

To calculate the unknown creatinine concentrations a calibration curve of 8 different concentrations was produced containing the following creatinine concentrations (mg / dL) 80, 40, 20, 10, 5, 2.25, 1.25 and 0.

Sample urine was diluted 1 in 10 (with d H_2O), and then 25 µl of each sample was added to wells of a 96 well flat bottomed plate. 125 µl of reagent A (5 ml of 0.5 M NaOH, 2.5 ml of 0.1 M sodium phosphate dibasic, 2.95 ml of 0.56 M borax, 2.5 ml SDS, 4.5 ml picric acid and 0.5 ml DMSO), was added to each well. After the addition of reagent A the plate was left for 2 minutes at room temperature, then 5 µl of reagent B (0.5 ml acetic acid, 0.1 ml H_2SO_4 and 4.4 ml d H_2O) was added to each well. The plate was then incubated at room temperature for 5 minutes on a plate shaker (300 rpm). The plate was then read at an absorbance of 490 nm using a plate reader (MRX Dynatech laboratories, London, UK)

5.2.5 The determination of sample Kidney Injury Molecule -1 concentrations using Meso Scale Discovery methods.

The Meso Scale Discovery (MSD) platform was selected for urinary KIM-1 analysis for several reasons. Firstly, previous work has demonstrated that MSD has 10 times increased sensitivity and a 2 fold increase in dynamic range compared to Enzyme-Linked Immuno-Sorbant Assay (ELISA) kits, which can also be used to detect urinary KIM-1. The MSD platform is also more time and cost effective compared to ELISA kits (MSD handout, 2012, personal correspondence University of Liverpool)

KIM-1 was chosen as the best bio-marker to look for TFV induced dysfunction as it is specific to damage caused in the proximal tubule (Ichimura et al., 2008).The MSD plates are based upon a sandwich principle (**Figure 5.3 A**), they have electrodes on the bottom of each pre-coated well that can conduct a voltage. The MSD plates used were pre-coated with KIM-1 capture antibodies. Once the sample and solution containing capture antibodies (which are conjugated to electrochemiluminescence labels, the unique MSD SULFO-TAG) are added to the plate, the analytes in the sample bind to the capture antibodies. The bound analytes then recruit the binding of the capture antibodies which completes the sandwich. When the MSD read buffer is added to the plate, it creates a chemical balance that is optimum for electrochemiluminescence. When the plate is added to the SECTOR imager (see **Figure 5.3 B**) a voltage is applied to the electrodes at the bottom of each well and causes the captured SULFO-TAG labels to emit light. The SECTOR imager measures the intensity of the emitted light to give a quantitative measurement of sample analyte concentration.

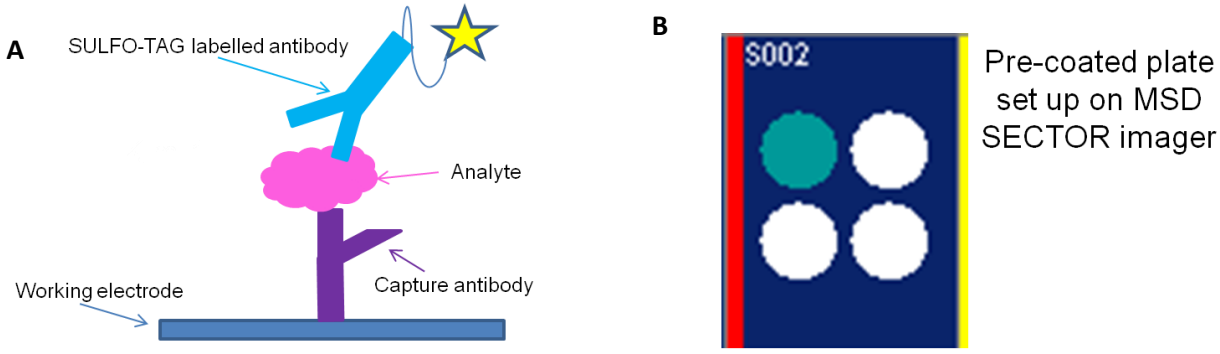

Figure 5.3 A- A schematic image of the MSD sandwich (modified from an image in the MSD handbook) and **5.3 B** – the set up of the SECTOR imager well

A KIM-1 calibration curve was produced in order to establish the unknown KIM-1 concentrations within the samples. The following concentrations of KIM-1 (pg/ml) were used; 5000, 1250, 313, 178, 20, 4.9 and a blank (diluent 37).

To the MSD plate 150 µl of Blocker A (1.25 g Blocker A and 20 ml de-ionised water) was added to each well. The plate was then sealed and shaken (30 minutes, 500 rpm, room temperature). The plate was washed 4 times in 150 µl / well of PBS-T. Urine samples were diluted 1 in 10 with diluent 37, then 50 µl of either calibrator or sample was added per well. The plate was sealed and shaken (2 hours, room temperature, 500 rpm). The plate was then washed with 150 µl / well of PBS-T (repeated 4 times). After washing, 25 µl of 1 x detection antibody solution (60 µl of 50 x SULFO-TAG anti-hu KIM-1 antibody and 2.94 ml diluent 37) was added to each well. The plate was sealed and incubated as before. After 2 hours the plate was washed in 150 µl / well of PBS-T, then 150 µl of read buffer (10 ml read buffer 4 x and 10 ml de-ionised water) was added to each well. The plate was read using a sector imager. Results were analysed using the MSD discovery workbench software.

5.2.6 The analysis of cellular KIM-1 in HEK293 KIM-1cells

HEK293 KIM-1 cells were incubated with TFV (10 μM and 100 μM) for a period of 5, 10, 15 and 20 days. After incubation cell supernatant was diluted 1 in 10, 1 in 100 or 1 in 1000 and were analysed using the MSD protocol. Neat concentrations were not used following the advice in the MSD manual

5.2.6 Statistical analysis

Statistical analysis was carried out on all data. Values are expressed as a mean $\pm$ standard deviation of the mean (SD), this is represented as error bars on all graphs. A Shapiro-Wilk test was first carried out on the data to see if they were considered normal. Univariate analysis was carried out on samples using a Spearman's rank correlation (calculated using the StatsDirect software). Multivariate analysis was carried out on data using a backwards linear model calculated with the SPSS version 20 software. Significance is indicated as follows * $P < 0.05$, ** $P < 0.01$, *** $P < 0.001$

5.3 Results

5.3.1 The analysis of cellular KIM-1 in HEK293 KIM-1 cells

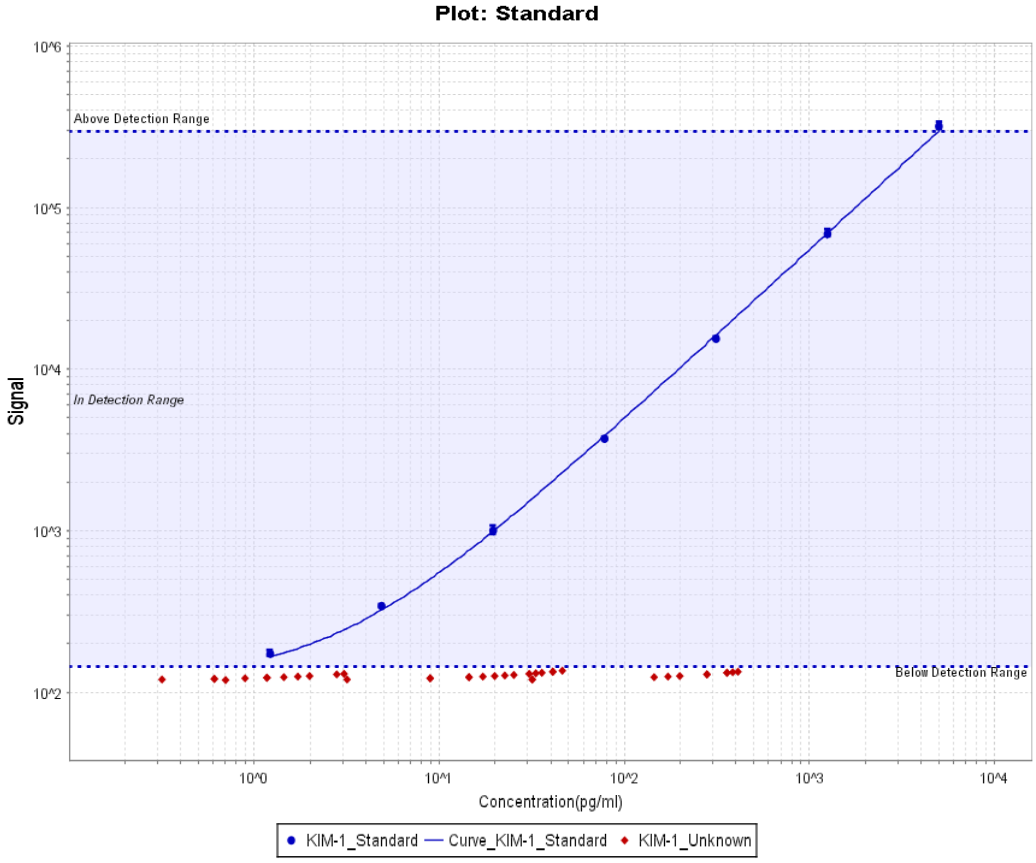

Figure 5.4: Calibration curve for detection of KIM-1 within HEK293 KIM-1 cells treated with varying concentrations of TFV, this was produced by the MSD SECTOR imager and shows that KIM-1 levels in the HEK293 KIM-1 cells (red dots)

The MSD SECTOR imager machine measures the amount of KIM-1 detected within the cells and then constructs a standard curve (TFV concentrations that cells were treated with are manually input into the MSD SECTOR imager) that the cells were dosed with. The calibration curve for the detection of KIM-1 within *in vitro* samples (**Figure 5.4)** shows that KIM-1 levels were undetectable. The samples (in red) were below the line of detection (dotted line). For all samples the value given from the MSD SECTOR imager was 0.

5.3.2 The validation of HIV-1 inactivation methods, using urine collected from healthy volunteers

Urine from healthy volunteers was use to analyse KIM-1 within the samples and to see how inactivation methods would influence these values. Samples were split into three categories and received different treatments; untreated, heat treated or formalin treated. These categories were also split in two, half of which were spiked with a known concentration of KIM-1. Then all samples were analysed for their KIM-1 levels.

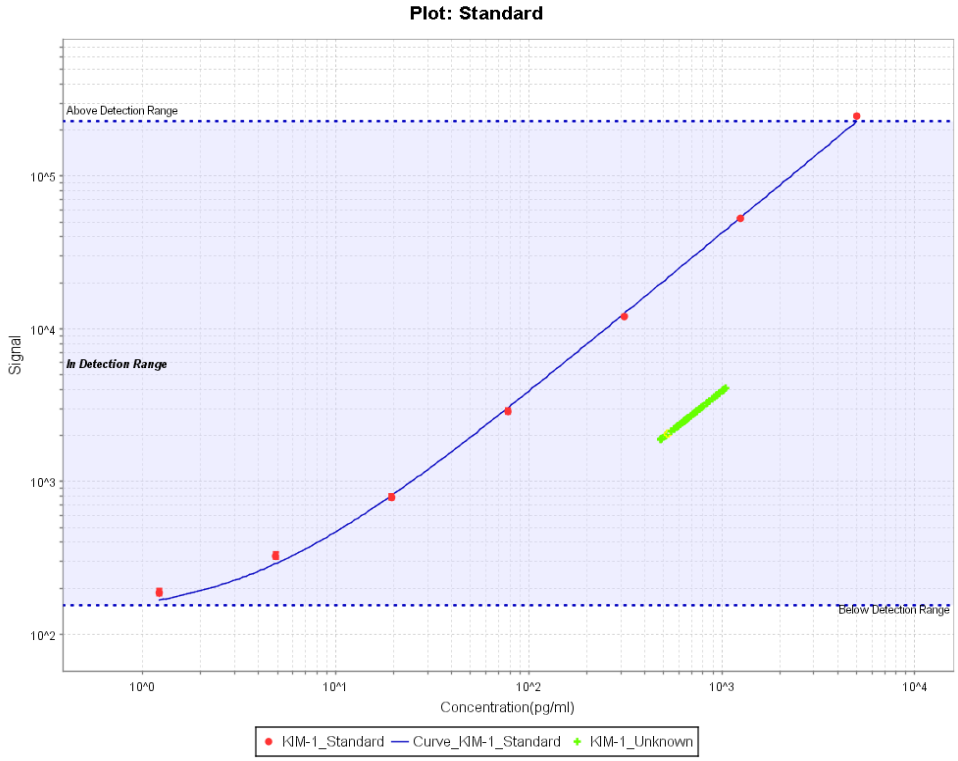

Figure 5.5: Calibration curve for detection of KIM-1 in urine samples treated with formalin or heat treated, this was produced by the MSD SECTOR imager and shows that KIM-1 levels in the samples are detectable represented by the green dots.

The calibration curve for the detection of KIM-1 in healthy volunteers urine (when untreated, heat treated and formalin treated) was produced by the MSD SECTOR imager (**Figure 5.5**) and shows that the KIM-1 can be detected in these samples.

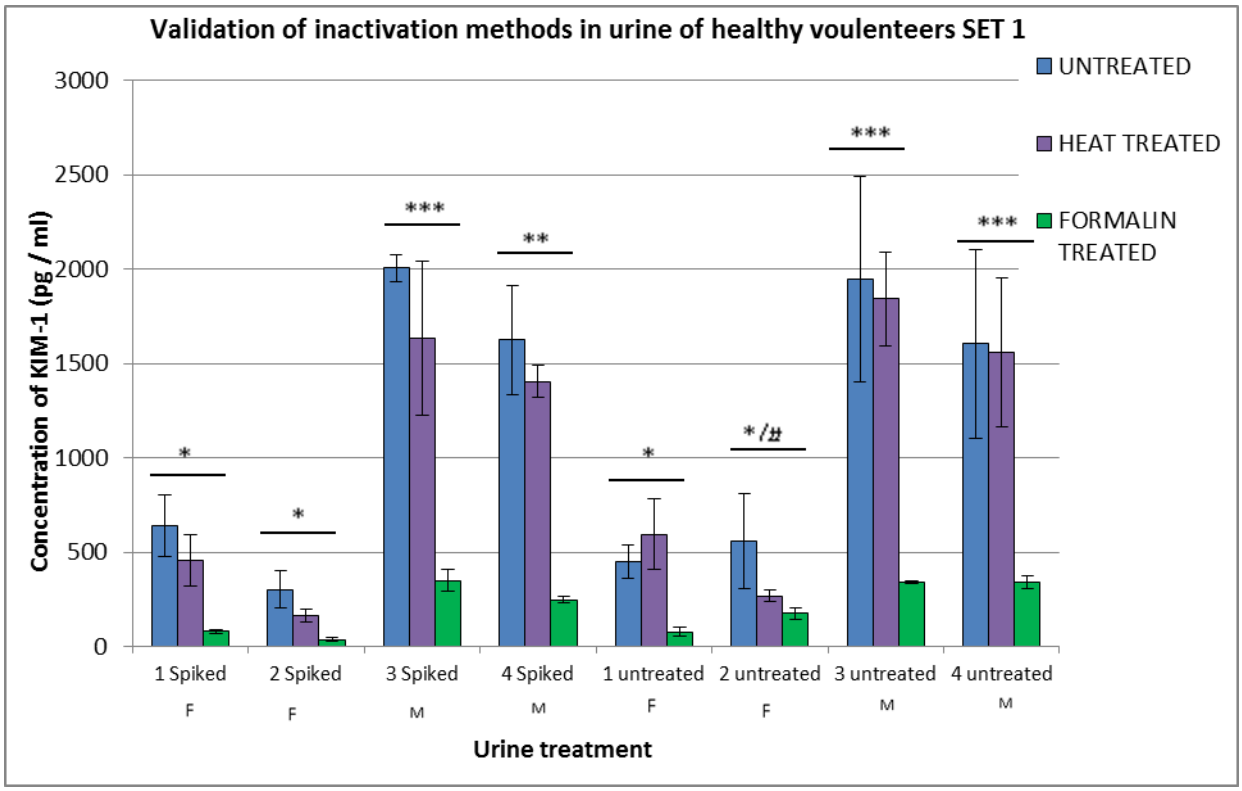

Figure 5.6: Graph showing KIM-1 values in healthy volunteer's urine, comparing untreated to formalin treated and heat treated (F = female and M = male). **KEY** * P <0.05, **P < 0.01, *** P < 0.001 for formalin treatment vs. untreated. # P< 0.05 for heat treatment vs. untreated.

SAMPLE	Heat Treated (expressed as % of untreated)	Formalin treated (expressed as % of untreated)
1 Spiked	71.0	25.2
2 Spiked	86.9	24.1
3 Spiked	81.4	34.8
4 Spiked	86.5	30.3
1 untreated	132.5	34.4
2 untreated	65.5	62.4
3 untreated	94.7	35.2
4 untreated	97.2	42.5

Table 5.1: Shows the values for urinary KIM-1 when formalin or heat treated expressed as a percentage of the UNTREATED KIM-1 values.

Measuring KIM-1 levels in healthy volunteer's urine (when untreated, heat treated and formalin treated – **Figure 5.6**), demonstrates that the levels of KIM-1 were reduced by both heat and formalin treatment, however heat treatment caused less of a reduction. This can be seen clearly when looking at the % of KIM-1 signal in the heat / formalin treatments in comparison to the untreated samples (**Table 5.1**). When heat treated the average % of KIM-1 recovery was 97.5 % (in un-spiked samples) in comparison to the average % of KIM-1 recovery for the formalin treatment which was 43.69%. The mean KIM-1 concentration for the untreated male samples was1773.6 and for the untreated females it was 503.6 pg/ ml

A second set of volunteer samples was used for the validation of the heat treatment.

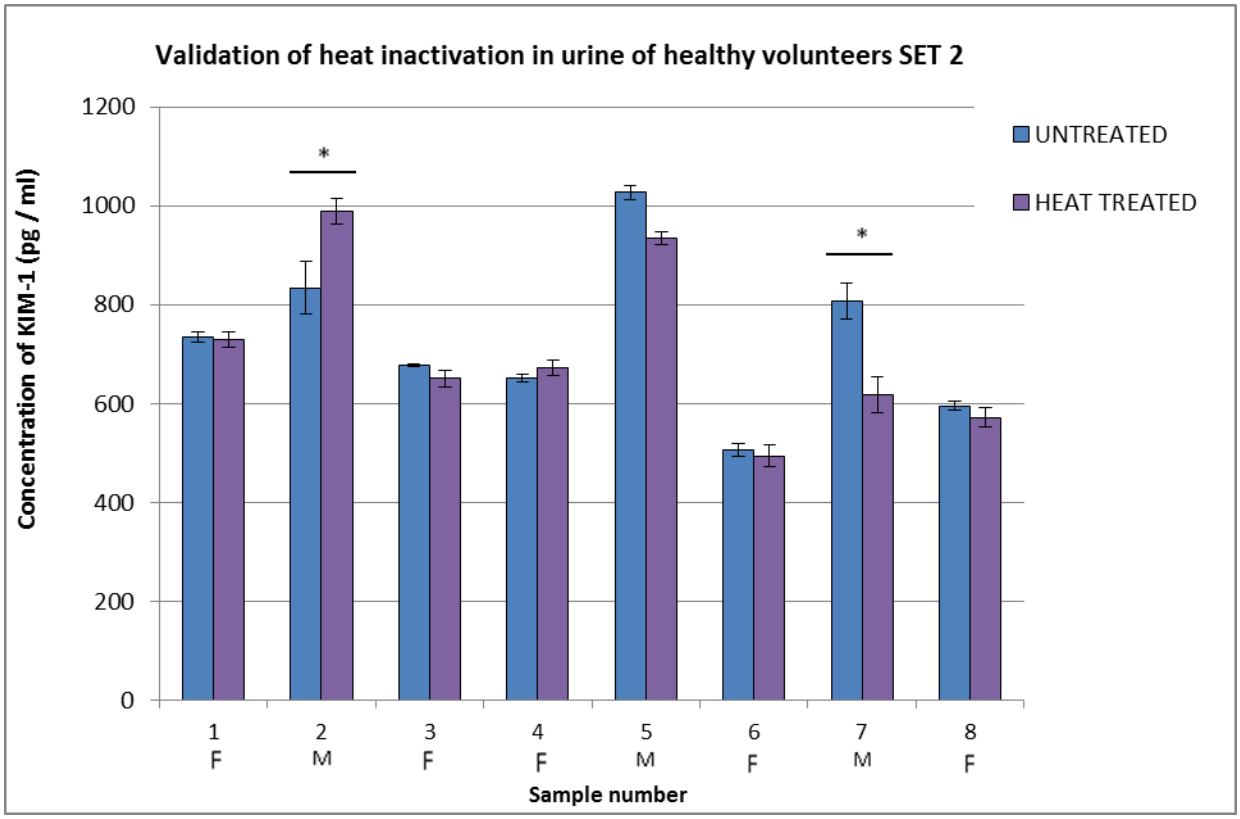

Figure 5.7: Graph showing KIM-1 values in healthy volunteer's urine when heat treated vs. untreated. (F = female and M = male). **KEY** * $P < 0.05$ for untreated vs. heat treated

The graph showing the KIM-1 detected within the urine of healthy volunteers in untreated and heat treated samples (**Figure 5.7**), shows that the heat treatment of the samples on average has not significantly reduced the value of KIM-1 detected within the urine. The maximum reduction in KIM-1 concentration due to the heat treatment was seen in sample 7 were KIM-1 reduced from 867.1 pg/ml to 617.6 pg/ml. The minimal reduction in KIM-1 concentration due to heat treatment was seen in sample 1 KIM-1 reduced from 735.3 pg/ml to 728.8 pg / ml. Unexpectedly for sample 2 and 4 there was an increase in KIM-1 when the sample was heat treated (In sample 2 KIM-1 increased from 834.2 pg /ml to 988.9 pg / ml and for sample 4 KIM-1 increased from 651.3 pg / ml to 671.4 pg / ml). The overall average % recovery of KIM-1 signal when the samples were heat treated was 97 % including sample 2 and 4 and 91.2 % when discounting sample 2 and 4. The mean KIM-1 concentration for the males was 850.7 pg /ml and for the females it was 607.6 pg/ ml.

A third set of volunteer urine samples was used to validate how heat treatment affects KIM-1, urinary creatinine and the widely used KIM-1 /creatinine ratio.

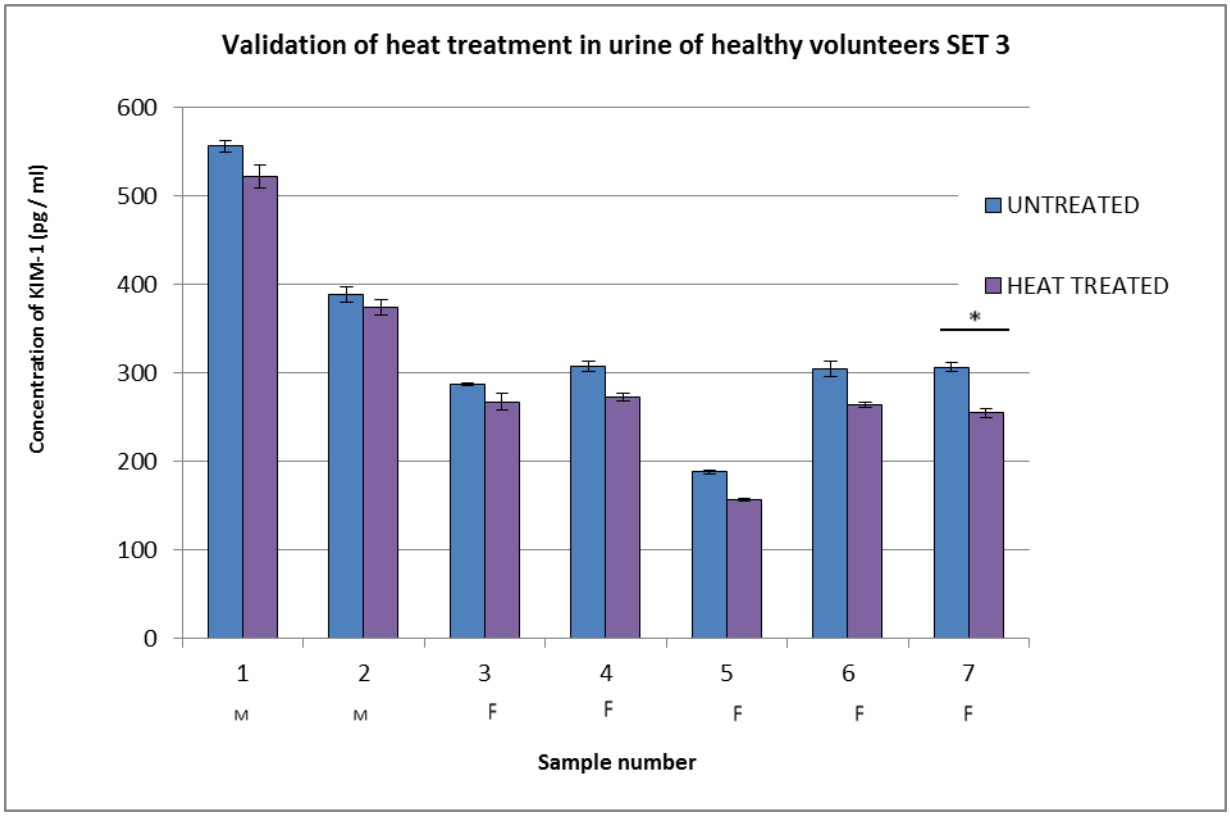

Figure 5.8: Graph showing KIM-1 values in healthy volunteer's urine when heat treated vs. untreated (F = female and M = male). **KEY** * P <0.05 for heat treatment vs. untreated.

The graph showing the determined KIM-1 concentrations (pg / ml) of urine from healthy volunteers when untreated and heat treated **(Figure 5.8)**, showed that heat treatment on average did not significantly decrease the KIM-1 within the urine samples. The maximum reduction in KIM-1caused by the heat treatment can be seen in 7, the KIM-1 reduced from 306.7 pg / ml to 254.5 pg / ml. The minimal reduction in KIM-1 caused by the heat treatment was observed in sample 2 KIM-1 reduced from 388.4 pg /ml to 374.3 pg / ml. The overall KIM-1 % recovery when the samples were heat treated was 90.2%. The mean KIM-1 concentration for the males 472 pg /ml was and for the females it was 278.9 pg /ml.

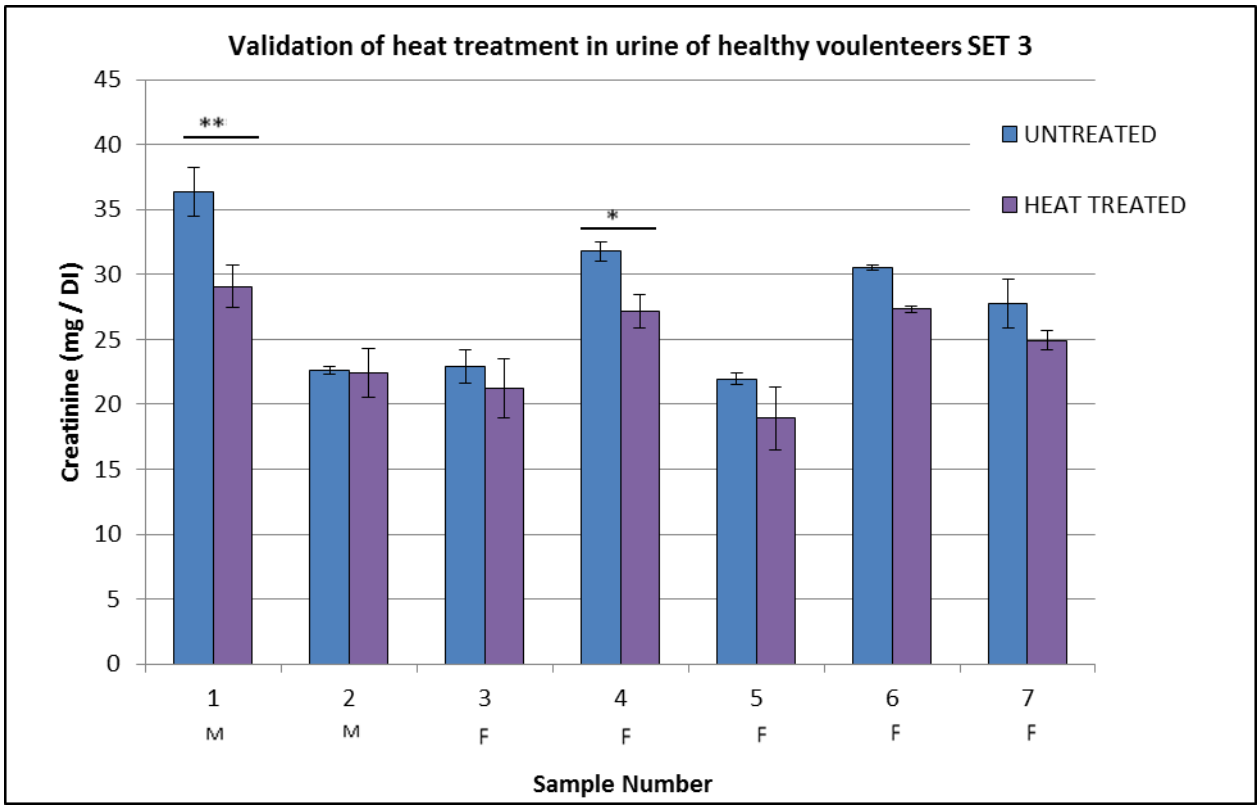

Figure 5.9: Graph showing creatinine values in healthy volunteer's urine when heat treated vs. untreated (F = female and M = male). **KEY** * P <0.05, ** P < 0.01 for heat treatment vs. untreated.

The graph showing the determined creatinine concentrations (mg/dL) of urine from healthy volunteers when untreated and heat treated **(Figure 5.9)**, showed that the heat treatment on average did not significantly decrease the creatinine concentrations within the urine samples. The maximal creatinine reduction induced by the heat treatment can be seen in sample 1, creatinine reduced from 36.37 mg/dL to 29.44 mg/dL. The minimal reduction in creatinine was observed in sample 2, creatinine reduced from 22.63 mg/dL to 22.47 mg/dL. The overall % of creatinine recovery when the samples were heat treated was 90.1%. The mean creatinine concentration for the males 29.5 mg / dL was and for the females it was 27 mg / dL.

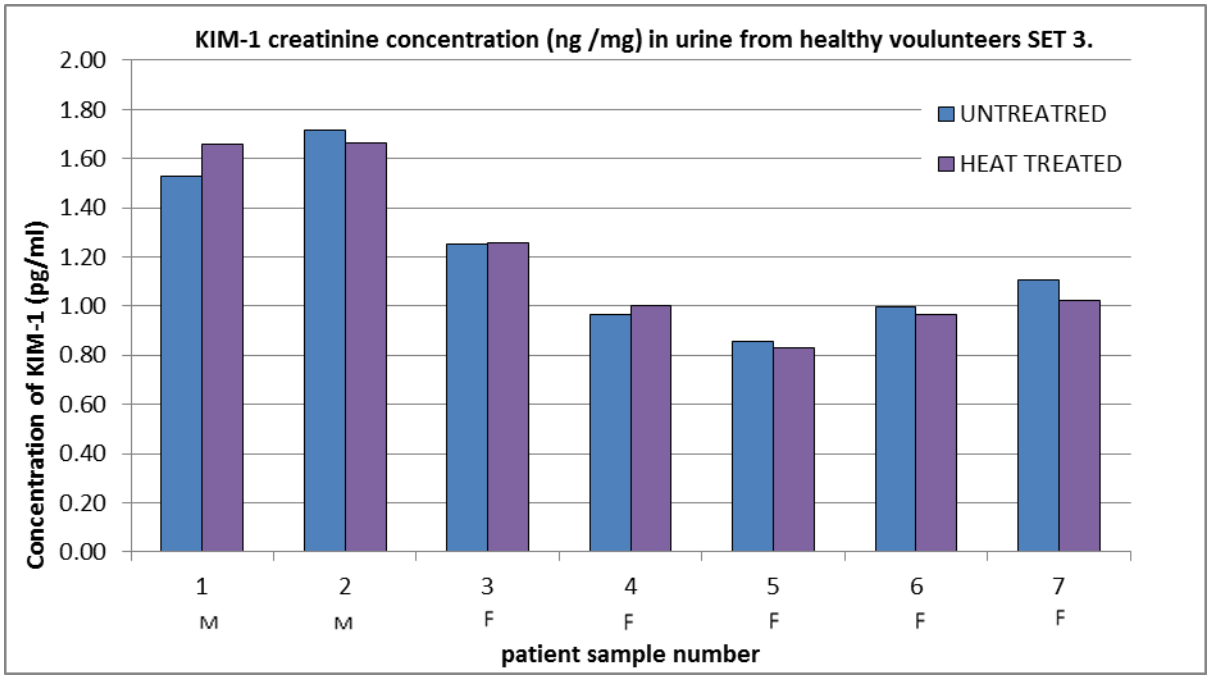

Figure 5.10: Graph showing KIM-1 / creatinine ratio in healthy volunteer's urine when heat treated vs. untreated (F = female and M = male).

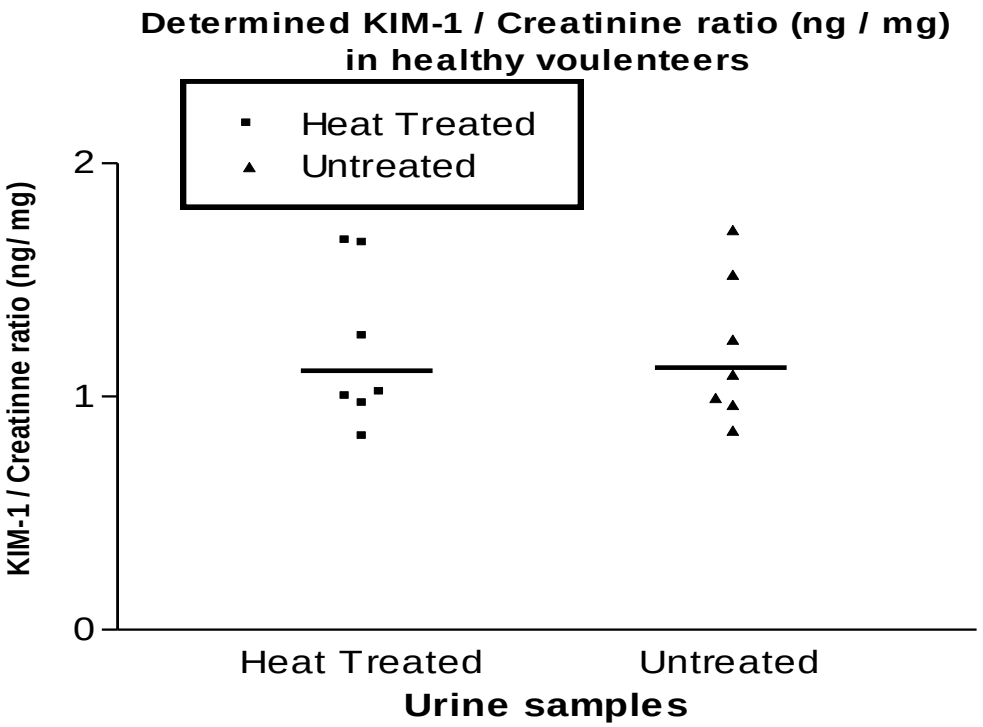

Figure 5.11: Strip Graph showing KIM-1/ Creatinine ratio (ng / mg) in healthy volunteer's urine when heat treated vs. untreated. The median values are shown on the graph represented by a line.

The graph showing the determined urine samples KIM-1/ creatinine ratios (**Figure 5.10**), shows that the KIM-1 / creatinine (ng / mg) ratio was not significantly reduced by heat treatment. The mean KIM-1 / creatinine ratio in untreated urine samples was 1.10 ng / mg, this was reduced to 1.02 ng / mg in heat treated samples. The overall % recovery of the KIM-1 / creatinine ratio within the heat treated samples when compared to untreated samples was 99.69 %. The spread of this validation data and the averages of each data set (untreated and heat treated) can be seen in **Figure 5.11**. The mean KIM-1 concentration for the males was 1.64 ng / mg and for the females it was 1.04 ng / mg .

5.5.4 The determination of the urinary KIM-1 in patient samples using MSD methods.

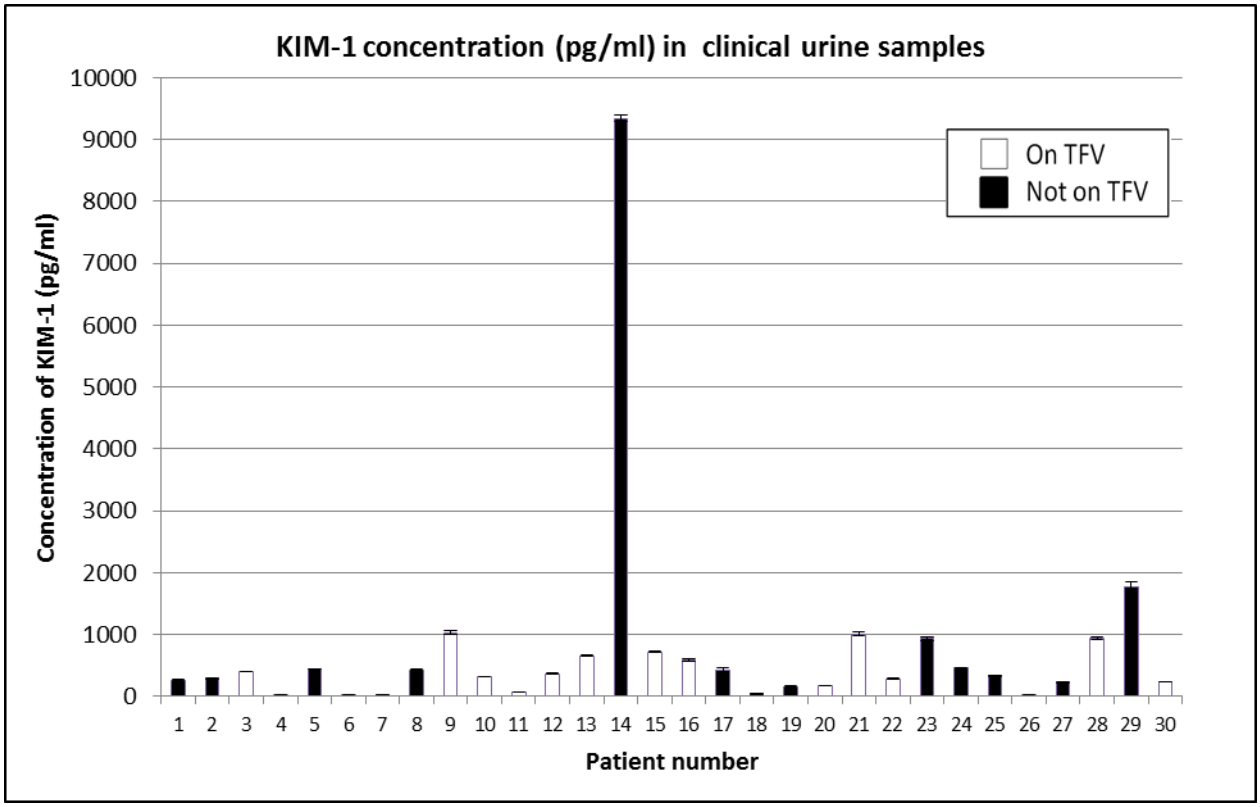

Figure 5.12: Graph showing determined KIM-1 (pg/ml) values in patient urine

When KIM-1 levels were determined within patient samples (**Figure 5.12**), results demonstrated that there was a wide range of KIM-1 levels within the patients (from 32.2pg/ml to 9342.2 pg /ml). It can be seen that several patients not taking TFV have similar levels of KIM-1 as patients taking TFV, for example patient 6 (on TFV treatment) has a KIM-1 value of 39.54 pg / ml and patient 7 (not on TFV treatment) has a KIM-1 value of 38.93 pg / ml. Patient 14 (not on TFV treatment) has the highest KIM-1 concentration of 9342.23 pg / ml and patient 26 (on TFV treatment) had the lowest KIM-1 value of 32.15 pg / ml. The mean KIM-1 value for all the data is 736.8 pg / ml, the mean KIM-1 for those patients on TFV was 433.1 pg / ml and the mean KIM-1 value for the patients not on TFV was 1084 pg / ml (when patient 14 is removed this value reduces to 448.7 pg / ml). The

median KIM-1 value for all the data was 352 pg / ml , the median KIM-1 for those patients on TFV was 344.8 pg / ml and the median KIM-1 for the patients not on TFV was 384.3 pg / ml (when patient 14 is removed this value reduces to 335.5 pg / ml).

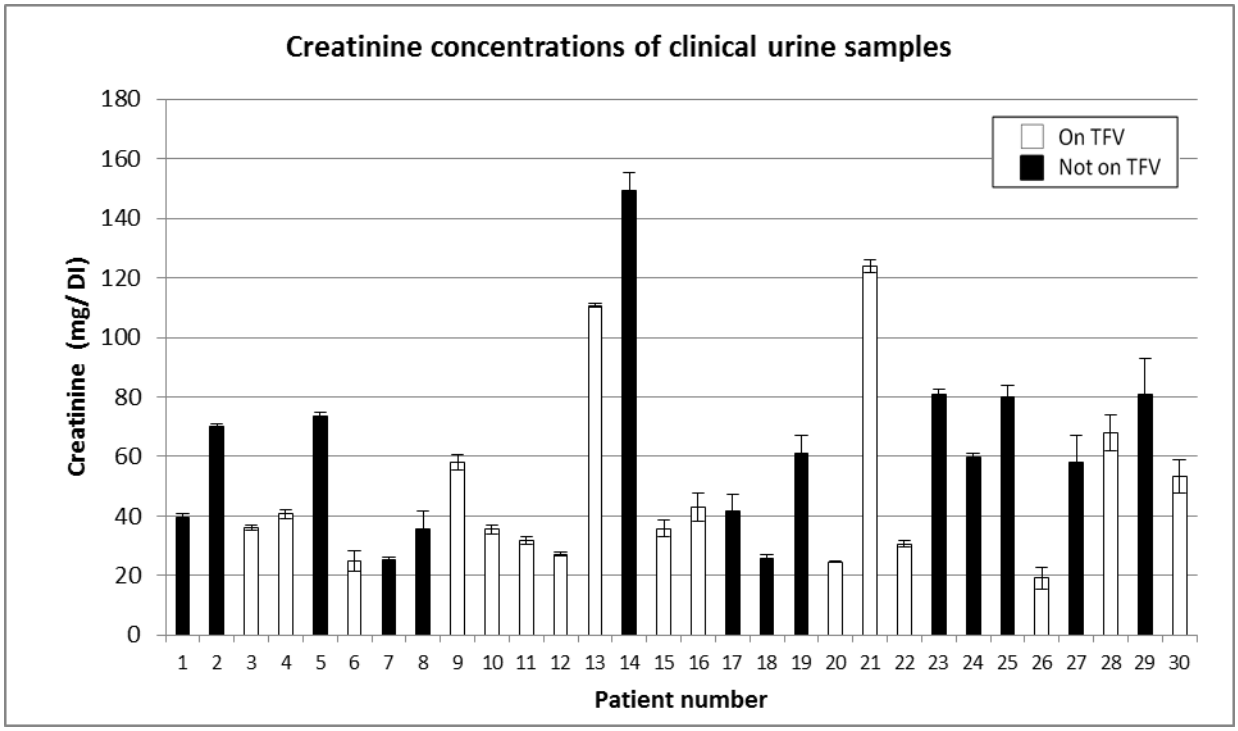

Figure 5.13: Graph showing determined creatinine (mg /dL) values in patient urine

The determined creatinine (mg / dL) levels within patient samples (**Figure 5.13**), demonstrates that there was a wide range of creatinine levels within the cohort patients. Patient 14 (not on TFV treatment) has the highest creatinine concentration of 149.32 mg/ dL and patient 26 (on TFV treatment) had the lowest creatinine value of 19.12 mg/ dL. The mean values for all the data was 54.8 mg/ dL , the mean creatinine concentration for those patients on TFV was 47.7 mg/ dL and the mean creatinine value for the patients not on TFV was 63.0 mg/ dL (when patient 14 is removed this value reduces to 50.3 mg/ dL).

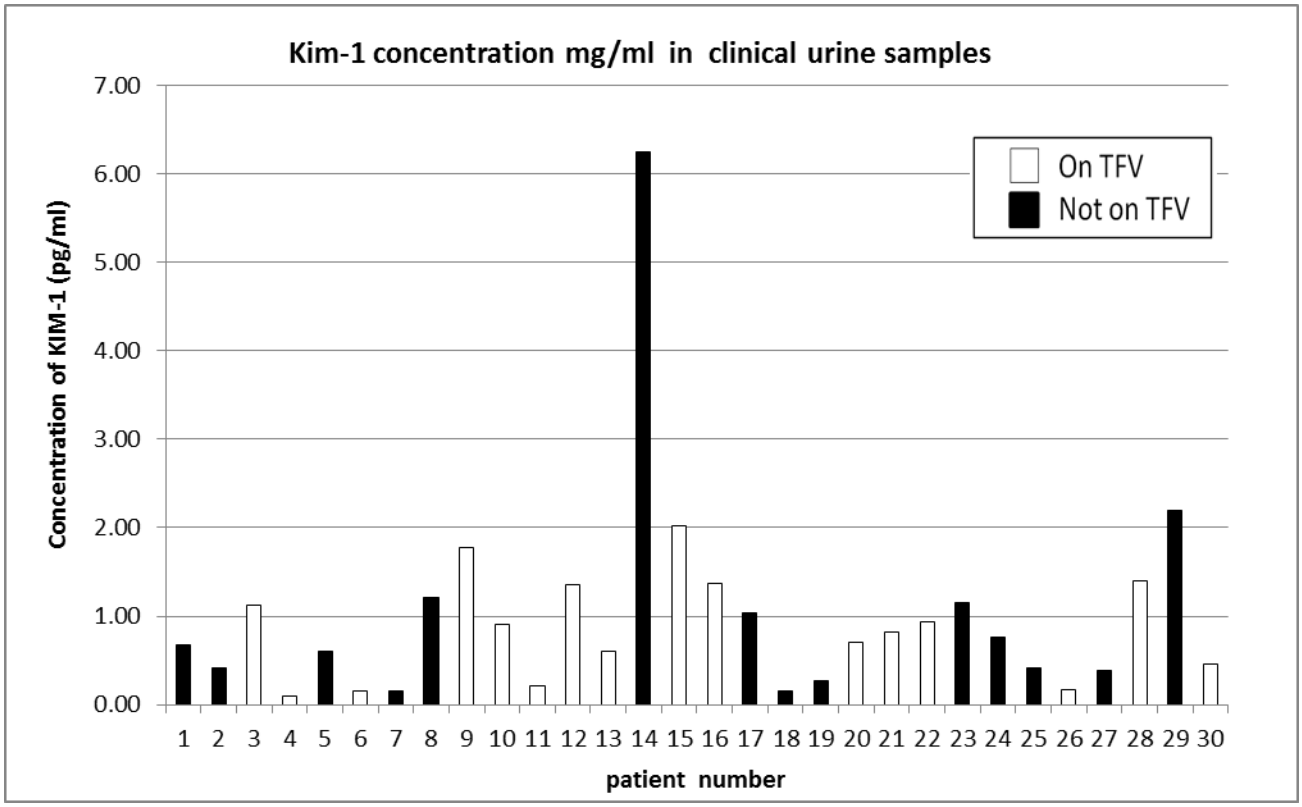

Figure 5.14: Graph showing determined KIM-1 / creatinine ratio in patient urine

patient Number	creatinine (mg/Dl)	KIM-1 (pg/ml)	KIM-1 ng/ creatinine (mg/ml)	TFV treatment	TDF detected in urine	FTC detected in urine	3TC detected in urine
1	39.55	265.31	0.67	NO	BLQ	BLQ	BLQ
2	69.90	288.64	0.41	NO	BLQ	BLQ	BLQ
3	36.08	403.58	1.12	YES	12576.04	9123.364	BLQ
4	40.66	38.78	0.10	YES	25522.91	10807.4	BLQ
5	73.44	443.73	0.60	NO	BLQ	BLQ	BLQ
6	24.91	39.54	0.16	YES	19232.71	7852.589	BLQ
7	25.39	38.93	0.15	NO	BLQ	BLQ	BLQ
8	35.74	432.93	1.21	NO	BLQ	BLQ	BLQ
9	58.10	1032.28	1.78	YES	BLQ	BLQ	170209
10	35.51	321.36	0.91	YES	90237.97	22487.09	BLQ
11	31.60	67.53	0.21	YES	17232.51	7258.936	BLQ
12	27.07	368.52	1.36	YES	47666.3	8286.948	BLQ
13	110.70	662.67	0.60	YES	289423.1	54920.59	BLQ
14	149.32	9342.23	6.26	NO	BLQ	BLQ	BLQ
15	35.74	721.94	2.02	YES	2750.006	757.818	BLQ
16	42.93	585.87	1.36	YES	66286.26	20725.63	BLQ
17	41.71	434.82	1.04	NO	BLQ	BLQ	BLQ
18	25.78	41.33	0.16	NO	BLQ	BLQ	BLQ
19	61.18	164.05	0.27	NO	BLQ	BLQ	BLQ
20	24.61	174.11	0.71	YES	33438.03	6091.926	BLQ
21	123.89	1006.57	0.81	YES	101156.3	45046.38	BLQ
22	30.63	286.21	0.93	YES	63316.8	8034.422	BLQ
23	80.75	933.24	1.16	NO	BLQ	BLQ	BLQ
24	59.69	458.14	0.77	NO	BLQ	BLQ	BLQ
25	80.15	335.52	0.42	NO	BLQ	BLQ	BLQ
26	19.12	32.15	0.17	YES	BLQ	BLQ	52806.84
27	57.85	220.93	0.38	NO	BLQ	BLQ	BLQ
28	67.99	947.03	1.39	YES	979466.1	120362.7	737.807
29	80.96	1776.29	2.19	NO	BLQ	BLQ	BLQ
30	53.16	240.93	0.45	YES	389121.5	38927.3	BLQ

Table 5.2: Table showing the determined KIM-1 (pg / ml) levels, creatinine (mg/dL) levels and KIM-1 /Creatinine ratios (ng / mg) within the patient urine samples. Also shown is the data obtained from The University of Liverpool BAF, showing the levels of TDF, FTC and 3TC found within these urine samples. BLQ is below limit of quantification

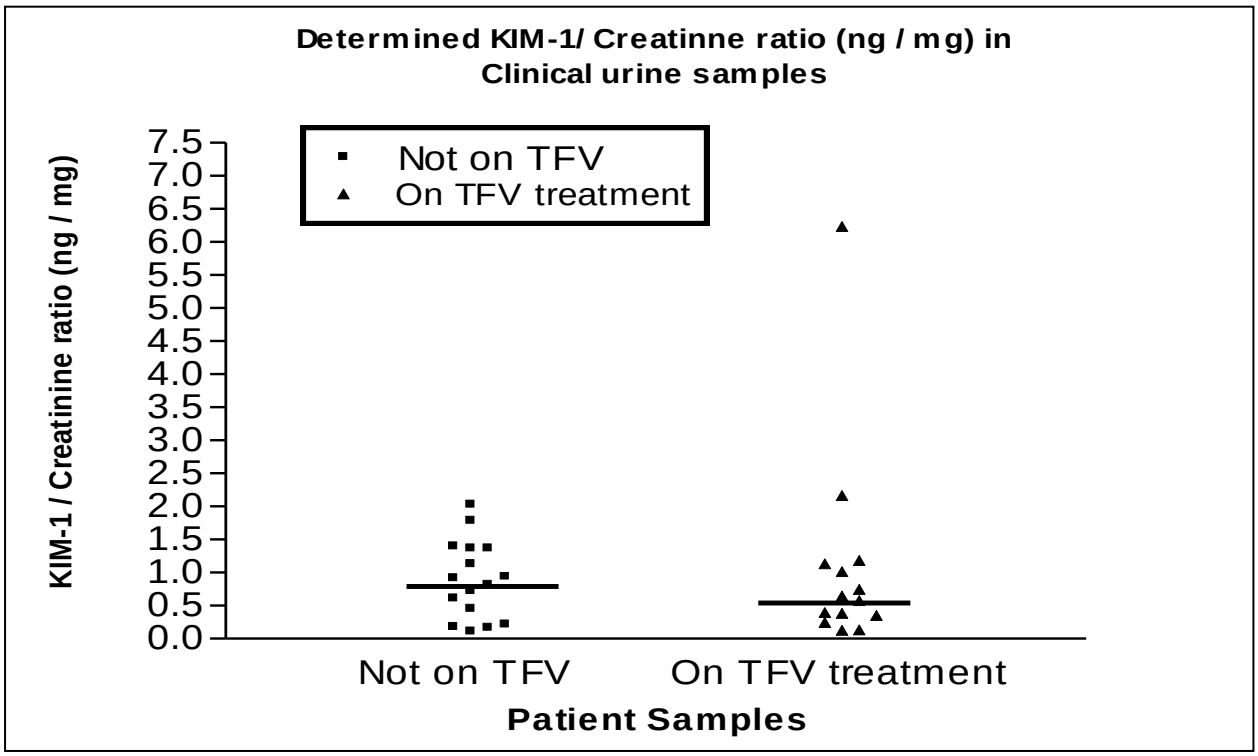

Figure 5.15: Strip Graph showing KIM-1/ Creatinine ratio (ng / mg) in clinical urine samples. The median values are shown on the graphs represented by a line.

The ratios of KIM-1 / creatinine (ng / mg) levels were determined within the patient samples (**Figure 5.14**), and the results demonstrated that there was a wide range of ratio levels within the patients. Patient 14 (not on TFV treatment) has the highest ratio of 6.25 ng /mg and patient 4 (on TFV treatment) had the lowest ratio value of 0.10 ng /mg. The mean ratio for all the data was 0.99 ng /mg, the mean ratio for those patients on TFV was 0.88 ng/mg and the mean creatinine value for the patients not on TFV was 1.22 ng/mg (when patient 14 is removed this value reduces to 0.64). The median ratio value for all the data was 0.74 ng/mg , the median ratio for those patients on TFV was 0.86 ng/mg and the median creatinine value for the patients not on TFV was 0.64 ng/mg (when patient 14 is removed this value reduces to 0.60 ng /mg). The spread of this clinical data and the averages of each data set (not taking TFV and on TFV treatment) can be seen in **Figure 5.15.**

When uni-variant analysis was carried out between TFV concentrations found within the patient's urine (**Table 5.2** all patients on TFV) and KIM-1 values the positive correlation p value was 0.09. When univariate analysis was carried out between TFV concentrations and creatinine values the positive correlation p values was 0.014. When univariate analysis was carried out between TFV concentrations and the KIM-1 /creatinine (ng/mg) ratio the positive correlation p values was 0.42. When univariate analysis was carried out between the KIM-1 values and the creatinine values the positive correlation p value was 0.01.

5.6 Discussion

This chapter has focused on using KIM-1 as a potential bio-marker to predict TFV-induced renal dysfunction. Within this chapter the association between TFV and KIM-1 levels *in vitro* using the supernatant from HEK293 KIM-1 cells was examined. The calibration curve for the detection of KIM-1 within the *in vitro* samples (**Figure 5.4)** demonstrated that the KIM-1 levels were undetectable in these samples irrespective of concentration of TFV and incubation length. Previous work within the department suggested that this could be due to the FBS interfering with this platform (Personal correspondence, The University of Liverpool). As the incubation periods required to see TFV-induced cytotoxicity are long (10 – 20 days as determined in Chapter 3 and 4), the cells could not be grown in a serum-free media without the cells phenotype becoming compromised. In conclusion in order to assess the influence of TFV on KIM-1 concentrations, the MSD platform will perform better with urine samples instead of *in vitro* samples due to this interference issue.

Following on from the *in vitro* analysis, KIM-1/creatinine (ng / mg) ratios were determined in urine samples from healthy volunteers. The MSD assay used for the determination of KIM-1 within urine samples was previously validated within this department using spiked urine; the lower limit of detection and lower limit of quantification were determined. Work was carried out to validate different inactivation methods that would be needed in order to analyse urine samples from HIV-1-infected patients. It can be seen in **Figure 5.6** that the formalin treatment of the urine samples has significantly reduced the KIM-1 signal within the urine samples, resulting in a lowered capacity to detect KIM-1. The heat treatment also caused a slight decrease in KIM-1 concentrations; however there was an average percentage loss of only 2.4% which is within the current accepted guidelines for recovery. The current guidelines for recovery state that an accepted percentage loss should be $\leq$ 10 % [27]

Further validation of heat treatment of urine samples from healthy volunteers was carried out. Firstly a further study of the effects of heat treatment on the urinary KIM-1 concentration was carried out in urine samples from 8 healthy volunteers. As seen in **Figure 5.7** this validation step again showed that the heat treatment caused an acceptable average percentage loss of 8.2%. Another set of urine samples from 7 healthy volunteers was obtained, and the effects of heat treatment on KIM-1, urinary creatinine levels and the KIM-1 / creatinine ratio was determined within these samples. In **Figure 5.8** it can be seen that the heat treatment has caused an accepted percentage loss of 9.8 % to the KIM-1 concentrations (comparing the untreated samples to heat treated samples). The creatinine concentrations determined within these samples can be seen in **Figure 5.9.** When comparing the untreated samples to the heat treated samples the average percentage loss was 9.9%, which is within the accepted 10 % guidelines. The KIM-1 concentrations were normalized to the creatinine concentration found within these urine samples, in order to obtain the KIM-1 / creatinine ratio (ng / mg). This is the currently used method to determine KIM-1 within urine samples [27]. When looking at **Figure 5.10** and **5.11** results show that the KIM-1 / creatinine ratio was not affected by the heat treatment and the average percentage loss was only 0.31%

After the validation work had been carried out the urinary KIM-1 / creatinine (ng/mg) ratios were determined in a cohort of 30 HIV-1 patients. This cohort was readily available from the Liverpool BAF and relevant to this work as it was possible to compare patients with and without TFV present in urine the patients were not well characterised and not much was known about them. Clinical urine samples were first inactivated via heat treatment, in order to be removed from a BL2 laboratory, and the influence of TFV on this ratio was determined.

Results demonstrated that there was a large degree of variability observed in these samples with respect to KIM-1 levels (**Figure 5.12**). Interestingly for both KIM-1 and creatinine

values within these patients samples; the group with the highest average is the patients not taking TFV, although this number does not reach significance. This trend was also seen in **Figure 5.14** when calculating the urinary KIM-1 / creatinine ratios within the patient samples. However, when the median values for each data set was calculated, as the median is not influenced by the spread of the group (patient 14 in those patients not taking TFV would cause the mean values to be higher), the median values were slightly higher but not significant for those patients on TFV compared to those not on TFV treatment. An increased KIM-1 for those patients on TFV can also be seen when patient 14 is left out of the mean calculations. These mean and median values could become significant if a bigger cohort of patients was used.

An interesting fact to note is that the average baseline urinary KIM-1 within healthy volunteers was 1.1 ng/mg. This was higher than the average baseline within the HIV-1 patients, which was 0.99 ng/ mg, although the difference is not significant. It could be a possibility that baseline KIM-1 levels within HIV-1 patients may be slightly lowered, due to the HIV-1 virus compromising kidney function and decreasing urinary output [28].

Patient 14 has the highest KIM-1(pg / ml) and creatinine (mg/Dl) concentrations and in **Figure 5.14** it can be seen that patient 14 also has the highest KIM-1 / creatinine (ng / mg) ratio. When looking at **Table 5.2** it is clear that this patient is not on any TFV containing regimens, as the current kidney function of this patient is not known the possibility that this patient has kidney dysfunction cannot be determined. It is a possibility that this patient is experiencing kidney dysfunction as a direct result of being HIV-1 positive. Studies have linked HIV-1 patients to development of kidney dysfunction due to the virus [28].

The univariate analysis of those patients on TFV, demonstrated that the urinary creatinine concentrations had a significant P value (P < **) compared to those patients not on TFV

treatment. However, KIM-1 did not show as significant within those patients on TFV. This shows that creatinine may not be as specific as KIM-1 when it comes to determining the onset of proximal tubule kidney dysfunction. As urinary creatinine is affected by factors that influence kidney function, such as chemical stress, using creatinine as a marker for proximal tubule toxicity may result in false positives. A false positive would lead to patient withdrawal from an effective treatment and for HIV-1 patients this could increase their risk factor for developing resistance.

The univariate analysis of all patients KIM-1 concentrations against creatinine concentrations showed KIM-1 and creatinine had a highly significant correlation (P < **); this was to be expected as urinary creatinine is linked to GFR, and therefore any increase in GFR will also increase urinary creatinine output. As GFR increases it is assumed that KIM-1 output will also increase as previous studies have shown that KIM-1 is shed through the urine [27].

There are conflicting reports in the literature with respect to the detection of KIM-1 in samples from healthy volunteers. Previous studies stated that urinary KIM-1 was undetectable within healthy populations [23]. However, others have shown this to not be the case [27], also work within the department using the MSD platform has found that there is an average KIM-1 / creatinine ratio of 1 ng / ml in neonates (Personal correspondence, The University of Liverpool). In **Figure 5.11** it can be seen that the average baseline ratio of KIM-1/ creatinine in urine of healthy volunteers was 1.1 ng/ml. The range of the healthy volunteer's baseline urinary KIM-1 / creatinine ratio was 1.72 ng/ml to 0.83 ng/ml. In a previous study, it was shown that the urinary KIM-1/ creatinine ratio was detectable in healthy volunteers and they had a range of 0.07 ng / ml to 0.988 ng / ml [27]. This range is slightly lower than the range that has been shown within this Chapter. It could be that the MSD platform used in this chapter was more sensitive and had a lower limit of quantification

than the ELISA kits that were used in previous studies. Therefore, these results could show a better of representation baseline urinary KIM-1 levels within a healthy population. Together, these findings suggest that there is always a higher than previously thought baseline level of KIM-1 within a seemingly healthy person. This background KIM-1 may be due to daily renal cellular shedding. More work needs to be carried out to find a true representation of this baseline urinary KIM-1 level within healthy populations, as well as within HIV-1 infected patients , before KIM-1 can be used as an effective bio-marker.

The validation work using the urine form healthy volunteers carried out within this study showed that males have a higher baseline KIM-1 level when compared to females. This difference could be due to the known fact that males have a higher metabolic rate than females, therefore males produce more waste produces than females leading to a higher concentration of KIM-1(KIM-1 is shed in urine). This leads to the questions of other factors that may influence an individual's baseline KIM-1 levels that are as yet unanswered. Demographic factors such as height, weight, genetics, race and age may affect their baseline urinary KIM-1 levels. Also certain over the counter medications such as ibuprofen (which affects kidney function [29] may affect a person's baseline KIM-1 level. These factors need to be studied further in order to establish a threshold that would give a positive result for proximal tubule dysfunction within patients.

For HIV-1 patients, their baseline urinary KIM-1 / creatinine ratio before treatment could be determined and monitored, in order to see any significant increase that would suggest onset of proximal tubule dysfunction.

A larger cohort of HIV-1 patients would provide a higher powered study to establish how TFV influences a HIV-1 patients urinary KIM-1 / creatinine. More information about the patients should be collected (age, race, height, weight, gender, period of time they have had

HIV-1, previous HARRT regimens taken, current HAART regimen being taken and concentrations and length on these treatments) as well as bloods (in order to establish GFR , protein urea and serum creatinine). These extra measurements would allow a clearer understanding of the variability in urinary KIM-1 / creatinine ratios and show the limitations of the current study.

Other biomarkers should also be considered in the future for use as TFV-specific biomarkers. Recent reports have highlighted the effectiveness of using mitochondrial DNA (mtDNA) levels within patient PBMC's as a good biomarker for the detection of mitochondrial dysfunction [30]. As work within this thesis has shown TFV to induce mitochondrial dysfunction, the use of mtDNA could be a potential marker for TFV-induced toxicity.

Overall, the work presented within this chapter highlights the feasibility of KIM-1 as a biomarker for TFV associated renal toxicity, additional information is needed to understand the effects of drug treatment on KIM-1 levels. Work has shown that heat inactivation would not influence the KIM-1 / creatinine ratios within clinical urine samples, and showed that future work needs to be carried out in order to establish healthy population's baseline urinary KIM-1 / creatinine levels. The possible use of KIM-1 as a biomarker for TFV-induced proximal tubule dysfunction could be used within a clinical setting once more confirmatory work has been carried out. Further study, in a larger cohort, is now warranted.

Chapter Six

GENERAL DISCUSSION

In this thesis, research has focused on the antiretroviral drug TFV in order to elucidate the mechanistic pathways of its toxicity. This work was essential for understanding the underlying mechanisms of proximal tubule toxicity that has been linked to TFV use clinically [1].

It is important to understand how TFV-induced proximal tubule dysfunction takes place as TFV is currently a front line antiretroviral drug that makes up the backbone of most HAART regimens due to its favourable pharmacokinetic and pharmacodynamic properties, which allows for a single daily dose [2]. If the toxicological mechanisms of TFV were elucidated patients that are at higher risk of developing proximal tubule toxicity could be identified and closely monitored [3].

The original aim of this thesis was to elucidate the mechanistic pathway of TFV-induced toxicity in order to develop safer HIV treatments in future, either via the identification of potential biomarkers to monitor TFV-induced renal dysfunction, or by identifying those patients who are more susceptible to TFV-induced renal dysfunction. Upon reflection, work presented within this thesis has fulfilled this aim as the research has led to the construction of a picture that demonstrates the mechanistic pathway of TFV-induced cytotoxicity (**Figure 6.1**). However, more work needs to be done in the future in order to support these findings and to expand on them especially with regards to the use of KIM-1 as a potential biomarker.

A key area that has changed since this thesis started is the use of TFV as an HIV preventative. A novel indication for TFV treatment has recently been approved in which TFV is used as chemoprophylaxis for the prevention of HIV infection in HIV negative patients [4-5]. This treatment is known as pre-exposure prophylaxis (PrEP). An idealistic tool for HIV prevention would be the use of a protective vaccine, however this still remains unfeasible due

issues surrounding the effectiveness [6]. PrEP uses antiretroviral drugs to prevent HIV contraction should HIV exposure occur (promiscuous sex / the sharing of needles/ contact with infected bodily fluids) [7-8]. Antiretroviral drugs are already currently used for the prevention of HIV in other high risk situations such as high risk sexual exposures, rape and prevention of mother to baby transmission [7-8]. The difference with PrEP treatment, compared to the other prevention strategies listed above, is that the target population will most likely be young adults in prime health that have no immediate risk of HIV exposure [9]. For this reason PrEP must have proven benefit in order to have a good risk benefit ratio; PrEP must be cost effective for patients and studies must show that it has a low toxic profile [10].

Recently TFV was approved to be used for PrEP treatment; it is the only drug that has been approved for this treatment type. A typical pre-exposure prophylaxis regimen is either oral tablets containing TFV alone (Viread) or as vaginal gel (1% tenofovir) [11]. The introduction of TFV as a PrEP reinforces the importance of understanding the mechanism of TFV-induced toxicity as a wider population of people will be exposed to TFV in the future and people who are at risk could be monitored via the use of biomarkers or offered an alternative treatment [3]. Based upon the findings within this thesis, people who take TFV for PrEP treatment should be monitored closely for signs of proximal tubule specific kidney damage; hopefully in the future this can be done by screening the patient's urine for changes in KIM-1 expression.

The research carried out within this thesis is of key importance for understanding the mechanistic pathway of TFV-induced toxicity. This work was required as previous in vitro studies have reported that TFV does not cause any cytotoxicity *in vitro* which could be due to them using immortalised cell lines grown in high glucose media [12]. These results conflict

with clinical data that has shown that as many as 20% of patients have presented with TFV-induced proximal tubule dysfunction clinically [3], this could be due to the patients having underlining renal dysfunction caused by the HIV-1 virus itself [3, 15-16]

The cell lines used for the research carried out within this thesis were modified via growing them in galactose media which forces cellular ATP production to proceed via mitochondrial OXPHOS [13]. This modification produces an *in vitro* model which better represents the physiological characteristics of the proximal tubule cell. These modifications were carried out as studies have shown that animal cells produce 95% of ATP via mitochondrial OXPHOS [13], whilst the cells used in previous TFV cytotoxicity studies have been immortalised cell lines grown in high glucose media that generate their energy mainly via glycolysis [14]. Therefore the data presented within this thesis better represent the mechanistic pathway of TFV (**Chapter 2**).

Although every effort was made to find an *in vitro* model that closely represented the phenotypical characteristics of human proximal tubule cells, the model still has flaws. These arise from the fact that they are immortalised, therefore have an altered cell cycle and proliferation and are grown in culture (so are not a part of an organ system). The development of an *in vitro* model that is phenotypically matched to a human proximal tubule cell is very difficult. The impact of the immortalisation of cells can be seen within this thesis. The HEK293 cells that were derived from human kidney cells did not contain the transporter OAT1 (**Figure 2.10C**); this was unexpected and shows that the phenotypical characteristics of the cells are altered by immortalisation process. However the *in vitro* models set up within this thesis was aerobically matched to proximal tubule cells and contained all the other major transporters required for TFV accumulation.

Recent advances within the *in vitro* field have led to the development of models that are more representative of the *in vivo* cells of interest, such as 3D spheroids [17]. Recently Human kidney epithelial cell spheroids became available, within this cell culture type 3D aggregates also called spheroids are formed. Recent data demonstrated that the kidney spheroids promoted an appropriate microenvironment, which generated the renal progenitor function [18]. These cells could be better representative models in order to study TFV-induced toxicity. Future work that could be carried out within different cell models involves the following: looking at the cytotoxicity of TFV in primary proximal tubule cells that have recently become available within our department. The study of TFV-induced cytotoxicity on cultured cells that have been isolated from the urine and have been shown to be a close phenotypical match to the proximal tubule cells (this work has recently become available within our department).

The work carried out within this thesis has built up a picture of the mechanistic pathway of TFV-induced cytotoxicity (**Figure 6.1**). Results showed that TFV-induces cell death via apoptosis and /or necrosis, dependent upon cellular ATP levels. Further work is required in order to determine the apoptotic mediators involved in TFV-induced cell death; the further work required is described in detail throughout the following discussion.

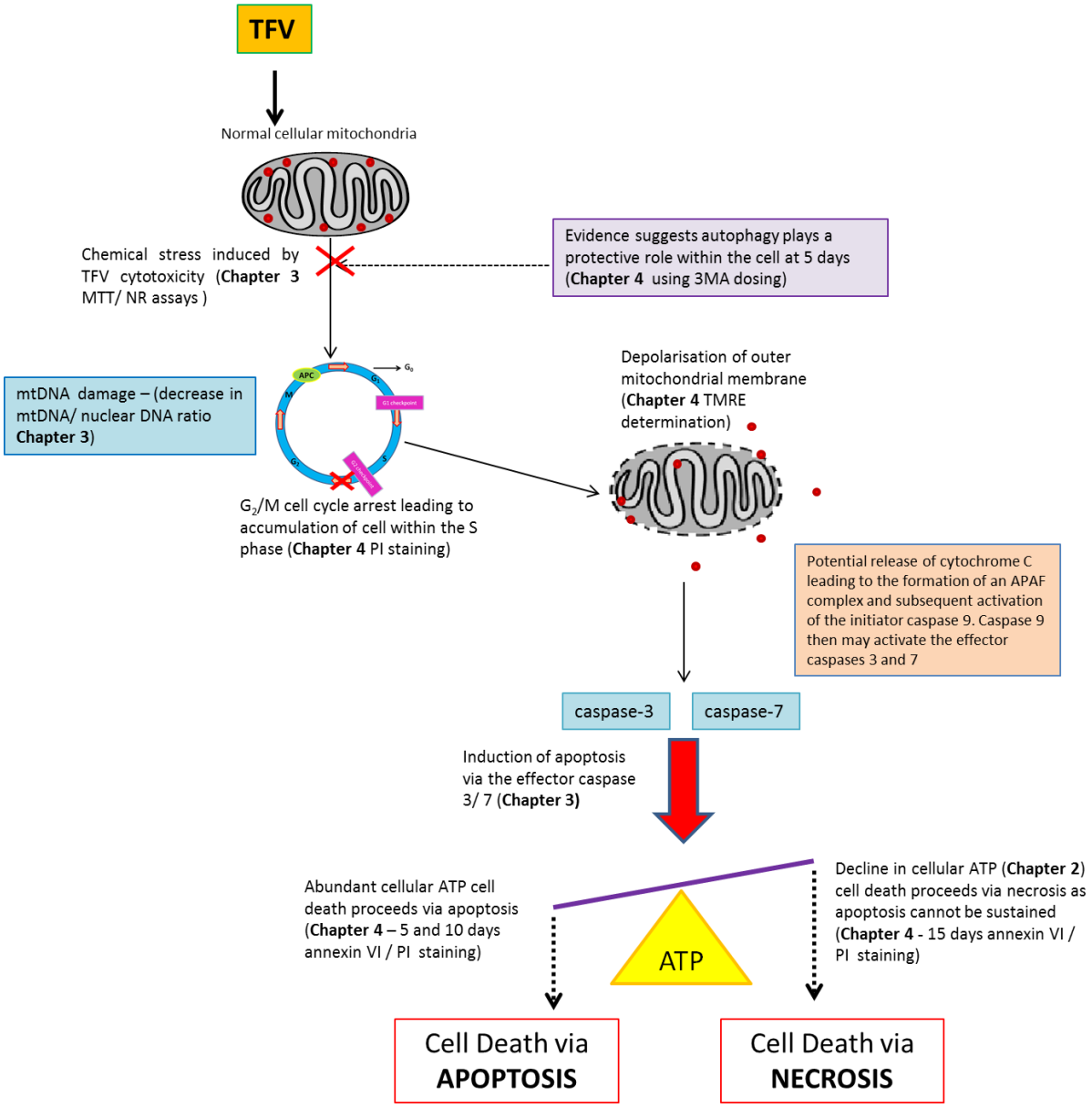

Figure 6.1: A Schematic image of the mechanistic pathway of TFV-induced cytotoxicity as determined by work carried out within this thesis

The preliminary work using both glucose-grown and galactose-grown cells and the classical mitochondrial toxin rotenone, demonstrated that rotenone-induced mitochondrial toxicity could only be determined within the galactose grown cells. This showed that the galactose cultured cells were more susceptible to mito-toxins. This work was carried forward and

repeated using TFV. It was demonstrated that TFV induces mitochondrial damage within the galactose cultured cells after 5 days (**Table 3.2, Figure 3.3A**).

Investigations were carried out into the possible protective role of autophagy induced by TFV. This study was performed as it has been reported that the antiretroviral drug efavirenz (EFV), induced autophagy at clinically relevant concentrations [19]. This previous study highlighted the importance of autophagy for cellular survival, TFV may induce autophagy masking the true extent of its cytotoxicity; therefore, the study of TFV and its possible induction of autophagy were determined within this thesis. It was found that autophagy plays a protective role at only the 5 day time point in HepG2 galactose and HepG2 WT cells (**Chapter 4**). These results were indicative that autophagy is induced by TFV and plays a protective role within the cells at the early time points. This may underline the long time periods required to see TFV-induced cytotoxicity. A further study looking into the role of autophagy could be carried out looking for other essential autophagy proteins such as LC-3 determined using western blot methods and using genetic and molecular modifications (siRNA ect) to determine the functional role of this pathway.

Cytotoxicity studies via MTT / NR assays have shown that TFV induces cellular death as cell viability was shown to decrease in HepG2 galactose cells after 5 days (**Chapter 3**). TFV dosing leads to the induction of mitochondrial membrane depolarisation which is the hallmark of early apoptosis [20]. This was shown by TMRE determination which increased with both time and dose in galactose grown HepG2 cells from 5 days (**Chapter 4**). The next hypothesised step involves the release of cytochrome C, which is widely reported to closely follow mitochondria membrane depolarisation [21-24]. Future studies could stain for cytochrome C release via western blot methods. Studies have shown that upon cellular

cytochrome C release the formation of an apoptosome is mediated [21]. The apoptosome is made up of cytochrome C and APAF-1 and its formation is dependent upon cellular ATP levels. The apoptosome recruits pro-caspase 9 which leads to its activation [21-24]. Caspase 9 is an initiator caspase that activates the effector caspases 3/7 [21-24]. Caspase 3/7 levels where shown to increase in HepG2 galactose cells after 5 days when determining caspase 3 / 7 levels using a luminescent kit (**Chapter 4**). Once activated , caspase 3/ 7 mediate cell death via apoptosis [25]. The involvement of the caspases could be studied further via the use of caspase inhibitors an example is X-linked IAP (XIAP) an inhibitor of caspase 3, 7 and 9 [26]. This would inhibit apoptotic cell death and show they are essential to the TFV-induced apoptotic pathway. This work supports the clinical case studies that have shown TFV to induce fanconi syndrome within patients [27-35]. Fanconi syndrome is a disease of the renal proximal tubule and one of its defining factors is cell death via apoptosis [36].

Following TFV dosing, TFV accumulates within the cell (shown by accumulation studies in **Chapter 2** and **Chapter 3**), possibly leading to its accumulation within the mitochondria possibly via the hENT1 transporter [37]. hENT1 is a member of a nucleoside transporter family; the gene encodes for a transmembrane glycoprotein that locates to either the plasma or mitochondrial membrane. hENT1 is responsible for the uptake of cellular nucleosides and nucleotides. TFV is an analogue of a nucleotide; therefore, hENT1 could play an important role in TFV uptake into the mitochondria [37]. Future studies could determine if TFV accumulates within the mitochondria and if hENT 1 is essential for this accumulation. The accumulation within the mitochondria could lead to inhibition of mitochondrial pol γ in a similar mechanism to how TFV inhibits HIV-1 reverse transcriptase. A decline in mitochondrial pol γ activity would result in a decline in mitochondrial DNA; such a decrease was shown to be induced post TFV dosing and was determined by a decrease in the mitochondrial DNA / nuclear DNA ratio in HepG2 galactose cells after 15 days (PCR

analysis **Chapter 3**). Previous studies have shown that TFV has low affinity to pol γ within immortalised cell lines [38-40]. The cell models used within this thesis have been modified to be dependent upon the mitochondria for ATP production, which may cause a higher rate of mitochondrial proliferation to support these energy requirements. Therefore, any damage inflicted by TFV would have a faster accumulation rate of dysfunctional mitochondria, thus making these cells more susceptible to TFV-induced mitochondrial damage and providing a better representation to proximal tubule cells. This decrease in mitochondrial DNA results in dysfunctional mitochondria within the cell; the levels of dysfunctional mitochondria gradually build up and eventually trigger the G_2 checkpoint (this checkpoint detects any DNA damage), within the cell cycle progression. After the G_2 checkpoint has been triggered, it mediates cell cycle arrest and results in cellular accumulation in the S phase. This was shown by the determination of cell cycle progression via PI staining within HepG2 galactose cells from 5 days (**Chapter 4**). A future study could determine quantitative mitochondrial DNA copy number against nuclear DNA copy number as this has been shown [41] to be a more reliable method of determining mitochondrial DNA damage to confidently show that TFV has reduced mitochondrial DNA. This method takes into account the structural variation that has been described recently as copy number variation [41]. The variable copy numbers within a sample are determined and compared to a standard reference genome this has been reported as a more reliable/accurate method [41]. This method was not used as the software required to carry it out was not available. Once the threshold point of dysfunctional mitochondria within the cell has been reached cellular ATP levels begin to decline [42]. Studies within this thesis showed that TFV (100µM) caused a significant decline in cellular ATP levels at 5 days in HepG2 galactose cells (**Chapter 3**).

Both the necrotic and apoptotic pathways were shown to be induced by TFV dosing after 5 days in HepG2 galactose cells. However, the necrotic pathway is time-delayed as it requires

the buildup of dysfunctional mitochondria and results show it is induced after 15 days in HepG2 galactose cells (**Table 3.2** and **3.5**). Once the threshold level of cellular dysfunctional mitochondria has been reached, the apoptotic pathway is inhibited as cellular ATP levels become too low to sustain apoptosis, which is an active process, leading to cell death via necrosis [43]. This balance of apoptotic against necrotic death which is dependent upon cellular ATP levels is depicted in **Figure 6.1.** These results match the clinical effects reported [43]. Apoptosis is induced as an early response to toxicity mainly as a protective role to prevent further damage (apoptosis is a clean and controlled event) [25]. When cellular damage becomes too overt, cell death proceeds predominantly via necrosis leading to irreversible damage [43].

The results presented within this thesis show that TFV-induced mitochondrial-specific cytotoxicity when cell lines were modified to better represent the physiological conditions of the human cells where toxicity has been reported. Throughout many of the studies presented in this thesis, the cytotoxicity of the antiretroviral ADEF was also assessed. The cytotoxic effects induced by ADEF were always more prominent and occurred faster than the cytotoxicity of TFV (**Figures 3.3 A, B, C** and **D**). ADEF also affected the HepG2 WT cells at the longer incubation periods. The difference between the toxicity induced by ADEF to that induced by TFV could be due to the difference in cellular accumulation between the two drugs (**Chapter 3**) as it was shown that ADEF had a higher rate of accumulation than TFV (**Figure 3.5 A** and **B**). This work also highlights how transporters could impact on TFV-induced toxicity. It has been hypothesised that a person with an increased OAT 1 / 3 activity or decreased MRP 2/ 4 activity may be at an increased risk of developing TFV-induced renal dysfunction [44]. If the increased cytotoxicity of ADEF compared to TFV is a direct result of the increased accumulation of ADEF, then any increase in TFV accumulation or decrease in elimination will lead to increased TFV cytotoxicity.

Within this thesis work was presented to look for a possible biomarker of TFV proximal tubule dysfunction. Kidney injury molecule -1 was selected as there is evidence that it is specific to proximal tubule cells [45]. Results demonstrated that TFV did not significantly alter the KIM-1 / creatinine ratio within patient urine samples. However, the data from this pilot study are novel (work looking at KIM-1 as a possible biomarker for TFV-induced toxicity has not been carried out) and can be used for future research into the possible use of KIM-1 as a biomarker for TFV-induced proximal tubule dysfunction. The data collected should be carried forward to power a future study using a larger patient cohort. This would benefit the patients and clinicians in future; patients on TFV could be easily monitored via a urine test that is non-invasive, which allows early detection of TFV-induced proximal tubule dysfunction and prevents the onset of irreversible renal damage. Future work could also determine if mtDNA levels within patients isolated PBMCs could be used as a predictive biomarker of TFV-induced mitochondrial dysfunction as previously reported data demonstrated that PBMCs can be used to detect mitochondrial damage within a patient [41].

The research carried out within this thesis has provided more detailed mechanistic information on the molecular pathways initiated by TFV. Overall, the research presented here has elucidated the molecular mechanism of TFV-induced cell death. Specifically, TFV causes delayed mitochondrial cytotoxicity, leading to cell cycle arrest, which is likely due to the inhibition of mitochondrial pol γ, leading to decreased mitochondrial DNA and increased cell death firstly via apoptosis (caused by the release of caspase 3/ 7), and then necrosis when cellular ATP levels become too low to sustain apoptosis. Work presented also showed that autophagy induced by TFV, could play a protective role within cells at lower time periods. Within this thesis *in vitro* cell models were modified in order to be more aerobically matched to human proximal tubule cells and allow the study of mitotoxins. This work showed TFV-induced cytotoxicity for the first time *in vitro;* proving the original hypothesis that growing

the cells in galactose media would make them more susceptible to mitochondrial toxicity and therefore TFV-induced cytotoxicity could be studied. This cell model could be useful for the industry to probe possible drug candidates for mitochondrial toxicity. This work has now opened doors for further study into the cytotoxicity of other antiretrovirals within these modified cell lines.

REFERENCES

CHAPTER ONE

[1] Gallant J.E, Staszewski S, Pozniak A.L, DeJesus E, Suleiman J.M, Miller M.D, Coakley D.F, Lu B, Toole J.J and Cheng A.K; Efficacy and safety of tenofovir DF vs stavudine in combination therapy in antiretroviral-naive patients: a 3-year randomized trial. JAMA 2004; Jul 14; 292(2):191-201

[2] Cooper D.A, Steigbigel R.T and Gatell J.M, Subgroup and resistance analyses of raltegravir for resistant HIV-1 infection. N Engl J Med 2008; 359: 355-65

[3] Cooper RD. Systematic review and meta-analysis: renal safety of tenofovir disoproxil fumarate in HIV-infected patients. Clin Infect Dis 2010; 51: 496-505

[4] Clerici, M, Stocks, NI and Zajac, RA. Detection of three distinct patterns of T helper cell dysfunction in asymptomatic human immunodeficiency virus-seropositive patients: independence of CD4+ cell numbers and clinical staging. *J Clin Invest* 1989;**84**:1892–1899

[5] Hebb, D.O. The Organization of Behavior. Wiley, New York, 1949

[6] Bailes E, Feng Gao F, Bibollet-Ruche, Courgnaud V, Peeters M, Marx P.A, Hahn B.H and Sharp P.M, Hybrid Origin of SIV in Chimpanzees Science 13 June 2003: Vol. 300 no. 5626 p. 1713

[7] Hahn B.H, Shaw G.M, De Cock KM and Sharp P.M. AIDS as a Zoonosis: Scientific and Public Health Implications Science 28 January 2000: Vol. 287 no. 5453 pp. 607-614

[8] Gao F, Bailes E, Robertson D.L, Chen Y, Rodenburg C. M, Michael S.F, Cummins L.B, Arthur L.O, Peeters M, Shaw G.M, Sharp P.M and Hahn B.H. Origin of HIV-1 in the chimpanzee Pan troglodytes troglodytes. Nature. 1999; 397(6718): 436-441.

[9] Courgnaud, V and Pourrut S.M, Characterization of a novel simian immunodeficiency virus with a vpu gene from greater spot-nosed monkeys (Cercopithecus nictitans) provides new insights into simian/human immunodeficiency virus phylogeny. J Virol 2002. 76, 8298–8309

[10] Fauci A.S. and Chun T.W. Latent reservoirs of HIV: obstacles to the eradication of virus. Proc Natl Acad Sci U S A. 1999 Sep 28; 96(20):10958-61.

[11] Fauci A.S. The AIDS epidemic- considerations for the 21st century. *N.Engl.J.Med*.1999;341,1046-1050

[12] Simon F, Mauclere P, Roques P, Loussert-Ajaka I, Muller-Trutwin M.C, Saragosti S, Georges-Courbot M.C, Barre-Sinoussi F and Brun-Vezinet F. Identification of a new human immunodeficiency virus type 1 distinct from group M and group O. Nat Med 1998; 4: 1032–1037.

[13] Anderson P.L, Kiser J.J, Gardner E.M, Rower J.E, Meditz A, and Grant G.M. Pharmacological considerations for tenofovir and emtricitabine to prevent HIV infection Antimicrob Chemother. 2011 February; 66(2): 240–250.

[14] UNIAIDS, 1998 *AIDS Epidemic Update: December 1998* (UNAIDS, Geneva, 1999)

[15] UNIAIDS, 2009 *AIDS Epidemic Update: December 2009* (UNAIDS, Geneva, 1999)

[16] Siliciano R.F and Greene W.C. HIV latency. Cold Spring Harbor perspectives in medicine. 2011;1, a007096

[17] Kim J.H, Cho A, Yin H, Schafer D.A, Mouneimne G, Simpson K.J, Nguyen K.V, Brugge, J.S., Montell, D.J. (2011). Psidin, a conserved protein that regulates protrusion dynamics and cell migration. Genes Dev. 25(7): 730--741.

[18] Mehandru S, Poles M.A, Tenner-Racz K, Horowitz A, Hurley A, Hogan C, Boden D, Racz P and Markowitz M. Primary HIV-1 infection is associated with preferential depletion of CD4+ T lymphocytes from effector sites in the gastrointestinal tract.J Exp Med. 2004 Sep 20;200(6):761-70.

[19]Douek D.C, Roederer M, and Koup R.A Emerging Concepts in the Immunopathogenesis of AIDS*Annual Review of Medicine 2009 Vol. 60: 471-484

[20] Briggs R.C, Shults K.E, Flye L.A, McClintock-Treep S.A, Jagasia M.H, Goodman SA, Boulos F.I, Jacobberger J.W, Stelzer G.T and Head D.R Dysregulated human myeloid nuclear differentiation antigen expression in myelodysplastic syndromes: evidence for a role in apoptosis. Cancer Res. 2006 May 1;66(9):4645-51.

[21] Ray N and Doms R.W. HIV-1 co-receptors and their inhibitors. Curr Top Microbiol Immunol 2006; 303: 97–120.

[22] Platt E.J, Durnin J.P and Kabat D. Kinetic factors control efficiencies of cell entry, efficacies of entry inhibitors, and mechanisms of adaptation of human immunodefi ciency virus. J Virol 2005; 79: 4347–56.

[23] Eckert D.M and Kim P.S. Mechanisms of viral membrane fusion and its inhibition. Annu Rev Biochem 2001; **70:** 777–810.

[24] Coffin J.M, Hughes S.H and Varmus H.E. Retroviruses. Plainview, NY, USA: Cold Spring Harbor Laboratory Press, 1997.

[25] Rus H, Cudrici and Niculescu F. The role of the complement system in innate immunity. Immunologic Research. 2005; 33 (2): 103–12.

[26] Shattuck T.M, Välimäki S, Obara T, Gaz R.D, Clark O.H, Shoback D, Wierman M.E, Tojo K, Robbins C.M, Carpten J.D, Farnebo L.O, Larsson C and Arnold A. Somatic and germ-line mutations of the HRPT2 gene in sporadic parathyroid carcinoma. N Engl J Med. 2003 Oct 30;349(18):1722-9.

[27] Scherdin U, Rhodes K and Breindl M. Transcriptionally active genome regions are preferred targets for retrovirus integration. J Virol 1990;**64:** 907.

[28] Schroder A. HIV-1 integration in the human genome favors activegenes and local hotspots. Cell 2002; **110:** 521–29.

[29] Martin-Serrano J, Zang T, Bieniasz PD. Role of ESCRT-I in retroviral budding. J Virol 2003; **77:** 4794–804.

[30] Bieniasz PD. Late budding domains and host proteins in enveloped virus release. *Virology* 2006; **344:** 55–63.

[31] Zhu T, Mo H and Wang N. Genotypic and phenotypic characterization of HIV-1 patients with primary infection. Science 1993; **261:** 1179–81.

[32] Chantry, D. HIV entry and fusion inhibitors. Expert Opin Emerg Drugs. 2004; **9**(1): 1-7.

[33] Boyd M.A and Andrew M. Clinical Management of Treatment- Experienced, HIV/AIDS Patients in the Combination Antiretroviral Therapy Era. Pharmacoeconomics 2010; 28 Suppl. 1: 17-34

[34] Abel S, Russell D, Whitlock L.A, Ridgway C.E, Nedderman A.N and Walker D.K. Assessment of the absorption, metabolism and absolute bioavailability of maraviroc in healthy male subjects. British Journal of Clinical Pharmacology. 2008; 65 (Suppl 1): 60–7

[35] Nolan D, Moore C, and Castley A. Tumour necrosis factor-alpha gene-238G/A promoter polymorphism associated with a more rapid onset of lipodystrophy. AIDS. 2003; 17(1):121-123

[36] Jacobson J.M, Saag M.S, Thompson M.A. Antiviral activity of single-dose PRO 140, a CCR5 monoclonal antibody, in HIV-infected adults. *J Infect Dis*. 2008 Nov 1;198(9):1345-52.

[37] Mocroft A, Ledergerber B and Katlama C. Decline in the AIDS and death rates in the EuroSIDA study: an observational study. Lancet 2003; 362: 22-9

[38] Sohl C.D, Singh K, Kasiviswanathan R, Copeland W.C, Mitsuya H, Sarafianos S.G and Anderson K.S. Mechanism of interaction of human mitochondrial DNA polymerase γ with the novel nucleoside reverse transcriptase inhibitor 4′-ethynyl-2-fluoro-2′-deoxyadenosine indicates a low potential for host toxicity. Antimicrob Agents Chemother. 2012; 56:1630–1634.

[39] Marcellin P, Chang T-T and Lim S.G. Adefovir dipivoxil for the treatment of hepatitis B e antigen-positive chronic hepatitis B. N Engl J Med 2003;348:808-816

[40] Balzarini J. Current status of the non-nucleoside reverse transcriptase inhibitors of human immunodeficiency virus type 1. Curr Top Med Chem 2004; 4: 921-44

[41] Cingolani A, Antinori A and Rizzo M.G. Usefulness of monitoring HIV drug resistance and adherence in individuals failing highly active antiretroviral therapy: arandomized study (ARGENTA). AIDS 2002; 16: 369-79

[42] Clavel F and Hance AJ. HIV drug resistance. N Engl J Med 2004; 350: 1023-35

[43] Hazuda DJ. Inhibitors of HIV integrase: antiviral activity and mechanism [abstract S2]. 7th Conference on Retroviruses and Opportunistic Infections; 2000 Jan 30–Feb 2;San Francisco, USA

[44] Wynn G.H, Zapor M.J and Smith B.H. Antiretrovirals, part 1: overview, history, and focus on protease inhibitors. Psychosomatics 2004; 45: 262-70

[45] Salzwedel K, Martin D.E and Sakalian M. Maturation inhibitors: a new therapeutic class targets the virus structure. AIDS Rev. 2007; **9**(3): 162-172.

[46] Gazzard BG. BHIVA Treatment Guidelines Writing Group. British HIV association guidelines for the treatment of HIV-1-infected adults with antiretroviral therapy 2008. HIV Med 2008; 9: 563-608

[47] King J.R, Yogev R, Jean-Philippe P, Graham B, Wiznia A, Britto P, Carey V, Hazra R and Edward P. Acosta E.P for the P1058 Protocol Team. Steady-State Pharmacokinetics of Tenofovir-Based Regimens in HIV-Infected Pediatric Patients Antimicrob Agents Chemother. 2011 September; 55(9): 4290–4294

[48] Riordan A, Judd A, Boyd K, Cliff D, Doerholt K, Lyall H, Menson E, Butler K and Gibb D. Tenofovir use in human immunodeficiency virus-1 infected children in the United Kingdom

[49] Boxall EH, Sira J and El-Shuhkri N. Long term persistence of immunity to hepatitis B after vaccination during infancy in a country where endemicity is low. *J Infect Dis.* 2004*;* 190: 1264–9.

[50] Terrault N, Roche B and Samuel D. Management of the hepatitis B virus in the liver transplantation setting: a European and an American perspective. *Liver Transpl.*2005; **11** (7): 716–32.

[51] Barditch-Crovo P, Deeks S.G, Collier A, Safrin S, Coakley D.F, Miller M, Kearney B.P, Coleman R.L, Lamy P.D, Kahn J.O, McGowan I and Lietman P.S. Phase I/II trial of the pharmacokinetics, safety, and antiretroviral activity of tenofovir disoproxil fumarate in human immunodeficiency virus-infected adults. Antimicrob Agents Chemother. 2001 Oct;45(10):2733-9.

[52] Hammer S.M, Eron Jr J.J and Reiss P. Antiretroviral treatment of adult HIV infection: 2008 recommendations of the International AIDS Society – USA panel. JAMA 2008; 300: 555-70

[53] Ray A, Olson L and Fridland A. Role of purine nucleoside phosphorylase in interactions ibetween 2,3-dideoxyinosine and allopurinol, ganciclovir, or tenofovir. Antimicrob Agents Chemother 2004;48(4):1089-95

[54] Taburet A, Piketty C, Chazallon C, Vincent I, Gérard L, Calvez V, Clavel F, Aboulker J ,Girard P and the ANRS Protocol 107 Puzzle 2 Investigators. Interactions between Atazanavir-Ritonavir and Tenofovir in Heavily Pretreated Human Immunodeficiency Virus-Infected Patients. Antimicrob Agents Chemother. 2004 June; 48(6): 2091–2096.

[55] Izzedine H, Isnard-Bagnis C, Hulot J.S, Vittecoq D, Cheng A, Jais C.K, Launay-Vacher V, and Deray J. Renal safety of tenofovir in HIV treatment-experienced patients. AIDS. 2004; 18:1074-1075

[56] Kohler J.J, Hosseini S.H, Green E, Abuin A, Ludaway T, Russ R, Santoianni R and Lewis W. Tenofovir renal proximal tubular toxicity is regulated by OAT1 and MRP4 transporters. Lab Invest. 2011; **91**(6): 852-858.

[57] Pavie J, Rachline A, Loze B, Niedbalski L, Delaugerre C, Laforgerie E, Plantier J-C, Rozenbaum W, Chevret S and Molina J-M. Sensitivity of Five Rapid HIV Tests on Oral Fluid or Finger-Stick Whole Blood: A Real-Time Comparison in a Healthcare Setting. PLoS ONE org 1 July 2010 / Volume 5 / Issue 7 /e11581

[58] Rodriguez-Novoa S, Labarga P and D'avolio A. Impairment in kidney tubular function in patients receiving tenofovir is associated with higher tenofovir plasma concentrations. AIDS. 2010;24:1064–1066.

[59] Baud V and Karin M. Signal transduction by tumour necrosis factor and its relatives. Trends Cell Biol 2001; 11:372-7.

[60] Kohler J, Hosseini S and Hoying-Brandt A. Tenofovir renal toxicity targets mitochondria of renal proximal tubules. Lab Invest 2009;89(5):513-9

[61] Rifkin BS, Perazella MA. Tenofovir-associated nephrotoxicity: Fanconi syndrome and renal failure. Am J Med 2004;117:282–284.

[62] Verhelst D, Monge M and Meynard J.L. Fanconi syndrome and renal failure induced by tenofovir: a first case report. Am J Kidney Dis 2002;40(6):1331-3

[63] Karras A, Lafaurie M and Furco A. Tenofovir-related nephrotoxicity in HIV-infected patients: three cases of renal failure, Fanconi syndrome, and nephrogenic diabetes insipidus. Clin Infect Dis 2003;36(8):1070-3

[64] James C, Steinhaus M, Szabo S and Dressier R. Tenofovir-related nephrotoxicity: case report and review of the literature. Pharmacotherapy 2004;24(3):415-8

[65] Izzedine H, Launay-Vacher V and Deray G. Antiviral drug-induced nephrotoxicity. Am J Kidney Dis. 2005 May;45(5):804-17.

[66] Creput C, Gonzalez-Canali G and Hill G. Renal lesions in HIV-1-positive patient treated with tenofovir. AIDS 2003;17(6):935-7

[67] Dupont C, Meier F and Loupy A. Acute renal failure and tenofovir: two new cases. Antivir Ther 2003;8(Suppl):76

[68] Schaaf B, Aries S and Kramme E. Acute renal failure associated with tenofovir treatment in a patient with acquired immunodeficiency syndrome. Clin Infect Dis 2003;37(3):e41-3

[69] Kapitsinou P and Ansari N. Acute renal failure in an AIDS patient on tenofovir: a case report. J Med Case Reports 2008;2:94

[70] Vallecillo-Sanchez G, Guelar-Grimberg A, Gonzalez-Mena A and Knobel-Freud H. Acute renal failure associated with the use of tenofovir combined with atazanavir in patients with HIV infection. Enferm Infecc Microbiol Clin 2008;26(5):316-17

[71] Abdissa S.G, Fekade D, Feleke, Y, Seboxa T and Diro E. Adverse drug reactions associated with antiretroviral treatment among adult Ethiopian patients in a tertiary hospital. Ethiop Med J.2012; 50(2): 107-113

[72] Ter H.R, Huitema A and Jansen R. Prolonged exposure to tenofovir monotherapy 1 month after discontinuation because of tenofovir-related renal failure. Antivir Ther 2009;14(2):299-301

[73] Wood S, Shah S and Steenhoff A. Tenofovir-associated nephrotoxicity in two HIV-infected adolescent males. AIDS Patient Care STDs 2009:23(1):1-4

[74] Callens S, De R and Colebunders R. Fanconi-like syndrome and rhabdomyolysis in a person with HIV infection on highly active antiretroviral treatment including tenofovir. J Infect 2003;47(3):262-3

[75] Peyriere H, Reynes J and Rouanet I. Renal tubular dysfunction associated with tenofovir therapy: report of 7 cases. J Acquir Immune Defic Syndr 2004;35(3):269-73

[76] Williams J and Chadwick D. Tenofovir-induced renal tubular dysfunction presenting with hypocalcaemia. J Infect 2006;52(4):e107-8

[77] Mathew G and Knaus S. Acquired Fanconi's syndrome associated with tenofovir therapy. J Gen Intern Med 2006;21(11):C3-5

[78] Bustamante C, Vejo-Puente E, Velasco-Montes J and Hernandez-Hernandez JL. Severe hypokalemia and tenofovir. Enferm Infecc Microbiol Clin 2008;26(5):317-18

[79] Earle K, Seneviratne T, Shaker J and Shoback D. Fanconi's syndrome in HIV+ adults: report of three cases and literature review. J Bone Miner Res 2004;19(5):714-21

[80] Di Biagio A, Rosso R and Monteforte P. Whole body bone scintigraphy in tenofovir-related osteomalacia: a case report. J Med Case Reports 2009;3:8136-9

[81] Irizarry-Alvarado J, Dwyer J and Brumble L. Proximal tubular dysfunction associated with tenofovir and didanosine causing Fanconi syndrome and diabetes insipidus: a report of 3 cases. AIDS Read 2009;19(3):114-21

[82] Rollot F, Nazal E.M and Chauvelot-Moachon L. Tenofovir-related Fanconi syndrome with nephrogenic diabetes insipidus in a patient with acquired immunodeficiency syndrome: the role of lopinavir-ritonavir-didanosine. Clin Infect Dis 2003;37(12):e174-6

[83] Badiou S, de Boever CM and Terrier N. Is tenofovir involved in hypophosphateamia and decrease of tubular phosphate reabsorption in HIV-positive adults? J Infect 2006;52(5):335-8

[84] Labarga P, Barreiro P and Martin-Carbonero L. Kidney tubular abnormalities in the absence of impaired glomerular function in HIV patients treated with tenofovir. AIDS 2009;23:689–696.

[85] Young B, Buchacz K and Baker R. HIV Outpatient Study Investigators. Renal function in tenofovir-exposed and tenofovir-unexposed patients receiving highly active antiretroviral therapy in the hiv outpatient study. J Int Assoc Physicians AIDS Care (Chic Ill) 2007;6(3):178-87,

[86] Zimmermann A, Pizzoferrato T and Bedford J. Tenofovir-associated acute and chronic kidney disease: a case of multiple drug interactions. Clin Infect Dis 2006;42(2):283-90

[87] de la Prada F, Prados A and Tugores A. Acute renal failure and proximal renal tubular dysfunction in a patient with acquired immunodeficiency syndrome treated with tenofovir. Nefrologia 2006;26(5):626-30

[88] Gupta S. Tenofovir-associated Fanconi syndrome: review of the FDA adverse event reporting system. AIDS Patient Care STDS 2008;22(2):99-103

[89] Goicoechea M, Liu S and Best B. Greater tenofovir-associated renal function decline with protease inhibitor-based versus nonnucleoside reverse-transcriptase inhibitor-based therapy. J Infect Dis 2008;197:102–108.

[90] Nelson M, Katlama C and Montaner J. The safety of tenofovir disoproxil fumaratefor the treatment of HIV infection in adults: the first 4 years. AIDS 2007;21(10):1273-81

[91] Jimbo R and Shimosawa T. Cardiovascular Risk Factors and Chronic Kidney Disease-FGF23: A Key Molecule in the Cardiovascular Disease Int J Hypertens. 2014;2014:381082

[92] Birkus G, Hitchcock M, Cihlar T. Assessment of mitochondrial toxicity in human cells treated with tenofovir: comparison with other nucleoside reverse transcriptase inhibitors. Antimicrob Agents Chem other 2002;46(3):716-23

[93] Cihlar T, Ho ES, Lin DC, and Mulato AS.Human renal organic anion transporter 1 (hOAT1) and its role in the nephrotoxicity of antiviral nucleotide analogs. Nucleosides Nucleotides. 2001;20: 641-648.

[94] Van Rompay K, Brignolo L and Meyer D. Biological effects of short-term or prolonged administration of 9-[2-(phosphonomethoxy)propyl]adenine (tenofovir) to newborn and infant rhesus macaques. Antimicrob Agents Chemother 2004;48(5):1469-87

[95] Djoko C.F, Rimoin A.W, Vidal N, Tamoufe U, Wolfe N.D, Butel C, LeBreton M, Tshala F.M, Kayembe P.K, Muyembe J.J, Edidi-Basepeo S, Pike B.L, Fair J.N, Mbacham W.F, Saylors K.E, Mpoudi-Ngole E, Delaporte E, Grillo M, and Peeters M. High HIV Type 1 Group M pol Diversity and Low Rate of Antiretroviral Resistance Mutations Among the Uniformed Services in Kinshasa, Democratic Republic of the Congo AIDS Res Hum Retroviruses. 2011 March; 27(3): 323–329

[96] Tong L, Phan T.K, Robinson K.L, Babusis D, Strab R, Bhoopathy S, Hidalgo I.J, Rhodes G.R, and Ray A.S. Effects of human immunodeficiency virus protease inhibitors on the intestinal absorption of tenofovir disoproxil fumarate in vitro. Antimicrob. Agents Chemother.2007; 51:3498–3504

[97] Venhoff N, Setzer B, Melkaoui K and Walker U.A. Mitochondrial toxicity of tenofovir, emtricitabine and abacavir alone and in combination with additional nucleoside reverse transcriptase inhibitors. Antivir Ther. 2007;12(7):1075

[98] Cihlar T, Ray A.S, Laflamme G, Vela J.E, Tong L, Fuller M.D, Roy A and Rhodes G.R. Molecular assessment of the potential for renal drug interactions between tenofovir and HIV protease inhibitors. Antivir Ther. 2007;12(2):267-72.

[99] Cihlar T, Birkus G, Greenwalt D.E and Hitchcock M.J.M. Tenofovir exhibits low cytotoxicity in various human cell types: comparison with other nucleoside reverse transcriptase inhibitors. Antiviral Research. 2002;54(1): 37-45.

[100] Bousquet L, Pruvost A, Didier N, Farinotti R and Mabondzo A. Emtricitabine: Inhibitor and substrate of multidrug resistance associated protein. Eur J Pharm Sci. 2008; 35:247-256.

[101] Maggi P, Montinaro V, Bellacosa C, Pietanza S, Volpe A, Graziano G, Strippoli G., and Angarano G. Early Markers of Tubular Dysfunctionin Antiretroviral-Experienced HIV-Infected Patients Treated with Tenofovir Versus Abacavir AIDS PATIENT CARE and STDs. 2012;Volume 26, Number 1.

[102] Ferraro R, Lillioja S, Fontvieille A.M, Rising R, Bogardus C, Ravussin E. Lower sedentary metabolic rate in women compared with men. J Clin Invest. 1992;90(3):780–784.

[103] Anderson P.L. Pharmacologic perspectives for once-daily antiretroviral therapy. Ann Pharmacother. 2004;38:1924–34.

[104] Kontorinis N and Dieterich D. Hepatatoxicity of Antiretroviral Therapy. AIDS. 2003; 5:36-43

CHAPTER TWO

[1] Barr A , Nelson M, Portsmouth S, Stebbing J, Atkins M, Matthews G, Pillay D, Fisher M, Bower M and Gazzard B. An open-label study of tenofovir in HIV-1 and Hepatitis B virus coinfected individuals. AIDS. 2003; Jan 3;17(1):F7-F10.

[2] Cihlar T, Birkus G, Greenwalt D.E and Hitchcock M.J.M. Tenofovir exhibits low cytotoxicity in various human cell types: comparison with other nucleoside reverse transcriptase inhibitors. Antiviral Research. 2002;54(1): 37-45.

[3] Chen K.C, Csikasz-Nagy A, Gyorffy B, Val J, Novak B and Tyson J.J. Kinetic analysis of a molecular model of the budding yeast cell cycle. Mol. Biol. Cell. 2000; 11:369-391.

[4] Birkus G, Hitchcock M, Cihlar T. Assessment of mitochondrial toxicity in human cells treated with tenofovir: comparison with other nucleoside reverse transcriptase inhibitors. Antimicrob Agents Chem other 2002;46(3):716-23
[5] Edwards R.I and Aronson J.K. Adverse drug reactions: definitions, diagnosis, and management Lancet. 2000; 356: 1255–59

[6] Rodriguez-Novoa S, Labarga P and D'avolio A. Impairment in kidney tubular function in patients receiving tenofovir is associated with higher tenofovir plasma concentrations. AIDS. 2010;24:1064–1066.
[7] Qi W, Johnson D.W, Vesey D.A, Pollock C.A And Chen X. Isolation, propagation and characterization of primary tubule cell culture from human kidney NEPHROLOGY 2007; 12, 155–159

[8] Marroquin LD, Hynes J, Dykens JA, Jamieson JD, Will Y. Circumventing the Crabtree effect: replacing media glucose with galactose increases susceptibility of HepG2 cells to mitochondria toxins, Toxicol Sci. 2007;97:539-547

[9] Pavie J, Rachline A, Loze B, Niedbalski L, Delaugerre C, Laforgerie E, Plantier J-C, Rozenbaum W, Chevret S and Molina J-M. Sensitivity of Five Rapid HIV Tests on Oral Fluid or Finger-Stick Whole Blood: A Real-Time Comparison in a Healthcare Setting. PLoS ONE org 1 July 2010 / Volume 5 / Issue 7 /e11581
[10] White A.J. Mitochondrial toxicity and HIV therapy Transm Inf 2001;77:158–173

[11] Golshani-Hebroni S.G and Bessman S.P. Hexokinase binding to mitochondria: A basis for proliferative energy metabolism. J. Bioenerg.Biomembr.1997; 29, 331–338.

[12] Dykens. J. A and Yvonne Will. Drug-induced Mitochondrial Dysfunctoion. 2008;Part 1, Wiley
[13] Warburg O, Geissler A.W and Lorenz S. On growth of cancer cells in media in which glucose is replaced by galactose. Hoppe Seylers Z. Physiol. Chem.1967; 348, 1686–1687.

[14] Barrientos A and Moraes CT. Titrating the effects of mitochondrial complex I impairment in the cell physiology. J Biol Chem. 1999; 274: 16188-16197

[15] Mosmann T. Rapid colorimetric assay for cellular growth and survival: application to proliferation and cytotoxicity assays. J Immunol Methods. 1983 Dec 16;65(1-2):55-63.

[16] Repetto G, del Peso A and Zurita J.L Neutral red uptake assay for the estimation of cell viability/cytotoxicity Nat Protoc. 2008;3(7):1125-31.

[17] Maggi P, Montinaro V, Bellacosa C, Pietanza S, Volpe A, Graziano G, Strippoli G., and Angarano G. Early Markers of Tubular Dysfunctionin Antiretroviral-Experienced HIV-Infected Patients Treated with Tenofovir Versus Abacavir AIDS PATIENT CARE and STDs. 2012;Volume 26, Number 1.

[18] Larson B. Overcoming the Crabtree Effect is Critical to Mitochondrial Toxicity. BioTek Instruments, Inc. 2011;published online
[19] Ray A, Olson L, Fridland A. Role of purine nucleoside phosphorylase in interactions ibetween 2¢,3¢-dideoxyinosine and allopurinol, ganciclovir, or tenofovir. Antimicrob Agents Chemother 2004;48(4):1089-95

[20] Notenboom S, Wouterse A.C, Peters B, Kuik L.H, Heemskerk S, Russel F.G.M and Masereeuw R. Increased Apical Insertion of the Multidrug Resistance Protein 2 (MRP2/ABCC2) in Renal Proximal Tubules following Gentamicin Exposure. J Pharmacol Exp Ther. 2006;318(3):1194-202.

[21] Koczor C.A, Torres R.A and Lewis W. The role of transporters in the toxicity of nucleoside and nucleotide analogs. Expert Opin Drug Metab Toxicol. 2012 ; 8(6): 665–676.;

CHAPTER THREE

[1] Kontorinis N and Dieterich D. Hepatatoxicity of Antiretroviral Therapy. AIDS. 2003; 5:36-43

[2] Barr A , Nelson M, Portsmouth S, Stebbing J, Atkins M, Matthews G, Pillay D, Fisher M, Bower M and Gazzard B. An open-label study of tenofovir in HIV-1 and Hepatitis B virus coinfected individuals. AIDS. 2003; Jan 3;17(1):F7-F10.

[3] Cihlar T, Birkus G, Greenwalt D.E and Hitchcock M.J.M. Tenofovir exhibits low cytotoxicity in various human cell types: comparison with other nucleoside reverse transcriptase inhibitors. Antiviral Research. 2002;54(1): 37-45.

[4] Chen K.C, Csikasz-Nagy A, Gyorffy B, Val J, Novak B and Tyson J.J. Kinetic analysis of a molecular model of the budding yeast cell cycle. Mol. Biol. Cell. 2000; 11:369-391.

[5] Birkus G, Hitchcock M, Cihlar T. Assessment of mitochondrial toxicity in human cells treated with tenofovir: comparison with other nucleoside reverse transcriptase inhibitors. Antimicrob Agents Chem other 2002;46(3):716-23

[6] Takekura H and T Yoshioka. Specific mitochondrial responses to running training are induced in each type of rat single muscle fibers. Jpn J Physiol. 1989; 39(4): 497-509.

[7] Morais V. A and De Strooper B. Mitochondria dysfunction and neurodegenerative disorders: cause or consequence. J Alzheimers Dis. 2010; 20 Suppl 2: S255-263.

[8] Cereghetti G.M, Stangherlin A, de Brito O.M, Chang C.R, Blackstone C, Bernardi P and Scorrano L. Dephosphorylation by calcineurin regulates translocation of Drp1 to mitochondria. Proc Natl Acad Sci USA .2006;105: 15803–15808.

[9] Koizumi K, Stivers C, Brody T, Zangeneh S, Mozer B, Odenwald W.F, Higashi S, Furuhara K., Ota K., Iwasaki K., Ozaki T, Kobayashi H and Higashida H. A search for Drosophila neural precursor genes identifies ran. Dev. Genes Evol. 2001; 211(2)**:** 67--75.

[10] Lewis W and Dalakas M.C. Mitochondrial toxicity of antiviral drugs. Nat Med. 1995: 1(5);417-422

[11] Lewis W, Kohler J.J and Hosseini S.H. Antiretroviral nucleoside, deoxynucleotide carrier and mitochondrial DNA: evidence supporting the DNA pol gamma hypothesis. AIDS. 2006; 20(5):675-684

[12] Lewis W, Gonzalez B, Chomyn A and Papoian T. Zidovudine induces molecular, biochemical, and ultrastructual changes in rat skeletal muscle mitochondria. J Clin Invest. 1992; 89(4): 1354-1360

[13] Bogenhagen D.F., Sakonju S. and Brown D.D. Cell. 1976; 19: 27-35

[14] Bestwick R, Ruta M, Kiessling A, Faust C, Linemeyer D, Scolnick E and Kabat D. Genetic structure of Rauscher spleen focus-forming virus. Journal of Virology. 1983; 45, 1217 1222.

[15] Kohler J. J, Cucoranu I Fields E, Green E, He S, Hoying A, Russ R, Abuin A, Johnson D, Hosseini S.H, Lewis W and Raper C.M. Transgenic mitochondrial superoxide dismutase and mitochondrially targeted catalase prevent antiretroviral-induced oxidative stress and cardiomyopathy. Lab Invest . 2009; 89(7): 782-790.

[16] Dykens. J. A and Yvonne Will. Drug-induced Mitochondrial Dysfunctoion. 2008;Part 1, Wiley

[17] Maher B, Alfirevic A, Vilar F.J, Wilkins E.G, Park B.K and Pirmohamed M. TNF-alpha promoter polymorphisms in HIV-positive patients with lipodystrophy. AIDS. 2002;16(15): 2013-2018

[18] Nolan D, Moore C and Castley A. Tumour necrosis factor-alpha gene-238G/A promoter polymorphism associated with a more rapid onset of lipodystrophy. AIDS. 2003; 17(1):121-123

[19] Yamanaka H, Gatanaga H, Kosalaraksa P, Matsuoka-Aizawa S, Takahashi T, Kimura S, and Oka S. Novel mutation of human DNA polymerase gamma associated with mitochondrial toxicity induced by anti-HIV treatment. J. Infect. Dis. 2007; 195:1419-1425

[20]Wierzbicki R and Bartkowiak J. The mitochondrial deoxyribonucleic acid. Postepy Biochem. 1966;12(4):577-86.

[21] Taanman, J.W, Bodnar A.G, Cooper J.M, Morris A.A.M, Clayton P.T, Leonard J.V and Schapira A.H.V. Molecular mechanisms in mitochondrial DNA depletion syndrome**.** Hum. Molec. Genet. 1997;6: 935-942

[22] Leonard J.V and Schapira A.H. Mitochondrial respiratory chain disorders I: mitochondrial DNA defects. Lancet. 2000; 355(9200): 299-304.

[23] Chinnery P.F, Johnson M.A, Wardell T.M, Singh-Kler R, Hayes C, Brown D.T, Taylor R.W, Bindoff L.A and Turnbull DM. The epidemiology of pathogenic mitochondrial DNA mutations. Ann Neurol. 1999;48:188–93

[24] Swerdlow R.H, Burns J.M and Khan S.M. The Alzheimer's disease mitochondrial cascade hypothesis. Alzheimers Dis. 2010;20 :2:S265-79.

[25] Ropp P.A and Copeland W.C. Cloning and characterization of the human mitochondrial DNA polymerase, DNA polymerase gamma. Genomics. 1996;36:449–458

[26] Davis A.F, Ropp P.A and Clayton D.A. And Copeland, W.C. Mitochondrial DNA polymerase gamma is expressed and translated in the absence of mitochondrial DNA maintenance and replication. Nucleic acids research. 1996; 24(14):2753-2759.

[27] Rasmussen A.K, Chatterjee A, Rasmussen L.J, Singh K.K. Mitochondria-mediated nuclear mutator phenotype in Saccharomyces cerevisiae. Nucleic Acids Res.2003; 31: 3909-3917.

[28] Stacpoole P.W, Henderson G.N, Yan Z, Cornett R and James M.O. Pharmacokinetics, metabolism, and toxicology of dichloroacetate. Drug Metab Rev . 1997; 30:499–539

[29] Marcellin P, Chang T-T and Lim SG. Adefovir dipivoxil for the treatment of hepatitis B e antigen-positive chronic hepatitis B. N Engl J Med 2003;348:808-816

[30] Cihlar T, Ho ES, Lin DC, and Mulato AS.Human renal organic anion transporter 1 (hOAT1) and its role in the nephrotoxicity of antiviral nucleotide analogs. Nucleosides Nucleotides.2001. 20: 641-648.

[31] Malik A.N, Shahni R, Rodriguez-de-Ledesma A, Laftah A and Cunningham P . Mitochondrial DNA as a non-invasive biomarker: Accurate quantificationusing real time quantitative PCR without co-amplification of pseudogenes and dilution bias. Elsevier. 2011; 412:1–7

[32] Schmittgen T.D, Jiang J, Liu Q and Yang L. A high-throughput method to monitor the expression of microRNA precursors. Nucleic Acids Res. 2008;32-43

[33] Kim J.H, Cho A, Yin H, Schafer D.A, Mouneimne G, Simpson K.J, Nguyen K.V, Brugge J.S and Montell D.J. Psidin, a conserved protein that regulates protrusion dynamics and cell migration. Genes Dev.2011; 25(7)**:** 730--741.

[34] Marroquin LD, Hynes J, Dykens JA, Jamieson JD, Will Y. Circumventing the Crabtree effect: replacing media glucose with galactose increases susceptibility of HepG2 cells to mitochondria toxins, Toxicol Sci. 2007;97:539-547

[35] Proskuryakov SY, Gabai VL and Konoplyannikov AG. Necrosis is an active and controlled form of programmed cell death. Biochemistry (Mosc) 2002; 67:387-408.

[36] Davis A.F, Ropp P.A, Clayton D.A. And Copeland W.C. Mitochondrial DNA polymerase gamma is expressed and translated in the absence of mitochondrial DNA maintenance and replication. Nucleic acids research. 1996; 24(14):2753-2759.

CHAPTER FOUR

[1] Zhaoyu J.W and El-Deiry S. Overview of Cell Death Signaling Pathways. Cancer Biology & Therapy. 2005; 4:2, 139-163

[2] Kerr J.F, Wyllie A.H and Currie A.R. Apoptosis: A basic biological phenomenon with wide-ranging implications in tissue kinetics. Br J Cancer 1972; 26:239-57.

[3] Mattson, M. P. Apoptosis in neurodegenerative disorders. Nat Rev Mol Cell Biol. 2000; 1(2): 120-129.

[4] Baud V and Karin M. Signal transduction by tumor necrosis factor and its relatives. Trends Cell Biol. 2001; 11:372-7.

[5] Green DR, Kroemer G. The pathophysiology of mitochondrial cell death. Science. 2004;305:626-9.

[6] Liu X, Kim CN, Yang J, Jemmerson R, Wang X. Induction of apoptotic program in cell free extracts: Requirement for dATP and Cytochrome C. Cell 1996; 86:147-57.

[7] Ortiz A, Justo P, Sanz A, Lorz C, Egido J. Targesting apoptosis in acute tubular necirsis. Biochem pharmacol. 2003; 66:1589-1594

[8] Degterev A, Boyce M and Yuan J. A decade of caspases. Oncogene. 2003; 22:8543-67.

[9] Woo M, Hakem R, Soengas M.S, Duncan G.S, Shahinian A, Kagi D, Hakem A, McCurrach M, Khoo W, Kaufman S.A, Senaldi G, Howard T, Lowe S.W and Mak T.W. Essential contribution of caspase 3/cpp32 to apoptosis and its associated nuclear changes. Genes Dev. 1998; 12:806-19.

[10] Kuida K, Zheng T.S, Na S, Kuan C, Yang D, Karasuyama H, Rakic P and Flavell R.A. Decreased apoptosis in the brain and premature lethality in cpp32-deficient mice. Nature 1996; 384:368-72.
[11] Proskuryakov SY, Gabai VL, Konoplyannikov AG. Necrosis is an active and controlled form of programmed cell death. Biochemistry (Mosc) 2002; 67:387-408.

[12] Lockshin R.A and Zakeri Z. Caspase-independent cell death? Oncogene. 2004; 23:2766-73.
[13] Oppenheim R.W, Flavell R.A, Vinsant S, Prevette D, Kuan C.Y and Rakic P. Programmed cell death of developing mammalian neurons after genetic deletion of caspases. J Neurosci. 2001; 21:4752-60.

[14] Edinger A.L and Thompson C.B. Death by design: apoptosis, necrosis and autophagy. Curr Opin Cell Biol 2004; 16:663-9.

[15] Nerurkar P.V, Pearson L, Frank J.E, Yanagihara R and Nerurkar V.R. Highly active antiretroviral therapy (HAART)- associated lactic acidosis: in vitro effects of combination of nucleoside analogues and protease inhibitors on mitochondrial function aqnd lactic acid production. Cell Mol Bio. 2003; 49:1205-1211

[16] Apostolova L.G, Hwang K.S, Medina L.D, Green A.E, Braskie M.N, Dutton R.A, Lai J, Geschwind D.H, Cummings J.L, Thompson P.M and Ringman J.M. Cortical and hippocampal atrophy in patients with autosomal dominant familial Alzheimer's disease. Dementia and Geriatric Cognitive Disorders. 2011;32:118-125.

[17] Blas-García A, Apostolova N, Ballesteros D, Monleón D, Morales J.M and Rocha M. Inhibition of mitochondrial function by Efavirenz increases lipid content in hepatic cells. Hepatology. 2010
[18] Tsukada M and Ohsumi Y. Isolation and characterization of autophagy-defective mutants of Saccharomyces cerevisiae. FEBS Lett. 1993; 333:169-74.

[19] Codogno, P. and Meijer A.J. Autophagy and signaling: their role in cell survival and cell death. Cell Death Differ. 2005; 12(S2): 1509-1518.

[20] Thumm M, Egner R, Koch B, Schlumpberger M, Straub M, Veenhuis M and Wolf D.H. Isolation of autophagocytosis mutants of Saccharomyces cerevisiae. FEBS Lett. 1994; 349:275-80.

[21] Son J.H, Hee J.S, Kyung-Hee K, Ji-Young H and Ji-Young H. Neuronal autophagy and neurodegenerative diseases. Exp Mol Med. 2012 44: 89-98.

[22] Yu L, Alva A, Su H, Dutt P, Freundt E, Welsh S, Baehrecke E.H and Lenardo M.J. Regulation of an ATG7-beclin 1 program of autophagic cell death by caspase-8. Science. 2004; 304:1500-2.

[23] Liang X.H, Jackson S, Seaman M, Brown K, Kempkes B, Hibshoosh H and Levine B. Induction of autophagy and inhibition of tumorigenesis by beclin 1. Nature 1999;402:672-6.

[24] Kim J.H, Cho A, Yin H, Schafer D.A, Mouneimne G, Simpson K.J, Nguyen K.V, Brugge, J.S., Montell, D.J. (2011). Psidin, a conserved protein that regulates protrusion dynamics and cell migration. Genes Dev. 25(7)**:** 730--741.

[25] Thabethe K, Adefolaju G and Hosie M. An *In Vitro* Study of the Effects of Emtricitabine, Tenofovir Disoproxil Fumarate and Efavirenz on a Breast Cancer Cell Line, MCF-7. *J. Basic. Appl. Sci. Res.*2003; 3(4)444-452.

[26] Rieger K.J, Kaniak A and Coppee J.Y. Large-scale phenotypic analysis — the pilot project on yeast chromosome III. Yeast 13. 1997; 1547–1562.

[27] Karpinich NO, Tafani M, Rothman R.J, Russo M.A, Farber J.L. The course of etoposide-induced apoptosis from damage to DNA and p53 activation to mitochondrial release of cytochrome c. J Biol Chem. 2002; 277: 16547–16552.

[28] Fadok, V.A, Bratton D.L, Rose D.M, Pearson A., Ezekewitz R.A and Henson P. M. A receptor for phosphatidylserine-specific clearance of apoptotic cells. Nature. 2000; 405, 85-90

[29] Scaduto A., Russell C.J, Grotyohann A and Lee W. Measurement of mitochondrial membrane potential using fluorescent rhodamine derivatives. Biophys.1999; J. 76, 469-477

[30] Vande Velde C, Cizeau J, Dubik D, Alimonti J, Brown T, Israels S, Hakem R and Greenberg A.H. BNIP3 and genetic control of necrosis-like cell death through the mitochondrial permeability transition pore. Mol Cell Biol 2000; 20:5454-68

[31] Owusu-Ansah E, Yavari A, Mandal S and Banerjee U. Distinct mitochondrial retrograde signals control the G1-S cell cycle checkpoint. Nat. Genet.2008; 40(3): 356--361.

[32] Gerasimenko J.V, Gerasimenko O.V, Palejwala A, Tepikin A.V, Petersen O.H and Alastair Watson J.M. Menadione-induced apoptosis: roles of cytosolic Ca2+ elevations and the mitochondrial permeability transition pore Journal of Cell Science. 2001; 115, 485-497

[33] Shiao1 Y-H, Lee S-H and Kasprzak K.S. Cell cycle arrest, apoptosis and p53 expression in nickel(II) acetate-treated Chinese hamster ovary cells. Carcinogenesis. 1998; vol.19 no.7 pp.1203–1207.

[34] Willis N, Rhind N and Li W.X. Studying G2 DNA Damage Checkpoints Using the Fission Yeast Schizosaccharomyces pombe. Cell Cycle Checkpoints, Methods in Molecular Biology 782

[35] Koczor C.A, Shokolenko I.N, Boyd A.K, Balk S.P, Wilson G.L and Ledoux S.P. Mitochondrial DNA damage initiates a cell cycle arrest by a Chk2-associated mechanism in mammalian cells. J. Biol. Chem. 2009;284, 36191–36201

[36] Simon F, Mauclere P, Roques P, Loussert-Ajaka I, Muller-Trutwin M.C, Saragosti S, Georges-Courbot M.C, Barre-Sinoussi F and Brun-Vezinet F. Identification of a new human immunodeficiency virus type 1 distinct from group M and group O. Nat Med 1998; 4: 1032–1037.

[37] Zamzami, N., and Kroemer, G. (2001). The mitochondrion in apoptosis: how Pandora's box opens. Nat. Rev. Mol. Cell Biol. 2, 67–71.

[38] Silva, M. T. Secondary necrosis: the natural outcome of the complete apoptotic program. FEBS Lett. 2010; 584(22): 4491-4499.

[39] Kim J.H, Cho A, Yin H, Schafer D.A, Mouneimne G, Simpson K.J, Nguyen K.V, Brugge, J.S., Montell, D.J. (2011). Psidin, a conserved protein that regulates protrusion dynamics and cell migration. Genes Dev. 25(7): 730--741.

[40] Rodriguez-Novoa S, Labarga P and D'avolio A. Impairment in kidney tubular function in patients receiving tenofovir is associated with higher tenofovir plasma concentrations. AIDS. 2010;24:1064–1066.

CHAPTER FIVE

[1] Karras A, Lafaurie M and Furco A. Tenofovir-related nephrotoxicity in HIV-infected patients: three cases of renal failure, Fanconi syndrome, and nephrogenic diabetes insipidus. Clin Infect Dis 2003;36(8):1070-3

[2] Malik A, Abraham P, Malik N. Acute renal failure and Fanconi syndrome in an AIDS patient on tenofovir treatment-case report and review of literature. J Infect 2005;51(2):E61-5

[3] Kohler J.J, Hosseini S.H, Green E, Abuin A, Ludaway T, Russ R, Santoianni R and Lewis W. Tenofovir renal proximal tubular toxicity is regulated by OAT1 and MRP4 transporters. Lab Invest. 2011; **91**(6): 852-858.
[4] Chaturvedi S, Farmer T and Kapke GF. Assay validation for KIM-1: human urinary renal dysfunction biomarker. Int J Biol Sci 2009;5:128-34.

[5] Rodriguez-Novoa S, Labarga P and D'avolio A. Impairment in kidney tubular function in patients receiving tenofovir is associated with higher tenofovir plasma concentrations. AIDS. 2010;24:1064–1066.
[6] Duarte C.G and Preuss H.G. Assessment of renal function–glomerular and tubular. Clin Lab Med 13. 1993; 33–52.
[7] Chiusolo A, Defazio R, Zanetti E, Mongillo M, Mori N, Cristofori P and Trevisan A. Kidney injury molecule-1 expression in rat proximal tubule after treatment with segment-specific nephrotoxicants: A tool for early screening of potential kidney toxicity. Toxicol Pathol. 2010; 38:338–345.

[8] Miller D. Nucleoside phosphonate interactions with multiple organic anion transporters in renal proximal tubule. J Pharmacol Exp Ther. 2001;299(2):567-74

[9] Labarga P, Barreiro P and Martin-Carbonero L. Kidney tubular abnormalities in the absence of impaired glomerular function in HIV patients treated with tenofovir. AIDS 2009;23:689–696.

[10] Taylor S, Little J, Halifax K, Drake S and Back D. Pharmacokinetics of nelfinavir and nevirapine in a patient with end stage renal failure on continuous ambulatory peritoneal dialysis. J Antimicrob Chemother. 2000;45(5): 716–717.
[11] Vaidya V.S, Ozer J.S, Frank D, Collings F.B, Ramirez V, Troth S, Muniappa N, Thudium D, Gerhold D, Holder D.J, Bobadilla N.A, Marrer E, Perentes E, Cordier A, Vonderscher J, Maurer G, Goering P.L, Sistare F.D, and Bonventre J.V. Kidney Injury Molecule-1 Outperforms Traditional Biomarkers of Kidney Injury in Multi-site Preclinical Biomarker Qualification Studies. Nat Biotechnol. 2010 ; 28(5): 478–485.

[12] Gallant J.E, Staszewski S, Pozniak A.L, DeJesus E, Suleiman J.M, Miller M.D, Coakley D.F, Lu B, Toole J.J and Cheng A.K; Efficacy and safety of tenofovir DF vs stavudine in combination therapy in antiretroviral-naive patients: a 3-year randomized trial. JAMA 2004; Jul 14; 292(2):191-201
[13] Izzedine H, Launay-Vacher V, Deray G. Antiviral drug-induced nephrotoxicity. Am J Kidney Dis. 2005 May;45(5):804-17.
[14] Arribas J.R, Pozniak A.L, Gallant J.E, Dejesus E, Gazzard B, Campo R.E, Chen S.S, McColl D, Holmes C.B, Enejosa J, Toole J.J and Cheng A.K. Tenofovir disoproxil fumarate, emtricitabine, and efavirenz compared with zidovudine/lamivudine and efavirenz in treatment-naive patients: 144-week analysis. J Acquir Immune Defic Syndr. 2008: 1:47(1):74-8.

[15] Kohler J, Hosseini S and Hoying-Brandt A, Tenofovir renal toxicity targets mitochondria of renal proximal tubules. Lab Invest 2009;89(5):513-9
[16] Lebrecht D, Venhoff A.C, Kirschner J, Wiech T, Venhoff N and Walker UA. Mitochondrial tubulopathy in tenofovir disoproxil fumarate-treated rats. J Acquir Immune Defic Syndr. 2009;1;51(3):258-63.

[17] Van Rompay K, Brignolo L and Meyer D. Biological effects of short-term or prolonged administration of 9-[2-(phosphonomethoxy)propyl]adenine (tenofovir) to newborn and infant rhesus macaques. Antimicrob Agents Chemother 2004;48(5):1469-87

[18] Buchacz K, Young B and Baker RK. Renal function in patients receiving tenofovir with ritonavir/lopinavir or ritonavir/atazanavir in the HIV Outpatient Study (HOPS) cohort.JAIDS. 2006;43:626-628.

[19] Goodsaid F.M, Blank M and Dieterle F. Novel biomarkers of acute kidney toxicity. Clin Pharmacol Ther. 2009; 86, 490–6.

[20] Ichimura T, Bonventre J.V, Bailly V, Wei H, Hession C.A, Cate R.L and Sanicola M. Kidney injury molecule-1 (KIM-1), a putative epithelial cell adhesion molecule containing a novel immunoglobulin domain, is up-regulated in renal cells after injury. J Biol Chem. 1998; 273:4135–4142.
[21] Zhang, Z., Humphreys, B.D and Bonventre J.V. Shedding of the Urinary Biomarker Kidney Injury Molecule-1 (KIM-1) Is Regulated by MAP Kinases and Juxtamembrane Region." Journal of the American Society of Nephrology.2007; 18(10): 2704-2714.

[22] Lim A.I, Tang S.C.W, Lai K.N and Leung J.C.K. Kidney Injury Molecule-1: More Than Just an Injury Marker of Tubular Epithelial Cells? J. Cell. Physiol. 2012; 228: 917–924, 2013.

[23] Amin RP. Identification of putative gene based markers of renal toxicity. Environ Health Perspect. 2004; 112:465–479.

[24] Bailly V. Shedding of kidney injury molecule-1, a putative adhesion protein involved in renal regeneration. J Biol Chem. 2002; 277:39739–39748.

[25] Zhou Y. Comparison of kidney injury molecule-1 and other nephrotoxicity biomarkers in urine and kidney following acute exposure to gentamicin, mercury, and chromium. Toxicol Sci. 2008; 101:159–170.

[26] Hahn B.H, Shaw G.M, De Cock K.M and Sharp P.M. AIDS as a Zoonosis: Scientific and Public Health Implications Science. 2000: Vol. 287 no. 5453 pp. 607-614

[27] Chaturvedi S, Farmer T, Kapke G.F. Assay validation for KIM-1: human urinary renal dysfunction biomarker. Int J Biol Sci. 2009;5:128-34.

[28] Fine D.M, Perazella M.A, Lucas G.M and Atta M.G. Kidney biopsy in HIV: beyond HIV-associated nephropathy. Am J Kidney Dis. 2008;51:504–514.

[29] Passmore A.P, Copeland S and Johnston G.D. A comparison of the effects of ibuprofen and indomethacin upon renal haemodynamics and electrolyte excretion in the presence and absence of frusemide. *Br J Clin Pharmacol.* 1989 Apr;**27**(4):483–490.

[30] Malik A.N, Shahni R, Rodriguez-de-Ledesma A, Laftah A and Cunningham P . Mitochondrial DNA as a non-invasive biomarker: Accurate quantificationusing real time quantitative PCR without co-amplification of pseudogenes and dilution bias. Elsevier. 2011; 412:1–7

CHAPTER SIX

[1] Cooper RD. Systematic review and meta-analysis: renal safety of tenofovir disoproxil fumarate in HIV-infected patients. Clin Infect Dis 2010; 51: 496-505

[2] Gallant J.E, Staszewski S, Pozniak A.L, DeJesus E, Suleiman J.M, Miller M.D, Coakley D.F, Lu B, Toole J.J and Cheng A.K; Efficacy and safety of tenofovir DF vs stavudine in combination therapy in antiretroviral-naive patients: a 3-year randomized trial. JAMA 2004; Jul 14; 292(2):191-201

[3] Rodriguez-Novoa S, Labarga P and D'avolio A. Impairment in kidney tubular function in patients receiving tenofovir is associated with higher tenofovir plasma concentrations. AIDS. 2010;24:1064–1066.
[4] Cohen M.S, Gay C and Kashuba A.D. Narrative review: antiretroviral therapy to prevent the sexual transmission of HIV-1. Ann Intern Med 2007; 146: 591–601.

[5] Garcia-Lerma J.G, Paxton L and Kilmarx P.H. Oral pre-exposure prophylaxis for HIV prevention. Trends Pharmacol Sci 2010; 31: 74–81.

[6] Dolin R. HIV vaccine trial results—an opening for further research.N Engl J Med 2009; 361: 2279–80.

[7] Panlilio A.L, Cardo D.M, Grohskopf LA, Heneine W and Ross C.S. U.S. Public Health Service.Updated U.S. Public Health Service guidelines for the management of occupational exposures to HIV and recommendations for postexposure prophylaxis. MMWR Recomm Rep. 2005; Sep 30;54(RR-9):1-17.
[8] Smith K, Weinberg W and DeJesus E. Once-daily ritonavir (100mg) boosting of fosamprenavir (FPV/r) or atazanavir (ATZ/r) with tenofovir (TDF)/emtricitabine (FTC) in antiretroviral-naive HIV-infected patients.2007; 48-50

[9] Peterson L, Taylor D, Roddy R, Belai G, Phillips P, Nanda K, Grant R, Essie E, Clarke K, Ridzon R, Doh A.S, Jaffe H.S, and Cates W. Tenofovir Disoproxil Fumarate for Prevention of HIV Infection in Women: A Phase 2, Double-Blind, Randomized, Placebo-Controlled Trial. PLoS Clin Trials. 2007; 2(5): e27
[10] Calmy A, Hirschel B and Cooper D.A. A new era of antiretroviral drug toxicity. Antivir Ther 2009; 14: 165–79.

[11] Anderson P.L, Kiser J.J, Gardner E.M, Rower J.E, Meditz A, and Grant G.M. Pharmacological considerations for tenofovir and emtricitabine to prevent HIV infection Antimicrob Chemother. 2011 February; 66(2): 240–250.

[12] Kim J.H, Cho A, Yin H, Schafer D.A, Mouneimne G, Simpson K.J, Nguyen K.V, Brugge, J.S., Montell, D.J. (2011). Psidin, a conserved protein that regulates protrusion dynamics and cell migration. Genes Dev. 25(7): 730--741.

[13] Marroquin LD, Hynes J, Dykens JA, Jamieson JD, Will Y. Circumventing the Crabtree effect: replacing media glucose with galactose increases susceptibility of HepG2 cells to mitochondria toxins, Toxicol Sci. 2007;97:539-547

[14] Rodriguez-Enriquez S, Kim I, Currin R.T and Lemasters, J.J. Tracker dyes to probe mitochondrial autophagy (mitophagy) in rat hepatocytes. Autophagy. 2006; 2, 39–46

[15] Ray A, Olson L and Fridland A. Role of purine nucleoside phosphorylase in interactions ibetween 2,3-dideoxyinosine and allopurinol, ganciclovir, or tenofovir. Antimicrob Agents Chemother 2004;48(4):1089-95

[16] Kohler J, Hosseini S and Hoying-Brandt A, Tenofovir renal toxicity targets mitochondria of renal proximal tubules. Lab Invest 2009;89(5):513-9
[17] Pampaloni F, Reynaud E.G and Stelzer E.H. K. The third dimension bridges the gap between cell culture and live tissue." Nat Rev Mol Cell Biol. 2007; 8(10): 839-845.

[18] Buzhor E , Harari-Steinberg O, Omer D, Metsuyanim S, Jacob-Hirsch J, Noiman T, Dotan Z, Goldstein R.S, and Dekel B. Tissue Engineering Part A. 2011; 17(17-18): 2305-2319.

[19] Apostolova L.G, Hwang K.S, Medina L.D, Green A.E, Braskie M.N, Dutton R.A, Lai J, Geschwind D.H, Cummings J.L, Thompson P.M and Ringman J.M. Cortical and hippocampal atrophy in patients with autosomal dominant familial Alzheimer's disease. Dementia and Geriatric Cognitive Disorders. 2011;32:118-125.

[20] Zamzami N and Kroemer G. The mitochondrion in apoptosis: how Pandora's Box opens. Nat. Rev. Mol. Cell Biol.2001; 2, 67–71

[21] Liu X, Kim CN, Yang J, Jemmerson R, Wang X. Induction of apoptotic program in cell-free extracts: requirement for dATP and cytochrome c. Cell. 1996;86:147–157.

[22] Kluck R, Bossy-Wetzel E, Green D, Newmeyer D. The release of cytochrome c from mitochondria: A primary site for Bcl-2 regulation of apoptosis. Science. 1997;275:1132–1136.

[23] Yang J, Liu X, Bhalla K, Kim C, Ibrado A-M, Cai J, Peng T-I, Jones D.P, Wang X. Prevention of apoptosis by Bcl-2: Release of cytochrome c from mitochondria blocked. Science. 1997;275:1129–1132

[24] Green DR, Reed JC. Mitochondria and apoptosis. Science. 1998;281:1309–1312.

[25] Zhaoyu J.W and El-Deiry S. Overview of Cell Death Signaling Pathways. Cancer Biology & Therapy. 2005; 4:2, 139-163
[26] Suzuki, Y. Ubiquitin-protein ligase activity of X-linked inhibitor of apoptosis protein promotes proteasomal degradation of caspase-3 and enhances its anti-apoptotic effect in Fas-induced cell death. Proceedings of the National Academy of Sciences.2001; 98(15): 8662-8667.

[27] Malik A, Abraham P, Malik N. Acute renal failure and Fanconi syndrome in an AIDS patient on tenofovir treatment-case report and review of literature. J Infect 2005;51(2):E61-5

[28] Callens S, De R and Colebunders R. Fanconi-like syndrome and rhabdomyolysis in a person with HIV infection on highly active antiretroviral treatment including tenofovir. J Infect 2003;47(3):262-3

[29] Peyriere H, Reynes J and Rouanet I. Renal tubular dysfunction associated with tenofovir therapy: report of 7 cases. J Acquir Immune Defic Syndr 2004;35(3):269-73

[30] Williams J and Chadwick D. Tenofovir-induced renal tubular dysfunction presenting with hypocalcaemia. J Infect 2006;52(4):e107-8

[31] Mathew G and Knaus S. Acquired Fanconi's syndrome associated with tenofovir therapy. J Gen Intern Med 2006;21(11):C3-5

[32] Rifkin BS and Perazella MA. Tenofovir-associated nephrotoxicity: Fanconi syndrome and renal failure. Am J Med 2004;117:282–284.

[33] Bustamante C, Vejo-Puente E, Velasco-Montes J and Hernandez-Hernandez J.L. Severe hypokalemia and tenofovir. Enferm Infecc Microbiol Clin. 2008;26(5):317-18

[34] Earle K, Seneviratne T, Shaker J and Shoback D. Fanconi's syndrome in HIV+ adults: report of three cases and literature review. J Bone Miner Res 2004;19(5):714-21

[35] Di Biagio A, Rosso R and Monteforte P. Whole body bone scintigraphy in tenofovir-related osteomalacia: a case report. J Med Case Reports 2009;3:8136-9

[36] Buchwald M. Moustacchi E. Is Fanconi anemia caused by a defect in the processing of DNA damage? Mutat Res. 1998;408:75–90.

[37] Son J.H, Hee J.S, Kyung-Hee K, Ji-Young H and Ji-Young H. Neuronal autophagy and neurodegenerative diseases. Exp Mol Med. 2012 44: 89-98.

[38] Barr A , Nelson M, Portsmouth S, Stebbing J, Atkins M, Matthews G, Pillay D, Fisher M, Bower M and Gazzard B. An open-label study of tenofovir in HIV-1 and Hepatitis B virus coinfected individuals. AIDS. 2003; Jan 3;17(1):F7-F10.

[39] Cihlar T, Birkus G, Greenwalt D.E and Hitchcock M.J.M. Tenofovir exhibits low cytotoxicity in various human cell types: comparison with other nucleoside reverse transcriptase inhibitors. Antiviral Research. 2002;54(1): 37-45.

[40] Birkus G, Hitchcock M, Cihlar T. Assessment of mitochondrial toxicity in human cells treated with tenofovir: comparison with other nucleoside reverse transcriptase inhibitors. Antimicrob Agents Chem other 2002;46(3):716-23

[41] Malik A.N, Shahni R, Rodriguez-de-Ledesma A, Laftah A and Cunningham P . Mitochondrial DNA as a non-invasive biomarker: Accurate quantificationusing real time quantitative PCR without co-amplification of pseudogenes and dilution bias. Elsevier. 2011; 412:1–7

[42] Stacpoole P.W, Henderson G.N, Yan Z, Cornett R and James M.O. (Pharmacokinetics, metabolism, and toxicology of dichloroacetate. Drug Metab Rev . 1997; 30:499–539

[43] Proskuryakov SY, Gabai VL and Konoplyannikov AG. Necrosis is an active and controlled form of programmed cell death. Biochemistry (Mosc) 2002; 67:387-408.

[44] Maggi P, Montinaro V, Bellacosa C, Pietanza S, Volpe A, Graziano G, Strippoli G and Angarano G. Early Markers of Tubular Dysfunctionin Antiretroviral-Experienced HIV-Infected Patients Treated with Tenofovir Versus Abacavir AIDS PATIENT CARE and STDs. 2012;Volume 26, Number 1.

[45] Ichimura T, Bonventre J.V, Bailly V, Wei H, Hession C.A, Cate R.L and Sanicola M. Kidney injury molecule-1 (KIM-1), a putative epithelial cell adhesion molecule containing a novel immunoglobulin domain, is up-regulated in renal cells after injury. J Biol Chem. 1998; 273:4135–4142.